

The University of Nottingham

UNITED KINGDOM · CHINA · MALAYSIA

Microglia respond to exogenous and endogenous activating stimuli differently during development

Rawan Edan (BSc, MSc)

A thesis submitted to the University of Nottingham

for the degree of Doctor of Philosophy

November 2019

Acknowledgements

I would like to express my deepest appreciation for my supervisors Dr Andrew Bennett and Dr Stephen Alexander, for their continuous support. PhD is a stressful journey, and their brilliant supervision created a stress-free environment. Secondly, I would like to thank my sponsor, Kuwait University and Kuwait's cultural office in London for providing me with this opportunity and for their financial support.

Many thanks to the FRAME lab team, especially, Monika Owen and Nicola De Vivo for their extraordinary lab management skills. The frame lab has been my second home for a few years, thanks to everyone who worked in it, especially Amer Imraish, who has been there for me at the beginning of my PhD. I am incredibly grateful for David Watson, Claire Spicer and Stephen Woodhams who trained and supervised the animal work. Many thanks to Tomas Bellamy, Federico Dajas-Bailador and Gareth Hathway for their valuable help and support.

I have been blessed to make friends with the most incredible people throughout my PhD journey who I can proudly call family. Alessandra Agostini, Andrea Bertoneri, Mathew Barron, Jessica Carpenter and Rawan Hareeri.

I have been blessed with the most supportive husband, Salem Salmain who left his job in Kuwait to come and support me. I am grateful for this man who inspires me every day by doing a degree in architecture at the age of 38 and

who gave me the most beautiful child in the world, Omar. Thank you Omar for making me a better person.

Finally, I would like to thank my parents, my in-laws and my family for their moral support.

Declaration

All of the experiments and analysis detailed in this thesis have been carried out by myself. This thesis has not been submitted for any other degree or qualification.

Abbreviations

TNP-ATP	2',3'-O-(2,4,6-Trinitrophenyl)adenosine-5'-triphosphate tetra(triethylammonium) salt
6-MP	6-mercaptopurine
A.MCM-ACM	Adult MCM-stimulated ACM
ACM	Astrocytes conditioned media
AD	Alzheimer's disease
AF-1	Ligand-independent domain
Akt	Serine/threonine-specific protein kinase
ALS	Amyotrophic lateral sclerosis
AP-	Activator protein-
ATP	Adenosine triphosphate
Aβ	Amyloid-beta
BBB	Blood-brain barrier
BCP	1-Bromo 3-Chloro-propane
BDNF	Brain-derived neurotrophic factor
BSA	Bovine serum albumin
c1q	complement component c1q
C3	Complement component
Ca^{2+}	Calcium
CCI	Chronic Constriction Injury
CNS	Central nervous system
CORM-2	Tricarbonyldichlorrutheniem II dimer
CREB	cAMP response element-binding protein
CyTOF	Multiplexed mass cytometry
DAMPs	Danger-associated molecular patterns
DAPI	4′,6-diamidino-2-phenylindole
DBD	DNA-binding domain
DEPC	Diethyl pyrocarbonate
DMSO	Dimethyl sulfoxide
DNase I	Deoxyribonuclease I
DRG	Dorsal root ganglion
EGF	Epidermal growth factor
EIA	Enzyme Immunoassay
ELISA	Enzyme-linked immunosorbent assay
Emilin2	Elastin microfibril interfacer 2
ERK	Extracellular signal-regulated kinases
FAM	6-carboxyfluorescein

FBS	Fetal bovine serum
Fcrls	Fc receptor-like molecules
FGF	Fibroblast growth factor
FKN	Fractalkine
GABA	γ-aminobutyric acid
GAPDH	Glyceraldehyde 3-phosphate dehydrogenase
Gda	Guanine deaminase
GDNF	Glial cell line-derived neurotrophic factor
GFAP	Glial fibrillary acidic protein
Gi	Heterotrimeric G protein-coupled to Gi protein
GLUT5	Glucose transporter member 5
GM-CSF2	Granulocyte-macrophage colony-stimulating factor 2
HBSS	Hanks balanced salt solution
HD	Huntington's disease
HDAC1	Histone-deacetylase 1
HMGB1	High mobility group box 1
Hp	Haptoglobin
I.p	Intraperitoneally
IBA1	Ionized Calcium-binding adapter molecule 1
IFN-	Interferon-
IkB	Inhibitor of kappa B
IKK	Inhibitor of kappa B kinase
IL-	Interleukin-
IP-10	IFN-γ-induced protein 10
JNK	c-Jun N-terminal kinase
KCC2	Potassium cloride transporter
LBPs	LPS binding proteins
LCN2	Lipocalin-2
L-LME	L-leucine methyl ester
LPS	Lipopolysaccharide
LXRs	Liver X receptors
MafB	MAF BZIP Transcription Factor B
MAPK	Mitogen-activated protein kinase
MCM	Microglia conditioned media
MCP-1	Monocyte chemoattractant protein -1
MEK	Mitogen-activated protein kinase kinase
MEKK	MAP3kinase
MHC-	Major histocompatibility complex-
miR-9	microRNA-9
MS	Multiple sclerosis
MWCO	Molecular weight cut off

N.MCM-ACM	Neonatal MCM-stimulated ACM
NADPH	Nicotinamide adenine dinucleotide phosphate
NBM	Neurobasal media
NF-kB	Necrosis factor-kappa B
NLRPs	NOD-like receptor proteins
NO	Nitric oxide
NR4A	Nuclear receptor 4 A
ORM2	Orosomucoid 2
p2ry12	Purinergic receptor P2Y, G-protein coupled,12
PAI-1	Plasminogen activator inhibitor-1
PAMPs	Pathogen-associated molecular patterns
PBS	Phosphate-buffered saline
PDL	Poly-D-lysine
Pen/strep	Penicillin/streptomycin
PGE2	Prostaglandin-E2
PI3K	Phosphatidylinositide 3-kinases
PKC	Protein kinase C
PLC	Phospholipase C
PLO	Poly-o-ornithine
PNI	Peripheral nerve injury
Pp38	Phosphorylated p38
PPARs	Peroxisome proliferator-activated receptors
PRRs	Pattern recognition receptors
Psat1	Phosphoserine Aminotransferase 1
PTX3	Pentraxin 3
qPCR	quantitative PCR
Raf	Small GTPase
Raf	Small GTPase
RXR	9-cis Retinoic acid receptor
Sall1	Sal-like protein 1
Scd2	stearoyl-Coenzyme A desaturase 2
SDS	Sodium dodecyl sulfate
Sell	Selectin-L
SEM	Standard error of mean
Serpina3n	Serine protease Inhibitor
SFM	serum-free media
Slc2a5	Solute carrier family 2, facilitated glucose transporter member 5
TAMRA	tetramethylrhodamine
TBST	Tris-buffered saline-tween 20

TGF-	Tumour growth factor
TLR-4	Toll-like receptor-4
TMEM119	transmembrane protein 119
TNF-	Tumour necrosis factor-
TREM2	Triggering receptor expressed on myeloid cells 2
TrkB	Tropomyosin-related kinase B
VEGF-B	Vascular endothelial growth factor B
β-actin	Beta-actin

Abstract

Background: Glial cells (microglia and astrocytes) facilitate inflammatory responses in the CNS by responding to pathogen-associated molecular patterns (PAMPs) or damage-associated molecular patterns (DAMPs). Dysregulation in their communication could affect their polarisation state and if not resolved, can give rise to the pathogenesis of several neurodegenerative disorders. The different morphologies acquired by microglia during development suggest a functional difference crucial for the development of the brain. During ageing microglial state is skewed to a pro-inflammatory phenotype. Lipopolysaccharide (LPS) stimulation of aged microglia augments gene expression of pro-inflammatory mediators. The extent of glial cell activation and their production of inflammatory mediators affects the fate of neurons. LPS stimulation of microglia caused death in neurons mediated by neurotoxic glial cross-talk. Microglial response to injury alters their physiological release of neuroprotective brain-derived neurotrophic factor (BDNF) and its persistent release from ATP-activated microglia via P2X4R can contribute to neuropathic pain. In this thesis, we investigated microglial sensitivity during development towards LPS and ATP and regional heterogeneity. We studied the effect of LPS on glial cell communication in early post-natal and adult microglia, and the impact of consequent produced inflammatory mediators on neuronal viability. We also compared the inflammatory state of adult and neonatal microglia in response to ATP. Orphan nuclear receptor NR4A subfamily members have anti-

inflammatory properties during neuroinflammation carried out by microglia and astrocytes. In this thesis, we studied their expression in response to PAMPs and DAMPs.

Methods: Sprague Dawley rats have been used for all primary cultures. Neonatal cortical or spinal cord microglia or astrocytes primary cultures were established from P 0-2 rats while P-40 rats were used for cortical or spinal cord adult primary microglia cultures. Cortical neurons were isolated from E18 rats. Serum or serum-free media were used to evaluate the effect of serum on gene expression. Microglia were treated with 100 ng/ml LPS. Astrocytes were incubated with LPS-stimulated microglia-conditioned media (MCM) for 1, 3, 6 and 24h. Real-time qPCR was performed to evaluate *Nur77*, *Nurr1*, *NOR-1*, *IL-1β* and *TGF- β* transcript levels in astrocytes in response to MCM stimulation. Primary cortical neurons were incubated with serum-free MCM-stimulated astrocyte's conditioned media for 24 hours and their viability was evaluated. In chapter four, adult or neonatal spinal cord or cortical microglia were stimulated with different concentrations of ATP and the effect of pretreating them with P2X inhibitor (TNP-ATP) or p38 MAPK inhibitor (SB202190) was evaluated. Immunoreactivity of P2X4R in adult and neonatal microglia was investigated. BDNF expression (through qPCR) and release (via ELISA) was determined in response to ATP stimulation and inhibitors. The anti-inflammatory mediators, *Nurr1* and *IL-10* mRNA expression in response to ATP and inhibitors were also studied in adult and neonatal microglia.

Results: LPS stimulation increased cortical (adult: 32-fold, neonatal:413-fold) and spinal cord (neonatal: 5-fold) microglial *Nur77* mRNA expression and also *NOR-1* mRNA expression rapidly in cortical (adult: 5-fold and neonatal: 57-fold) and spinal cord microglia (neonatal: 98-fold). Astrocytes orphan nuclear receptors mRNA levels significantly increased when stimulated with neonatal or adult MCM for 24 hrs. Adult cortical LPS-stimulated MCM appeared to increase the level of *IL-1β* mRNA (59-fold) in a higher manner compared to astrocytes stimulated with neonatal cortical LPS-stimulated MCM (12-fold) in serum rich media and the same effect was notable in spinal cord astrocytes treated with spinal cord MCM. Levels of MCM-induced *NOR-1* mRNA was higher (~ 100-fold in cortical astrocytes and ~ 60-fold in spinal cord astrocytes) than *Nur77* (~15-fold in spinal cord astrocytes and ~80-fold in cortical astrocytes) and *Nurr1* transcript levels (~13-fold in spinal cord astrocytes and ~55-fold in cortical astrocytes. Morphological observations based on neuronal axons integrity suggested that neonatal cortical microglia promoted proliferation in cortical neurons sustained by cortical astrocytes conditioned media (ACM). Cell proliferation assay confirmed that neonatal cortical MCM-ACM increased the viability (153%) of cortical neurons in comparison to controls (99%) and adult unstimulated-MCM-ACM (150%) or LPS-stimulated MCM-ACM (122%) treated. Microglial stimulation with ATP significantly up-regulated NR4A subfamily members after 1 hour of stimulation in cortical and spinal cord microglia. ATP stimulation significantly up-regulated *BDNF* expression levels in adult microglia (4-fold in spinal cord and 4.8-fold in cortical) and not

neonatal microglia (1.6-fold in spinal cord and 1.4-fold in cortical). Pre-treatment with TNP-ATP down-regulated mRNA expression (≤ 3-fold) and release of BDNF in adult cortical and spinal cord microglia while p38 MAPK inhibitor down-regulated ATP –induced *BDNF* transcript levels (3-fold) but failed to significantly reduce BDNF release from adult cortical and spinal cord microglia. Pre-treatment with both inhibitors attenuated ATP-induced *Nurr1* and *IL-10* expression in adult and neonatal microglia.

Conclusion: The extent of microglial activation and their polarisation is dependent on the type, duration and concentration of the stimulus. Microglial developmental and regional heterogeneity was evident in the event of external (LPS) and endogenous (ATP) stimuli. Glial cell communication and their responses to activating stimuli are modulated by both developmental stage and physical location.

Table of contents

Acknowledgements ..... *ii*

Declaration ..... *iii*

Abbreviations ..... *iv*

Abstract ..... *viii*

Table of contents ..... *xii*

1) Chapter One: General Introduction *1*

1.1 Neuroinflammation **2**

1.2 Glial cells **3**

1.2.1 Microglia 5

1.2.1.1 Microglial development 9

1.2.1.2 Activators of Microglia 10

1.2.1.3 LPS and Microglia 11

1.2.1.4 ATP and Microglia 13

1.2.1.5 Microglia and neuropathic pain 15

1.2.1.6 Cytokines and Microglia 17

1.2.1.7 Chemokines and Microglia 18

1.2.1.8 M1/M2 paradigm 20

1.2.1.9 Microglial heterogeneity 23

1.2.1.10 Microglia and ageing 27

1.2.1.11 Limitations of microglial cultures 29

1.2.2 Astrocytes 31

1.2.3 Glia-neuron crosstalk 35

1.3 Nuclear receptors 39

1.3.1 Orphan Nuclear Receptors 40

1.3.1.1 NR4A1/Nur77 41

1.3.1.2 NR4A2/Nurr1 43

1.3.1.3 NR4A3/NOR-1 44

2) Chapter two: Materials and Methods 48

2.1 Animals 49

2.1.1 Primary microglia culture isolated from adult rats 49

2.1.2 Primary microglia culture isolated from neonatal rats 51

2.1.3 Primary astrocyte culture isolated from neonatal rats 52

2.1.4 Primary cortical neuron culture isolated from rat embryos 54

2.2 Reagents 55

2.3 Collection of microglia and astrocytes conditioned media 56

2.3.1.1 LPS treatment and collection of conditioned media from microglia 56

2.3.1.2 Astrocyte treatment with adult or neonatal microglial conditioned media (MCM) 57

2.3.1.3 Neuron treatment with Astrocytes conditioned media (ACM) 58

2.4 RNA extraction 58

2.5 Reverse Transcription (cDNA synthesis) 60

2.6 Taqman qPCR 60

2.7 Western blotting 63

2.8 Immunocytochemistry 67

2.9 MTS assay 68

2.10 Enzyme-linked immunosorbent assay (ELISA) 69

2.10.1 Rat IL-1β/IL-1F2 ELISA..... 69

2.10.2 BDNF Enzyme Immunoassay (EIA)..... 70

2.11 Cloning of Nur77 from microglia..... 72

2.12 Statistical analysis..... 74

3) Chapter Three: Microglia-astrocyte crosstalk during in vitro LPS-induced neuroinflammation, a study of regional and developmental heterogeneity 75

3.1 Introduction 76

3.2 Aim 77

3.3 Results 79

3.3.1 Validation of the purity of neonatal and adult microglia *in vitro*..... 79

3.3.2 Validation of neonatal and adult microglia phenotypes *in vitro*..... 84

3.3.3 LPS-induces *IL-1β* and *IL-10* mRNA expression rapidly in primary microglia 86

3.3.4 LPS-induces *Nur77* and *NOR-1* mRNA expression rapidly in primary microglia..... 90

3.3.5 LPS-induces Nur77 protein expression rapidly in primary cortical microglia 96

3.3.6 LPS-induces IL-1β release in primary microglia..... 98

3.3.7 Astrocyte expression of Nurr1 and splice variants..... 100

3.3.8 Effect of treatment with LPS-stimulated serum-rich MCM on spinal cord astrocytes' expression of *Nur77*, *NOR-1*, *Nurr1*, *TINUR*, *Nurr1a, IL-1β, and TGF-β* mRNA..... 102

3.3.9 Effect of treatment with LPS-stimulated serum-free MCM on spinal cord astrocytes' expression of *Nur77*, *NOR-1*, *Nurr1, TINUR*, *Nurr1a, IL-1β*, and *TGF-β* mRNA..... 117

3.3.10 Effect of adult or neonatal cortical MCM-stimulated ACM on cortical neurons 130

3.4 Discussion 134

3.4.1 Microglia retain their developmental gene expression profile *in vitro* 134

3.4.2 LPS-induced pro-inflammatory and anti-inflammatory cytokine mRNA expression in microglia 137

3.4.3 LPS induces the expression of orphan nuclear receptors in microglia 138

3.4.4 Astrocytes' expression of Nurr1 and splice variants 141

3.4.5 GFAP immunoreactivity of primary Astrocytes cultured in serum/serum-free media 141

3.4.6 Effect of treatment with LPS-stimulated MCM on astrocyte expression of *Nur77*, *NOR-1*, *Nurr1*, *TINUR*, *Nurr1α*, *IL-1β* and *TGF-β* mRNA 143

4) Chapter four: Developmental differences in microglial responses to ATP 147

4.1 Introduction 148

4.2 Aim 149

4.3 Results 150

4.3.1 ATP-induced NR4A expression in microglia 150

4.3.1.1 Different concentrations of ATP induced mRNA expression of *Nur77*, *NOR-1* and *Nurr1* in microglia after 60 min of stimulation 150

4.3.1.2 Induced transcript levels of *Nur77* and *NOR-1* in microglia stimulated with 100µM ATP at different time points 159

4.3.1.3 ATP-induced Nur77 protein expression in microglia in a time-dependent manner 163

4.3.2 P2X4R protein expression and localisation in neonatal or adult microglia 165

4.3.3 *BDNF* mRNA expression in response to ATP stimulation of microglia 168

4.3.3.1 ATP-induced BDNF expression and release was changed in adult microglia upon interference with P2X or P38 MAPK pathways in a time-dependent manner 174

4.3.4 ATP-induced anti-inflammatory mediators' expression is altered in adult microglia upon inhibition with P2X or P38 MAPK pathways in a concentration-dependent manner . 189

4.3.4.1 ATP-induced *Nurr1* mRNA expression decreased with p38 MAPK inhibitor In adult spinal cord microglia 189

4.3.4.2 100μM ATP-induced *Nurr1* and *IL-10* mRNA expression was decreased with TNP-ATP and SB202190 pretreatment 193

4.4 Discussion 198

4.4.1 ATP stimulation rapidly induces NR4A subfamily members of nuclear receptors expression in microglia 199

4.4.2 P2X4R expression and localisation in microglia 201

4.4.3 ATP-induces BDNF expression and release in adult microglia only 201

4.4.3.1 P2X and p38 MAPK inhibitors affect BDNF mRNA and release 202

4.4.3.2 P2X and p38 MAPK inhibitors regulate ATP-induced *Nurr1* and *IL-10* mRNA expression 203

5) Chapter Five: General Discussion and future directions 206

5.1 Summary of findings 207

5.2 Markers for developmental microglia..... 208

5.3 Microglia-astrocyte communication after LPS stimulation..... 209

5.4 Microglial responses to ATP stimulation 213

5.5 Future directions 216

Appendix 218

Data presented at conferences..... 218

6) Chapter six: Bibliography 219

1) Chapter One:

General Introduction

1.1 Neuroinflammation

Neuroinflammation is a term used when describing inflammation occurring in the central nervous system (CNS). Neuroinflammation can occur as a result of an invading pathogen or may be caused by trauma or injury. Resident immune cells in the CNS, such as microglia, and other glial cells including astrocytes are responsible for eliciting an inflammatory response. Their activation and production of inflammatory mediators lead to neuroinflammation. Importantly, dysregulation in their activated states can be deleterious to CNS tissues (Harry and Kraft, 2012, Taupin, 2008).

The blood-brain barrier (BBB) is a highly selective membrane barrier that is composed of astrocytes, pericytes and endothelial cells connected by tight junctions (Daneman and Prat, 2015). The integrity of the BBB alters during neuroinflammation (Erickson et al., 2012). Infiltrating peripheral immune cells such as lymphocytes and macrophages aid in restoring a healthy state of the damaged tissue in the CNS (Harry and Kraft, 2008). Neutrophils are the first type of leukocytes to be recruited towards the site of insult (Kolaczkowska and Kubes, 2013). The cascade of their recruitment involves their rolling across endothelial tissues, a process associated with increased expression of surface integrins and selectins (Ma et al., 2013). Chemical signalling attracts neutrophils to the area of damage. For instance, local immune cells can release cytokines, leukotrienes, and histamines that guide neutrophils in the direction of the insult (Kolaczkowska and Kubes, 2013). That migration eventually ends with neutrophil extravasation through

endothelial tissues of the BBB to the site in question (Ubogu et al., 2006, Kolaczkowska and Kubes, 2013). Mechanisms underlying neuroinflammation determine if the outcome is beneficial or deleterious to CNS tissues, for example, whether the damage is caused by pathogen infection or tissue trauma (Ransohoff, 2016). Another critical factor is the behaviour of cells surrounding the site of insult. In addition, the type of infiltrating peripheral immune cells can have a major impact on the immune responses (Carson et al., 2006).

Neuroinflammation can be either acute or chronic, while acute inflammation might be relevent to CNS injury, the term chronic neuroinflammation can be associated with degenration due to the chronicity of diseases (Streit et al., 2004a). Acute neuroinflammation is beneficial to the body by facilitating healing either by eliminating the pathogen or by repairing the wound. Its duration is generally short (Streit et al., 2004a). On the other hand, chronic neuroinflammation can damage tissues due to persistent production of inflammatory mediators (Sudduth et al., 2013). Molecules constantly being produced by infiltrating and/or resident immune cells can result in cell death or alteration of neighbouring cell phenotypes (Franceschi and Campisi, 2014).

1.2 Glial cells

Cumulative histological studies made by scientists in the 1800-1900s shaped the field of neurobiology. Rudolf Virchow was the first to introduce

the term neuroglia (Somjen, 1988). Virchow laid the building blocks for other scientists; for instance, Camillo Golgi developed silver nitrate staining in 1873 and discriminated between neurons and glial cells (Golgi, 1873). This technique has been modified and is still utilised despite the availability of advanced technologies (Baloyannis, 2015). He also paved the way to differentiate between protoplasmic and fibrous astrocytes. The Spanish scientist Santiago Ramon y Cajal developed gold chloride sublimate staining that differentiated astrocytes from other types of glial cells (Cajal, 1913). Cajal's and Nicolas Achuccaro's work defined the heterogeneity in astrocyte distribution and morphology in the CNS. The term, astrocyte, was defined at that time by Michael von Lehnossek (Ndubaku and de Bellard, 2008, Patrylo and Nowakowski, 1994, Tremblay et al., 2015, Oberheim et al., 2012). These findings helped Pio Rio del Hortega to distinguish microglia from other cells in the CNS.

Pio del Rio-Hortega is known as the father of microglia. He hypothesised microglial functions and distinguished them from astrocytes and oligodendrocytes (del Rio-Hortega, 1939). Not only did he describe the ability of microglia to nourish and protect neurons, but he also predicted the phagocytic functions of microglia. Moreover, he identified microglia and astrocytes with respect to their origin and differential phenotypic properties during different developmental stages. In mammals, microglia are mesodermal in origin and are derived from the yolk sac. On the other hand, astrocytes arise from the neuroectoderm (del Rio-Hortega, 1939, Rock et

al., 2004). Astrocytes form 35% of the total CNS cell population. Their cell extensions (feet processes) are found in close association with blood vessels in the brain; therefore, they regulate the BBB (Daneman and Prat, 2015). Astrocytes produce cytokines when activated to promote extravasation of leukocytes to the site of stimulus in the CNS (Carson et al., 2006).

The interaction between microglia and astrocytes is crucial to sustaining functions and biology of the CNS (da Fonseca et al., 2014).

1.2.1 Microglia

Microglial cells comprise about 15% of residing cells in the CNS. They are considered to be the resident macrophages in the CNS due to shared features with mononuclear phagocytes (Prinz and Priller, 2014). Microglia are derived from myeloid progenitor populations in the yolk sac during earlier developmental stages (Haage et al., 2019). In spite of sharing several common features with CNS populations of macrophages (I.e. Choroid plexus macrophages, meningeal macrophages, and perivascular macrophages), structural, molecular and functional differences were observed (Perry and Teeling, 2013, Sevenich, 2018).

Furthermore, peripheral macrophages exhibit high turnover rate and can be replaced by bone marrow-derived cells, unlike microglia that have a self-renewal rate of 0.8% per day (Hickey and Kimura, 1988, Reu et al.,

2017, Sousa et al., 2017). Moreover, the microglial self-renewal process is independent of circulating blood-stream monocytes or progenitor cells (Ajami et al., 2007). Studies focusing on CNS microglia and macrophages demonstrated the possibility of discriminating between both types of cells by examining their size and extension density (Giulian et al., 1995). However, it is challenging to distinguish between microglia and blood-derived infiltrating macrophages with respect to gene expression since both types of cells express common surface markers such as CD45 and the fractalkine receptor CX3CR1 (Haage et al., 2019). Recent transcriptomic and proteomic studies have identified genes expressed differently in microglia than macrophages (Satoh et al., 2016, Butovsky et al., 2014, Haage et al., 2019, Sa and Hoover-Plow, 2011).

For instance, microglia have been shown to uniquely express transmembrane protein 119 (*TMEM119*) (Satoh et al., 2016) the G-protein-coupled purinergic receptor P2Y12 (*p2ry12)* (Butovsky et al., 2014), solute carrier family 2, facilitated glucose transporter member 5 (*Slc2a5)* and Fc receptor-like molecules (*Fcrls) (Haage et al., 2019)*. Some of these markers have known functions in microglia. For example, P2ry12 is involved in chemotaxis where the movement of microglial cell processes are directed to the site of CNS injury (Lou et al., 2016) while Slc2a5 (also known as GLUT5) regulates fructose transport in human and rat brain (Sasaki et al., 2004), yet the functions of TMEM119 and Fcrls are still unclear (Bennett et al., 2016). Interestingly, DePaula-Silva and colleagues reported that homeostatic

microglia expressed high levels of *P2ry12* and *Fcrls* in comparison to reactive microglia (DePaula-Silva et al., 2019) suggesting that microglia biomarkers can be altered during microglial activation. However, the reported differential expression of microglial signature genes between homeostatic and reactive microglia could be solely linked to their model of neuroinflammation; an induced encephalomyelitis in mice via Theiler's murine encephalomyelitis virus.

On the other hand, unique peripheral monocyte/macrophages biomarkers have been identified including Elastin microfibril Interfacer 2 (*Emilin2);* a suggested modulator of thrombosis (Sa and Hoover-Plow, 2011), Guanine deaminase (*Gda)*; an enzyme that regulates intracellular levels of purine derivatives (Fernandez et al., 2009), Haptoglobin (*Hp)*; which controls trafficking of extracorpuscular haemoglobin (Murray et al., 1961), and Selectin L (*Sell)*; a cell adhesion molecule that facilitates migration and adhesion of immune cells (Ivetic et al., 2019, Haage et al., 2019)

Microglia have critical roles in health and disease (as shown in Figure 1-1). For instance, they sustain neuronal survival through their production of neurotrophic and anti-inflammatory mediators (Pocock and Piers, 2018). Moreover, neurogenesis occurs upon the recruitment of stem cells to the site of injury, a process facilitated by microglia (McPherson et al., 2011, Aarum et al., 2003). However, aberrant functions of microglia lead to deleterious and toxic effects (Block et al., 2007, Roy et al., 2008, Luo et al., 2010).

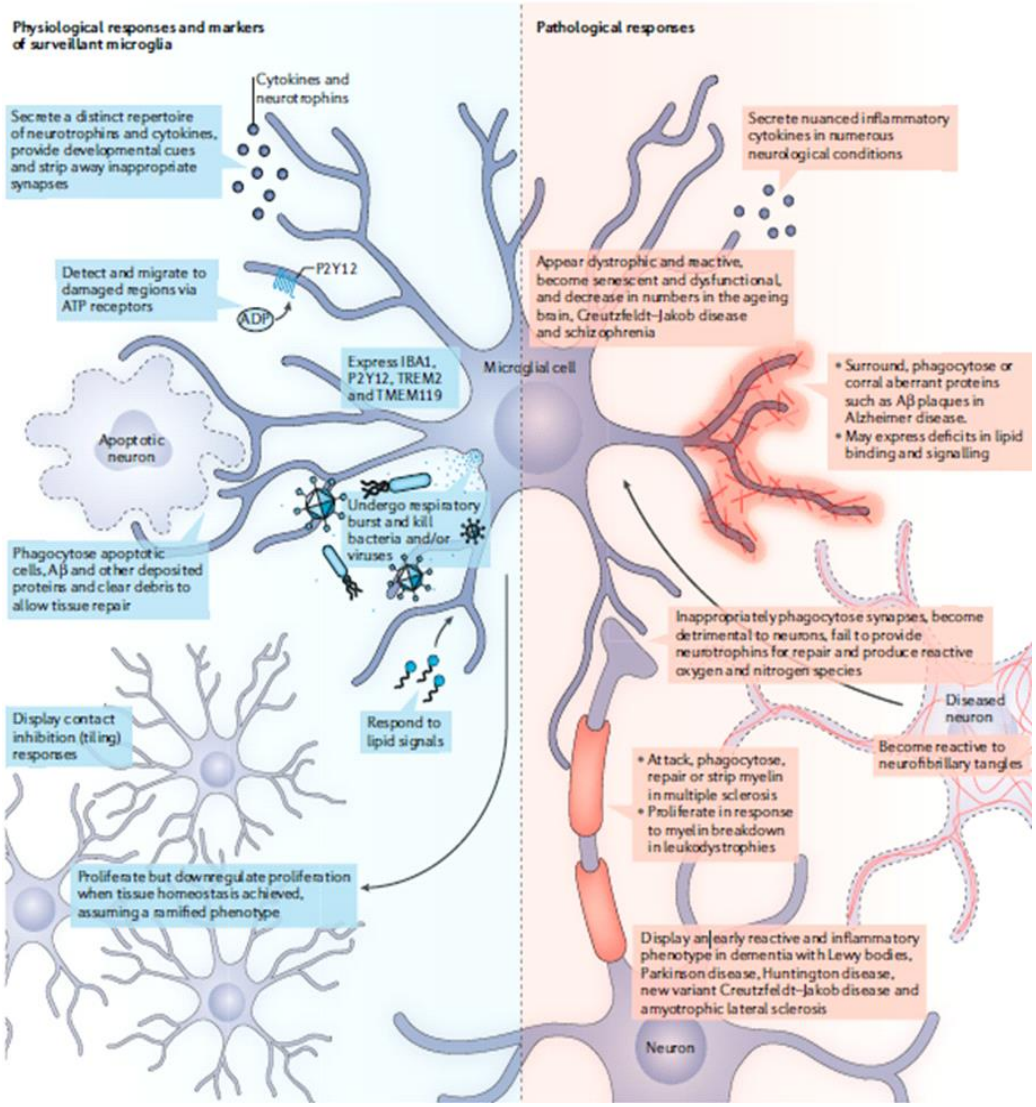

Figure 1-1 Schematic representation describing a few of many roles of microglia in health and disease. In the healthy brain, microglia regulate cell death by phagocytosis of apoptotic cells, they are involved in synaptic pruning and plasticity through the elimination of inactive synapses and promoting neurogenesis, they provide constant surveillance for the microenvironment for any damaging agent including released products from cells (such as adenosine triphosphate (ATP) via P2X and P2Y receptors) or a pathogen invasion (viruses or bacteria). Microglial migratory and phagocytic properties aid in maintaining tissue homeostasis by neutralising such insults. Aberrant functions of microglia or their overactivation are highlighted in neurological disorders. For example, malfunctions in the triggering receptor expressed on myeloid cells 2 (TREM2) pathway in microglia is associated with Alzheimer's disease (AD). Moreover, in multiple sclerosis (MS), a loss of myelin sheath is often associated with dysfunction of microglial phagocytic properties. Microglial overactivation is also observed in patients with Huntington's disease (HD) and amyotrophic lateral sclerosis (ALS). Adapted from (Pocock and Piers, 2018). IBA1, ionized Calcium-binding adapter molecule 1

1.2.1.1 Microglial development

Epigenetics and RNA sequencing studies have categorised microglia in terms of development into early (E10.5-E12.5), pre-microglia (E14-P9) and adult microglia (more than a few weeks postnatal) as summarised in Figure 1-2 (Salter and Stevens, 2017, Matcovitch-Natan et al., 2016b).

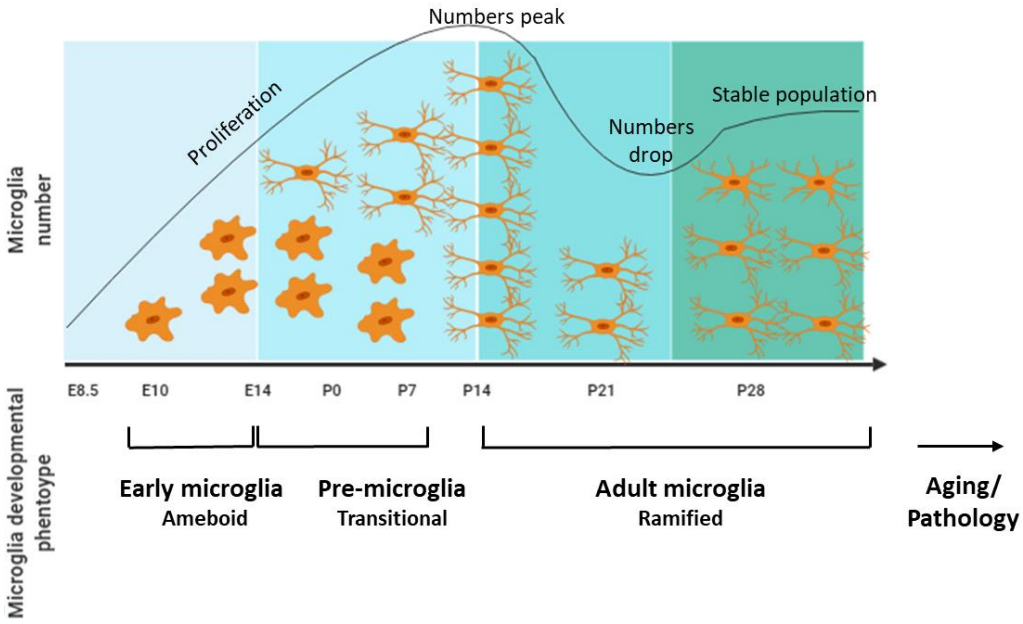

Figure 1-2 Rodent Microglia during brain development. Microglial development from progenitors derived from the yolk sac occurs at early embryonic stages. Early microglia acquire an ameboid morphology and proliferate from E8.5-E14. Pre-microglia then continues to proliferate until they peak in numbers at post (P) natal day 14 (P14). During adulthood, numbers of microglia decrease significantly either due to cell death or migration from region to region and they increase again to reach a stable population number (P14-P28). Microglial numbers and morphology are altered during ageing or pathological conditions.

As shown in the figure above, microglia undergo different morphological changes during development. During earlier developmental

stages, microglia acquire an amoeboid phenotype, a characteristic morphology of activated microglia. This acquired morphology by developmental microglia is crucial for synaptic pruning and efficient removal of redundant synapses and dead cells (Michell-Robinson et al., 2015). On the other hand, adult microglia have a distinctive ramified morphology. Extending and moving their processes facilitate continuous surveillance of immune challenges and neurons' health-state (Hammond et al., 2019, Rossi and Lewis, 2018, Lenz and Nelson, 2018).

1.2.1.2 Activators of Microglia

Different inflammatory stimuli, either exogenous or endogenous, stimulate the immune system to achieve homeostasis. Exogenous stimuli are often termed pathogen-associated molecular patterns (PAMPs) that include pathogen-derived molecules (Kigerl et al., 2014). Endogenous stimuli, on the other hand, are self-produced and are known as damage-associated molecular patterns (DAMPs) or alarmins (Kigerl et al., 2014). DAMPs are released by necrotic cells or damaged tissues (Venegas and Heneka, 2017). As mentioned earlier, resting microglia are neuroprotective, however, when activated by PAMPs or DAMPs they produce inflammatory mediators that could be challenging to tissues if such activation is not resolved (Streit et al., 2004b, Lucas et al., 2006). Microglial activation is defined by alteration in microglial cell morphology, gene expression and function (Cho et al., 2019).

Specific receptors initiate signalling cascades upon their binding their particular PAMPs or DAMPs. Such receptors are known as pattern recognition receptors (PRRs) (Kigerl et al., 2014). For instance, the most studied bacterial-derived PAMP is lipopolysaccharide (LPS), a component of the Gram-negative cell wall. It binds to toll-like receptor (TLR)- 4, a type of PRR. The binding of LPS to TLR-4 activates microglia (Akira et al., 2006, Kielian, 2006). In order to maintain the intracellular environment, stressed or necrotic cells produce cytosolic or nuclear peptides, DAMPs. Chromatin-associated high mobility group box 1 (HMGB1), Interleukin (IL)-1 family members, histones and S100 family of calcium-binding proteins are all examples of DAMPs (Bianchi, 2007). In addition to peptides, cells are also capable of orchestrating inflammatory signalling pathways through encountering non-protein molecules such as ATP, DNA or RNA (Zhang et al., 2013). Here, we focus on the signalling pathways involved in LPS and ATP stimulation of microglia.

1.2.1.3 LPS and Microglia

LPS presence is essential for bacterial survival (Li et al., 2012). LPS can be liberated in small amounts during the pathogen's cell division and during the destruction of bacteria by antibiotic treatment (Kirikae et al., 1998, Zhang et al., 1998). LPS can be toxic when produced in large amounts thus is referred to as an endotoxin (Rietschel et al., 1994, Caroff et al., 2002, Qin et al., 2008, Hines et al., 2013). It is recognised by PRRs as a PAMP, therefore triggering an immune response (Kigerl et al., 2014).

LPS binding proteins (LBPs) found in the blood transfer LPS to CD14, the latter is either expressed on cell surfaces of phagocytes or in a soluble form (Fenton and Golenbock, 1998, Triantafilou and Triantafilou, 2002, Akira et al., 2006). Myeloid Differentiation factor 2 (MD-2) is co-expressed with TLR-4 and is found in association with its extracellular domain. MD-2 initiates TLR-4 downstream signalling cascade after receiving LPS from CD-14 (Dobrovolskaia and Vogel, 2002). TLR-4 is expressed by microglia; hence, their activation occurs upon binding of LPS to TLR-4. Despite the importance of TLR-4 expression in eliciting an immune response, TLR-4-independent activation of microglia has been reported at high doses of LPS (Kielian, 2006). Once LPS associates with TLR-4, recruitment of the adapter protein Myd88 initiates a cascading event that leads to the translocation of necrosis factor (NF)-κB from the cytoplasm to the nucleus. The signalling pathway results in activating the expression of inflammatory mediators such as cytokines (e.g. IL-1β, tumour necrosis factor [TNF-]-α, IL-6) and chemokines (e.g. C-X-C motif chemokine ligand 1 [CXCL1]) (Barger et al., 2005, Brambilla et al., 2005, Chhor et al., 2013).

In spite of the BBB's function as a protective shield against blood-borne molecules, this role can be jeopardised. High doses of LPS alter the permeability of the BBB; therefore disrupting its integrity which makes it permeable and leaky to certain molecules (Banks et al., 2015). Moreover, certain areas of the BBB are susceptible to LPS-induced loss of integrity (Banks et al., 2015). Previous studies confirm that LPS binding is restricted

to microglia and not neurons in the cortex. Such confirmation was achieved by fluorescently labelled LPS assays. Microglia activation due to the presence of LPS can, therefore, result in neuronal toxicity and death (Dutta et al., 2008, Lehnardt, 2010). Moreover, LPS potentially contributes to neurodegeneration by altering BBB permeability. Jaeger et al., (2009) reported that radiolabelled amyloid β (Aβ) peptides injected intravenously were transported from the blood to brain across the BBB when mice were subjected to multiple doses of LPS. The aggregation of Aβ is a hallmark of Alzheimer's disease (AD). Dysregulation of transport and accumulation of these peptides in the brain triggers chronic neuroinflammation and potentiates AD (Jaeger et al., 2009).

1.2.1.4 ATP and Microglia

Purinergic receptors are activated by purines (ADP, ATP) or pyrimidines (UTP, UDP). They are divided into two families: the P2X family (ligand-gated ion channels) and P2Y family (G-coupled receptors) (Inoue, 2002). Functional P2X receptors are expressed in microglia including P2X4 and P2X7. Moreover, microglia express multiple P2Y receptors like P2Y2, P2Y4, P2Y6, P2Y12 and P2Y14 (Koizumi et al., 2013). As mentioned earlier, microglia respond to apoptotic cells to either induce apoptosis through reactive oxygen species bursts or phagocytosis of remnant debris (Arcuri et al., 2017, Lull and Block, 2010). Following trauma, ATP is released by

apoptotic or damaged cells, hence increased extracellular levels of ATP induce neuroinflammation and microglial activation (Bernier, 2012).

Increased Interleukin-1β (IL-1β) production is a characteristic of several CNS pathologies. Inflammasomes are necessary for cytokine processing (Gross et al., 2011). Inflammasomes are multimeric complexes that assemble in the cytosol in response to physiological (DAMPs) or pathogenic stimuli (PAMPs). Although inflammasomes differ depending on the type of stimulus, they generally form a platform to recruit the in-active pro-caspase-1. The conversion of pro-caspase-1 to active caspase-1 is initiated by the oligomerisation of pro-caspase-1 that induces the autoproteolytic cleavage from pro to caspase-1. A proteolytic reaction involving the cleavage of Immature IL-1β by caspase-1 to release mature IL-1β is facilitated by NOD-like receptor proteins (NLRPs) present in inflammasomes (Guo et al., 2015). High levels of ATP (500 μM-1 mM) have been shown to activate NLRP2 inflammasome and subsequently caused IL-1β release in human astrocytes through the purinergic receptor P2X7 and pannexin-1 (Panx-1) channel (Minkiewicz et al., 2013). Lower doses of ATP, however, activate P2X4R, a purinergic receptor also involved in the regulation of inflammasomes (North and Surprenant, 2000). P2X4R responds to ATP by increasing potassium efflux, thus increasing extracellular ATP levels due to the opening of Panx-1. Increased extracellular ATP levels result in the activation of P2X7R that eventually leads to the activation of inflammasomes (Bernier, 2012).

Trang and colleagues, (2009) showed that microglial expression and release of brain-derived neurotrophic factor (BDNF) is mediated by ATP-activation of P2X4R. Although BDNF is an important signalling molecule between microglia and neurons, it has been found to be associated with neuropathic pain (Trang et al., 2009).

1.2.1.5 Microglia and neuropathic pain

Neuropathic pain is a chronic pathological state of pain caused by nerve injury during infections, trauma, cancer, autoimmune diseases, and diabetes. Patients become more sensitive to noxious (hyperalgesia) and non-noxious (tactile allodynia) stimuli (Zhuo et al., 2011). The pain transmission pathway starts from the dorsal root ganglion (DRG) to the spinal dorsal horn, thalamus, and cortex (Tsuda, 2016). Microglia and astrocytes seem to play their parts in neuropathic/inflammatory pain progression and pathology (Zhuo et al., 2011).

Under physiological conditions, BDNF is released by microglia and astrocytes to promote neuronal growth and survival (Miwa et al., 1997). Lai and colleagues, (2018) showed promising anti-inflammatory effects of BDNF in glial cells communication during induced neuroinflammation. For instance, recombinant BDNF attenuated LPS-induced cyclooxygenase-2 (COX2) protein expression in microglia in a concentration-dependent manner. Interestingly, treating microglia with astrocytes conditioned media down-

regulated LPS-induced COX-2 protein and up-regulated BDNF protein expression in microglia (Lai et al., 2018). Nevertheless, BDNF release has been associated with neuropathic pain in peripheral nerve injury (PNI) models (Coull et al., 2005, Ulmann et al., 2008). Microglial release of BDNF is induced by ATP-activation of P2X4R (Trang et al., 2009) and it has been shown that extracellular ATP abundance due to mechanical stimuli enhances the excitability of nociceptive nerve fibres (Irnich et al., 2002). Moreover, spinal cord microglial activation has been observed in models of neuropathic pain. In a rat model of, chronic constriction injury of the sciatic nerve (CCI), blocking of P2X4R through intrathecal administration of an antagonist (Tricarbonyldichlorrutheniem II dimer [CORM-2]) reduced thermal and mechanical hypersensitivity (Jurga et al., 2017). Moreover, inhibiting P2X4R restored cytokines physiological levels and reduced glial cells activation marked by decreased glial fibrillary acidic protein (GFAP) and Iba-1 levels in the spinal cord and DRG (Jurga et al., 2017). Similarly, interfering with P2X4R with a selective antagonist (NP-1815-PX) in a mouse model of viral-induced pain resulted in diminished allodynia (Matsumura et al., 2016). ATP-mediated synthesis of BDNF through P2X4R in microglia signalling pathway is illustrated in Figure 1-3. Decoding the mystery behind microglial activation and their contribution to neuropathic pain Is important for developing targeted therapies.

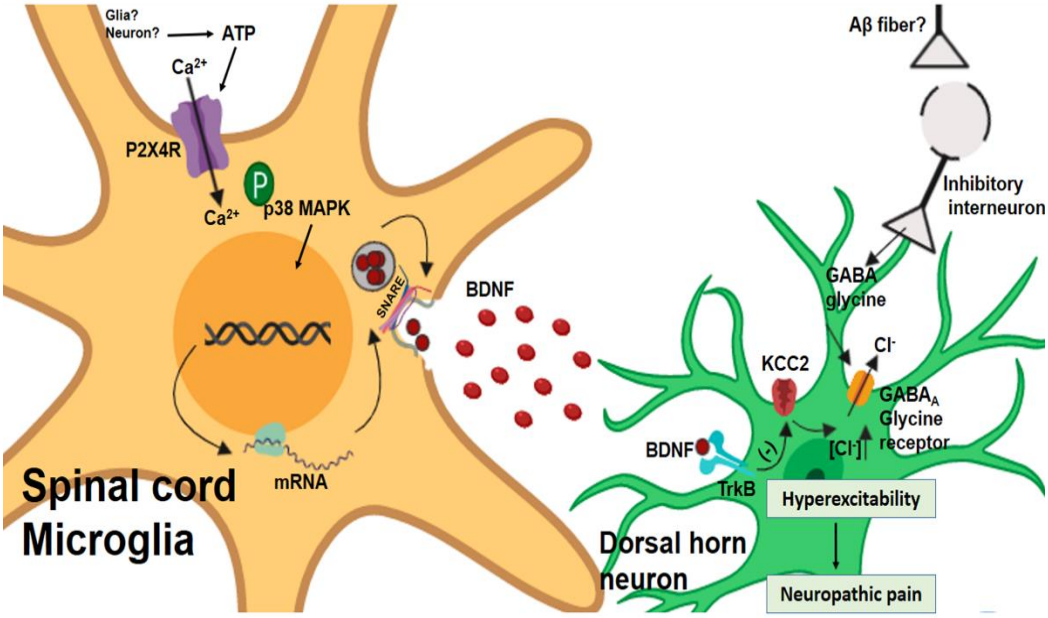

Figure 1-3 **Schematic representation of neuropathic pain induced by ATP-stimulated P2X4R and BDNF release from spinal cord microglia.** Extracellular ATP produced by glia or neurons activates P2X4R on microglia resulting in an increase in calcium (Ca^{2+}) influx. Increased intracellular calcium activates p38 MAPK leading to upregulation in BDNF expression. BDNF synthesis and release is mediated by SNARE. Downregulation of the potassium chloride transporter (KCC2) is driven by the binding of BDNF to its receptor tropomyosin-related kinase B (TrkB) on dorsal horn neuron. Intracellular chloride levels increase leads to dorsal horn neuron depolarisation due to a collapsed transmembrane anion gradient especially after stimulation of the γ-aminobutyric acid (GABA) and glycine receptor possibly in response to Aβ fibre stimulation. Thus, hyperexcitability could lead to neuropathic pain. Modified from (Trang et al., 2009, Tsuda, 2016).

1.2.1.6 Cytokines and Microglia

Measuring cytokine levels is a way to evaluate the activated phenotype of microglia as opposed to its physiological resting state (Li et al.,

2003). Cytokines are secreted polypeptides (8-26 kDa) that have significant roles in cell survival by promoting growth, differentiation, and activation of immune cells (Zhao and Schwartz, 1998, Hanisch, 2002). Cytokines are characterised as pro-inflammatory or anti-inflammatory based on their functions (Smith et al., 2012). Depending on the stimulus encountered or level of activation, microglia can be harmful or beneficial to tissues. While activated microglia is crucial for the healing process in the CNS post an insult or an injury, exacerbated production of pro-inflammatory mediators by persistently activated microglia could lead to CNS pathologies like neuropathic pain, hypoxia, AD, MS and other diseases (Lull and Block, 2010).

Classically activated microglia, M1, defend against pathogenic infections or tissue insults via their release of pro-inflammatory cytokines such as IL-1, TNF-α, Interferon (IFN)- γ and reactive oxygen species (free radicals). On the other hand, during alternative activation, M2, microglia promote angiogenesis, tissue healing, and repair through producing anti-inflammatory cytokines including IL-10, IL-4, IL-13 and tumour growth factor (TGF)- β (Wang et al., 2015).

1.2.1.7 Chemokines and Microglia

Chemokines are small secreted molecules belonging to the cytokine family. As their name implies, they attract responsive cells via chemical signals in a process known as chemotaxis. They can be either homeostatic or inflammatory depending on their biological activity. During inflammation,

chemokines recruit innate and adaptive immune cells to the site of damage. (Ramesh et al., 2013).

Microglia-neuron communication is facilitated by fractalkine (FKN) and its receptor (CX3CR1). FKN is a chemokine released by neurons under physiological conditions (Paolicelli et al., 2014) to promote microglial migration (Maciejewski-Lenoir et al., 1999). Figure 1-4 summarises the FKN signalling pathway between neurons and microglia.

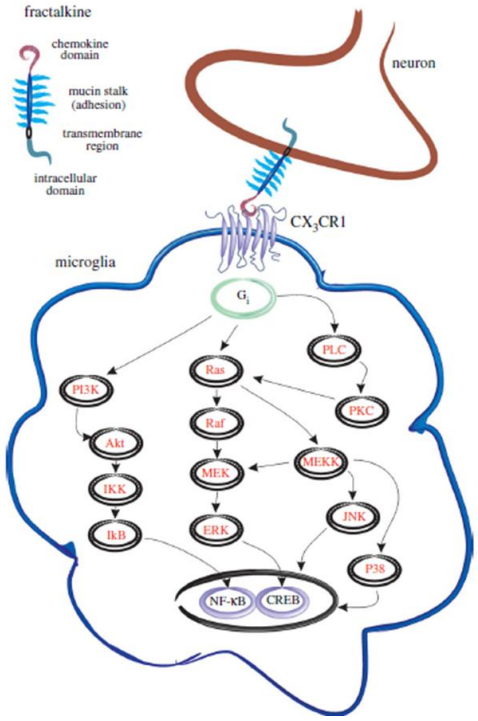

Figure 1-4 Schematic representation of FKN and CX3CR1 signalling pathways. Fractalkine consists mainly of four functional regions. Firstly the N-terminal chemokine domain is susceptible to cleavage by metalloproteinases or lysosomal cysteine protease including ADAM10, TACE or Cathepsin S, respectively. Secondly, the mucin stalk involved in cell adhesion especially towards migrating leukocytes during inflammation. Thirdly, it possesses a hydrophobic transmembrane region and finally, an intracellular C-terminal domain. Several transcription factors (e.g. NF-kB, nuclear factor kappa B; CREB, cAMP response element-binding protein) can be activated when the membrane-bound or the soluble form of fractalkine bind to its receptor CX3CR1. The latter is a G-protein coupled receptor. Gi, heterotrimeric G protein-coupled to Gi protein; PI3K, phosphatidylinositide 3-kinases; Akt, serine/threonine-specific protein kinase; IKK, an inhibitor of kappa B kinase; IkB, inhibitor of kappa B; Ras, small GTPase; Raf, small GTPase; MEK, mitogen-activated protein kinase; ERK, extracellular signal-regulated kinases; PLC, phospholipase C; PKC, protein kinase C; MEKK, MAP3kinase; JNK, c-Jun N-terminal kinase; p38, p38 mitogen-activated protein kinase. Taken from (Sheridan and Murphy, 2013).

Although FKN shows potential anti-inflammatory properties in attenuating LPS-induced TNF-α release from microglia (Zujovic et al., 2000), the cross-talk between neurons and microglia through FKN/CX3CR1 signalling, respectively, could be a player in several CNS-linked pathologies. Intrathecal injection of the soluble form of FKN resulted in neuropathic pain manifested by mechanical allodynia and hyperalgesia (Milligan et al., 2004). Microglia play an essential role in maintaining neuropathic pain through their expression of the cysteine protease Cathepsin S, a proteolytic enzyme responsible for releasing the soluble form of FKN (Clark et al., 2007).

LPS and neurotropic virus stimulation of microglia result in their release of a number of chemokines CCL3, CCL4, CCL5, CXCL8 and CXCL10 (Kielian, 2004). Anti-inflammatory cytokines like IL-10 and TGF-β attenuate the microglial release of CCL5 (RANTES) (Hu et al., 1999) and CXCL8 (IL-8) (Ehrlich et al., 1998).

1.2.1.8 M1/M2 paradigm

The oversimplified M1/M2 nomenclature can create more harm than good by missing the opportunity to study the different subtypes of microglia and their possible differential functions and responses during health and disease. Those terms were derived from macrophage-activating T-lymphocyte clones that produce IFN-γ and IL-2 (Th1) in contrast with Th2 lymphocytes that release IL-4, IL-5 and IL-10 to inhibit macrophage activation (O'Garra and Murphy, 1994). Mills and colleagues, (2000)

proposed the terms M1 and M2 for peripheral macrophages based on their studies on a Th1-strain (C57BL/6 mice) in comparison to Th2-strain mice (BALB/c) and the association of M1 macrophages with NO production (Mills et al., 2000). Importantly, despite the similarities between peripheral macrophages and microglia, several differences were reported as mentioned earlier; thus the classification of microglia as proinflammatory (M1) or anti-inflammatory (M2) needs to be addressed. Furthermore, a refined microglial terminology is necessary that considers microglial regional (Li et al., 2016b) and developmental (Hammond et al., 2019) heterogeneity, sexual dimorphism (Villa et al., 2018), proteomic and transcriptomic profiles (Grabert et al., 2016, Matcovitch-Natan et al., 2016b) and their differential responses to activating stimuli .

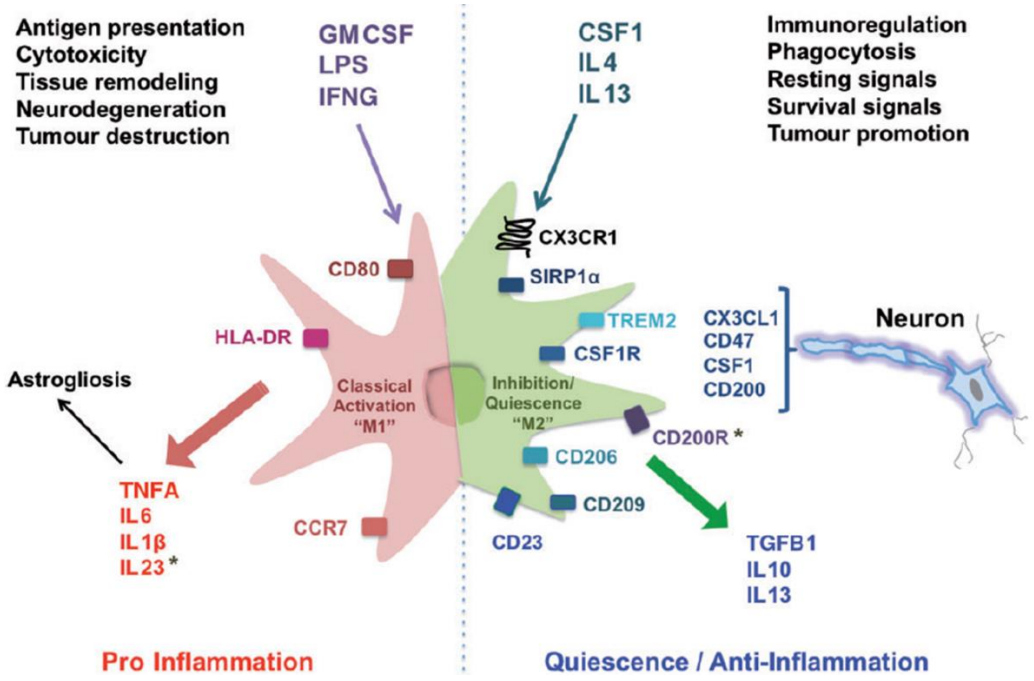

Figure 1-5 M1 and M2 polarization in microglia. Microglia respond differently depending on the stimulus and can acquire an M1 or M2 phenotype. Triggering microglia with pro-inflammatory stimuli (e.g. LPS, granulocyte-macrophage colony-stimulating factor [GM-CSF2], interferon [IFN]) up-regulates surface markers (CD80, CCR7) and inflammatory mediators. Classically activated microglia, release pro-inflammatory cytokines including IL-1β, TNF-α, IL-23 and IL-6 that cause further activation of astrocytes that in turn recruit immune cells to maintain tissue homeostasis. Microglia respond to anti-inflammatory molecules such as CSF1, IL-4, and IL-13 to initiate the process of tissue repair, and produce neurotrophic factors that improve neuronal survival. M2 microglia upregulate the expression of various Fc receptors (like CD23), c-type lectins (CD206 and CD209), and the release of IL-10, IL-13 and TGF-β1. M2 microglia can achieve homeostasis in the brain through interacting with neurons and astrocytes; such interaction is facilitated by fractalkine, CD47, CSF1 and CD200. Taken from (Michell-Robinson et al., 2015).

1.2.1.9 Microglial heterogeneity

Microglia respond to insults or ageing by proliferating, changing their morphology, migrating to the site of damage, phagocytosing debris or dead cells and producing cytokines and chemokines that in turn activate microglia and other immune cells to sustain tissue homeostasis. Yet, recent studies have been focusing on understanding the enigma surrounding microglial M1/M2 polarisation.

In the developing brain, maturation of microglia is dependent on signals produced by neurons (Wu et al., 2018). Perhaps that is why microglia have different gene transcription profiles, morphologies, and cell numbers during different developmental stages (Lenz and Nelson, 2018). In addition, due to the fact that their functions are region-specific, changes in the distribution and morphology occur as the brain is developing. Hammond and colleagues, (2019) identified subsets of microglia based on single-cell sequencing of mouse microglia. They observed a more diverse population of microglia during embryogenesis and early development that becomes more homogeneous during adulthood. Nonetheless, during ageing or pathological conditions, microglia become heterogeneous. Interestingly, early embryonic and postnatal microglia have shown to overexpress genes associated with regulating the metabolic activity, cell growth and cell proliferation. Notably, the TGF-β signalling pathway drives microglial differentiation and interfering with this pathway alters gene expression profiles in microglia (Hammond et al., 2019).

Microglial heterogeneity has also been observed in CNS disorders. Current neuropathological therapies focus on the pharmacological modulation of microglial activation; however, understanding microglial heterogeneity can enhance drug efficacy. For instance, in a rat model of neuropathic pain, spinal cord microglia showed differential responses to minocycline than prefrontal cortex microglia. Despite the low efficacy of minocycline, administering the drug before or after SNI induction resulted in attenuating spinal cord microglia activation demonstrated by dampening of pro-inflammatory markers while the same effect was not shown in brain microglia. Moreover, in pain-induced animals, prefrontal cortex microglia showed less anti-inflammatory biomarker expression ($CD172a^{+}$) and adopted an M1 polarised phenotype, whereas, under physiological conditions, spinal cord microglia state was more M1 skewed than brain microglia. This suggests that spinal cord and cortical microglia may have region-specific immune properties under both physiological and pathological conditions (Li et al., 2016b).

Moreover, transcriptional studies of adult rodent brain showed that microglia residing in the cerebellum exert a more robust immune response, as opposed to hippocampal, striatal and cortical microglia, suggested by the increased expression of genes responsible for bacterial or viral recognition, genes involved in Interferon pathway and genes involved in major histocompatibility complex- (MHC-) I and II pathways (Grabert et al., 2016). Although microglial metabolism and immunological functions are region-

specific, during ageing, immune-related genes are sensitive while metabolic genes are not affected. For instance, Immune-related genes are upregulated during ageing in the cerebellum. Some gene expression networks are preserved in ageing microglia perhaps due to their functional importance while others can be altered (Grabert et al., 2016). Microglial regional heterogeneity is also observed in human brain samples from AD patients in which different morphological subclasses of microglia occur at a result of ageing and pathology. It has been shown that M1/M2 phenotypes of microglia are acquired differentially during the progression of AD (Bachstetter et al., 2015). Bottcher and colleagues (2019) confirmed human microglial heterogeneity on a single-cell level using a multiplexed mass cytometry (CyTOF) deep profiling. They reported the detection of higher expression of microglial activation markers (e.g. CD68, CD86, CD45, CD11c, CD64, CX3CR1) in the subventricular zone and thalamus in comparison to the cerebellum, temporal lobe and frontal lobe. Furthermore, subpopulations of human microglia in the temporal and frontal lobe showed lower expression of mannose receptor 206, an anti-inflammatory marker of microglia/macrophages (Bottcher et al., 2019).

Not only do microglia show regional, morphological and functional heterogeneity in health and disease but also sex differences in microglia gene expression (Gosselin et al., 2017) and function have been reported. For instance, male microglia show a more homogeneous transcriptional profile than female microglia. Altogether, male microglia acquire a more pro-

inflammatory polarised state than female microglia. Morphological observations indicate that male microglia are pro-inflammatory skewed in comparison to female microglia (Villa et al., 2018). These observations are confirmed by RNA-seq data obtained from adult mice suggesting that male microglia highly express genes associated with cytokine production and cell migration. Moreover, inducing permanent ischemia in mice resulted in a larger damaged area in males rather than females. Interestingly, transplanting adult male rats with male or female microglia did not affect the volume of the damaged area; however, the progression of damage was lower in mice transplanted with female microglia. This protective role could be maintained by adult female microglia because of estrogen priming at earlier developmental stages (Villa et al., 2018). Furthermore, intrathecal injection of ATP-stimulated neonatal male microglia induced mechanical allodynia in naive female and male rats. On the contrary, injection with female ATP-stimulated microglia didn't result in mechanical hypersensitivity in naïve female or male rats (Mapplebeck et al., 2018).

Microglia cell density and size increase upon traumatic spinal cord injury; however, microglial morphology and MHC-II expression differ in the grey matter than white matter (McKay et al., 2007). As mentioned earlier, aberrant phagocytic properties of microglia could contribute to MS due to demyelination. Microglia express type I-Interferon (IFN) differently between grey matter and white matter in non-inflamed samples. Additionally, genes associated with NF-kB pathway are expressed in white matter microglia

more than grey matter microglia under normal conditions. Inhibitors of the NF-kB signalling pathway are upregulated in white matter microglia (van der Poel et al., 2019).

In vitro studies of mice cortical microglia, identified a change in morphology and increase in microglia heterogeneity when microglia were kept in culture for long periods. They displayed an aged irresponsive phenotype upon day 16 *in vitro* in comparison to day 2 in culture (Caldeira et al., 2014).

1.2.1.10 Microglia and ageing

Studies reported that ageing microglia experience changes in their phagocytic activity leading to an immune-underprivileged CNS (Rawji et al., 2016). Another feature that is adapted by ageing microglia is their excessive production of pro-inflammatory factors and their decreased production of anti-inflammatory molecules (Rock et al., 2004, Dheen et al., 2007, Damani et al., 2011, Harry, 2013). Moreover, it has been reported that LPS stimulation of aged microglia augments their pro-inflammatory mediator gene expression (Nikodemova et al., 2016). Studies also described an increase in MHCII expression on microglia during ageing, a phenotype associated with activated microglia relating to their antigen presentation features. Streit and colleagues (2004) stated changes in human microglia with respect to cytoplasmic structures in ageing brains. They demonstrated that microglia undergo senescence with age (Streit et al., 2004b).

One way of cells to change their phenotype from young to old is via loss of telomere ends that occur at the end of each cell cycle of DNA replication. Telomeres are the functional physical ends of eukaryotic linear chromosomes (Olovnikov, 1996). Cells reach senescence when they are incapable of replicating due to shortening of telomeres, thus experiencing altered gene expression and functions. Isolated microglia from both young and old rats showed differences in telomeres lengths in which aged rat microglia possessed shorter telomeres than young rat microglia (Flanary et al., 2007).

Alteration of gene expression in ageing microglia shows an increase in M1 related cytokines in comparison to M2 cytokines in response to stimulating agents such as LPS (Ye and Johnson, 2001, Luo et al., 2010). Impaired microglial surveillance mechanism of the microenvironment is a consequence of ageing leading to loss of neurons. Not only do microglia experience differences in functions, but also structure and morphology.

Ageing microglia exert ramified and shorter structures than young microglia (Colonna and Butovsky, 2017). Studying structural and functional differences between young and ageing microglia can give some insight regarding the mechanisms involved in neurodegenerative diseases and chronic neuroinflammation-associated disorders.

1.2.1.11 Limitations of microglial cultures

In vitro studies have utilised microglial cell lines, stem cells-derived microglia (such as embryonic stem cells [ESCs] or induced pluripotent stem cells [iPSCs]) and primary dissociated microglia (Timmerman et al., 2018). Table 1-1 summarises the advantages and limitations of each *in vitro* microglial model. As most neurodegenerative diseases develop during ageing, studying adult microglia *ex vivo* would be more ideal than neonatal microglia due to their differences in surface marker expression, their physiological functions and phenotypes (Galatro et al., 2017). Recent studies provided valuable insight into the transcriptome profile of *ex vivo* microglia; however, culture conditions play an essential role in altering microglial gene expression *in vitro* (Bohlen et al., 2017).

Table 1-1 Overview of advantages and limitations of current *in vitro* microglia models

Model	Advantages	Limitations	Reference
Microglia cell-lines	Can be derived from mice, rats, non-human primates and humans.	Altered microglial gene expression, function and phenotype than *in vivo* microglia.	(Garcia-Mesa et al., 2017, Cheepsunthorn et al., 2001, Bohlen et al., 2017, Das et al., 2016)
	Easy to maintain. Highly abundant due to immortalisation thus increased proliferation.	Prone to dedifferentiation. Challenging for comparative	(Stansley et al., 2012, Timmerman et al., 2018)

		developmental studies (lines generated from neonatal or embryonic retain developmental phenotypes).	
Stem cell-derived microglia	Facilitate comparative studies between healthy donors and patients due to their retention of genetic background.	Reflect a fetal human mRNA expression profile. Lack of exposure to CNS micro-environment.	(Timmerman et al., 2018, Speicher et al., 2019)
Primary microglia	Can be isolated from mice, rats, non-human primates and humans. Can be derived from different develop-mental stages and transgenic rodents.	Variation in gene expression between rodents and human primary microglia. Scarce sources of healthy human donors.	(Galatro et al., 2017, Yip et al., 2009, Tamashiro et al., 2012, Rustenhoven et al., 2016) (Giulian and Baker, 1986, Butovsky et al., 2014, Weydt et al., 2004, Watkins and Hutchinson, 2014) (Mizee et al., 2017)

	Facilitate our understanding of pathogenesis by isolating microglia from human donors post-mortem.	Post-mortem delay effect on microglial phenotypes and gene expression.

1.2.2 Astrocytes

As mentioned earlier, astrocytes are the most predominant glial cells and are found in the brain and spinal cord. Their feet processes are in close association with endothelial cells and pericytes, and due to that intimate contact, they regulate the functions of the BBB (Matias et al., 2019). Similar to microglia, astrocytes' physiological functions vary during development (illustrated in Figure 1-6). In spite of astrocytes' essential regulatory functions, their role extends beyond sustaining metabolic support for neuronal networks and maintaining homeostasis in the CNS. Therefore, aberrant astrocytes' functions have a negative impact on the CNS (Sofroniew and Vinters, 2010).

Astrocytes form a heterogeneous cell population that is comprised of two major subtypes, protoplasmic and fibrous astrocytes (Miller and Raff, 1984). They are classified based on morphological (Miller and Raff, 1984), structural (Oberheim et al., 2009), functional and distributional differences

(Oberheim et al., 2012). Protoplasmic astrocytes are mainly distributed in the brain's grey matter. Their cell processes are finely branched. On the other hand, fibrous astrocytes have straight and long processes and are localised mainly in the white matter (Matias et al., 2019). Gap junctions not only connect fine processes of a single astrocyte but also connect neighbouring astrocytes, thus, facilitating communication. Astrocyte-astrocyte and astrocyte-neuron communication occur as a result of regulated Calcium (Ca^{2+}) influx-efflux In astrocytes that contributes to astrocyte excitability (Ding, 2014, Sofroniew and Vinters, 2010, Agulhon et al., 2008).

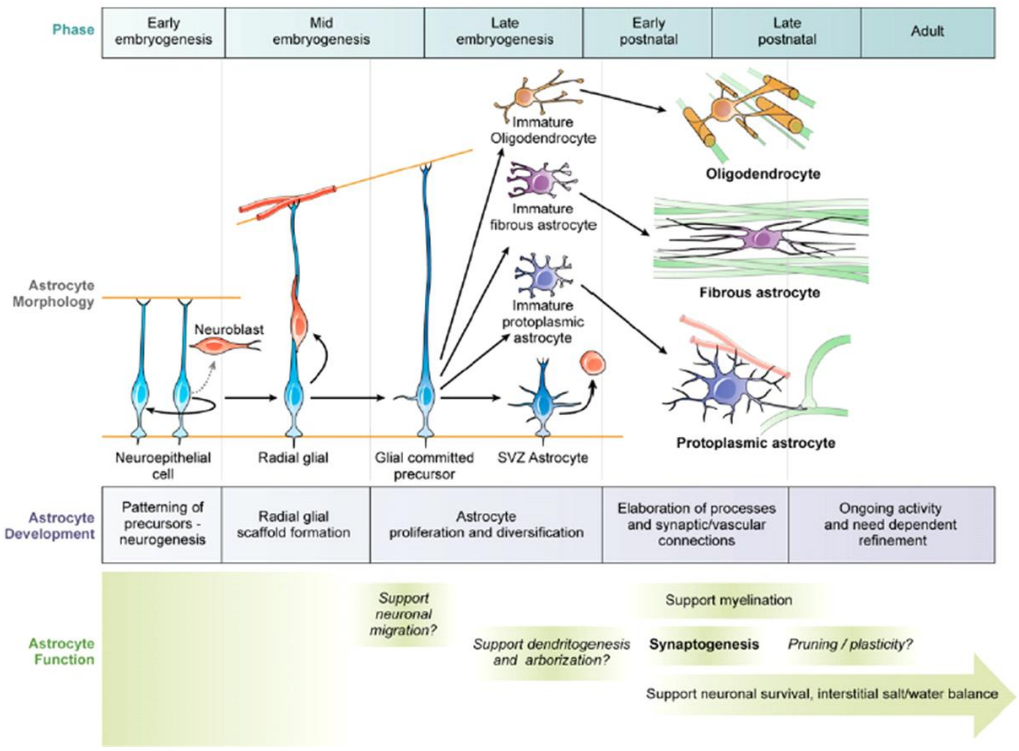

Figure 1-6 Morphological and functional changes in astrocytes during development. Radial glial cells and neuroblasts are derived from neuroepithelial cells; they then become glial-committed, generating proliferative precursors that differentiate into fibrous and protoplasmic astrocytes that further mature postnatally. Adult astrocytes maintain homeostasis and sustain neuronal survival. Taken from (Molofsky et al., 2012).

Recently, researchers have focused on the important role of astrocytes during health and disease. Astrocytes alter their phenotypes and gene expression profiles during neurodegenerative diseases, trauma, infection and ageing due to their reactive state (Rozovsky et al., 1998, Hidano et al., 2016, Liddelow et al., 2017a, Sofroniew and Vinters, 2010). An important biomarker of reactive astrocyte is the intermediate filament protein, GFAP. Immunohistochemical studies of reactive astrocytes *in vivo*

showed differences in GFAP immunoreactivity. Moreover, GFAP expression is higher in fibrous than protoplasmic astrocytes (Shehab et al., 1990, Tabata, 2015). Nonetheless, finding alternative markers that give a better description of reactive astrocytes is important because GFAP expression is exhibited by most astrocytes. In addition, astrocyte heterogeneity in expressing GFAP makes interpreting research outcomes very challenging.

Two candidate biomarkers are up-regulated in reactive astrocytes following either LPS stimulation or induced ischemia; the acute phase protein lipocalin-2, *Lcn2* and the serine protease inhibitor, *Serpina3n*. Moreover, genetic profiling of reactive astrocytes showed that astrocytes could either acquire a pro-inflammatory phenotype (A1) following systemic LPS stimulation or an anti-inflammatory (A2) phenotype after induced ischemia (Zamanian et al., 2012). A1 astrocytes are believed to be neurotoxic while A2 astrocytes show potential neuroprotective effects (Liddelow et al., 2017a).

Recent studies highlighted the importance of microglial-astrocyte crosstalk during physiological and pathological conditions, hence studying their molecular communication can provide better identification of the various stimuli that regulate the switch from a neuroprotective role to a neurotoxic one (Liddelow and Barres, 2017, Jha et al., 2019).

1.2.3 Glia-neuron crosstalk

Communication is key between neurons and glial cells. For instance, FKN expression and release have been associated only with neurons and astrocytes but not microglia. Despite that, microglia highly express the receptor for FKN (CX3CR1) in the brain, suggesting an essential role for this chemokine to mediate glial-neuron interaction (Sheridan and Murphy, 2013). Stimulating primary microglia with FKN *in vitro* enhanced their survival and metabolic activities (Boehme et al., 2000). Conversely, ablation of CX3CR1 in microglia induced neurotoxicity in a model of LPS-induced neuroinflammation (Cardona et al., 2006).

Neurons can also communicate with glial cells through metabolic crosstalk, as observed during development. Synaptic activity is modulated through lactate production from cortical astrocytes after glutamate uptake (Voutsinos-Porche et al., 2003). Interaction between neurons and glial cells in health and disease is summarised in Figure 1-7.

Interestingly, not only secreted molecules affect the biology of glial cells and neurons but also emerging evidence showed that physical contact with neurons and astrocytes affect astrocytes morphogenesis and synaptogenesis through Neuroligin-2 (Stogsdill et al., 2017). Dysregulation of any glial-neuron communication can affect the homeostasis of the CNS. Alterations in gene expression have been reported in reactive astrocytes in response to microglia and other CNS cell populations (Sofroniew, 2009). Zamanian et al. (2012) suggested that LPS stimulation of glial cells can be

destructive to synapses through activating the classical complement pathway. Moreover, IL-10 has been identified as a critical player in microglia and astrocyte communication during inflammation (Zamanian et al., 2012). It is produced in a time-dependent manner in the event of LPS stimulation of microglia and astrocytes leading to decreasing pro-inflammatory cytokines' gene expression (Ledeboer et al., 2002). Intriguingly, IL-10 release by microglia stimulates the expression of TGF-β by astrocytes leading to attenuation of microglial activation (Norden et al., 2014). In contrast, activated microglia secrete IL-1α, TNF-α, and c1q upon LPS stimulation and induce neurotoxic A1 astrocytes (Liddelow et al., 2017a).

Molecular communication between microglia and astrocytes is summarised in Table 1-2 and Table 1-3. Although microglia-astrocyte communication is bidirectional, it is believed that microglial activation occurs earlier than reactive astrogliosis during pathologies. Evidently, pro-inflammatory mediators released by activated microglia drive astrocyte activation, however, the nature of such communication is highly variable and dependent upon the physiological state of the surrounding tissue, and its effect on either cell type's polarisation remains to be elucidated (Liu et al., 2011).

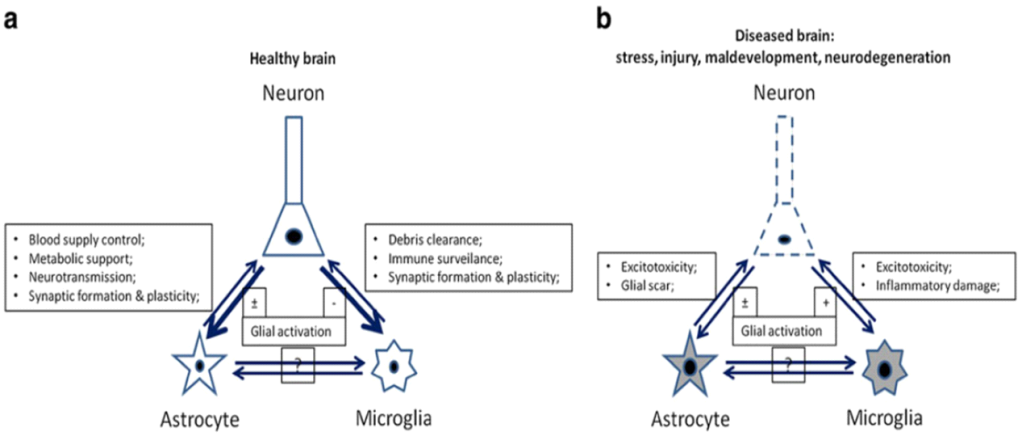

Figure 1-7 Simplified schematic representation of neuron-glia crosstalk in health and disease. (a) In the healthy CNS, molecular signalling between neurons and glial cells maintain physiological functions of glial cells and consequently promote neuronal survival. **(b)** Contrary under pathological or abnormal conditions neurons produce damage signals leading to microglia and astrocyte activation that often result in neurotoxicity. Taken from (Tian et al., 2012).

Table 1-2 Effects of molecules secreted from microglia on astrocytes. Nitric oxide (NO), complement component c1q (C1q), vascular endothelial growth factor B (VEGF-B). Modified from (Jha et al., 2019).

Microglial molecules	Effects on astrocytes	References
TNF- α	↑ NO and TNF- α production	(Chen et al., 2015)
NO	↑ NO and TNF- α production	(Iizumi et al., 2016)
Type I IFN (IFN α/β	↓ Chemokines expression (e.g CCL2)	(Finsen and Owens, 2011)
NADPH oxidase-derived H_2O_2	Regulates astrogliosis	(Hou et al., 2017)
IL-1 α, TNF- α, C1q	Induce A1 reactive astrocytes	(Liddelow et al., 2017)
TGF- α-, VEGF-B	Regulate the pathogenic activities of astrocytes in a mouse MS model.	(Rothhammer et al., 2018)

Table 1-3 Effects of molecules secreted from astrocytes on microglia. Orosomucoid 2 (ORM2), Lipocalin-2 (LCN2), Monocyte chemoattractant protein -1 (MCP-1), IFN-γ-induced protein 10 (IP-10), Plasminogen activator inhibitor-1 (PAI-1), Glial cell line-derived neurotrophic factor (GDNF), Pentraxin 3, (PTX3), Complement component (C3), microRNA-9 (miR-9). Modified from (Jha et al., 2019).

Astrocytic molecules	Effects on microglia	References
ORM2	Inhibits activation, pro-inflammatory cytokine release, and migration through blocking CCL4-CCR5 interaction	(Jo et al., 2017)
LCN2	Enhances microglial activity	(Kim et al., 2017, Jha et al., 2015)
MCP-1/CCL2	Promotes activation and motility	(Tanuma et al., 2006)
IP-10/CXCL10	Promotes migration and activation, and regulate phagocytosis	(Tanuma et al., 2006, Skripuletz et al., 2013)
TGF-β	Attenuates activation	(Norden et al., 2014)
PAI-1	Regulates migration and phagocytosis	(Jeon et al., 2012)
GDNF	Modulates microglial activation and phagocytosis	(Rocha et al., 2012)
PTX3	Inhibits phagocytosis of apoptotic cells	(Jeon et al., 2010)
C3	Regulate phagocytosis	(Lian et al., 2016)
Exosomal miR-9	Mediates migration in HIV-mediated neuropathogenesis	(Yang et al., 2018)

Altogether, microglial activation, astrogliosis and the recruitment of peripheral immune cells from the bloodstream are essential to maintain homeostasis; however, dysregulation in this intricate communication triggers deleterious events in the CNS causing exacerbated neuronal loss. Current anti-inflammatory drugs block microglial and astrocytes activation entirely.

Realistic approaches focusing on the M1/M2 or A1/A2 polarisation can be more neuroprotective. Thus, modulating the switch between a pro-inflammatory to an anti-inflammatory phenotype is promising in treating several CNS pathologies caused and maintained by glial cells activation.

1.3 Nuclear receptors

In humans, the family of nuclear receptors includes 48 members that have various roles in development, immunity, reproduction, and homeostasis (Sever and Glass, 2013, Saijo et al., 2013). They have the potential to positively or negatively regulate gene expression by acting as transcription factors (Saijo et al., 2009). This process is either induced by ligand binding or through signal detection (Saijo et al., 2013). Transcription can be repressed via the interaction of sequence-specific transcription factors and specific gene response elements. The communication between nuclear receptors and the inflammatory signalling pathways modulates innate and adaptive immunity (Huang and Glass, 2010).

Different nuclear receptors including glucocorticoid receptors (GRs) or peroxisome proliferator-activated receptors (PPARs) demonstrated anti-inflammatory properties by interfering with NF-κB and activator protein (AP) -1-driven gene transcription (Delerive et al., 1999, Ogawa et al., 2005, Pascual et al., 2005). In addition, the expression of several genes that participate in inflammatory events is downregulated upon binding of liver X

receptors (LXRs) to their ligands. Ligand-receptor crosstalk promotes SUMOlyation of LXRs by small ubiquitin-like modifier proteins (SUMOs). SUMOlayted receptors have been reported to interact with corepressor complexes, nuclear receptor corepressor (NCoR)/SMRT, to repress transcription of genes participating in pro-inflammatory signalling (Ghisletti et al., 2007). Orphan nuclear receptors show interesting roles in regulating cytokine expression and growth factors during inflammatory events that would often lead to neuropathology (McMorrow and Murphy, 2011).

1.3.1 Orphan Nuclear Receptors

The orphan nuclear receptor subfamily includes NR4A1 (Nur77), NR4A2 (Nurr1) and NR4A3 (NOR-1) (Murphy and Crean, 2015). No natural ligands, whether endogenous or exogenous, that modulate these receptors' activities have been identified as yet (Maxwell and Muscat, 2006), however, studies showed the possibility of pharmacologically activating these receptors by using 6-mercaptopurine (6-MP) (Huang et al., 2016) or Isoxazdo-pyridinone 7e (Montarolo et al., 2014). Due to their pivotal roles, they are expressed throughout the body including T-cells, skeletal muscles, cardiac tissues, adipose tissue, liver, brain, and kidney (Maxwell and Muscat, 2006).

All three NR4A receptors share a similar structure. They possess a ligand-independent domain (AF-1) that is located at the N-terminus. They

have a DNA binding domain (DBD) which contains two zinc fingers that facilitate the interaction with specific DNA segments. The structure of the DBD is highly conserved amongst the three receptors. Their structure is also composed of AF-2 transactivation ligand-binding domain at the C-terminus (Castro et al., 1999, Zhao et al., 2010). They can bind to response elements as monomers or homodimers. NR4A1 and NR4A2 can form heterodimers with 9-cis retinoic acid receptor (RXR), while NR4A3 cannot (Aarnisalo et al., 2002, Maxwell and Muscat, 2006). Pei et al. (2005) demonstrated the regulatory role of NR4As during inflammation proposing the possibility of their interaction with NF-κB. They showed that LPS induces NR4A expression in macrophages through the NF-κB pathway (Pei et al., 2005). Understanding the role that each member of NR4A subfamily plays during inflammation, particularly in neuroinflammation, is key to tailor therapeutic approaches that modulate microglial activation.

1.3.1.1 NR4A1/Nur77

Nur77 is expressed broadly in the CNS, more importantly, in microglia. A recent study reported that over-expression of Nur77 downregulated the expression of LPS-induced pro-inflammatory mediators. Nur77 interferes with both p38 mitogen-activated protein kinase (MAPK) and NF-κB signalling pathways, thus exerting a negative regulatory role and eventually prevent neurotoxicity caused by microglial overactivation (Liu et al., 2017).

The substance, 6-MP, structurally mimics endogenous purine bases (i.e. adenine, guanine and hypoxanthine) and is found to attenuate *TNF-α* expression in LPS-activated primary microglia *in vitro* in a dose-dependent manner. Knocking down Nur77 in BV2 microglia restored LPS-induced *TNF-α* expression. Importantly, 6-MP evidently inhibits NF-kB p65 subunit phosphorylation (Huang et al., 2016). Similarly, ablation of Nur77 in microglia affected the expression of several proteins participating in inflammatory signalling pathways with respect to LPS stimulation. Migratory, phagocytic and inflammatory microglial functions were affected by knocking down Nur77 (Chen et al., 2017). The accumulation of Aβ aggregates is one of the leading causes of chronic microglial activation that contributes to neurodegeneration and possibly, AD. A study explored the potential role of the endogenous anti-inflammatory mediators to alleviate the pro-inflammatory consequences of Aβ aggregates. Upon treating microglia with an agonist for EP4, a G-protein coupled receptor for prostaglandin-E2 (PGE2), Nur77 and Nurr1 expression increase significantly. While the accumulation of Aβ42 suppresses the expression of Nur77 and Nurr1, therefore, the study suggested that EP4 signalling can restore the suppressed expression of Nur77 and Nurr1 caused by Aβ42 (Woodling et al., 2014). Hanna et al. (2012) reported that macrophages isolated from Nur77 deficient mice showed altered expression of TLRs including TLR-4. They also elaborated that macrophages lacking Nur77 acquired an M1 phenotype and experienced increased phosphorylation of p65 subunit of NF-κB, which facilitates the expression of the latter (Hanna et al., 2012). In

addition to its anti-inflammatory roles, Nur77 is essential in promoting apoptosis especially during T cell maturation (Calnan et al., 1995). Moreover, Nur77 participates in the process of promoting tumorigenesis in various types of cancer (Lee et al., 2011). In conclusion, Nur77 plays a central role in cell differentiation, growth, and survival.

1.3.1.2 NR4A2/Nurr1

Similar to Nur77, Nurr1 has a protective role in preventing neurotoxicity by suppressing pro-inflammatory mediators produced by microglia and astrocytes, and it is possibly the most studied of all orphan nuclear receptors. Recent findings suggest that Nurr1 inhibits the amplification of the inflammatory signal as a result of microglia-astrocyte communication (Saijo et al., 2009). In a mouse model, the presence of Nurr1 appeared to be necessary for the survival of neonates; offsprings of Nurr1 deficient mice did not survive due to abnormal movement and suckling behaviour (Zetterström et al., 1997). Lallier et al., (2016) have shown that exposing neonatal mice to hyperoxia following maternal LPS treatment resulted in a significant increase in Nurr1 by microglia (Lallier et al., 2016).

Nurr1 suppresses microglial activation in response to TLR-4 stimulation. A mechanism of Nurr1 transrepression of NF-κB has also been proposed (illustrated in Figure 1-8). It involves the interference of Nurr1 with p65 subunit that communicates with the promoters of pro-inflammatory genes. Nurr1 binding to a corepressor complex enables the negative regulation of NF-κB transcriptional activity (Saijo et al., 2013). In astrocytes,

a compensatory upregulation in Nur77 or Nurr1 mRNA was observed when either of these receptors was knocked down, contrary to knocking down NOR-1 that showed no effect on the expression of neither Nurr1 nor Nur77 (Popichak et al., 2018). Intriguingly, in a rat model of Parkinson's disease (PD), transplantation of Nurr1-overexpressing microglia and ventral mesencephalic neural stem cells improved rotational behaviour in rats and induced dopaminergic neuron differentiation (Qian et al., 2019). Kinoshita and colleagues (2019) showed that the antimalarial drug amodiaquine Is a potential agonist for Nurr1. Glial cells activation and pro-inflammatory cytokines and chemokines expression were suppressed upon amodiaquine-induced Nurr1 increased expression in a mouse model of Induced intracerebral haemorrhage (Kinoshita et al., 2019).

1.3.1.3 NR4A3/NOR-1

The least studied of all NR4As is NOR-1. Inflammatory mediators such as LPS, IL-1β, and TNF –α induce its expression in endothelial cells. Induction of NOR-1 by TNF-α is NF-κB pathway-dependent. The process involves the recruitment of p65 subunit with respect to TNF-α stimulation (Zhao et al., 2010). In IL-4-induced M2 macrophages, knocking down NOR-1 significantly decreased the expression of M2 markers. Importantly, inducing M2 polarisation resulted in NOR1-induction only but not Nurr1 nor Nur77 (De Paoli et al., 2015).

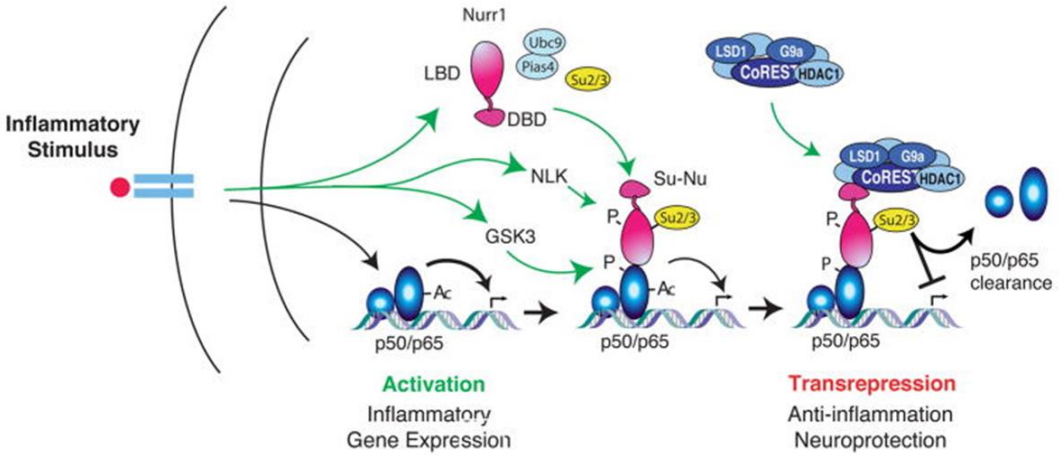

Figure 1-8 Inhibitory effect of Nurr1 in microglia and astrocytes concerning neurotoxic gene expression, a model of CoREST-mediated transrepression. GSK-3β phosphorylation of S468 of NF-kB p65 subunit recruits Nurr1 to pro-inflammatory gene promoters. The co-repressor complex, Co-REST is further recruited through serine-threonine protein kinase NLK. Histone-deacetylase 1 (HDAC1) is a component of the Co-REST complex, and it plays an essential role in regulating p65 transcriptional activity; thus Nurr1/Co-REST signalling is critical for inhibiting inflammatory responses through the clearance of p65 from pro-inflammatory mediators' promoters. Taken from (Saijo et al., 2009).

A key question is whether microglial polarisation is affected by development or is it a matter of regional heterogeneity. In this study, we investigated the activation state of cortical or spinal cord microglia in response to DAMPs and PAMPs during two stages of development (neonatal and adult). To assess the expression of orphan nuclear receptors and M1/M2 inflammatory markers in resting or activated adult and neonatal microglia, we adapted existing microglia isolation methods to generate pure,

non-activated primary microglia cultures. We used an *in vitro* model of disease and injury to induce microglial activation through stimulation with LPS and ATP, respectively. We aimed to create a physiologically relevant model of microglial activation rather than to induce cytotoxicity.

In chapter three, the main objective was to assess the effect of developmental microglial secretome on astrocytes in the event of LPS-induced microglial activation. As described earlier, Liddelow and colleagues reported that LPS-treated microglia release pro-inflammatory factors that induce a neurotoxic phenotype in astrocytes (Liddelow et al., 2017a). Surprisingly, our results suggest a neuroprotective role of activated microglia rather than a neurotoxic one.

Chapter four focuses on the other objective of this study which is to assess the effect of ATP stimulation on microglia activation. Previous reports suggested that neonatal microglia are activated by ATP through activation of the P2X4R. Moreover, this activation could lead to neuropathic pain in rats through intrathecal injection of ATP-stimulated microglia (Mapplebeck et al., 2018). Our findings indicate that both adult and neonatal microglia respond to ATP stimulation. Although neuropathic pain has been associated with BDNF release from ATP-stimulated neonatal microglia (Trang et al., 2009), our results suggest that only adult microglia release BDNF upon ATP stimulation.

To our knowledge, this study is the first to report differential orphan nuclear receptor expression in LPS or ATP-stimulated microglia during

development. These receptors are crucial in dampening inflammation through their anti-inflammatory roles as illustrated in Figure 1-9. Understanding the role that each member of NR4A subfamily plays during inflammation, particularly neuroinflammation, is critical to tailor therapeutic approaches that focus on modulating microglial polarisation.

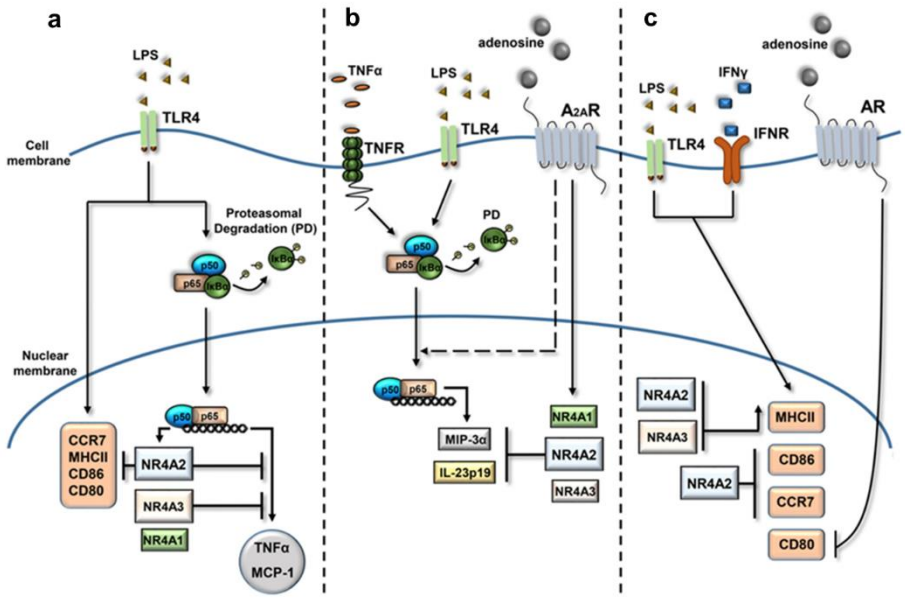

Figure 1-9 Orphan nuclear receptors regulate immunity; a) LPS-induces activation through TLR-4 activates NF-κB which in turn activate the expression of orphan nuclear receptors and inflammatory mediators such as TNF-α and monocyte-chemoattractant protein (MCP)-1. Expressions of biomarkers of classical activation including CCR7, major histocompatibility complex (MHC) –II, CD 86 and CD80 are increased upon TLR-4 activation. Decreased expression of orphan nuclear receptors results in increased pro-inflammatory mediators' expression. b) NF-κB expression can be induced by activating TNF-α receptor, TLR-4 by LPS and A2a receptor by adenosine. This activation results in increased expression of macrophage inflammatory protein (MIP)-3a and IL-23p19 in addition to orphan nuclear receptors. NR4A2 blocks the production of pro-inflammatory mediators in response to adenosine stimulation. c) IFN-γ induction of pro-inflammatory mediators and surface markers (CD86, CD80, CCR7 and MHC-II). NR4A2 inhibits the production of surface markers and inflammatory mediators. Adapted from (Crean et al., 2015).

2) Chapter two:

Materials and Methods

2.1 Animals

All animals were supplied by Charles River, UK. Animals were housed in a temperature-controlled room in individually ventilated cages (IVCs) following 12 hours dark-light cycle, where food and water were available *ad-libitum*. Adult male Sprague-Dawley rats at postnatal day 40 (P40) were used for microglia isolation and mixed-gender neonates (P0-2) were used for microglia or astrocytes isolation. Embryonic Sprague-Dawley rats at gestational day 18 (E18) were used for isolation of cortical neurons. All procedures were in accordance with UK Home Office regulations on operations of the Animals (Scientific Procedures) Act (ASPA) 1986. Adult rats were subjected to regulated procedures under license PP3DA999F. Neonatal rats were used under Animal Welfare and Ethical Review Body (AWERB) non-ASPA 000148 while embryonic rats were used under non-ASPA 000154.

2.1.1 Primary microglia culture isolated from adult rats

Four P40 male rats were anaesthetized with sodium pentobarbital intraperitoneally (i.p). Trans-cardiac perfusion via the left ventricle was performed using sterile 1x phosphate-buffered saline (PBS) supplemented with 2 units/ml heparin sodium (Wockhardt, UK) at a hydrostatic pressure of approximately 80 mmHg to wash out all contaminating blood cells from both brain and spinal cord. After 5 minutes of perfusion, or until the animal's internal organs are pale, the brains and spinal cords were aseptically

removed, submerged in sterile PBS and carefully dissected free of the meninges under a stereomicroscope. The brains and spinal cords were approximately cut into 500 µm thick sections using a sterile scalpel. Tissues were then transferred into 6 ml Hibernate A media (Gibco, Thermofisher Scientific) supplemented with 130U papain (Worthington biochemical corporation, USA). Tissues were subjected to gentle rotation at 37°C in a CO_2 incubator (Thermo, UK) for 15 minutes. Tissues were removed from the incubator and gentle trituration was applied by pipetting up and down, and then tissues were incubated again at 37°C for another 15 minutes. Tissue dissociation was terminated by adding an equal volume of DMEM, high glucose, GlutaMAX™ Supplement (Gibco, ThermoFisher Scientific) supplemented with 10% heat-inactivated fetal bovine serum (FBS) (Gibco, ThermoFisher Scientific) and 1% penicillin/streptomycin (Sigma-Aldrich, St Louis, MO, USA). The cell suspension was filtered by passing it through a 100µm cell strainer (Falcon, Corning) and then sieving the flow-through further using a 70µm strainer. The cell suspension was centrifuged at 397 x g for 5 minutes at room temperature. The supernatant was discarded and cells were re-suspended with DMEM, high glucose, GlutaMAX™ Supplement. Poly-D-lysine (PDL) (Sigma-Aldrich, St Louis, MO, USA) was used to coat T-75 flasks for one hour at 37 °C followed by washing twice with sterile high-performance liquid chromatography (HPLC) grade water. The cell suspension was transferred to pre-coated T-75 tissue culture flasks. Following incubation at 37°C for 24 hours, flasks were tapped to remove

non-adherent cells. Flasks were washed twice with DMEM, high glucose, GlutaMAX™ Supplement followed by incubation with 15 ml fresh media. Microglial cells were maintained in the same culture media for one week until they spread their processes and were ready to be used for experiments (Yip et al., 2009, Rustenhoven et al., 2016).

2.1.2 Primary microglia culture isolated from neonatal rats

Microglia were isolated from forebrains and spinal cords of neonatal rats as described by (Tamashiro et al., 2012). Pups (10-14 pups per litter) were sacrificed by cervical dislocation, rinsed with 70% alcohol and death was confirmed by decapitation with sterile sharp scissors. Heads and bodies were rinsed in 70% ethanol, then transferred to sterile PBS. Brains and spinal cords were removed and placed in Petri dishes containing chilled 5 ml L-15 Leibovitz media with L-glutamine (HyClone, GE Healthcare Life Sciences) supplemented with 0.1% w/v bovine serum albumin (BSA) (Sigma-Aldrich, St Louis, MO, USA) + 1% pen/strep. Meninges were removed from both brains and spinal cords, and tissues were transferred to sterile Petri dishes containing L-15 media. Brains and spinal cords were transferred to sterile 50 ml Falcon tubes using a 10 ml serological pipette. Tubes were centrifuged at 2,500 x g for 5 minutes at 4°C (Allegra™ X-22R Centrifuge, Beckman Coulter, UK). Supernatants were aspirated and 5 ml fresh L-15 media were added. Cells were re-suspended by gently pipetting up and down using a 10 ml serological pipette, and then the suspensions

were passed through a 100µm cell strainer to remove aggregates and tissue debris. The flow-through for each tissue was centrifuged at 2,500 x g for 5 minutes at 4°C. Supernatants were discarded and fresh culture media (DMEM, high glucose, no glutamine, no calcium (Gibco, ThermoFisher Scientific) supplemented with 10% FBS and 1% pen/strep were added to cell pellets. The volume was brought up to 12 ml then equal volumes were transferred to T-75 tissue culture flasks. Cells were incubated at 37°C and media were changed on day five and then changed every three days until cells reached confluence (12-14 days). Microglia were shaken-off the astrocytes bottom layer gently using an orbital shaker (Heidolph Rotamax 120, Fisher Scientific) at 100 rpm for 2 hours, at 37°C. Supernatants were collected and centrifuged at 2,500 x g for 5 min at 4°C. Cells were re-suspended in 1 ml fresh microglial plating media (DMEM, high glucose, no glutamine, no calcium supplemented with heat-inactivated horse fetal serum [Gibco, ThermoFisher Scientific] and 1% pen/strep).

2.1.3 Primary astrocyte culture isolated from neonatal rats

Microglia were isolated from neonatal forebrains or spinal cords. Pups (10-14 pups per litter) were sacrificed by cervical dislocation, rinsed with 70% alcohol and death was confirmed by decapitation with sterile sharp scissors. Heads and bodies were rinsed in 70% ethanol then transferred to sterile PBS. Brains and spinal cords were removed and placed in universal tubes containing chilled 5 ml glial media (Dulbecco's Modified Eagle's

Medium-high glucose, Sigma-Aldrich). Media were removed and 5 ml of media were used to reconstitute a vial of papain. Cortical and spinal cord tissues were digested with papain. Tissues were subjected to trituration with pipette followed by Incubation at 37°C for 40 minutes. A volume of 500µl Deoxyribonuclease I (DNase I), from Bovine Pancreas (Applichem Lifescience, VWR) was added to digested tissues that were then transferred to universal tubes. Tubes were centrifuged at 212 x g for 6 minutes. Supernatants were discarded and complete glial media (10% FBS, 500µg/ml L-proline [Sigma-Aldrich, St Louis, MO, USA] and 1% P/S) with the addition of 500µl DNase I were added to each tissue and followed by trituration with a pipette. Tubes were centrifuged at 182 x g for 3 minutes. Supernatants were collected in universal tubes. Remaining pellets were triturated in 10 ml of the glial medium then centrifuged again at 182 x g for 3 minutes. Supernatants were added to the previously collected supernatants in universal tubes. Pellets were triturated again in 10 ml glial medium, followed by centrifugation at 182 x g for 3 minutes. Supernatants were also collected in the previous universal tube, centrifuged at 212 x g for 6 min and followed by discarding the supernatant and re-suspending the pellet with 10 ml of glial medium. Suspensions were strained through 100µm cell strainer followed by adding fresh media and transferring to T-75 flasks. Astrocytes were left to adhere to the bottom of flasks for 24 hours and were then shaken at 120 rpm overnight to remove microglia and oligodendrocytes. Media was refreshed every four days for ten days. Astrocytes were trypsinised and seeded in PDL coated 12 well plates in a density of 80,000 cells/ml.

2.1.4 Primary cortical neuron culture isolated from rat embryos

Twelve well plates (for cell proliferation assay) or 24 wells plate (for immunocytochemistry) were coated with Poly-L-Ornithine-hydrobromide (PLO) (50µg/ml, Sigma-Aldrich, St Louis, MO, USA) 24 hours before neuron culture. Embryos at gestational day E18 were used. The pregnant dam was sacrificed using a carbon dioxide chamber. The dam's abdomen was sterilised with 70% ethanol. The uterus was extracted and placed in a 90mm Petri dish containing neurobasal media (Gibco, Thermofisher Scientific). Embryos were cut free from the amniotic sac and placenta. Embryos heads were removed and placed in a universal tube containing neurobasal media. The brains were dissected out under a stereomicroscope in a sterile environment and placed in a 35mm in diameter Petri dish containing Hanks balanced salt solution (HBSS/HEPES) [Sigma-Aldrich, St Louis, MO, USA] PH 7.3. After the removal of the meninges, approximately seven brain hemispheres were transferred to a 35mm petri dish with 2 ml HBSS/HEPES solution. Brains were triturated into small pieces with a pipette to facilitate tissue digestion. Tissues were digested by adding 200µl of trypsin (Sigma-Aldrich) and 20µl of DNase (Sigma-Aldrich) to each 35 mm Petri dish for 30 minutes at 37°C. Tissue digestion was terminated by adding 200µl of trypsin inhibitor (Sigma-Aldrich, St Louis, MO, USA) to each Petri dish. Digested tissue solutions were transferred to a universal tube containing 6 ml of

neurobasal media (supplemented with B27 supplement [Invitrogen] and Glutamax-supplement [Gibco, Thermofisher Scientific]). After waiting for the tissue to settle at the bottom of the tube, 6ml of media were removed. A volume of 10µl DNase was added to the digested tissue followed by gentle swirling to ensure proper mixing. Next, 5ml of media was added to the tissue and the tissue was allowed to sink to the bottom of the tube as previously mentioned. Most of the media were removed except for about 1.5-2ml. Once more, 10µl of DNase was added to the remaining solution followed by gentle swirling. A single-cell suspension was created by gentle trituration of the tissue using a pipette cautiously avoiding creating air bubbles. The process was repeated for ten times. A volume of 10 ml of neurobasal media was added to the solution followed by centrifugation for 5 minutes at 250 x g. The supernatant was aspirated and the cell pellet was resuspended in a volume of neurobasal media equal to the number of brains used. This protocol generates approximately $10x10^6$/ml cells. Neurons were seeded in a density of $0.5x10^6$ cells/ml and media was half changed every four days.

2.2 Reagents

Table 2-1 summarises reagents, drugs and inhibitors used for cell treatment.

Table 2-1 Bioreagents and inhibitors used for cell treatment

Name	Supplier
ATP	Sigma-Aldrich, St Louis, MO, USA
LPS from *Escherichia coli* (strain O111: B4	Sigma-Aldrich, St Louis, MO, USA
BSA	Sigma-Aldrich, St Louis, MO, USA
SB202190 (p38 MAPK inhibitor)	Sigma-Aldrich, St Louis, MO, USA
TNP-ATP triethylammonium salt (P2X inhibitor)	Tocris, UK
A438079 hydrochloride (P2X7R inhibitor)	Tocris, UK
5-BDBD (P2X4R inhibitor)	Tocris, UK

All inhibitors were prepared as stocks in dimethyl sulfoxide (DMSO) except for TNP-ATP as it is supplied pre-dissolved in water. A stock of 1mg/ml LPS in PBS was prepared. No effect of solvents was detected in all experiments.

2.3 Collection of microglia and astrocytes conditioned media

2.3.1.1 LPS treatment and collection of conditioned media from microglia

Twelve well plates pre-coated with PDL were used for seeding. Adult or neonatal microglia isolated from rat forebrains or spinal cords were either seeded in 10% serum-supplemented media or serum-free media (DMEM/F-12 advanced [Gibco, ThermoFisher Scientific]+ 1% P/S, L-glutamine

[Sigma-Aldrich, St Louis, MO, USA] and 1x G-5 supplement [Gibco, Thermofisher Scientific]). The cells were left to adhere overnight in serum-rich media. Next, the media was aspirated, and each well was washed with sterile PBS. Cells were refreshed with serum-rich or serum-free media. After 24 hours of refreshing cells with media, 100ng/ml of LPS was used to stimulate microglia for 6 hours. Media was aspirated, cells were washed with PBS, and fresh serum-rich or serum-free media were added correspondingly. After 24 hours post LPS stimulation, microglial conditioned media were filtered using a 0.45µM Minisart Syringe Filter (Sartorius, UK) and stored at -80°C in aliquots. Cells were lysed in TriReagent for RNA extraction.

2.3.1.2 Astrocyte treatment with adult or neonatal microglial conditioned media (MCM)

Neonatal cortical or spinal cord astrocytes were seeded in serum-rich media in PDL pre-coated 12 wells plates. Cells were left to adhere for 48 hours. Media was aspirated, and cells were washed with PBS, followed by the addition of fresh serum-rich or serum-free media as described earlier. After 24 hours of media change, astrocytes were treated with adult or neonatal untreated or LPS-stimulated MCM in a dilution of 1:2 (i.e. 50% astrocyte media: 50% microglial conditioned media) for different time points (1, 3, 6, and 24 hours). Control astrocytes were not treated with microglial conditioned media. Astrocyte conditioned media were filtered with 0.45µM

filter and stored at -80°C in aliquots. Cells were lysed with Tri-Reagent and processed for RNA extraction.

2.3.1.3 Neuron treatment with Astrocytes conditioned media (ACM)

Embryonic cortical neurons were treated with

MCM-stimulated ACM. On the eighth day following isolation, neurons were treated with serum-free cortical ACM for 24 hours in a dilution of 1:5 (i.e. 80% neurobasal media: 20% ACM media). Controls were treated with fresh serum-free media with a dilution of 1:5. After 24 hours of stimulation, a cell viability assay was carried out.

2.4 RNA extraction

RNA was isolated from cell lysates in Tri reagent ® (Sigma-Aldrich, St Louis, MO, USA). Samples were incubated for 5 minutes at room temperature to allow dissociation of nucleoprotein complexes. An amount of 60µl 1-Bromo 3-Chloro-propane (BCP) (Sigma-Aldrich, St Louis, MO, USA) was added to each 300µl of lysis reagent. Each sample was vortexed vigorously for 15 seconds, followed by separating the mixture into two phases by centrifugation at 12,000 x g for 15 minutes at 4 °C. The upper aqueous layer was transferred into a sterile nuclease-free tube. RNA was precipitated by adding 150µl of 2-propanol (Fisher Chemical) and 1µl of glycogen (Thermo Scientific) to each sample. To increase the amount of

precipitated RNA, samples were incubated at -20 °C overnight. Microtubes were centrifuged at maximum speed for 10 minutes at 4°C and precipitated RNA was collected by aspirating the supernatant while keeping the pellet intact. Pellets were washed twice with 70% ethanol. After aspiration of ethanol, the lids were opened to allow the ethanol to evaporate however, the pellet was not allowed to dry fully. A volume of 87.5 µl diethylpyrocarbonate (DEPC)-treated HPLC grade water was added to each sample followed by heating on a Biometra Trio-Thermoblock (Thistle Scientific, UK) at 65°C for 5 minutes. To purify RNA from contaminating DNA, 2.5µl of DNase I and 10µl of RDD buffer (Qiagen) were added to each sample. Samples were incubated at room temperature for 10 minutes. The volume was adjusted to 400µl with DEPC-treated HPLC grade water. An equal amount of phenol/chloroform/isoamyl alcohol was added to each sample followed by mixing and centrifugation at 12,000 x g for 10 minutes at 4°C. The upper aqueous phase was transferred to a sterile Eppendorf tube. Further precipitation of RNA was achieved by incubating samples with 40µl 3M sodium acetate (PH 5.2) and 800µl absolute ethanol at -20°C overnight. RNA pellets were collected by centrifugation at maximum speed for 10 minutes at 4°C. RNA was washed twice with 70% ethanol. The RNA pellet was left to air dry at room temperature. RNA was re-suspended in 40µl DEPC-treated water. Concentrations and purity of RNA were estimated by measuring the absorbance at 260 nm and 280 nm using FLUOstar® Omega microplate reader (BMG, Labtech).

2.5 Reverse Transcription (cDNA synthesis)

AffinityScript Multiple Temperature cDNA Synthesis Kit (Agilent Technologies) was used to synthesise 500ng cDNA from RNA samples. DEPC-treated HPLC grade water was added to calculated RNA volumes to total the volume up to 10.7µl. Random primers (0.1µg/µl) (Promega) were added in a volume of 3µl. Samples were incubated at 65°C at 10 minutes. The reaction was cooled at room temperature for about 10 minutes. To total the reaction volume to 20µl; 2.0µl of 10x AffinityScript RT Buffer, 2.0µl 100 mM DTT, 0.5µl of dNTP mix (25 mM each dNTP), 0.5µl of RNase Block Ribonuclease Inhibitor (40U/µl) (Invitrogen) and 1 µl of AffinityScript Multiple Temperature RT were added to each sample. Reactions were placed on a heat block that controls their incubation at 25°C for 10 minutes, 55°C for 60 minutes, 70°C for 15 minutes and finally holds at 4°C.

2.6 Taqman qPCR

Following reverse transcription, 60µl of nuclease-free water was used to dilute each sample. Standards were prepared by generating a pool of all samples which forms the neat standard sample to use for the standard curve. From the neat standard sample, in a dilution of 1:4, standards of 5 points were prepared. The reaction mixture is composed of 6.5µl of PrecisionPLUS qPCR Master Mix low ROX (Primer Design), 0.4µl forward primer (10µM), 0.4µl reverse primer (10 µM), 0.25µl probe (10 µM), 2.45µl

DEPC-treated HPLC grade water and 3µl of sample or standards. Conditions of the PCR cycles were according to TaqMan master mix manufacturers' recommendations. Genes of interest were normalised to rat GAPDH gene; the latter was used as an endogenous control. Primers and probes were designed using Primer Express 3 software (Applied Biosystems, UK) and synthesised either by Eurofins or Sigma-Aldrich. Probes were labelled with the fluorophore, FAM (6-carboxyfluorescein) and a quencher, TAMRA (tetramethylrhodamine). Primers and probes sequences are listed in Table 2-2. AriaMx Real-time PCR system (Agilent Technologies) were used. Results were analysed using the standard curve method and $2^{-\Delta\Delta ct}$ method (Livak and Schmittgen, 2001).

Table 2-2 Sequences of primers and probes used for quantitative real-time PCR

Rat Gene	**Full name**	**Sequence 5'-3'**
GAPDH	Glyceraldehyde 3-phosphate dehydrogenase	Sense: TCTGCTCCTCCCTGTTCTAGAGA Anti-sense: CGACCTTCACCATCTTGTCTATGA Probe:ATCTTCTTGTGCAGTGCCAGCCTCGT
NR4A1/Nur77	Nuclear receptor subfamily 4, group A, member 1	Sense: TGTTGCTAGAGTCCGCCTTTC Anti-sense: CAGGCCTGAGCAGAAGATGAG Probe: TTATCCTCCGCCTGGCCTACCGATCTAA
NR4A2/Nurr1	Nuclear receptor subfamily 4, group A, member 2	Sense: TTGCAGAATATGAACATCGACATTT Anti-sense: CCCGTGTCTCTCTGTGACCAT Probe: TCTCCTGCATTGCTGCCCTGGC
NR4A3/NOR-1	Nuclear receptor subfamily 4, group A, member 3	Sense: CGCCCTTGTCCGAGCTTTA Anti-sense: CGGTGGGACAGTATCTGGAGTAA Probe: CAGACGCAACGCCCAGAGACCTTG

TINUR	Transcriptionally-inducible nuclear receptor	Sense: TCCACCTTTATTTTCCTCGAAAAC Anti-sense: CGTCGTAGCCTGTGCTGTAGT Probe: CACTCGGCTGAAGCT MGB
Nurr1a	-	Sense: AGCATACAGAATATGAACATCGACATT Anti-sense: CCCGTGTCTCTCTGTGACCAT Probe: CCTTCTCCTGCATTGCTGCCCTGT
Psat1	Phosphoserine Aminotransferase 1	Sense: CAGCTAAGGCTGCGGAAGAA Anti-sense: GCGTCCGGGTTGAGGTT Probe: TTACACAAAAATTCCAGACCCAAGCACCTG
Scd2	stearoyl-Coenzyme A desaturase 2	Sense: TTCCAGAACGATGTGTACGAATG Anti-sense: CCAACCCACGTGAGAGAAGAA Probe: CTCAGAGACACACGCCGACCCTCA
MafB	MAF BZIP Transcription Factor B	Sense: GCCTTCTTCTCCCAGCTTCA Anti-sense: TTGCTCGCCATCCAGTACAG Probe: TCCGACTGAACAGAAGACCCATCTCGA
Sall1	Sal-like protein 1	Sense: AGTCGCCCCACTAAGAGCAA Anti-sense: GGAGCAGAAGGTCTGATAATTCAAA Probe: CCCACGTCTGTGGCCGGTGC
BDNF	Brain-derived neurotrophic factor	Sense: CCATAAGGACGCGGACTTGT Anti-sense: GAGGCTCCAAAGGCACTTGA Probe: CACTTCCCGGGTGATGCTCAGCA
TGFβ-1	Transforming Growth Factor Beta 1	Sense: CGTGGAAATCAATGGGATCAG Anti-sense: GGAAGGGTCGGTTCATGTCA Probe: CGAGGTGACCTGGGCACCATCC
IL-1β	Interleukin 1 beta	Sense: CACCTCTCAAGCAGAGCACAG Anti-sense: GGGTTCCATGGTGAAGTCAAC Probe: TGTCCCGACCATTGCTGTTTCCTAGG
IL-10	Interleukin-10	Sense: CCCTGGGAGAGAAGCTGAAGA Anti-sense: CACTGCCTTGCTTTTATTCTCACA Probe: CAGCTGCGACGCTGTCATCGATTTC

2.7 Western blotting

Following phase separation of RNA, DNA and protein using TriReagent and BCP, the lower phase was used for protein extraction. A volume of 90µl of absolute ethanol (0.3 ml of ethanol for 1 ml of Tri-reagent) was added to the protein phase and mixed by inverting followed by incubation at room temperature for 2-3 minutes. Tubes were centrifuged for at 2,000 x g for 5 minutes at 4°C. The supernatant was transferred to a fresh tube. A volume of 450µl isopropanol (1.5ml of isopropanol for 1ml of TriReagent) was added to the supernatant followed by incubation at room temperature for 10 minutes. After the incubation, tubes were centrifuged at 12,000 x g for 10 minutes at 4°C. The supernatant was discarded, and the protein pellet was washed with 0.3 M guanidine hydrochloride (Sigma-Aldrich, St Louis, MO, USA)/95% ethanol solution by incubation at room temperature for 20 minutes. Tubes were centrifuged at 7,500 x g for 5 minutes at 4°C. The supernatant was discarded and the wash and spin steps were repeated for a total of 3 times. After the third wash, the supernatant was discarded and 2 ml of absolute ethanol was added to the protein pellet followed by vortexing and incubation at room temperature for 20 minutes. The protein pellet was centrifuged at 7,500 x g for 5 minutes and the supernatant was discarded. The pellet was air-dried for a few minutes followed by dissolving proteins in 7M Urea 2X Lamaelli buffer (100mM Tris HCL pH 6.8, 4% of 10% Sodium dodecyl sulfate [SDS], 0.1M Dithiothreitol [DTT], 7M Urea, 0.2mg/ml Bromophenol blue, 1mM of 0.5M

Ethylenediaminetetraacetic acid [EDTA] and 20% glycerol) that has protease and phosphatase inhibitor (Sigma-Aldrich, St Louis, MO, USA) added. Insoluble materials were removed by centrifugation at 10,000 x g for 10 minutes at 4°C followed by the transfer of supernatant to a fresh tube. Samples were boiled with the loading buffer for 5 min at 95°C. An approximately equal amount of proteins were loaded into 10% SDS polyacrylamide gel. Gels were run at 60 V through the stacking gel followed by increasing power to 200 V using mini-PROTEAN Electrophoresis System from Biorad. The stacking gel was cut off after the run finished and gels were sandwiched in a cassette (Mini Trans-Blot® Cell, Biorad) to transfer protein bands to nitrocellulose membrane (GE Healthcare, Life Sciences). The transfer was run for 90 minutes at 200 mA (for one gel) or for two gels, the transfer was run at 300 mA for 120 minutes. Following transfer, membranes were stained with 1x Ponceau Red S solution (Sigma-Aldrich, St Louis, MO, USA) to confirm transfer success and washed with water and 0.1% Tris-buffered saline-tween 20 (TBST). Membranes were incubated with 5% skimmed milk in TBST for blocking on an orbital shaker for 60 minutes at room temperature. Primary antibodies (see Table 2-4) were diluted with 5% milk in TBST. Antibodies were prepared in 50 ml Falcon tube that was used to incubate membrane with antibody overnight on a roller at 4°C. Membranes were washed three times, each for 10 minutes with TBST. Secondary antibodies (shown in Table 2-5) were prepared in foil-wrapped 50 ml tubes. Membranes were incubated in 50 ml tubes on a roller at room

temperature for 60 min. Membranes were washed three times with TBST, each for 5 minutes taking care not to expose membranes to light. Blots were imaged using LiCor Odyssey detection system (LI-COR Biosciences).

Table 2-3 Solutions used for Western blot

10X running buffer (500ml)	Tris base 15g (250mM) Glycine 72g (1.92M) 1% SDS 5g (or 50ml 10% SDS) Volume to 500 ml with deionised water
10X transfer buffer (500ml)	Tris base 15g Glycine 72g Volume to 500ml with deionised water
1X transfer buffer (1L)	10X transfer buffer 100ml Methanol 200ml Deionised water 700ml
10X TBS pH 7.4 (2.5L)	Tris 75g (250mM) NaCl 200g (2M) KCl 5g (27mM)
0.1% TBST (1L)	Deionised water 899ml 10X TBS 100ml Tween 20 1ml

Table 2-4 Primary antibodies used for Western blot

Primary Antibody	Dilution	Supplier	Catalogue number
Rabbit anti-Nur77 antibody	1:1000	Abcam	ab109180
Mouse anti-beta actin	1:5000	Sigma-Aldrich	A5441
Mouse anti-alpha tubulin	1:5000	Sigma-Aldrich	T9026
Rabbit anti-p38 MAPK	1:1000	Cell signaling	9212s
Rabbit anti-phospho p38MAPK	1:1000	Cell signaling	9211s
Rabbit anti-BDNF	1:1000	Novusbio	NB100-98682

Table 2-5 Secondary antibodies used for western blot

Primary Antibody	Dilution	Supplier	Catalogue number
IRDye ® 800CW Donkey (polyclonal) anti-rabbit IgG (H+L)	1:5000	LI-COR	926-32213
IRDye ® 680LT Goat (polyclonal) anti-mouse IgG (H+L)	1:5000	LI-COR	926-68020

2.8 Immunocytochemistry

Cells seeded on coverslips or in 24 wells plate were fixed with 200µl prewarmed 4% paraformaldehyde solution for 10 minutes followed by washing for three times with 200µl 1x PBS. Triton X-100 solution (0.1%) was added to cells in a volume of 200µl and incubated at room temperature for 10 minutes, followed by washing with 200µl PBS for three times. Blocking was achieved by adding 200µl 0.5% w/v bovine serum albumin (BSA) for 1 hour at room temperature. Fixed cells were incubated overnight with diluted primary antibody (see Table 2-6) in 0.5% BSA at 4 °C. Following washing with PBS three times, cells were incubated with secondary antibody (

Table **2-7**) diluted in 0.5% BSA for 45 minutes at room temperature while protected from light exposure. After three times washing with PBS, diluted 4′,6-diamidino-2-phenylindole (DAPI) in PBS was added to cells for 1 minute at room temperature avoiding exposure to light. Cells were rinsed with PBS once. Coverslips were mounted on glass slides using DABCO (5ml PBS/45ml glycerol) mounting media and secured with clear nail varnish. Cells in 24 wells plate were kept in the PBS solution. Imaging was performed using a fluorescence microscope with a Zyla 4.2 sCMOS camera (Andor Technology, Belfast, UK) and an Olympus 10x objective lens, wide-field microscope (Zeiss Exciter) in a magnification of 20x or a confocal microscope (Zeiss LSM710 Confocal Microscope) with a magnification of 60x.

Table 2-6 Primary antibodies used for Immunocytochemistry

Primary Antibody	Dilution	Supplier	Catalogue number
Rabbit anti-P2X4R	1:2000	Alomone labs	APR-002
Mouse anti-GFAP	1:100	Thermofisher	MS-1376-P1
Rabbit anti-Iba1	1:100	Abcam	ab178847
Mouse anti-NeuN	1:100	Millipore	MAB377

Table 2-7 Secondary antibodies used for Immunocytochemistry

Secondary Antibody	Dilution	Supplier	Catalogue number
Goat anti-rabbit Alexa Fluor 488	1:250	Molecular Probes	R37116
Goat anti-mouse Alexa Fluor 488	1:250	LifeTechnologies, ThermoFisher Scientific	A11001
DAPI	1µg/ml (1:1000)	Sigma-Aldrich	32670

2.9 MTS assay

Embryonic cortical neurons were seeded in a 12 wells plate and treated with cortical MCM-stimulated ACM. Cell viability was determined using CellTiter 96® AQ_{ueous} One Solution Cell Proliferation Assay (MTS) by Promega. CellTiter 96 ® AQ_{ueous} One solution reagent was thawed at 37°C. A volume of 200µl/ml of one solution reagent was pipetted to each well. A positive control was used by adding 0.1% Triton-X to cells. The plate was

incubated at for 1 hour In a humidified, 5% CO_2 incubator at 37°C. The absorbance was measured at 490nm using the FLUOstar® Omega microplate reader.

2.10 Enzyme-linked immunosorbent assay (ELISA)

2.10.1 Rat IL-1β/IL-1F2 ELISA

IL-1β release into the supernatant was quantified using rat IL-1β /IL-1F2 (R&D systems) Quantikine® ELISA kit. Using the microplate strips provided with the kit, 50µl of assay diluent RD1-21 were added to each well. Standards were prepared according to the manufacturer's instructions in concentrations of 2000, 1000, 500, 250, 125, 62.5, 31.3 and 0 pg/ml. A volume of 50µl of standards, controls or samples was added to each well. Plates were tapped gently for one minute to ensure good mixing, covered with an adhesive and followed by incubation for two hours at room temperature. The plate sealer was gently removed and the plate was washed five times with 250µl of diluted wash buffer (provided with the kit) using a multichannel pipette. Fluids were removed from each well through inverting the plate over a container or a sink followed by tapping on clean paper towels. Rat IL-1β Conjugate (provided with the kit) was added to each well in a volume of 100µl. The plate was covered again with an adhesive strip and incubated at room temperature for another 2 hours. The washing step was repeated for a total of five washed. A volume of 100µl of Substrate Solution (prepared by mixing reagents A and B in equal volumes no longer than 15 minutes before use) was added to each well followed by incubation

for 30 minutes at room temperature while protected from light. The reaction was stopped by adding 100µl of stop solution to each well followed by gentle tapping of the plate to guarantee thorough mixing. Optical density readings were measured at 450 nm using FLUOstar® Omega microplate reader. Concentrations were obtained using linear regression analysis via Omega MARS data analysis software (BMG, Labtech).

2.10.2 BDNF Enzyme Immunoassay (EIA)

Released BDNF from adult cortical or spinal cord microglia was measured using Chemikine™ Brain-Derived Neurotrophic Factor (BDNF) Sandwich ELISA kit (CYT306, Millipore, UK). The assay detects human and rats BDNF. Provided microplates were pre-coated with mouse monoclonal antibodies raised against human BDNF. Treatment groups included; untreated microglia, microglia treated with 100µM ATP for 1 hour, microglia pre-incubated with a broad P2X inhibitor (30µM TNP-ATP) for 3 minutes before treatment with ATP for 1 hour and microglia pre-treated with p38 MAPK inhibitor (10µM SB202190) for 45 minutes before ATP treatment for 1 hour. BDNF released from microglia into the supernatant was recovered using Vivaspin® centrifugal concentrators (Sartorius, UK) with a 5,000 molecular weight cut off (MWCO). A volume of 1 ml per sample was loaded to each concentrator, centrifuged for 8 minutes at 20°C, washed once with PBS and followed by centrifugation for another 8 minutes at 20°C. A volume of 200µl of concentrate was used for BDNF ELISA. BDNF provided with the kit was reconstituted and diluted to generate standards of the following

concentrations: 250, 125, 62.5,31.3, 15.6, 7.8, 3.9 and 0 pg/ml. A volume of 100µl of standards, negative control (dose 0) and samples were added to each well (run in duplicates). The plate was sealed with a plate sealer and incubated overnight at 4°C on a shaker. The plate sealer was gently removed and the plate was washed four times with 250µl of diluted wash buffer (provided with the kit) using a multichannel pipette. Fluids were removed from each well through inverting the plate over a container or a sink followed by tapping on clean paper towels. Diluted biotinylated mouse anti-BDNF monoclonal antibody (prepared according to the manufacturer's instructions) was added to each well in a volume of 100µl. The plate was sealed and incubated at room temperature for 2 hours on a shaker. Each well was washed four times as described earlier followed by adding 100µl of diluted streptavidin-RP conjugate solution (prepared as instructed by the manufacturer) to each well. The plate was sealed and incubated for 1 hour at room temperature on a shaker. Washing was performed as mentioned above. Room temperature-warmed TMB/E Substrate was added to each well in a volume of 100µl. The plate was covered and incubated at room temperature for 15 minutes. The reaction was stopped was by 100µl of stop solution to each well. Optical density readings were measured at 450 nm using FLUOstar® Omega microplate reader. Concentrations were obtained using linear regression analysis via Omega MARS data analysis software (BMG, Labtech).

2.11 Cloning of Nur77 from microglia

Full-length Nur77 cDNA was amplified using Phusion ® high fidelity PCR kit (New England BioLabs, UK) and cloning primers summarized in Table 2-8 using three-step PCR as follows: initial denaturation 95 °C for 3 min; 95°C for 30 secs, 70°C for 30 secs, 72°C for 1:30 sec (30 cycles); final extension 72°C for 5 min; hold at 4°C. Restriction enzymes (NotI and HindIII, New England BioLabs, UK) were used to digest Nur77 sequence and pcDNA3.1(+) plasmid followed by running on 1% agarose gel electrophoresis. Corresponding bands were cut and extracted from gel using GeneElute™ Gel extraction kit (Sigma-Aldrich, St Louis, MO, USA). Nur77 DNA was ligated to plasmid using T4 DNA ligase. NEB® 10-beta Competent E. coli (High Efficiency) (New England BioLabs, UK) were used for transformation using heat shock then plated on Ampicillin agar plates overnight at 37°C. Screening by colony PCR (Phusion ®, New England BioLabs, UK) was performed using T7 and BGHR primers (Table 2-8). PCR conditions as follows:

Initial denaturation 96°C for 5 min; 96°C for 15 secs, 55°C for 50 secs, 72°C for 1 min (30 cycles); final extension 72° for 5 min; hold at 4°C.

Nur77 constructs were extracted from positive colonies using plasmid miniprep kit (Qiagen). Constructs were confirmed by sequencing and stored at -80°C in 50% glycerol.

The same protocol was applied to clone full rat NOR-1 from microglia; however, amplification of full-length NOR-1 has not been successful. Different sets of primers were designed to amplify two segments of the full-length product that include PstI restriction endonuclease site to ligate both sequences to generate a full-length NOR-1 (NCBI NM_031628.1). Surprisingly, primers designed for NOR-1 B (amplifying from 1893 to 2616, 5`-3`) resulted in successful amplification shown by a visible band on agarose gel while primers designed for NOR-1A (amplifying from 661 to1954) didn't result in the same outcome.

Table 2-8 Sequences of primers used for cloning

Primer	**Sequence 5'-3'**
Full length Nur77	Sense: TAAAAGCTT GAAAGTTGGGGTAGTGTGCGAG Anti-sense: TAAGCGGCCGCTGGGTGACAAGAAGAACATGCAC
T7	TAATACGACTCACTATAGGG
BGHR	TAGAAGGCACAGTCGAGG
Full length NOR-1	Sense: TAAAAGCTTACCTCCACAGAACCCAAAGC Anti-sense: TAAGAATTCCCTTTTGCTCACTTAATGACCAGTG
NOR-1 A	Sense: CCACCATTCAGCGCGCAAGATAC Anti-sense: CACCATCCCGACACTGAGACACTTC
NOR-1 B	Sense: AACTGCCCGGTAGACAAGAGACG Anti-sense: AAGTAGCTCTCTGCTCAGGCTTCC

2.12 Statistical analysis

Statistical analysis was performed using Graph Pad Prism software (version 8.0). The type of test used is mentioned in figure legends. Differences were considered significant when $p < 0.05$. Significant outliers were determined using the Grubbs test. Figures were plotted using the Prism software. The results in the text and figures were expressed as the standard error of the mean (SEM) obtained from independent samples stated in the figure legend.

3) Chapter Three:

Microglia-astrocyte crosstalk during in vitro LPS-induced neuroinflammation, a study of regional and developmental heterogeneity

---

3.1 Introduction

As described in chapter one, LPS is a bacterial cell wall component that acts as a PAMP and subsequently induces neuroinflammation. LPS has been widely used *in vivo* and *in vitro* studies to induce glial cells activation. Although LPS evidently provoked a pro-inflammatory response in the CNS, yet it is not a common insult that causes CNS injury and pathology (Lively and Schlichter, 2018). Systemic LPS stimulation evoked morphological changes (Kloss et al., 2001) and induced pro-inflammatory cytokines gene expression (e.g. IL-1β and TNF-α) in mouse brain microglia (Edan et al., 2013). Moreover, LPS was suggested to trigger microglia to release TNF-α, IL-1α, and c1q that activates astrocytes to acquire an A1 pro-inflammatory phenotype *in vivo* and *in vitro* (Liddelow et al., 2017a). Although several *in vitro* studies concluded that LPS-activates astrocytes in a TLR-4-dependant mechanism (Gorina et al., 2011, Li et al., 2016a), misinterpretation of such data could be due to residual contaminating microglia. For instance, induction of IL-1β, TNF-α, and IL-6 release by LPS-stimulated astrocytes was abolished when cultures were treated with the lysosomal disruptive agent, L-leucine methyl ester (L-LME) (Facci et al., 2014a, Marinelli et al., 2015), which specifically targets microglia and induces apoptosis (Jebelli et al., 2015). Moreover, cultured human fetal microglia increase the expression and release of pro-inflammatory cytokines when stimulated with LPS, contrary to human fetal astrocytes that showed no response to LPS, yet responded to cytokine stimulation (Lee et al., 1993). These observations

support the idea that activated –microglial secretome activates astrocytes and contributes to their acquired phenotypes (A1/A2).

3.2 Aim

Studying glial cells *in vivo* is challenging due to invasiveness of current approaches and limitations of current technologies but most importantly because of their heterogeneity. Primary cell cultures provide a better understanding of each cell type function and response. Moreover, real-time imaging technologies enable the identification of molecules that facilitate their communication. In the present study, we were interested in unravelling the effect of PAMPs (LPS as an example) on microglial activation at different developmental stages. Moreover, due to reported region-specific functions and responses of glial cells, we studied the impact of activated cortical and spinal cord microglia on neonatal cortical and spinal cord astrocytes. The way we addressed glial cell activation and the consequent impact on neurons is summarised in Figure 3-1.

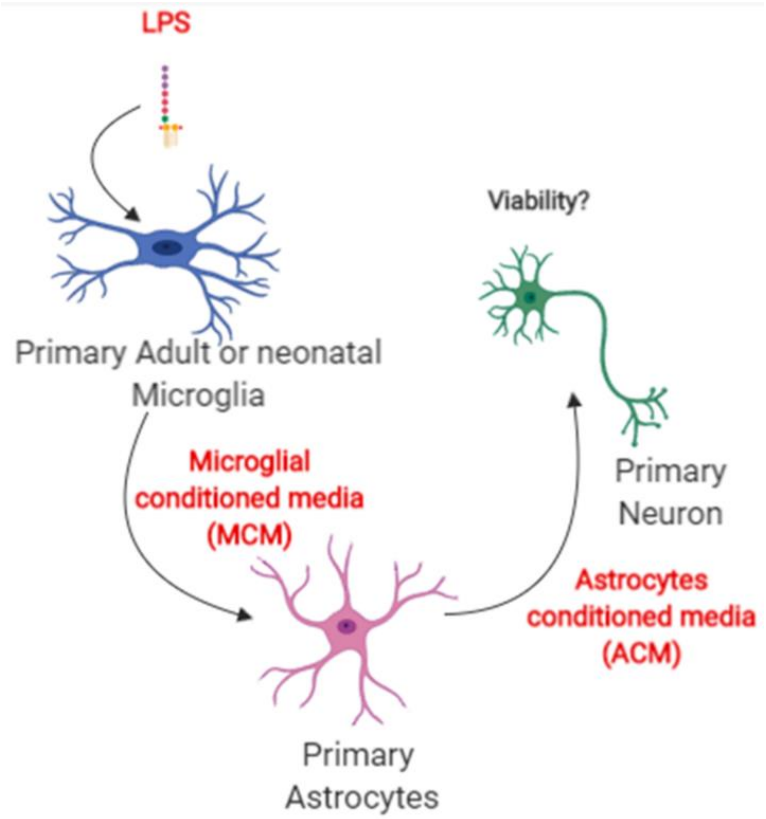

Figure 3-1 Study design for glial cells communication *in vitro* during an LPS challenge. LPS-stimulated microglial conditioned media (MCM) was used to stimulate astrocytes. MCM-stimulated astrocytes conditioned media (ACM) was used to stimulate cortical neurons only. Viability of neurons was evaluated.

3.3 Results

3.3.1 Validation of the purity of neonatal and adult microglia *in vitro*

In the present study, we follow a protocol for isolation of both neonatal and adult microglia designed not to skew their immunological responses into a false positive direction. Microglia isolation method used by our lab group (Imraish, 2018) produced high purity primary microglia cultures from neonatal (Figure 3-2 and Figure 3-3) and adult (Figure 3-4 and Figure 3-5) rat forebrains and spinal cords as suggested by Immunocytochemistry. Microglial specific cell surface marker Iba-1 immunoreactivity (rabbit anti-Iba1 [1:500], Wako, Cat#019-19741) indicated that microglia cultures were >90% pure. In addition, staining for cell-specific markers for astrocytes (rabbit anti-GFAP [1:1000], Abcam, Cat#ab48050) demonstrated minimal contamination while no oligodendrocytes (mouse anti-CC [1:500], Calbiochem., Cat#D001762 44) and neurons (Mouse anti-NeuN [1:100], Temecula, Cat#2453249) were observed. Neonatal cortical microglia isolation yielded about 1.5 x 10^6 cells/brain and spinal cord microglia isolation yielded approximately 1.1 x 10^6 cells/cord.

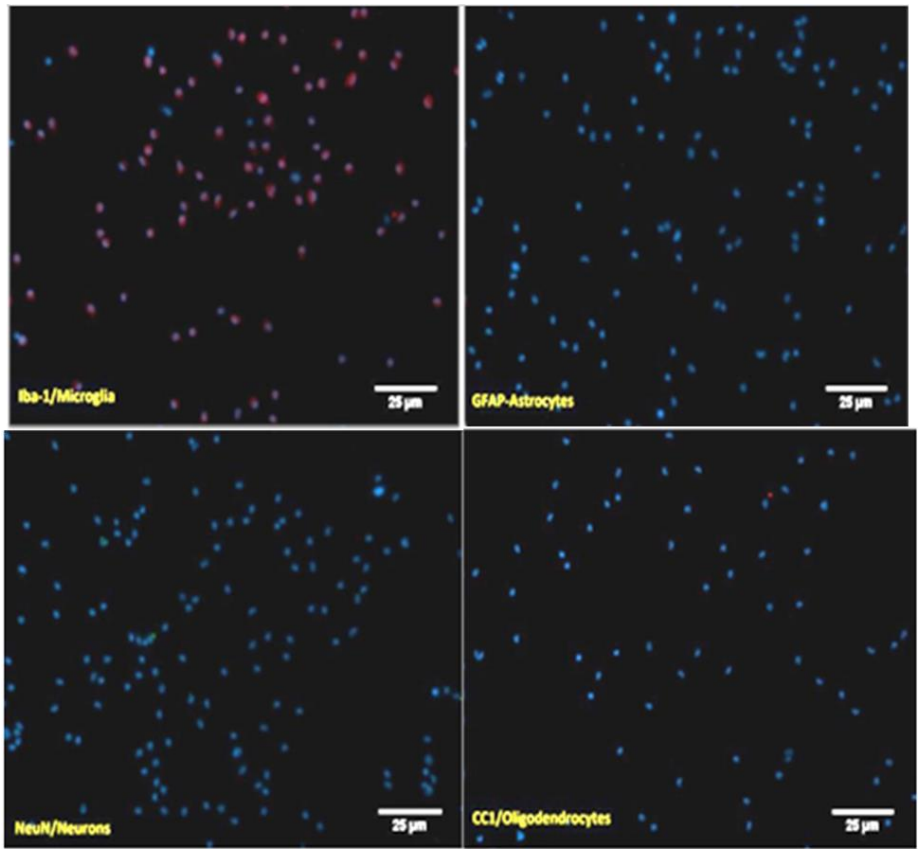

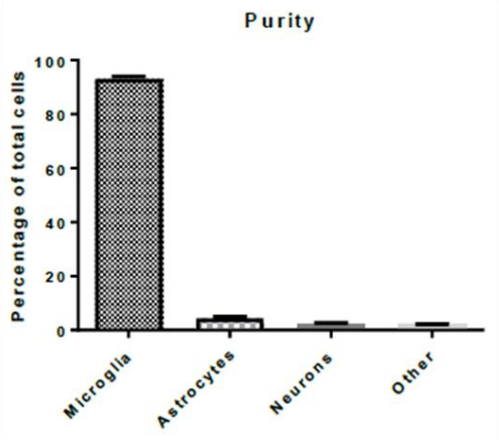

Figure 3-2 Purity of microglia isolated from neonatal rat spinal cords. The purity of primary microglia culture was determined via immunocytochemistry using specific cell surface markers for: (a) microglia (Iba-1), (b) astrocytes (GFAP), (c) oligodendrocytes (CC1) and (d) neurons (NeuN). Nuclei were stained with DAPI (blue) The graphs represent standard error of the mean (SEM) derived from three independent experiments. Scale bar 25 µm. Taken from (Imraish, 2018).

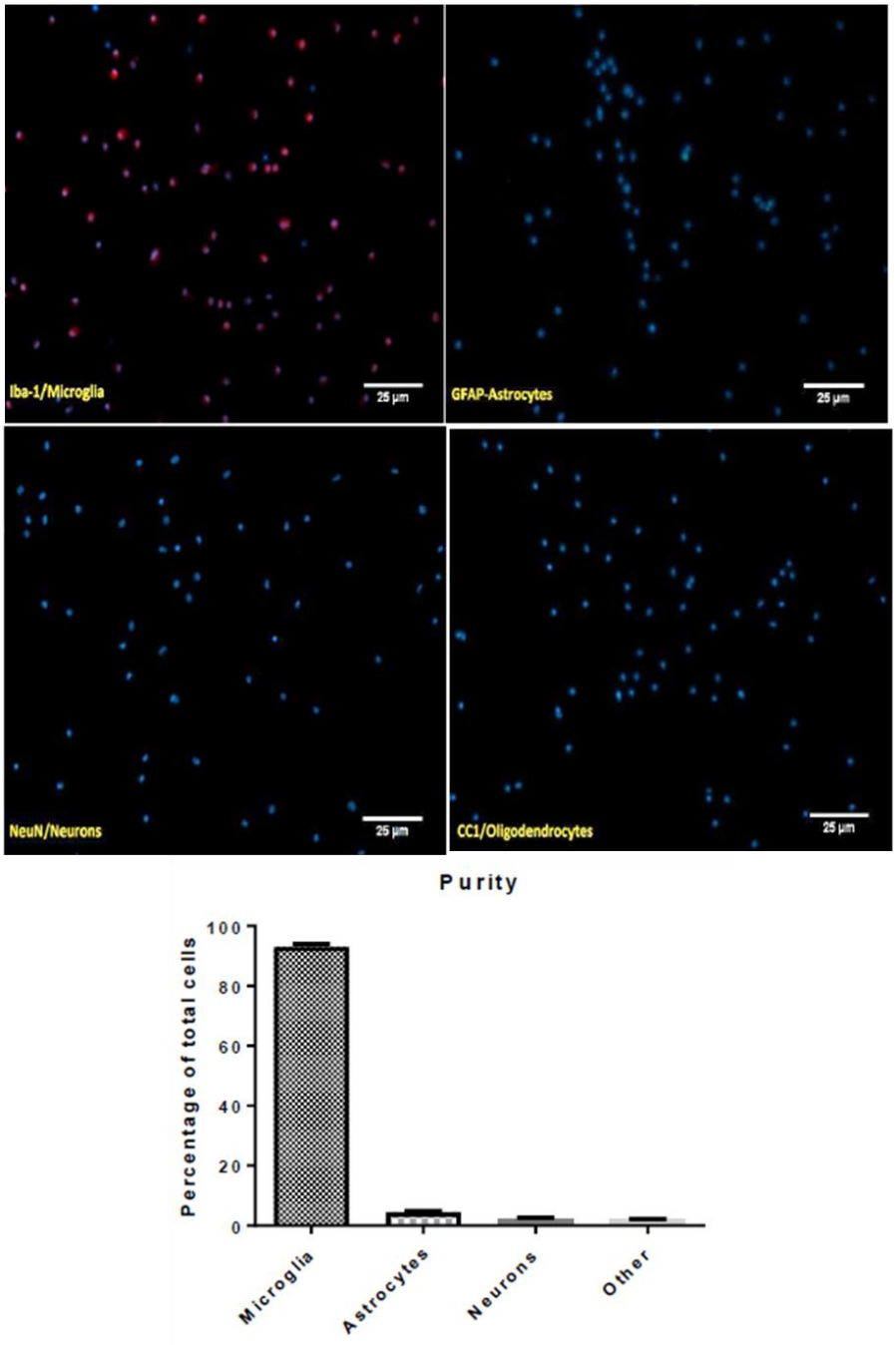

Figure 3-3 Purity of microglia isolated from neonatal rat forebrains. The purity of primary microglia culture was determined via immunocytochemistry using specific cell surface markers for: (a) microglia (Iba-1), (b) astrocytes (GFAP), (c) oligodendrocytes (CC1) and (d) neurons (NeuN). Nuclei were stained with DAPI (blue) The graphs represent standard error of the mean (SEM) derived from three independent experiments. Scale bar 25 µm. Taken from (Imraish, 2018).

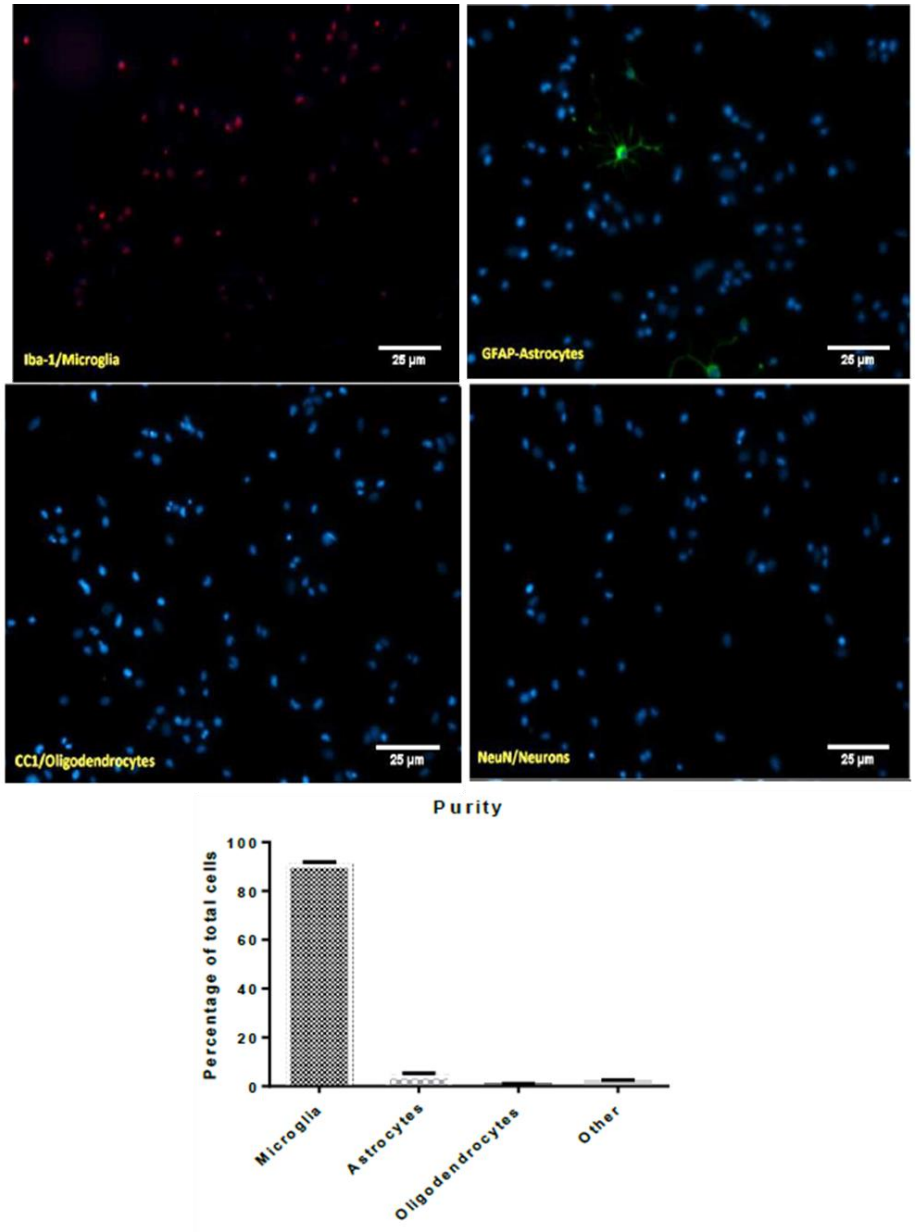

Figure 3-4 Purity of microglia isolated from adult rat spinal cords. The purity of primary microglia culture was determined via immunocytochemistry using specific cell surface markers for: (a) microglia (Iba-1), (b) astrocytes (GFAP), (c) oligodendrocytes (CC1) and (d) neurons (NeuN). Nuclei were stained with DAPI (blue) The graphs represent standard error of the mean (SEM) derived from three independent experiments. Scale bar 25 µm. Taken from (Imraish, 2018).

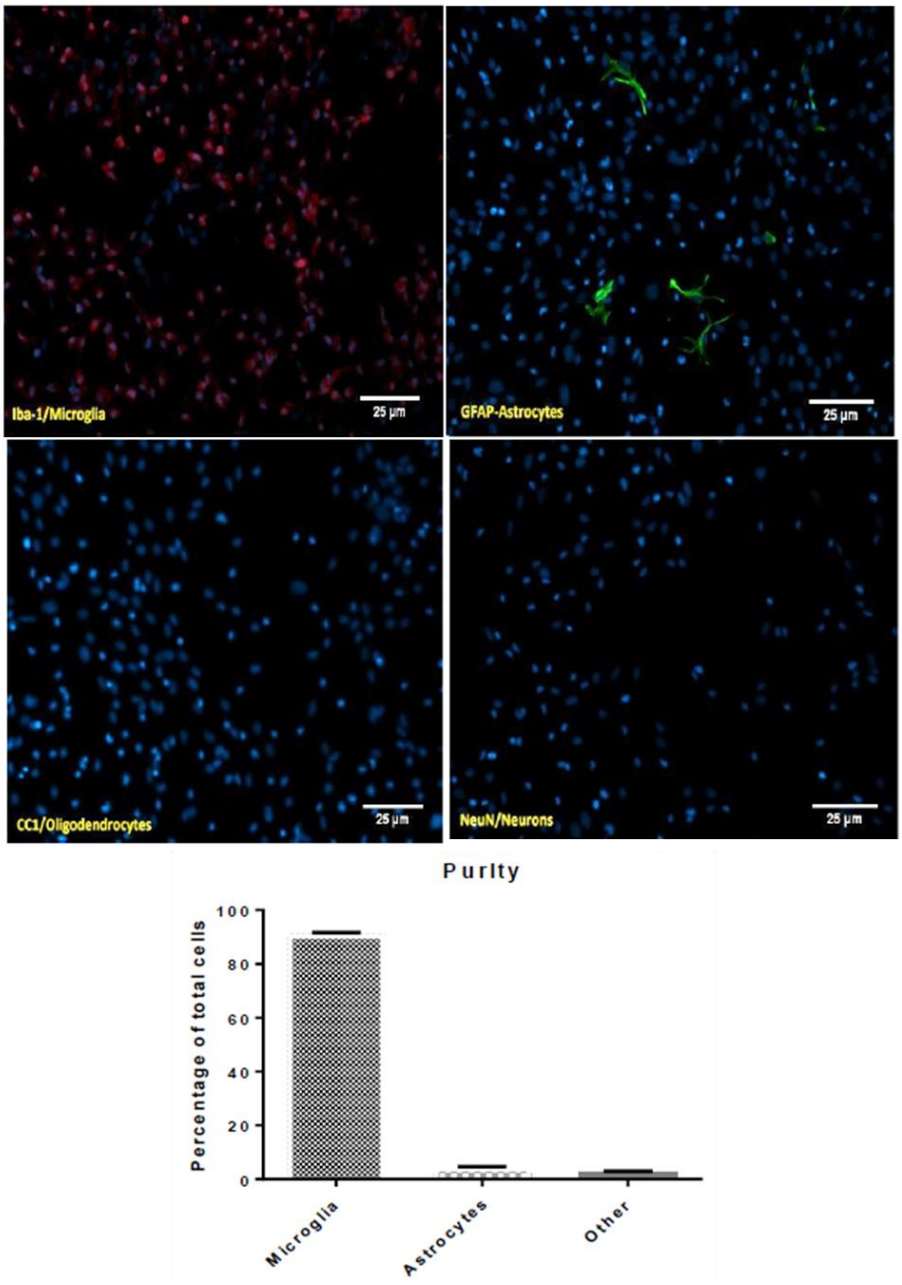

Figure 3-5 Purity of microglia isolated from adult rat forebrains. The purity of primary microglia culture was determined via immunocytochemistry using specific cell surface markers for: (a) microglia (Iba-1), (b) astrocytes (GFAP), (c) oligodendrocytes (CC1) and (d) neurons (NeuN). Nuclei were stained with DAPI (blue) The graphs represent standard error of the mean (SEM) derived from three independent experiments. Scale bar 25 µm. Taken from (Imraish, 2018).

3.3.2 Validation of neonatal and adult microglia phenotypes *in vitro*

Although many studies focus on studying microglial immunological responses *in vitro*, altered gene expression profiles have been reported in cultured mouse (Gosselin et al., 2014) and human microglia (Gosselin et al., 2017) in comparison to *in vivo* microglia. Therefore, distinctive biomarkers are essential to evaluate the phenotype of isolated cells. Different developmental markers have been characterised in cortical microglia (Matcovitch-Natan et al., 2016). We evaluated some of these markers in our adult or neonatal microglia considering the possibility of (1) altered gene expression, (2) ageing during culture (as mentioned earlier in chapter one), (3) loss of developmental characteristics, and (4) microglial heterogeneity. The selection of the developmental markers (MafB and Sall1 for adult microglia, Psat1 and Scd2 for neonatal microglia) was based on their differential expression between early postnatal microglia (P3-P9) and adult microglia from four weeks old mice onwards (Matcovitch-Natan et al., 2016).

As for cortical microglia, *MafB* and *Sall1* mRNA expression levels were higher in adult (relative mRNA expression: 2 and 0.9, respectively) compared to neonatal microglia (relative mRNA expression: 0.3 and 0.4) (Figure 3-6 a,b) whereas Scd2 and Psat1 transcript levels were significantly higher in neonatal (relative mRNA expression: 2.5 and 1.7) microglia than adult microglia (relative mRNA expression: 0.5 and 0.2) (Figure 3-6 c,d).

Spinal cord microglia showed a similar pattern; however, overlap in gene expression profiles was apparent. For instance, *Sall1* and *Psat1* transcript levels were similar in adult (relative mRNA expression: 0.9 and 0.8) and neonatal microglia (relative mRNA expression: 0.8 and 1) Figure 3-6 b,c). These observations hence indicate that our primary microglia retain their developmental characteristics and phenotypes in culture despite isolation and subjection to culture conditions.

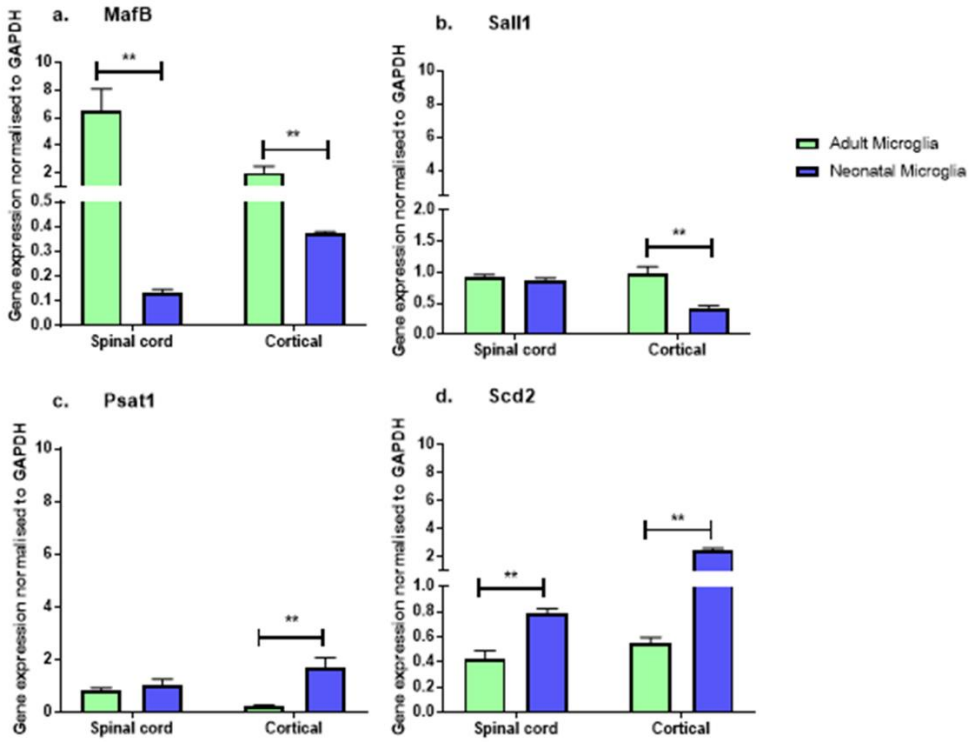

Figure 3-6 Adult and neonatal microglia maintain their developmental biomarkers *in vitro*. Relative expression of adult microglia biomarkers; (a) *MafB* and (b) *Sall1* or neonatal microglia biomarkers; (c) *Psat1* and (d) *Scd2* (normalised to *GAPDH* using standard curve method as described in methods) in microglia isolated from adult rat forebrains or spinal cords. Bars represent the standard error mean of values n=3. Statistical significant difference: **$p < 0.001$ (Multiple t-tests). MafB (v-maf avian musculoaponeurotic fibrosarcoma oncogene homolog B), Sall1 (Spalt Like Transcription Factor 1), Psat1 (Phosphserine Aminotransferase 1) and Scd2 (Acyl-CoA desaturase 2).

3.3.3 LPS-induces *IL-1β* and *IL-10* mRNA expression rapidly in primary microglia

As described earlier, LPS triggers immunological responses in microglia; therefore, LPS was chosen as an activator of microglia to investigate their responses to PAMPs. Firstly, we evaluated the mRNA expression of *IL-1β* after LPS stimulation at different time points. A significant rapid increase in LPS- induced *IL-1β* expression was observed in both adult and neonatal microglia, especially at three hours of LPS stimulation as shown in Figure 3-7 (adult microglia, 49-fold in cortical and 36-fold in spinal cord) and Figure 3-8 (neonatal microglia, 380-fold in cortical and 79-fold in spinal cord).

In adult cortical microglia, LPS-induced *IL-1β* mRNA levels decreased after six hours of LPS stimulation (29-fold compared to three hours of stimulation), while transcript levels remained significantly high in spinal cord microglia after six hours (5-fold increase from three hours of stimulation) (Figure 3-7 a,b). On the other hand, in neonatal microglia, LPS-induced *IL-1β* mRNA expression gradually increased in cortical microglia after one, three and six hours of stimulation (33-, 380- and 413-fold) whereas *IL-1β* transcript levels were induced after one (8-fold) and three (79-fold) hours of stimulation but slightly decreased after six hours of stimulation (67-fold). Despite that, the pattern of *IL-1β* mRNA expression appears to be similar between cortical and spinal cord microglia, although the fold change

is higher in neonatal cortical microglia in comparison to spinal cord microglia (Figure 3-8 a,b).

When comparing adult and neonatal microglia, a greater fold change was observed in neonatal rather than adult microglia. Moreover, adult cortical microglial expression of *IL-1β* decreased after 6 hours of LPS stimulation (29-fold) while it remained significantly elevated in neonatal cortical microglia.

We also evaluated the expression of *IL-10* as an anti-inflammatory cytokine. LPS stimulation resulted in a significant induction in *IL-10* transcript levels in both adult and neonatal microglia (Figure 3-7 c,d and Figure 3-8 c,d respectively). Maximum LPS-induced *IL-10* mRNA expression was significant after six hours of stimulation in adult (55-fold in cortical and 70-fold in spinal cord) and neonatal (158-fold in cortical and 119-fold in spinal cord) microglia, however, a higher fold change in *IL-10* mRNA expression was observed in neonatal cortical microglia in comparison to adult cortical microglia while *IL-10* transcript levels were higher in adult spinal cord as opposed to neonatal spinal cord microglia.

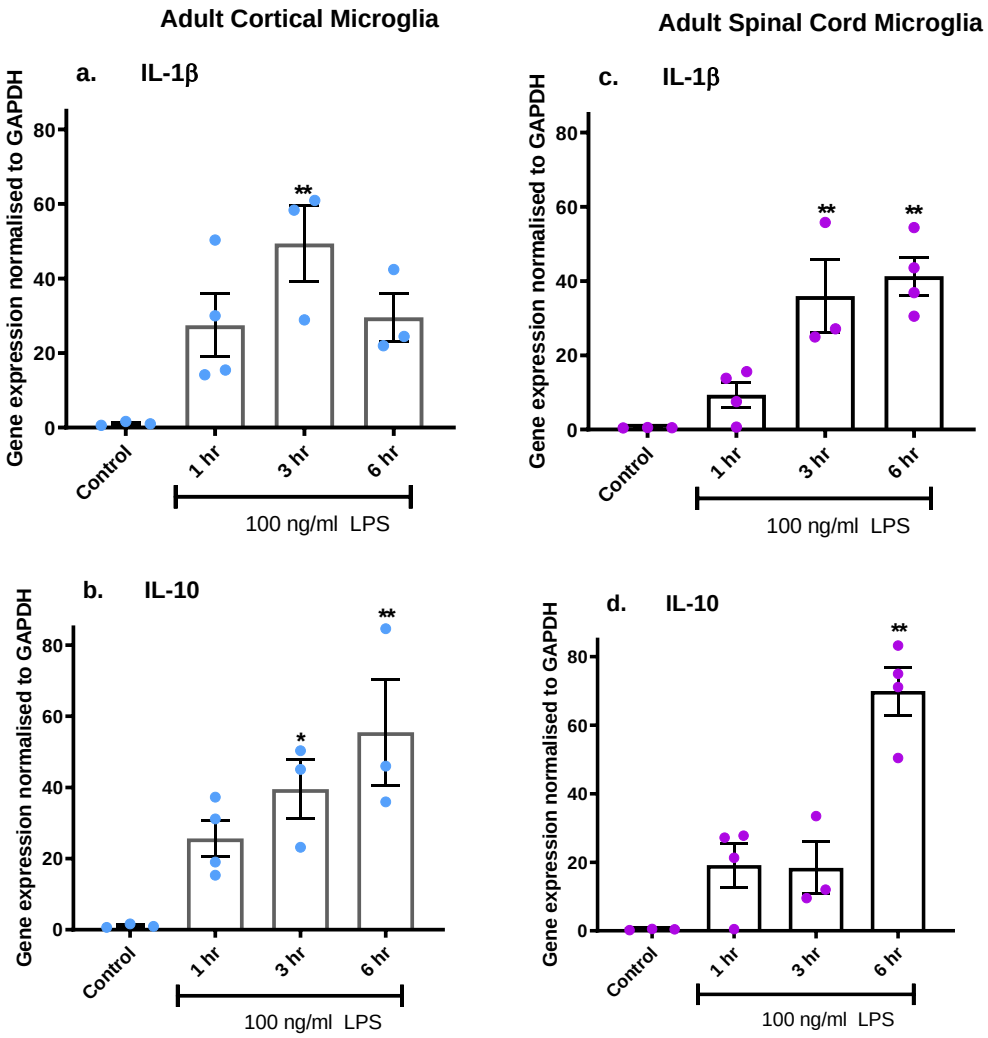

Figure 3-7 Effect of treatment with LPS on the adult microglial expression of *IL-1β* and *IL-10* mRNA. Relative expression of *IL-1β* and *IL-10* mRNA (normalised to *GAPDH* using Livak method as described in methods) in microglia isolated from adult rat forebrains **(a,b)** and spinal cords **(c,d)**. Treatment groups involved controls (vehicle-treated only), 100ng/ml LPS-treated for 1, 3 and 6 hours. Bars represent the standard error mean of the values.Statistically significant differences with controls (untreated): *p < 0.05, **p < 0.001 (one-way ANOVA followed by Bonferroni's multiple comparisons).

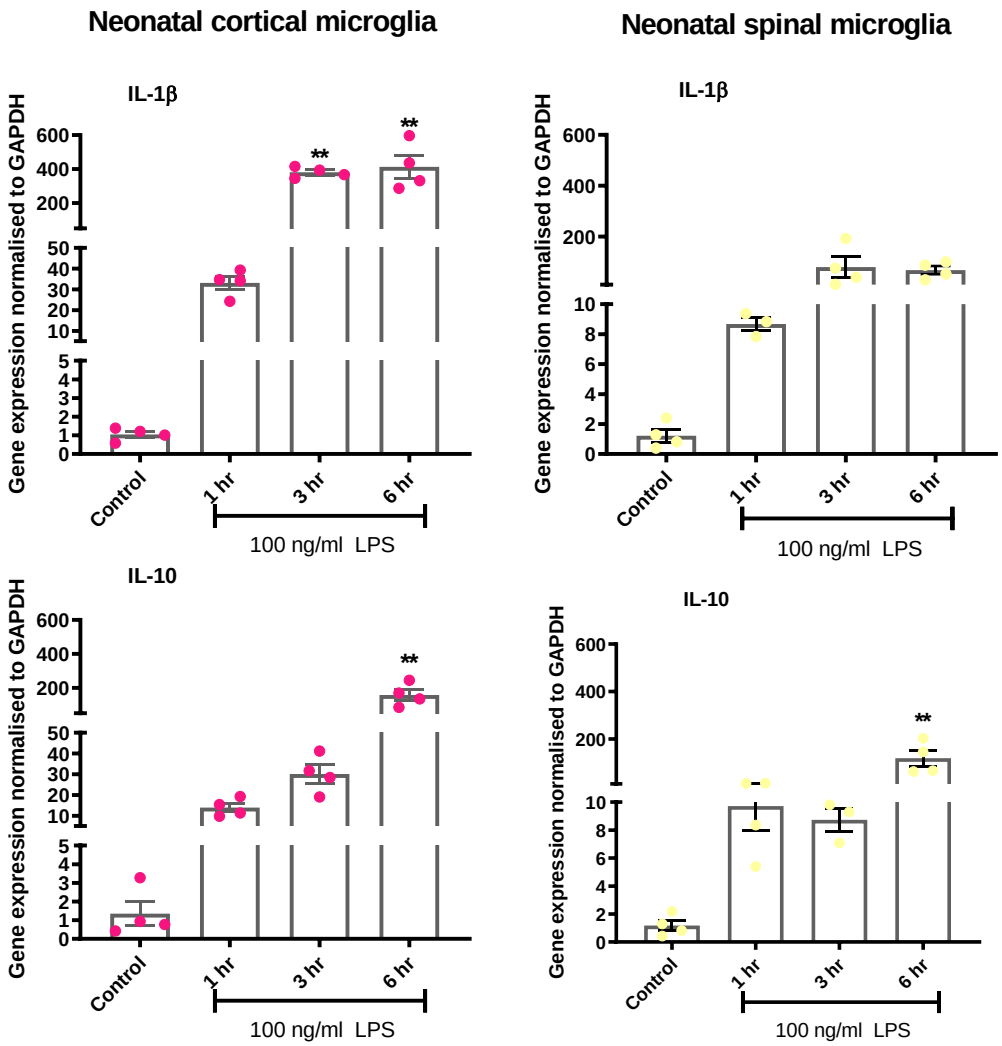

Figure 3-8 Effect of treatment with LPS on the neonatal microglial expression of *IL-1β* and *IL-10* mRNA. Relative expression of *IL-1β* and *IL-10* mRNA (normalised to *GAPDH* using Livak method as described in methods) in microglia isolated from neonatal rat forebrains **(a,b)** and spinal cords **(c,d)**. Treatment groups involved controls (untreated), 100ng/ml LPS-treated for 1, 3 and 6 hours. Bars represent the standard error mean of the values. Statistically significant differences with controls (untreated): **$p < 0.001$ (one-way ANOVA followed by Bonferroni's multiple comparisons).

Table 3-1 Summary of Relative mRNA expression of *IL-1β* and *IL-10* in response to 100 ng/ml LPS treatment of microglia

Region	Developmental stage	Gene	Treatment group	Mean relative expression of mRNA	P-value	Statistical test
Cortical microglia	Adult	*IL-1b*	LPS 1 hr	27.4	0.1034	One-way ANOVA/Bonferroni
			LPS 3 hr	49.4	0.0063	
			LPS 6 hr	29.6	0.0987	
	Neonatal		LPS 1 hr	33.1	>0.9999	
			LPS 3 hr	380.5	<0.0001	
			LPS 6 hr	413.1	<0.0001	
Spinal cord microglia	Adult		LPS 1 hr	9.3	0.8387	
			LPS 3 hr	35.9	0.0050	
			LPS 6 hr	41.3	0.0011	
	Neonatal		LPS 1 hr	8.6	>0.9999	
			LPS 3 hr	79.7	0.0930	
			LPS 6 hr	67.2	0.1849	
Cortical microglia	Adult	*IL-10*	LPS 1 hr	25.6	0.1850	
			LPS 3 hr	39.5	0.0371	
			LPS 6 hr	55.5	0.0051	
	Neonatal		LPS 1 hr	13.9	>0.9999	
			LPS 3 hr	30.1	0.7602	
			LPS 6 hr	158.4	<0.0001	
Spinal cord microglia	Adult		LPS 1 hr	19.1	0.1992	
			LPS 3 hr	18.3	0.2866	
			LPS 6 hr	69.9	<0.0001	
	Neonatal		LPS 1 hr	9.7	>0.9999	
			LPS 3 hr	8.7	>0.9999	
			LPS 6 hr	118.9	0.0019	

3.3.4 LPS-induces *Nur77* and *NOR-1* mRNA expression rapidly in primary microglia

Pro-inflammatory cytokine expression increases through the activation of the NF-kB pathway. Orphan nuclear receptors have a unique mechanism in interfering with the NF-kB pathway and consequently diminishing pro-inflammatory cytokine expression in the event of LPS-

induced microglial activation, hence modulating inflammation (Saijo et al., 2013). In this study, we used LPS to trigger microglial activation to evaluate NR4As expression in microglia isolated from different CNS regions (forebrain and spinal cord) and also to investigate any potential differences in response between adult and neonatal microglia. Here, we show a significant upregulation in *Nurr7* and *NOR-1* mRNA expression in response to LPS-induced microglial activation; however, such response suggested both developmental and regional heterogeneity.

Firstly, concerning regional differences, *NOR-1* transcript levels increased upon one hour of LPS stimulation in adult cortical microglia (5-fold). Such response was not observed in adult spinal cord microglia; nevertheless, LPS-induced *NOR-1* upregulation was noticeable after twenty-four hours of stimulation in both adult cortical (15-fold) and spinal cord microglia (17-fold). Similarly, *Nur77* transcript levels were significantly increased after one hour of LPS stimulation in adult cortical microglia (8-fold), but not in adult spinal cord microglia (Figure 3-9). Unlike *NOR-1*, LPS did not induce *Nur77* mRNA expression after twenty-four hours in adult microglia.

Interestingly, neonatal microglia response to LPS (Figure 3-10) was more similar than adult microglia (Figure 3-9). For instance, in neonatal cortical and spinal cord microglia, LPS-induction of *Nur77* was observed after one hour (5-fold in cortical and spinal cord) and three hours (3-fold in cortical and 5-fold in spinal cord) of stimulation, however, due to variability

in values of spinal cord microglia the differences were not statistically significant. On the other hand, the up-regulation of *NOR-1* transcript levels after LPS stimulation was significant after three hours of stimulation in both neonatal cortical (57-fold) and spinal cord microglia (98-fold). *NOR-1* mRNA expression gradually decreased after six hours of LPS stimulation in cortical (26-fold) and spinal cord (16-fold) microglia

Importantly, LPS induced death in neonatal microglia after twenty-four hours of stimulation, unlike adult microglia. This conclusion was based on morphological observations and low RNA and protein levels of housekeeping genes.

Intriguingly, differential regional and developmental expression levels were observed in unstimulated microglia. Although LPS induced higher transcript levels of *NOR-1* and *Nur77* in neonatal microglia compared to adult microglia, adult spinal cord microglia showed significantly higher basal levels of *Nur77* mRNA (0.0008) In contrast to neonatal spinal cord microglia (0.0002) (Figure 3-11 b). On the other hand, basal levels of *Nur77* mRNA were higher in neonatal cortical microglia (0.001) than adult cortical (0.0003) microglia while *NOR-1* transcript levels were similar in neonatal (0.0004) and adult cortical (0.0005) microglia. Moreover, basal levels of *NOR-1* mRNA were significantly higher in neonatal spinal cord (0.4) than adult spinal cord (0.0008) microglia.

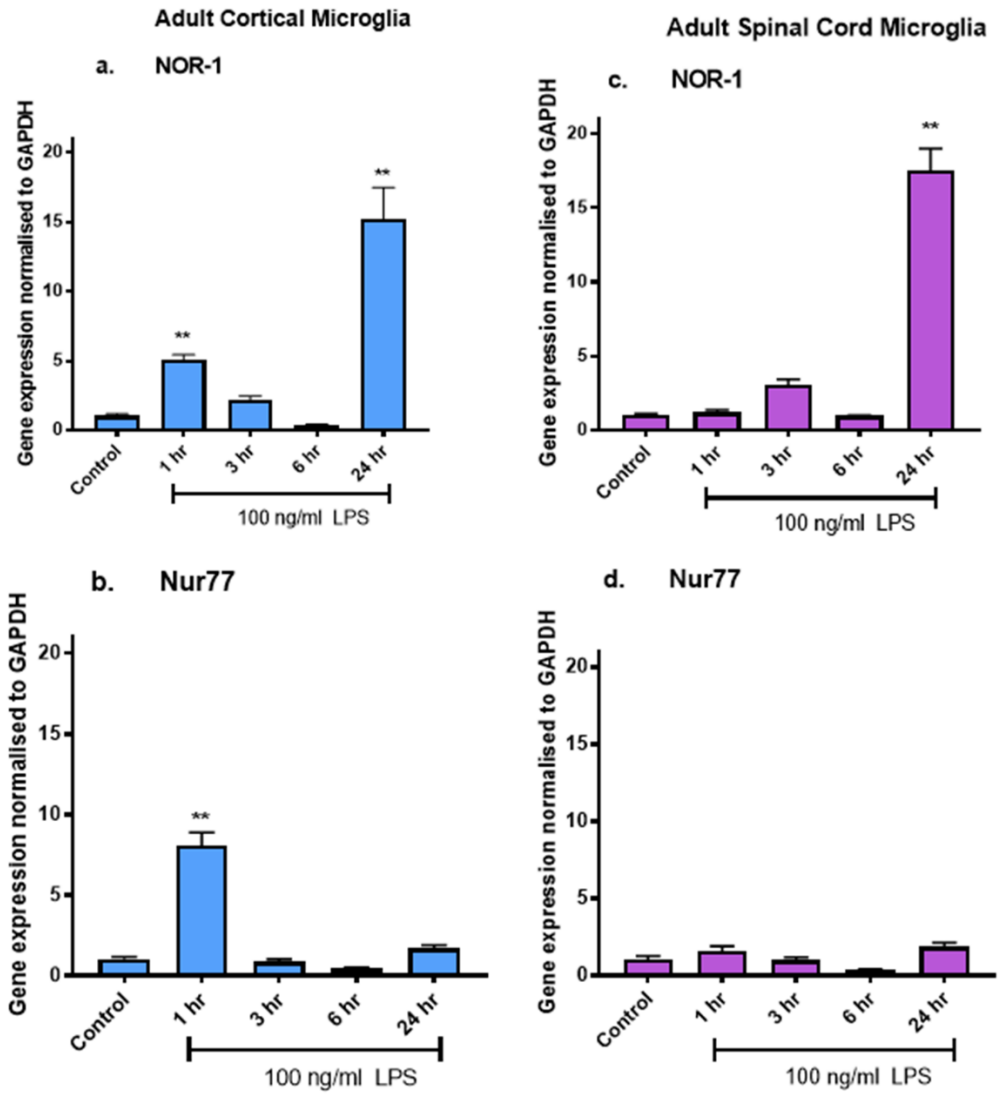

Figure 3-9 Effect of treatment with LPS on the adult microglial expression of *Nur77* and *NOR-1* mRNA. Relative expression of *Nur77* and *NOR-1* mRNA (normalised to *GAPDH* using Livak method as described in methods) in microglia isolated from adult rat forebrains **(a,b)** and spinal cords **(c,d)**. Treatment groups involved controls (untreated), 100ng/ml LPS-treated for 1, 3, 6 and 24 hours. Bars represent the standard error mean of the values n=4. Statistically significant differences with controls (untreated): **$p < 0.001$ (one-way ANOVA followed by Bonferroni's multiple comparisons).

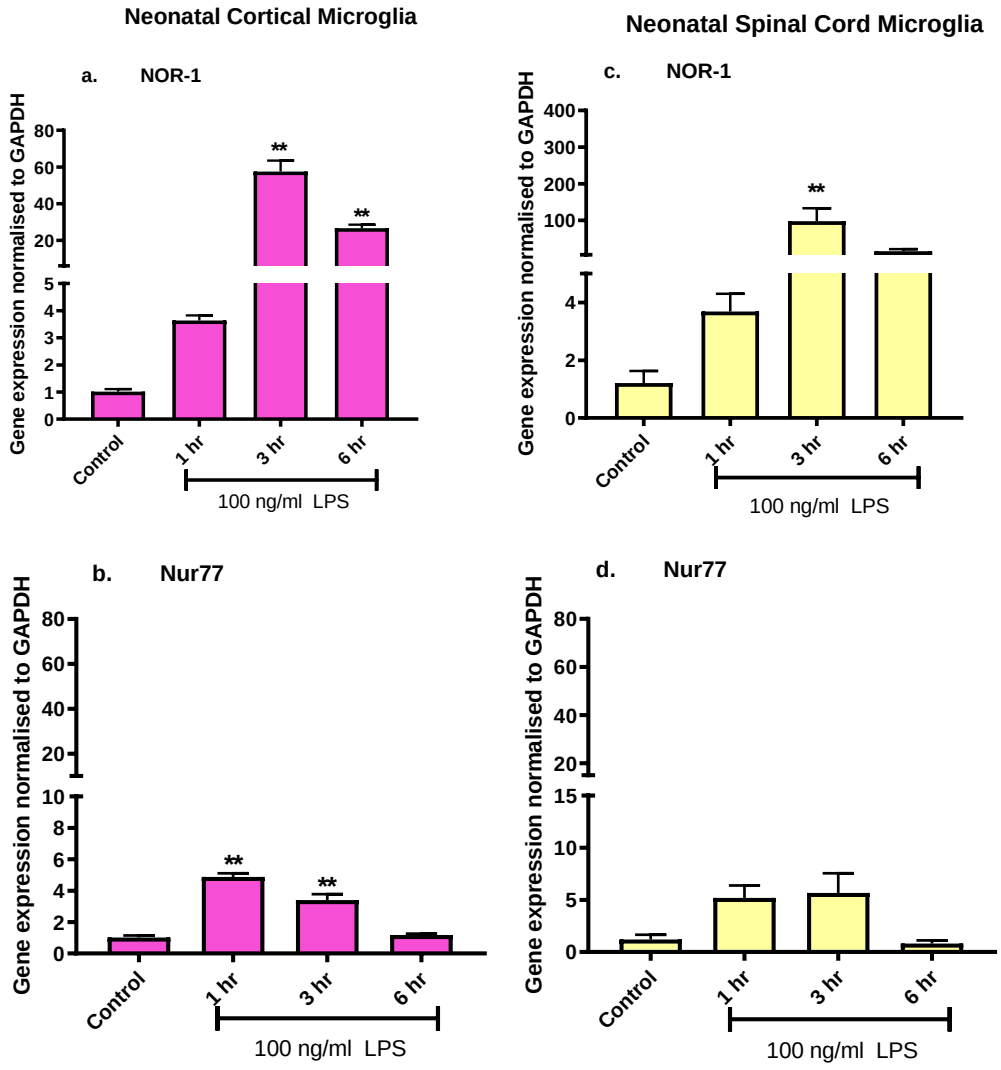

Figure 3-10 Effect of treatment with LPS on the neonatal microglial expression of *Nur77* and *NOR-1* mRNA. Relative expression of *Nur77* and *NOR-1* mRNA (normalised to *GAPDH* using Livak method as described in methods) in microglia isolated from neonatal rat forebrains **(a,b)** and spinal cords **(c,d)**. Treatment groups involved controls (untreated), 100ng/ml LPS-treated for 1, 3, 6 and 24 hours. Bars represent the standard error mean of the values n=4. Statistically significant differences with controls (untreated): **p < 0.001 (one-way ANOVA followed by Bonferroni's multiple comparisons).

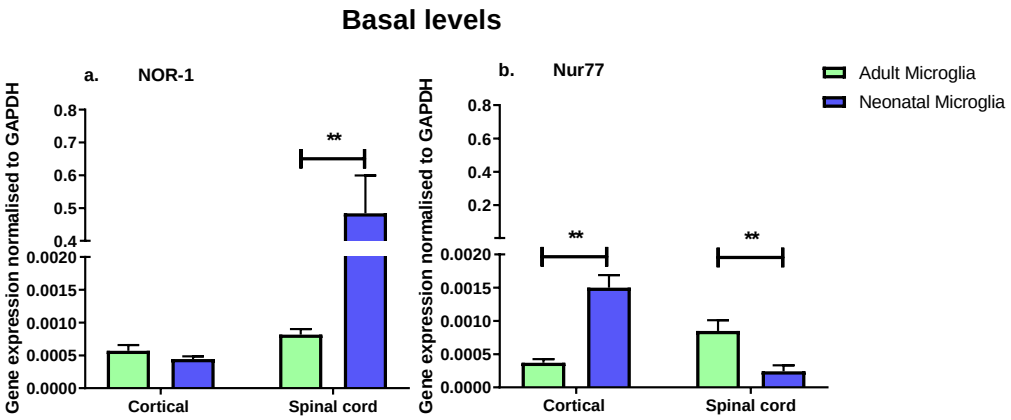

Figure 3-11 Regional and developmental heterogeneity concerning *NOR-1* and *Nur77* transcript levels. Basal mRNA levels of (a) *NOR-1* and (b) *Nur77* (normalised to *GAPDH*) in untreated microglia isolated from adult or neonatal rat forebrains and spinal cords. Bars represent the standard error mean of the values n=4. Statistically significant differences between adult and neonatal microglia: **$p < 0.001$ (Multiple t-tests).

Table 3-2 Summary of Relative mRNA expression of *Nur77* and *NOR-1* in response to 100 ng/ml LPS treatment of microglia

Region	Developmental stage	Gene	Treatment group	Mean relative expression of mRNA	P-value	Statistical test
Cortical microglia	Adult	*Nur77*	LPS 1 hr	8.1	<0.0001	One-way ANOVA/Bonferroni
			LPS 3 hr	0.8	>0.9999	
			LPS 6 hr	0.4	0.7815	
			LPS 24 hr	1.6	0.7043	
	Neo-natal		LPS 1 hr	4.8	<0.0001	
			LPS 3 hr	3.4	<0.0001	
			LPS 6 hr	1.1	>0.9999	
Spinal cord microglia	Adult		LPS 1 hr	1.5	0.4298	
			LPS 3 hr	0.9	>0.9999	
			LPS 6 hr	0.3	0.1698	
			LPS 24 hr	1.8	0.0777	
	Neo-natal		LPS 1 hr	5.1	0.0941	
			LPS 3 hr	5.6	0.0550	
			LPS 6 hr	0.8	>0.9999	
Cortical microglia	Adult	*NOR-1*	LPS 1 hr	5.1	0.0095	
			LPS 3 hr	2.2	>0.9999	
			LPS 6 hr	0.3	>0.9999	
			LPS 24 hr	15.2	<0.0001	
	Neo-natal		LPS 1 hr	3.6	>0.9999	
			LPS 3 hr	57.4	<0.0001	
			LPS 6 hr	26.5	0.0003	
Spinal cord microglia	Adult		LPS 1 hr	1.1	>0.9999	
			LPS 3 hr	3.0	0.2293	
			LPS 6 hr	0.9	>0.9999	
			LPS 24 hr	17.5	<0.0001	
	Neo-natal		LPS 1 hr	3.6	>0.9999	
			LPS 3 hr	98.1	0.0066	
			LPS 6 hr	16.2	>0.9999	

3.3.5 LPS-induces Nur77 protein expression rapidly in primary cortical microglia

Nur77 protein expression was evaluated with respect to a higher dose of LPS (1µg/ml) used for treatment at different time points in both neonatal and adult cortical microglia. As shown in Figure 3-12, LPS-induced Nur77 protein expression increased after three hours of LPS stimulation in

comparison to untreated controls in neonatal cortical microglia. Adult cortical microglia protein profiles differed in which the expression of Nur77 protein was not detectable in the blot whereas β-actin, an endogenous control, protein expression remained constant throughout LPS treatment, except for twenty-four hours of LPS stimulation where β-actin protein levels were affected in both neonatal and adult microglia. As mentioned earlier, LPS-induced cytotoxicity was also observed with a lower concentration of LPS after twenty-four hours of stimulation.

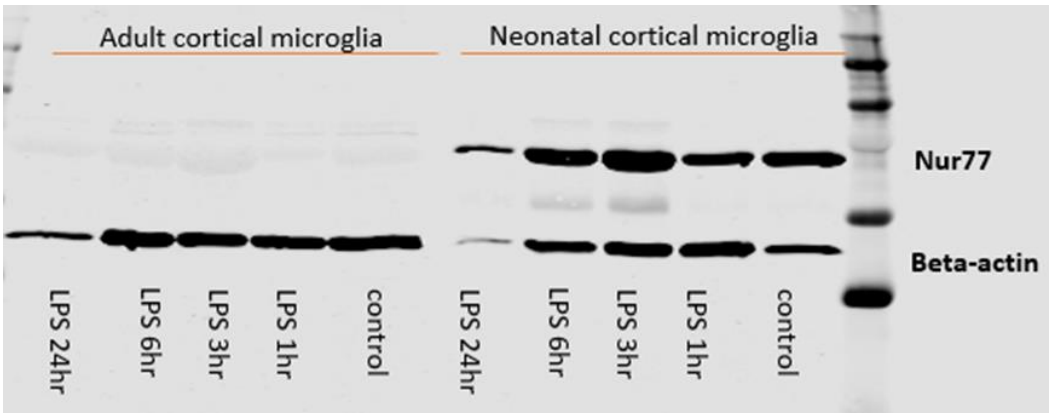

Figure 3-12 Immunoblot showing Nur77 protein expression in neonatal and adult cortical microglia treated with 1µg/ml LPS. Treatment groups include controls (vehicle-only treated microglia), LPS-treated for 1, 3, 6 and 24 hours. Top bands correspond to Nur77 (~64 kDa) while lower bands correspond to β-actin (~43 kDa).

3.3.6 LPS-induces IL-1β release in primary microglia

As we were interested in evaluating the effect of activated microglia secretome on astrocytes, here we evaluated the state of microglia in response to LPS stimulation through measuring IL-1β release via ELISA. In chapter two, we described our method for LPS stimulation of microglia for six hours to collect conditioned media. Our approach ensured the removal of LPS from the media to investigate the effect of activated microglia rather than LPS-induced toxicity on astrocytes. Here we confirm a significant release of IL-1β from activated microglia as a result of LPS stimulation.

In adult cortical microglia, a significant release of IL-1β was observed by microglia treated with LPS for six hours (127 pg/ml, MCM was not used for astrocyte stimulation) and by microglia treated with LPS for six hours, washed and then incubated with fresh media for a further eighteen hours for a total of twenty-four hours since LPS stimulation (141 pg/ml, MCM used for astrocyte stimulation) (Figure 3-13, left).

Although IL-1β release was significant in both LPS-treated groups in neonatal cortical microglia, LPS-treatment for a total of twenty-four hours (where LPS was removed) showed higher levels of IL-1β release (188 pg/ml) than microglia treated with LPS for six hours (119 pg/ml) (Figure 3-13, right).

LPS stimulation also caused a significant release of IL-1β from spinal cord microglia (Figure 3-14). The release of the pro-inflammatory cytokine

appears to be lower in LPS-treated neonatal spinal cord microglia (233 pg/ml) in comparison to LPS-treated adult spinal cord microglia (305 pg/ml).

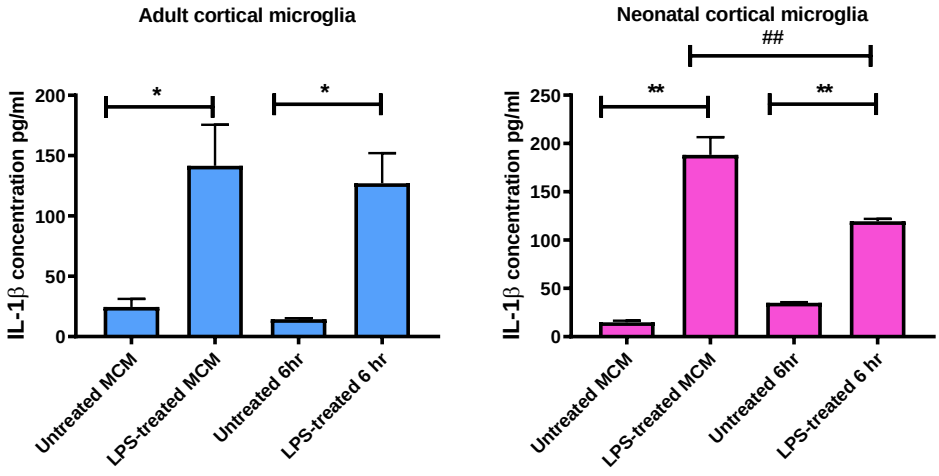

Figure 3-13 Effect of treatment with 100ng/ml LPS on cortical adult or neonatal microglial release of IL-1β in serum-rich media. The concentration of IL-1β released into the supernatant of cultured cortical adult (left) or neonatal (right) microglia in response to LPS treatment. Treatment groups involved controls (untreated MCM used to stimulate astrocytes), LPS-treated MCM (used for astrocytes stimulation), controls (untreated MCM for 6 hours) and LPS-treated MCM for 6 hours. Bars represent the standard mean of error (SEM) n=3. Statistically significant differences with untreated controls: *****p < 0.05, **p < 0.001; statistical differences with LPS-treated: ##p < 0.001. (one-way ANOVA followed by multiple comparisons).

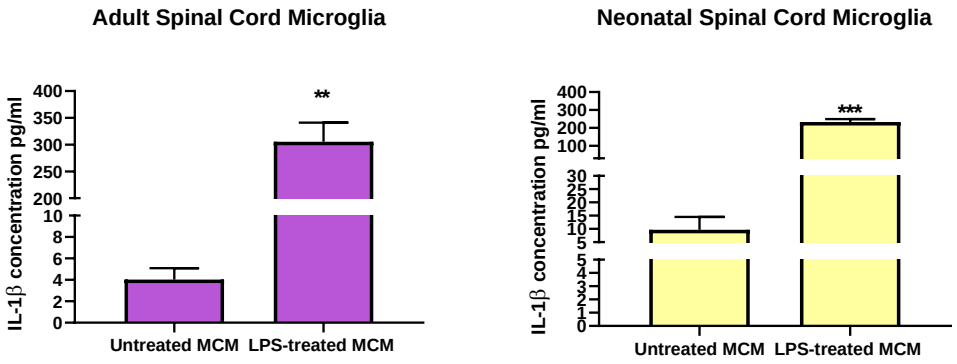

Figure 3-14 Effect of treatment with 100ng/ml LPS on spinal cord adult or neonatal microglial release of IL-1β in serum-rich media. The concentration of IL-1β released into the supernatant of cultured spinal cord adult (left) or neonatal (right) microglia in response to LPS treatment. Treatment groups involved controls (untreated MCM used to stimulate astrocytes) and LPS-treated MCM (used for astrocytes stimulation). Bars represent the standard mean of error (SEM) n=3. Statistically significant differences with untreated controls: *****p < 0.05, **p < 0.001; statistical differences with LPS-treated: ##p < 0.001. (t-test).

3.3.7 Astrocyte expression of Nurr1 and splice variants

Neurotoxicity is often associated with overactivation of microglia and astrocytes and the resultant continuous expression of inflammatory genes regulated by NF-$_k$B (Liddelow et al., 2017a). Potentially, pharmacological targetting of Nurr1 in astrocytes can attenuate the expression of NF-kB regulated genes (Popichak et al., 2018); therefore, more research is essential to understand Nurr1 structure. Nurr1 structure contains two activation function- (AF-) domains, AF-1 in the N-terminal region while AF-2 in the LBD region near the C-terminal (Wang et al., 2003). Previously, different Nurr1 isoforms (splice variants) have been identified in dopaminergic neurons. One of these is the transcriptionally inducible nuclear receptor (TINUR) that possess a truncated AF-1 domain due to alternative

splicing in exon 3. Another one lacks the C-terminus due to alternative splicing in exon 7 (AF-2/LBD) and is known as Nurr1a. Importantly, full-length Nurr1 is suggested to activate transcription more than Nurr1 isoforms (Michelhaugh et al., 2005). Moreover, in our lab, differential developmental expression of Nurr1 splice variants (Nurr1a and TINUR) has been recognised in primary rat microglia (Imraish, 2018). However, the astrocytic expression of these variants has not been explored yet. PCR amplification of full-length Nurr1 in neonatal cortical astrocytes showed a potential expression of at least one Nurr1 splice variant (Figure 3-15). Although cloning has not been performed to identify the splice variant, qPCR analysis confirmed the expression of TINUR and Nurr1a in both cortical and spinal cord neonatal astrocytes. Further studies are needed to assess their transcriptional activities in astrocytes.

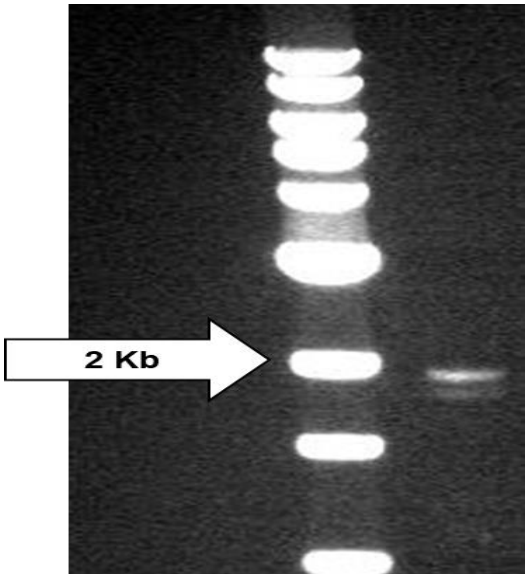

Figure 3-15 Potential Nurr1 splice variant in neonatal cortical astrocytes. Agarose gel electrophoresis (0.7%) displaying full-length cDNA of Nurr1 and Nurr1 splice variant(s) expressed by unstimulated Astrocytes. 1 Kb ladder has been used. Corresponding bands are about 2000 bp.

3.3.8 Effect of treatment with LPS-stimulated serum-rich MCM on spinal cord astrocytes' expression of *Nur77*, *NOR-1*, *Nurr1*, *TINUR*, *Nurr1a, IL-1β, and TGF-β* mRNA

Liddelow and colleagues, (2017) reported that LPS triggers postnatal microglia (both *in vivo* and *in vitro*) to produce pro-inflammatory mediators (e.g. TNF-α, IL-1α and C1q). Consequently, activated microglia induced a neurotoxic A1 phenotype in astrocytes resulting in neuronal death (Liddelow et al., 2017a). In the present study, we stimulated isolated microglia (adult or neonatal) from rats' forebrains or spinal cords with LPS. Then, to understand how activated microglia communicate with astrocytes, we stimulated neonatal rat (cortical or spinal cord) astrocytes correspondingly with either un-treated MCM or LPS-stimulated MCM for different periods (one, three, six and twenty-four hours). We investigated the expression of orphan nuclear receptors in astrocytes post-stimulation with MCM. Next, we evaluated the expression of the pro-inflammatory cytokine *IL-1β* or the anti-inflammatory cytokine *TGF-β* in astrocytes.

Firstly, we focused on comparing adult with neonatal spinal cord astrocytes in terms of adult and neonatal spinal cord MCM stimulation. Our results showed a significant increase in astrocytes expression of *Nurr1* (adult-MCM; 13-fold, neonatal-MCM: 7-fold) mRNA and its variants (*Nurr1a* and *TINUR*) after twenty-four hours of LPS treated-MCM stimulation in comparison to controls (untreated astrocytes) or astrocytes stimulated with non-treated MCM (see Figure 3-16). Stimulating astrocytes with LPS-

stimulated adult-spinal cord MCM increased Nurr1 mRNA expression in astrocytes more than LPS-stimulated neonatal spinal cord MCM.

Similarly, *Nur77* transcript levels were induced twenty-four hours after stimulation with LPS treated-MCM (Figure 3-17 a,c). Interestingly, Adult untreated-MCM significantly induced the expression of *Nur77* mRNA (9-fold), an effect similar to twenty-four hours stimulated-MCM. This effect was also observed in astrocytes stimulated with neonatal un-treated MCM (7-fold); however, three hours of neonatal LPS treated-MCM stimulation significantly induced *Nur77* mRNA levels (10-fold). Such induction of *Nur77* expression was increased after twenty-four hours of stimulation (15-fold).

The third subfamily member of NR4A, *NOR-1* mRNA levels were also upregulated after twenty-four hours of LPS-treated MCM stimulation. Adult LPS-treated spinal cord MCM increased *NOR-1* mRNA by 70 folds in astrocytes whereas LPS-stimulated neonatal MCM induced *NOR-1* mRNA levels by 57 folds (Figure 3-17 b,d)

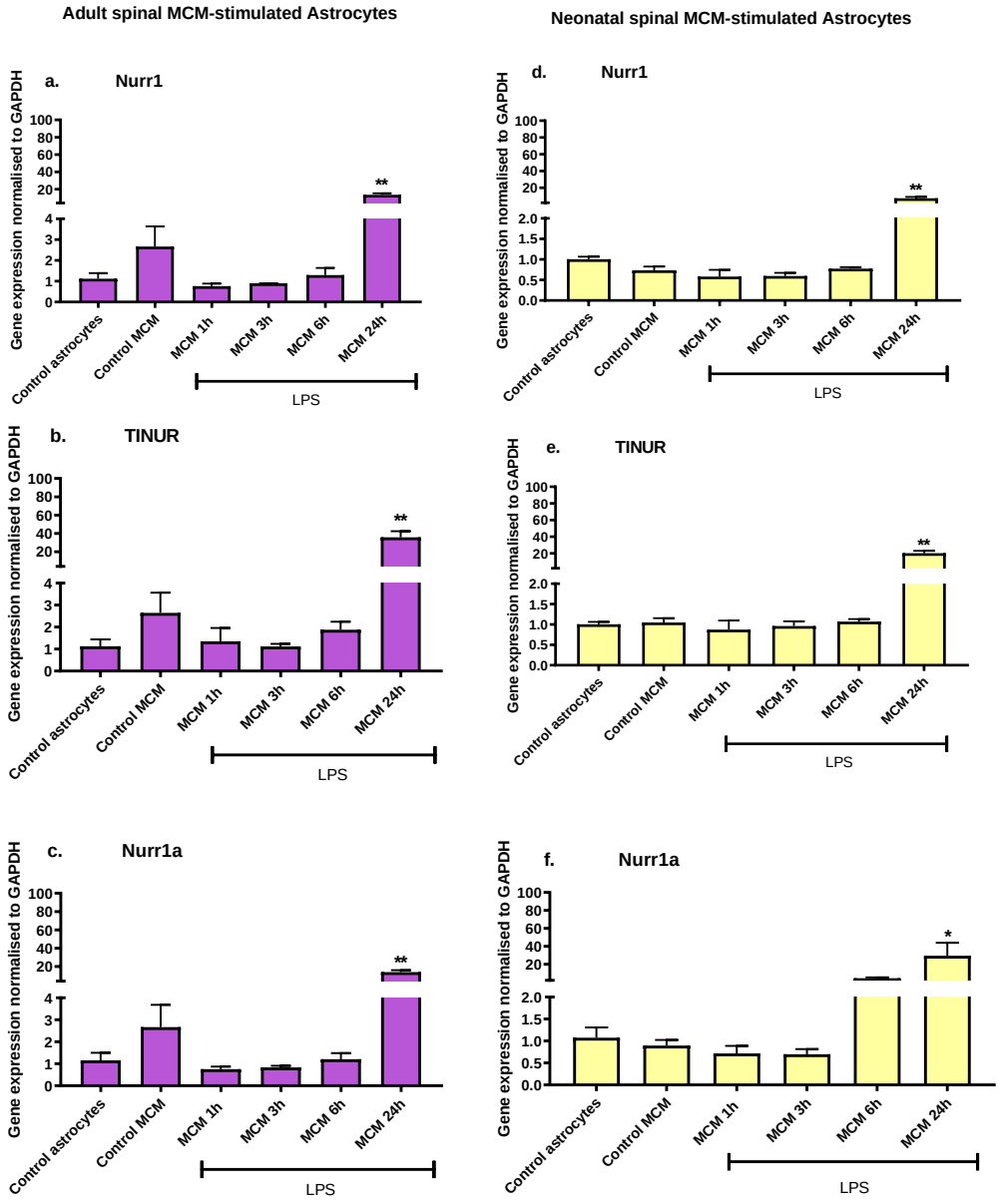

Figure 3-16 **Effect of treatment with LPS-stimulated adult (a-c) or neonatal (d-f) spinal cord MCM on neonatal spinal cord astrocytes expression of *Nurr1*, *TINUR* and *Nurr1a* mRNA.** Relative expression of *Nurr1*, *TINUR* and *Nurr1a* mRNA (normalised to *GAPDH following the Livak method*) in astrocytes isolated from neonatal rat spinal cord. Treatment groups involved control astrocytes (untreated astrocytes), control MCM (1:1; untreated MCM: untreated astrocytes), MCM stimulation for 1, 3, 6 and 24h. Bars represent the mean S.E.M of the values n=4. Statistically significant differences with control astrocytes: *p< 0.05, **p < 0.001. (one-way ANOVA followed by Bonferroni's multiple comparisons).

Altogether, orphan nuclear receptors expression significantly increased in spinal cord astrocytes after twenty-four hours of stimulation, regardless of the developmental stage of LPS-treated microglia. Importantly, Induction of *NOR-1* expression was the highest in spinal cord astrocytes in comparison to *Nurr1* or *Nur77.*

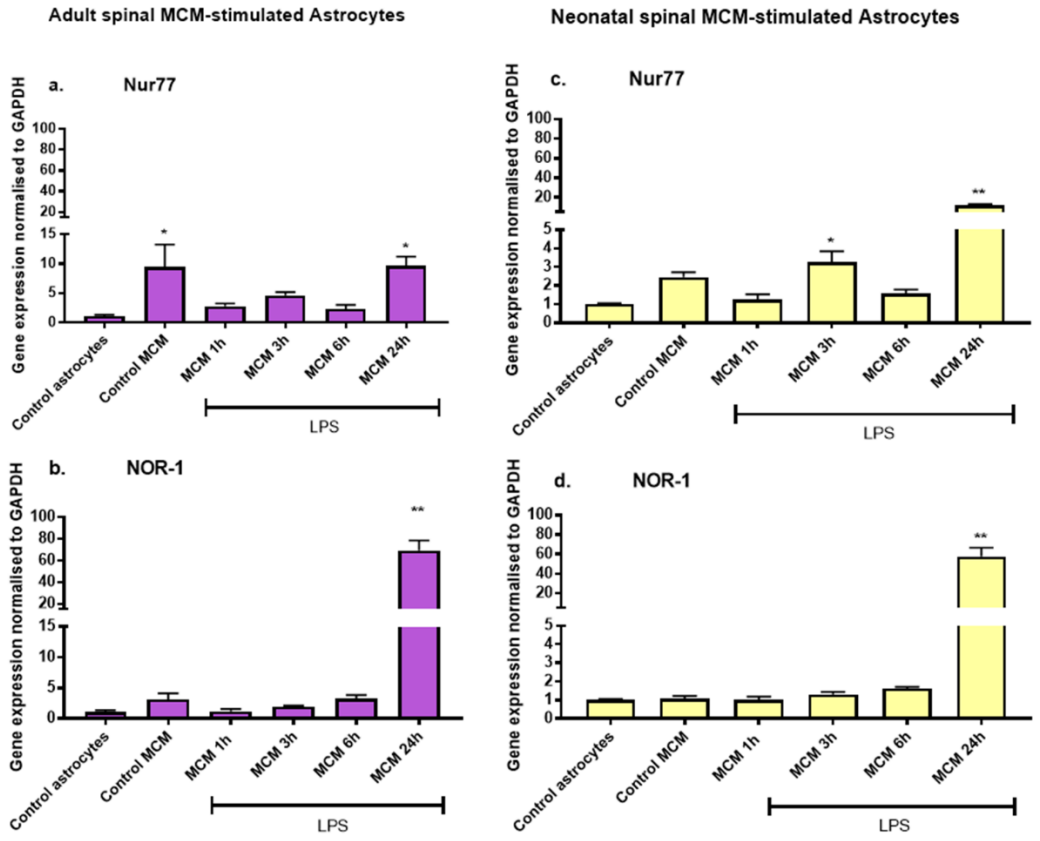

Figure 3-17 Effect of treatment with LPS-stimulated adult (a-b) or neonatal (c-d) spinal cord MCM on neonatal spinal cord astrocytes expression of *Nur77* and *NOR-1* mRNA. Relative expression of *Nur77* and *NOR-1* mRNA (normalised to *GAPDH* following the Livak method) in astrocytes isolated from neonatal rat spinal cord. Treatment groups involved control astrocytes (untreated astrocytes), control MCM (1:1; untreated MCM: untreated astrocytes), MCM stimulation for 1, 3, 6 and 24h. Bars represent the mean S.E.M of the values n=4. Statistically significant differences with control astrocytes: *p< 0.05, **p < 0.001. (one-way ANOVA followed by Bonferroni's multiple comparisons).

Since high levels of pro-inflammatory cytokine transcripts is a characteristic of A1 astrocytes, we investigated the expression of *IL-1β* mRNA after MCM stimulation. As seen in (Figure 3-18), treating astrocytes with both adult and neonatal spinal cord MCM significantly induced the expression of *IL-1β* (111-fold and 60-fold, respectively) after twenty-four hours of treated-MCM stimulation. Markedly, un-treated neonatal MCM upregulated the expression of *IL-1β* mRNA levels (3-fold) in astrocytes. However, adult treated-MCM's induction of *IL-1β* transcript levels is more robust than neonatal treated-MCM effect.

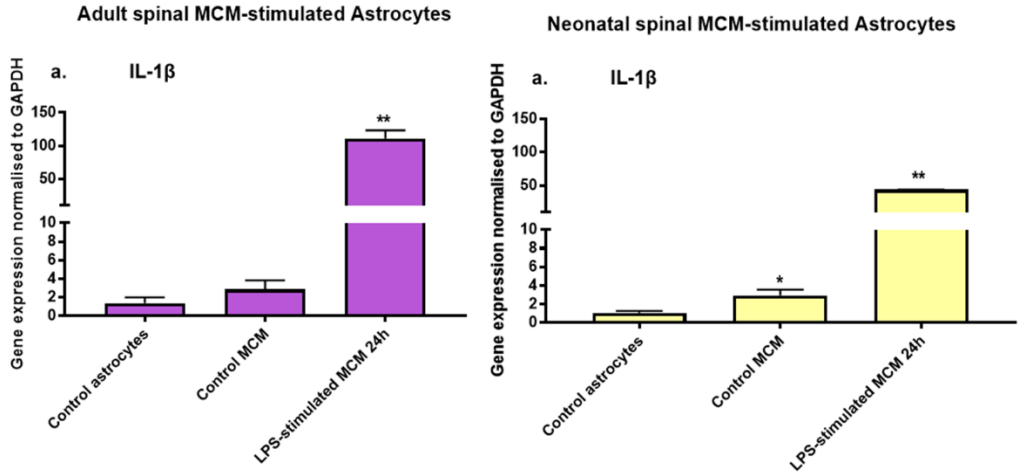

Figure 3-18 Effect of treatment with LPS-stimulated adult (a-b) or neonatal (c-d) spinal cord MCM on neonatal spinal cord astrocytes expression of *IL-1β* mRNA. Relative expression of *IL-1β* mRNA (normalised to *GAPDH* following the Livak method) in astrocytes isolated from neonatal rat spinal cord. Treatment groups involved control astrocytes (untreated astrocytes), control MCM (1:1; untreated MCM: untreated astrocytes), MCM stimulation for 1, 3, 6 and 24h. Bars represent the mean S.E.M of the values n=4. Statistically significant differences with control astrocytes: *p< 0.05, **p < 0.001. (one-way ANOVA followed by Bonferroni's multiple comparisons).

While changes were observed in *IL-1β* mRNA levels in response to MCM-stimulation, TGF-β expression (Figure 3-19) was not affected by adult or neonatal MCM treatment.

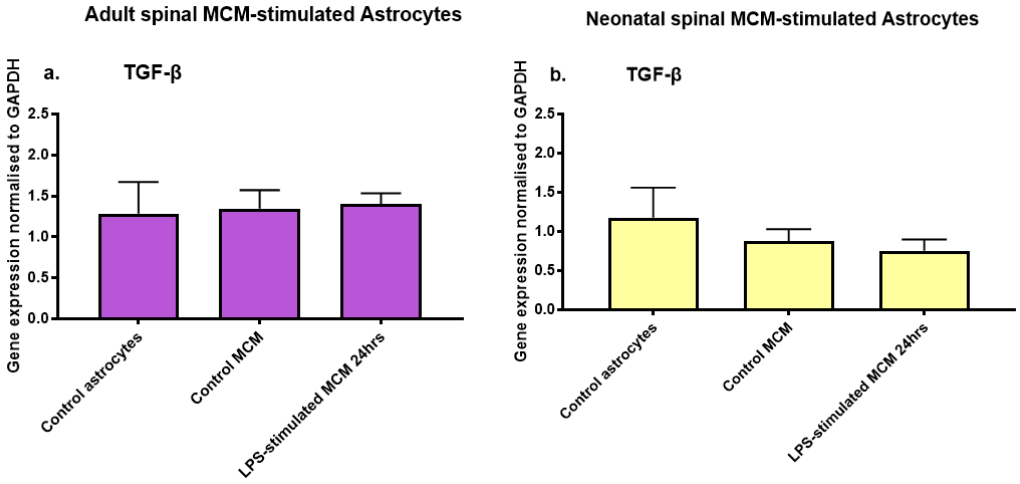

Figure 3-19 Effect of treatment with LPS-stimulated adult (a-b) or neonatal (c-d) spinal cord MCM on neonatal spinal cord astrocytes expression of *TGF-β* mRNA. Relative expression of *TGF-β* mRNA (normalised to *GAPDH* following the Livak method) in astrocytes isolated from neonatal rat spinal cord. Treatment groups involved control astrocytes (untreated astrocytes), control MCM (1:1; untreated MCM: untreated astrocytes), MCM stimulation for 1, 3, 6 and 24h. Bars represent the mean S.E.M of the values n=4. (one-way ANOVA followed by Bonferroni's multiple comparisons).

Secondly, we investigated the expression of NR4As and cytokines in cortical astrocytes in response to adult or neonatal cortical MCM stimulation. Resembling spinal cord MCM, both adult and neonatal treated-MCM upregulated the expression of *Nurr1* (52-fold and 32-fold, respectively) and its variants after twenty-four hours in astrocytes (Figure 3-20).

Moreover, *Nur77* mRNA levels increased in astrocytes treated with adult (64-fold) or neonatal (80-fold) LPS-stimulated MCM after twenty-four hours (Figure 3-21 a,c). Un-treated neonatal-MCM increased the mRNA expression of *Nur77* (90-fold) in astrocytes in a higher manner than untreated adult MCM (15-fold) or LPS-treated neonatal MCM. Furthermore, stimulating astrocytes with LPS treated-MCM for three hours significantly upregulated the expression of *Nur77* (adult LPS-stimulated MCM 55-fold and neonatal LPS-stimulated MCM 60-fold) in a similar manner to LPS-treated MCM for twenty-four hours.

Like the other NR4A subfamily members, *NOR-1* transcript levels were induced after twenty-four hours of treatment with LPS-stimulated adult (155-fold) or neonatal MCM (115-fold) as shown in Figure 3-21 b,d.

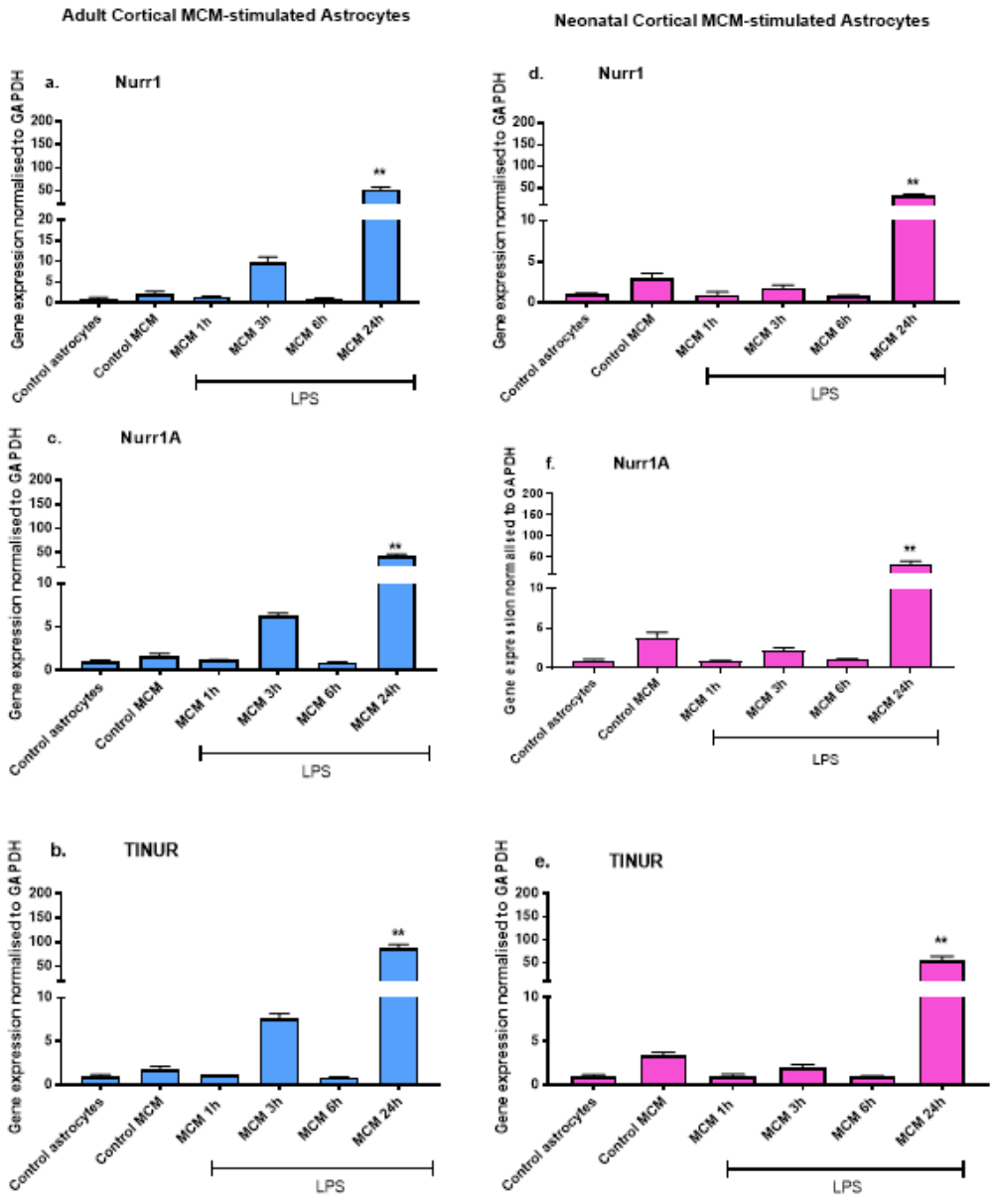

Figure 3-20 Effect of treatment with LPS-stimulated adult (a-c) or neonatal (d-f) cortical MCM on neonatal cortical astrocytes expression of *Nurr1*, *TINUR* and *Nurr1a* mRNA. Relative expression of *Nurr1*, *TINUR* and *Nurr1a* mRNA (normalised to *GAPDH* following the Livak method) in astrocytes isolated from neonatal rat forebrains. Treatment groups involved control astrocytes (untreated astrocytes), control MCM (1:1; untreated MCM: untreated astrocytes), MCM stimulation for 1, 3, 6 and 24h. Bars represent the mean S.E.M of the values n=4. Statistically significant differences with control astrocytes: **$p < 0.001$. (one-way ANOVA followed by Bonferroni's multiple comparisons).

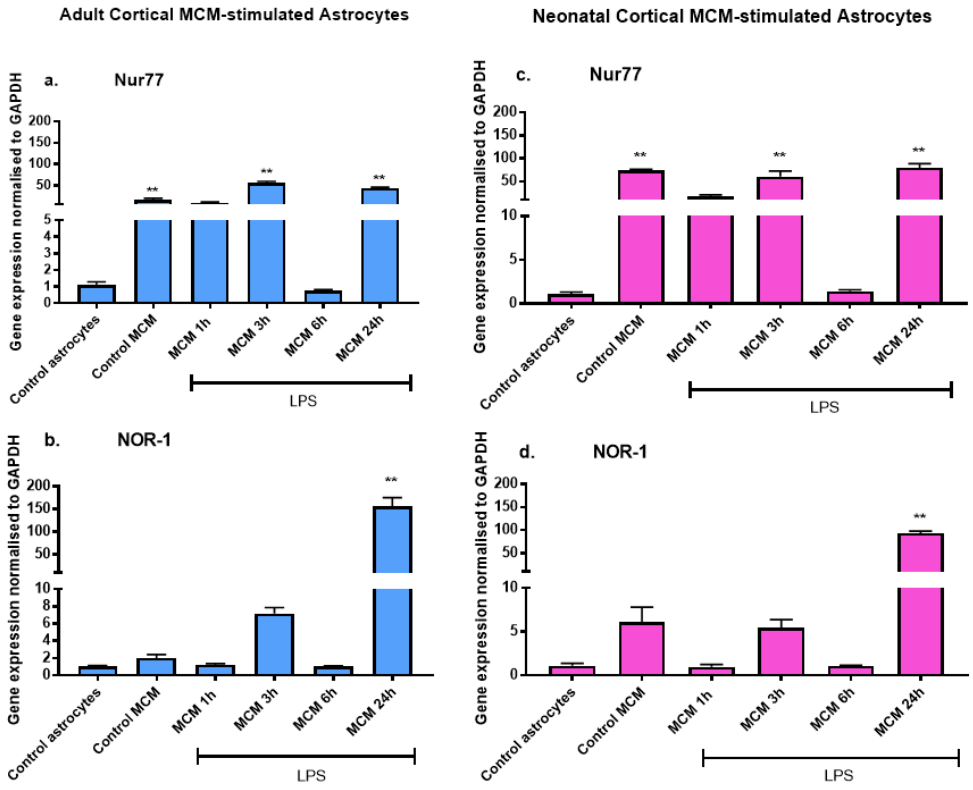

Figure 3-21 Effect of treatment with LPS-stimulated adult (a-b) or neonatal (c-d) cortical MCM on neonatal cortical astrocytes expression of *Nur77* and *NOR-1* mRNA. Relative expression of *Nur77* and *NOR-1* mRNA (normalised to *GAPDH* following the Livak method) in astrocytes isolated from neonatal rat forebrains. Treatment groups involved control astrocytes (untreated astrocytes), control MCM (1:1; untreated MCM: untreated astrocytes), MCM stimulation for 1, 3, 6 and 24h. Bars represent the mean S.E.M of the values n=4. Statistically significant differences with control astrocytes: **p < 0.001. (one-way ANOVA followed by Bonferroni's multiple comparisons).

Both spinal cord and cortical LPS-stimulated MCM have a similar effect on astrocytes in which *IL-1β* expression was significantly upregulated after twenty-four hours of stimulation (Figure 3-22). In addition, adult LPS-stimulated MCM highly upregulated *IL-1β* mRNA (53-fold) levels in astrocytes compared to *IL-1β* mRNA (12-fold) levels expressed by astrocytes stimulated with neonatal LPS-stimulated MCM.

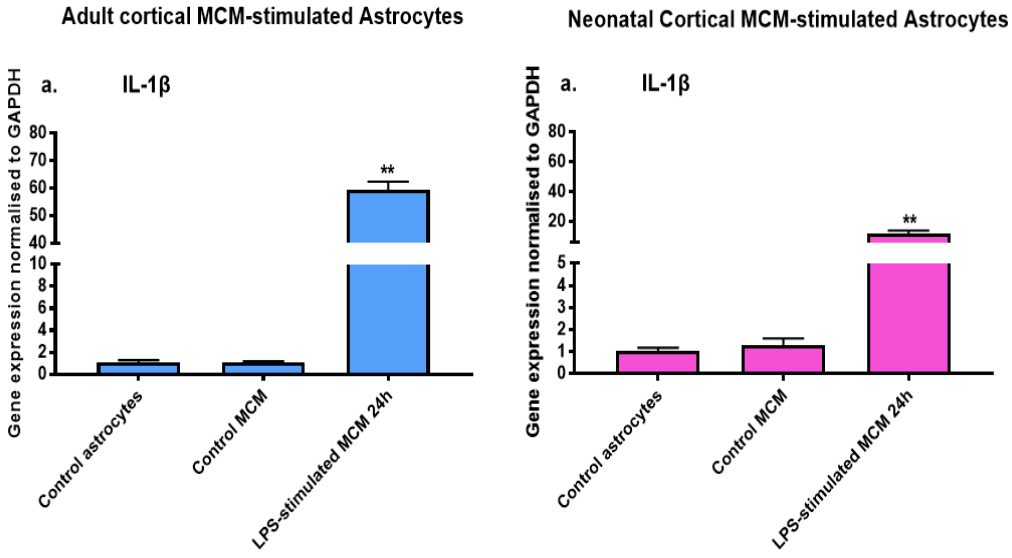

Figure 3-22 Effect of treatment with LPS-stimulated adult (a-b) or neonatal (c-d) cortical MCM on neonatal cortical astrocytes expression of *IL-1β* mRNA. Relative expression of *IL-1β* mRNA (normalised to *GAPDH* following the Livak method) in astrocytes isolated from neonatal rat forebrains. Treatment groups involved control astrocytes (untreated astrocytes), control MCM (1:1; untreated MCM: untreated astrocytes), MCM stimulation for 1, 3, 6 and 24h. Bars represent the mean S.E.M of the values n=4. Statistically significant differences with control astrocytes: ******p < 0.001. (one-way ANOVA followed by Bonferroni's multiple comparisons).

A different pattern of *TGF-β* expression was noticed in astrocytes treated with cortical MCM. As shown in Figure 3-23, untreated adult MCM decreased the expression of *TGF-β* in astrocytes by 0.3-fold. Stimulating astrocytes with adult LPS-stimulated MCM for twenty-four hours caused a further decrease in *TGF-β* mRNA expression by 0.1 fold. The same effect was not observed in astrocytes treated with neonatal MCM.

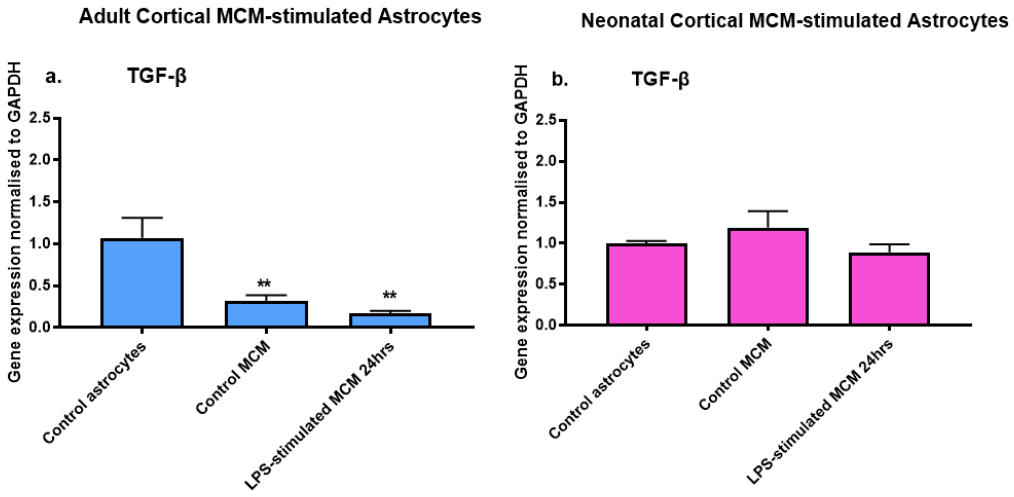

Figure 3-23 Effect of treatment with LPS-stimulated adult (a-b) or neonatal (c-d) cortical MCM on neonatal cortical astrocytes expression of *TGF-β* mRNA. Relative expression of *TGF-β* mRNA (normalised to *GAPDH* following the Livak method) in astrocytes isolated from neonatal rat forebrains. Treatment groups involved control astrocytes (untreated astrocytes), control MCM (1:1; untreated MCM: untreated astrocytes), MCM stimulation for 1, 3, 6 and 24h. Bars represent the mean S.E.M of the values n=4. Statistically significant differences with control astrocytes: **$p < 0.001$. (one-way ANOVA followed by Bonferroni's multiple comparisons).

Table 3-3 Summary of relative expression of *NR4A* subfamily members, *IL-1β* and *TGF-β* mRNA in astrocytes in response to MCM treatment (serum-supplemented media)

Region	MCM developmental stage	Gene	Treatment group	Mean relative expression of mRNA	P-value	Statistical test
Cortical Astrocytes	Adult MCM	*Nurr1*	Control-MCM	2.2	>0.9999	One-way ANOVA/Bonferroni
			1 hr	1.4	>0.9999	
			3 hr	9.7	0.0938	
			6 hr	1.1	>0.9999	
			24 hr	52.3	<0.0001	
	Neonatal MCM		Control-MCM	3.0	>0.9999	
			1 hr	1.0	>0.9999	
			3 hr	1.8	>0.9999	
			6 hr	0.8	>0.9999	
			24 hr	32.1	<0.0001	
Spinal cord Astrocytes	Adult MCM		Control-MCM	2.6	>0.9999	
			1 hr	0.7	>0.9999	
			3 hr	0.8	>0.9999	
			6 hr	1.2	>0.9999	
			24 hr	13.5	<0.0001	
	Neonatal MCM		Control-MCM	0.7	>0.9999	
			1 hr	0.5	>0.9999	
			3 hr	0.5	>0.9999	
			6 hr	0.7	>0.9999	
			24 hr	7.4	<0.0001	
Cortical Astrocytes	Adult MCM	*TINUR*	Control-MCM	1.7	>0.9999	
			1 hr	1.1	>0.9999	
			3 hr	7.5	>0.9999	
			6 hr	0.8	>0.9999	
			24 hr	86.9	<0.0001	

Region	MCM developmental stage	Gene	Treatment group	Mean relative expression of mRNA	P-value	Statistical test
Spinal cord Astrocytes	Neonatal MCM		Control-MCM	3.3	>0.9999	
			1 hr	1.0	>0.9999	
			3 hr	2.0	>0.9999	
			6 hr	0.9	>0.9999	
			24 hr	55.8	<0.0001	
	Adult MCM		Control-MCM	2.6	>0.9999	
			1 hr	1.3	>0.9999	
			3 hr	1.1	>0.9999	
			6 hr	1.8	>0.9999	
			24 hr	35.8	<0.0001	
	Neonatal MCM		Control-MCM	1.0	>0.9999	
			1 hr	0.8	>0.9999	
			3 hr	0.9	>0.9999	
			6 hr	1.0	>0.9999	
			24 hr	20.0	<0.0001	
Cortical Astrocytes	Adult MCM	*Nurr1a*	Control-MCM	1.6	>0.9999	
			1 hr	1.1	>0.9999	
			3 hr	6.2	0.0670	
			6 hr	0.9	>0.9999	
			24 hr	43.8	<0.0001	
	Neonatal MCM		Control-MCM	3.8	>0.9999	
			1 hr	1.2	>0.9999	
			3 hr	2.2	>0.9999	
			6 hr	1.1	>0.9999	
			24 hr	34.2	<0.0001	

Region	MCM developmental stage	Gene	Treatment group	Mean relative expression of mRNA	P-value	Statistical test
Spinal cord Astrocytes	Adult MCM	*Nur77*	Control-MCM	2.6	>0.9999	
			1 hr	0.7	>0.9999	
			3 hr	0.8	>0.9999	
			6 hr	1.2	>0.9999	
			24 hr	13.8	<0.0001	
	Neonatal MCM		Control-MCM	0.8	>0.9999	
			1 hr	0.7	>0.9999	
			3 hr	0.7	>0.9999	
			6 hr	4.3	>0.9999	
			24 hr	29.4	0.0161	
Cortical Astrocytes	Adult MCM		Control-MCM	15.5	0.0044	
			1 hr	9.3	0.1645	
			3 hr	55.5	<0.0001	
			6 hr	0.7	>0.9999	
			24 hr	64.3	<0.0001	
	Neonatal MCM		Control-MCM	90.9	<0.0001	
			1 hr	17.2	0.4629	
			3 hr	60.8	<0.0001	
			6 hr	1.4	>0.9999	
			24 hr	79.5	<0.0001	
Spinal cord Astrocytes	Adult MCM		Control-MCM	9.3	0.0179	
			1 hr	2.8	>0.9999	
			3 hr	4.6	0.8352	
			6 hr	2.3	>0.9999	
			24 hr	9.5	0.0148	
	Neonatal MCM		Control-MCM	7.7	0.4826	
			1 hr	4.9	>0.9999	
			3 hr	10.6	0.0452	

Region	MCM developmental stage	Gene	Treatment group	Mean relative expression of mRNA	P-value	Statistical test
			6 hr	2.2	>0.9999	
			24 hr	15.1	<0.0001	
Cortical Astrocytes	Adult MCM	*NOR-1*	Control-MCM	2.0	>0.9999	
			1 hr	1.2	>0.9999	
			3 hr	7.1	>0.9999	
			6 hr	1.0	>0.9999	
			24 hr	155.8	<0.0001	
	Neonatal MCM		Control-MCM	6.1	0.2092	
			1 hr	0.9	>0.9999	
			3 hr	5.4	0.3509	
			6 hr	1.1	>0.9999	
			24 hr	114.9	<0.0001	
Spinal cord Astrocytes	Adult MCM		Control-MCM	3.1	>0.9999	
			1 hr	1.1	>0.9999	
			3 hr	1.9	>0.9999	
			6 hr	3.2	>0.9999	
			24 hr	69.5	<0.0001	
	Neonatal MCM		Control-MCM	1.1	>0.9999	
			1 hr	1.0	>0.9999	
			3 hr	1.3	>0.9999	
			6 hr	1.6	>0.9999	
			24 hr	57.8	<0.0001	
Cortical Astrocytes	Adult MCM	*IL-1b*	Control-MCM	1.2	>0.9999	
			24 hr	53.4	<0.0001	
	Neonatal MCM		Control-MCM	1.3	>0.9999	
			24 hr	12.1	0.0002	

Region	MCM developmental stage	Gene	Treatment group	Mean relative expression of mRNA	P-value	Statistical test
Spinal cord Astrocytes	Adult MCM	*TGF-β*	Control-MCM	2.8	>0.9999	
			24 hr	111.1	<0.0001	
	Neonatal MCM		Control-MCM	2.9	>0.9999	
			24 hr	60.9	0.0042	
Cortical Astrocytes	Adult MCM		Control-MCM	0.3	0.0099	
			24 hr	0.1	0.0034	
	Neonatal MCM		Control-MCM	1.1	0.6550	
			24 hr	0.8	>0.9999	
Spinal cord Astrocytes	Adult MCM		Control-MCM	1.3	>0.9999	
			24 hr	2.1	>0.9999	
	Neonatal MCM		Control-MCM	0.8	0.8507	
			24 hr	0.7	0.5309	

3.3.9 Effect of treatment with LPS-stimulated serum-free MCM on spinal cord astrocytes' expression of *Nur77*, *NOR-1*, *Nurr1, TINUR*, *Nurr1a, IL-1β*, and *TGF-β* mRNA

As described earlier in chapter one, microglia gene expression can alter *in vitro* (Gosselin et al., 2017). Perhaps this is due to their cultivation in serum-rich media. Serum-containing media does not correspond to the glial cells physiological environment (Guttenplan and Liddelow, 2019); therefore, we utilised a chemically modified serum-free media that is rich in growth factors necessary for the survival of glial cells. Serum-free media triggered

morphological changes in astrocytes displayed by GFAP immunoreactivity (Figure 3-24).

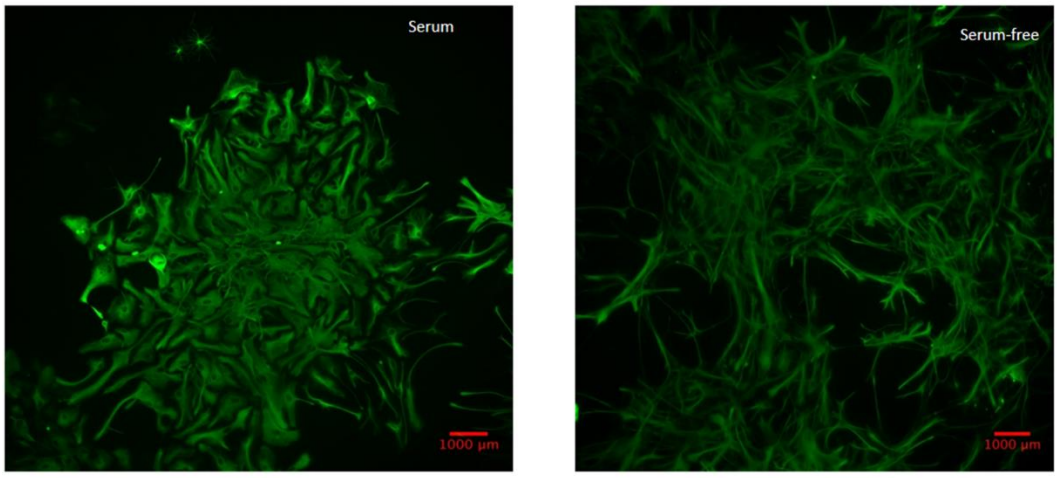

Figure 3-24 Immunoreactivity of GFAP in primary neonatal cortical rat astrocytes cultured in serum-supplemented media (left) or serum-free media (right) for 48 hours. Morphological changes in astrocytes cultured in serum-rich and serum-free media. Magnification 10x. Scale bar (1000 µm).

Stimulating astrocytes with serum-free MCM showed a similar pattern of gene expression to serum-rich MCM. Firstly, treating spinal cord astrocytes with adult LPS-stimulated MCM or neonatal LPS-stimulated MCM increased the expression of *Nur77* mRNA by 11 fold and 33 fold, respectively after twenty-four hours of treatment (shown in Figure 3-25 a,d).

Moreover, adult LPS-stimulated MCM upregulated the expression of *NOR-1* mRNA in astrocytes by 5 folds after three hours of treatment and by 93 folds after 24 hours of treatment. On the other hand, neonatal LPS-stimulated MCM elevated *NOR-1* mRNA levels by 110 folds after twenty-four hours of treatment (Figure 3-25 b,e).

Thirdly, adult LPS-stimulated MCM increased *Nurr1* mRNA expression by 10 folds while neonatal LPS-stimulated MCM upregulated *NOR-1* transcript levels by 22 folds in astrocytes treated for twenty-four hours as shown in Figure 3-25 c,f.

We evaluated the expression of *IL-1β* in astrocytes in response to serum-free MCM stimulation. The results mimic the ones obtained by serum-rich MCM in which treated-MCM-induced *IL-1β* mRNA levels were higher in astrocytes treated with adult LPS-stimulated MCM (212-fold) compared to astrocytes treated with neonatal LPS-stimulated MCM (54-fold) (Figure 3-26). Moreover, the relative expression of mRNA levels was higher in serum-free media as opposed to serum-rich media.

TGF- β expression in astrocytes was not affected by adult nor neonatal MCM stimulation (Figure 3-27).

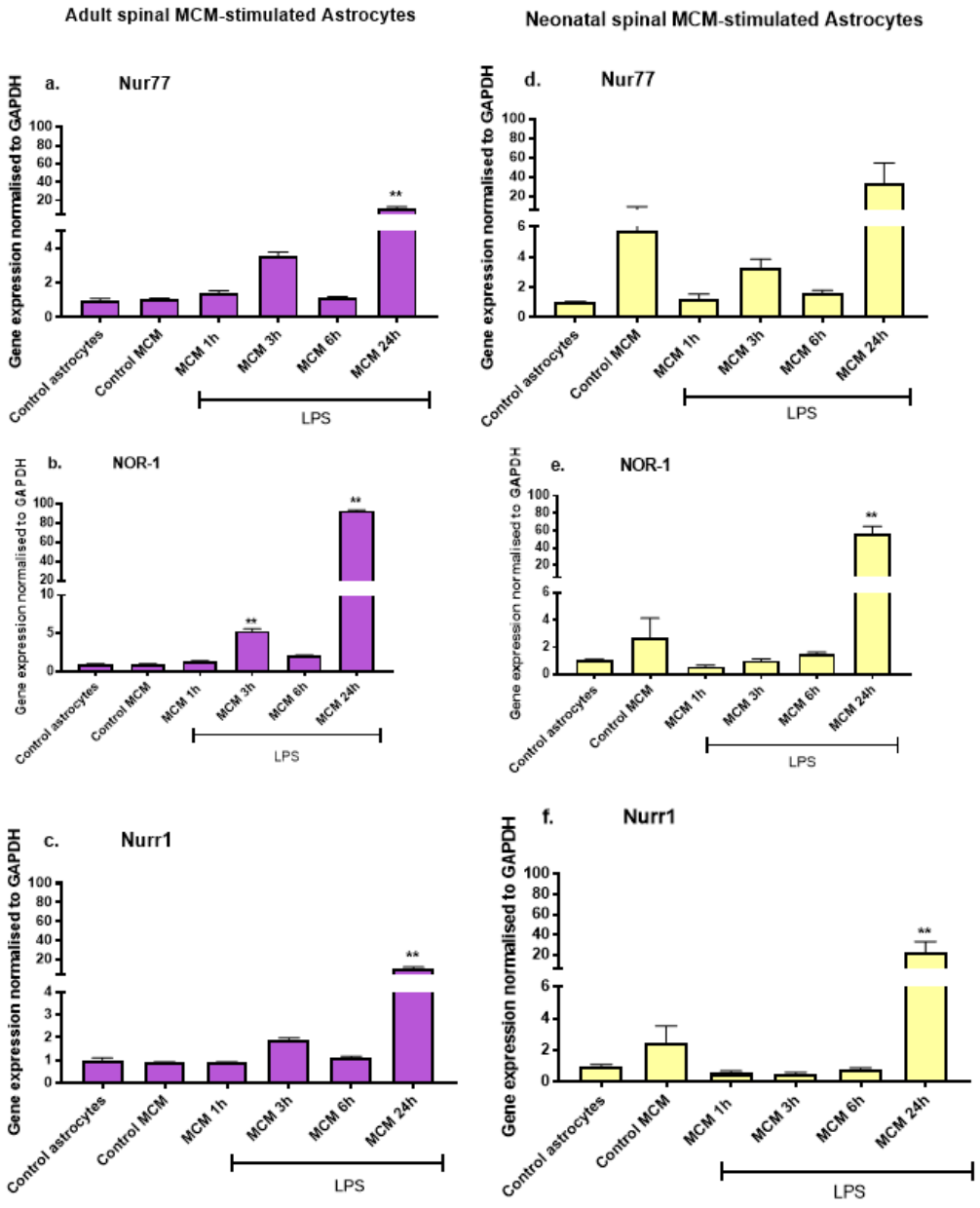

Figure 3-25 Effect of treatment with LPS-stimulated adult (a-b) or neonatal (c-d) spinal cord MCM on neonatal spinal cord astrocytes expression of *Nur77*, *NOR-1, and Nurr1* mRNA. Relative expression of *Nur77*, *NOR-1,* and *Nurr1* mRNA (normalised to *GAPDH* following the Livak method) in astrocytes isolated from neonatal rat spinal cord. Treatment groups involved control astrocytes (untreated astrocytes), control MCM (1:1; untreated MCM: untreated astrocytes), MCM stimulation for 1, 3, 6 and 24h. Bars represent the mean S.E.M of the values n=4. Statistically significant differences with control astrocytes: **$p < 0.001$. (one-way ANOVA followed by Bonferroni's multiple comparisons).

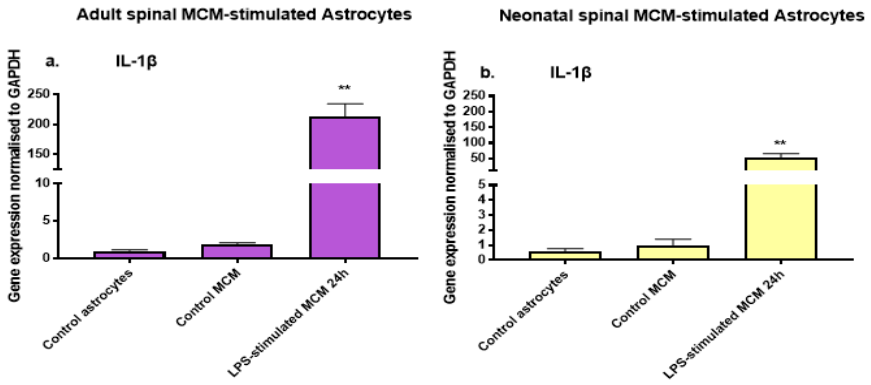

Figure 3-26 Effect of treatment with LPS-stimulated adult (a-b) or neonatal (c-d) spinal cord MCM on neonatal spinal cord astrocytes expression of *IL-1β* mRNA. Relative expression of *IL-1β* mRNA (normalised to *GAPDH* following the Livak method) in astrocytes isolated from neonatal rat spinal cord. Treatment groups involved control astrocytes (untreated astrocytes), control MCM (1:1; untreated MCM: untreated astrocytes), MCM stimulation for 1, 3, 6 and 24h. Bars represent the mean S.E.M of the values n=4. Statistically significant differences with control astrocytes: **p < 0.001. (one-way ANOVA followed by Bonferroni's multiple comparisons).

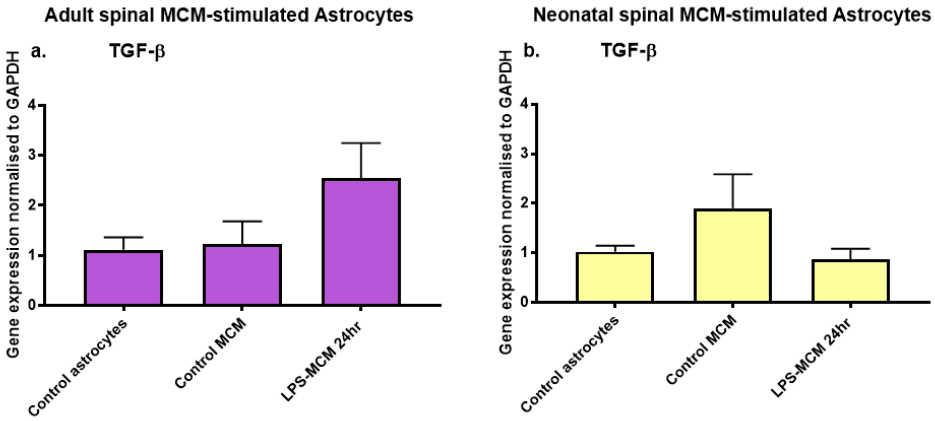

Figure 3-27 Effect of treatment with LPS-stimulated adult (a-b) or neonatal (c-d) spinal cord MCM on neonatal spinal cord astrocytes expression of *TGF-β* mRNA. Relative expression of *TGF-β* mRNA (normalised to *GAPDH* following the Livak method) in astrocytes isolated from neonatal rat spinal cord. Treatment groups involved control astrocytes (untreated astrocytes), control MCM (1:1; untreated MCM: untreated astrocytes), MCM stimulation for 1, 3, 6 and 24h. Bars represent the mean S.E.M of the values n=4. (one-way ANOVA followed by Bonferroni's multiple comparisons).

Next, we investigated the expression of NR4As and cytokines in cortical astrocytes in serum-free media and stimulated with serum-free cortical MCM. Treatment of astrocytes with adult LPS-stimulated MCM or neonatal LPS-stimulated MCM increased the expression of *Nur77* mRNA after twenty-four hours by 69 and 65 folds, respectively (Figure 3-28 a,d). Furthermore, adult LPS-stimulated MCM induced *NOR-1* mRNA levels by 929 folds whereas neonatal LPS-stimulated MCM elevated *NOR-1* mRNA levels by 137 folds (Figure 3-28 b,e). Transcript levels of *Nurr1* were also increased after twenty-four hours of treating astrocytes with adult LPS-stimulated MCM (83-fold) and neonatal LPS-stimulated MCM (37-fold) (Figure 3-28 c,f).

Although both adult and neonatal LPS-stimulated MCM increased the expression of *IL-1β* after 24 hours of stimulation in astrocytes (60-fold and 18-fold, respectively), adult treated-MCM seem to induce *IL-1β* levels more robustly (Figure 3-29). Surprisingly, *TGF-β* mRNA levels were not affected by serum-free MCM stimulation (Figure 3-30), a different observation to the one reported earlier in serum-rich media (Figure 3-23).

We compared basal levels of *NOR-1* expression between astrocytes and microglia isolated from either forebrains or spinal cords. As shown in Figure 3-31, neonatal spinal cord astrocytes highly expressed *NOR-1* (0.001) in comparison to cortical astrocytes (0.0003) or both cortical (0.0004) and spinal cord (0.0001) microglia. Variation in cortical astrocytes' expression of *NOR-1* mRNA is due to a different set of primary astrocyte

culture. Notably, microglial expression of *NOR-1* appeared to be similar between adult and neonatal microglia, whereas cortical microglia express higher levels of *NOR-1* than spinal cord microglia.

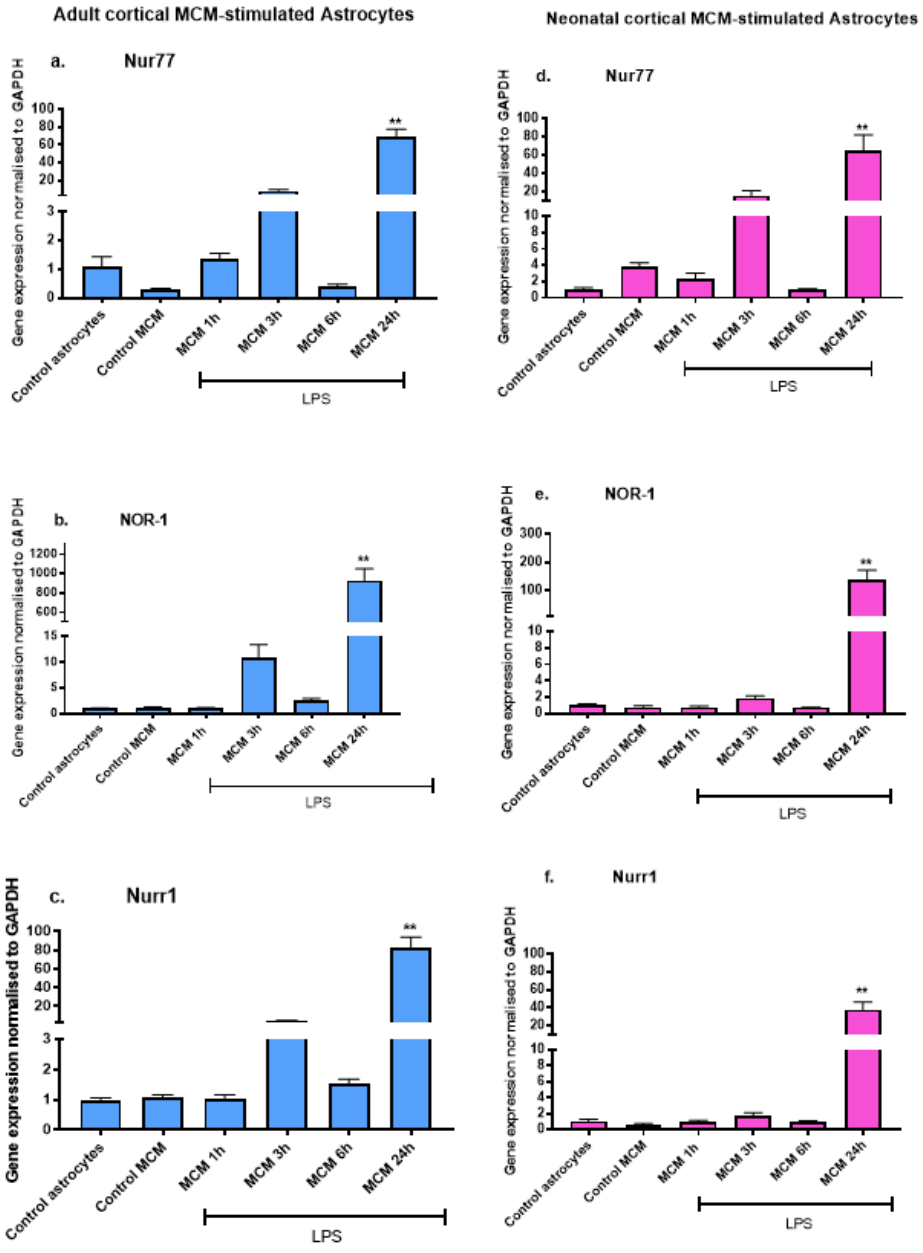

Figure 3-28 Effect of treatment with LPS-stimulated adult (a-b) or neonatal (c-d) cortical MCM on neonatal cortical astrocytes expression of *Nur77*, *NOR-1,* and *Nurr1* mRNA. Relative expression of *Nur77, NOR-1*, and *Nurr1* mRNA (normalised to *GAPDH* following the Livak method) in astrocytes isolated from neonatal rat forebrains. Treatment groups involved control astrocytes (untreated astrocytes), control MCM (1:1; untreated MCM: untreated astrocytes), MCM stimulation for 1, 3, 6 and 24h. Bars represent the mean S.E.M of the values n=4. Statistically significant differences with control astrocytes: **p < 0.001. (one-way ANOVA followed by Bonferroni's multiple comparisons).

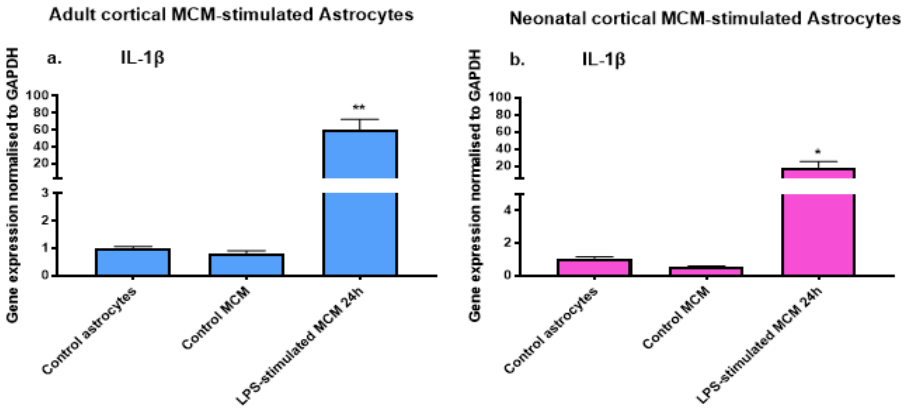

Figure 3-29 Effect of treatment with LPS-stimulated adult (a-b) or neonatal (c-d) cortical MCM on neonatal cortical astrocytes expression of *IL-1β* mRNA. Relative expression of *IL-1β* mRNA (normalised to *GAPDH* following the Livak method) in astrocytes isolated from neonatal rat forebrains. Treatment groups involved control astrocytes (untreated astrocytes), control MCM (1:1; untreated MCM: untreated astrocytes), MCM stimulation for 1, 3, 6 and 24h. Bars represent the mean S.E.M of the values n=4. Statistically significant differences with control astrocytes: *****p < 0.05, ******p < 0.001. (one-way ANOVA followed by Bonferroni's multiple comparisons).

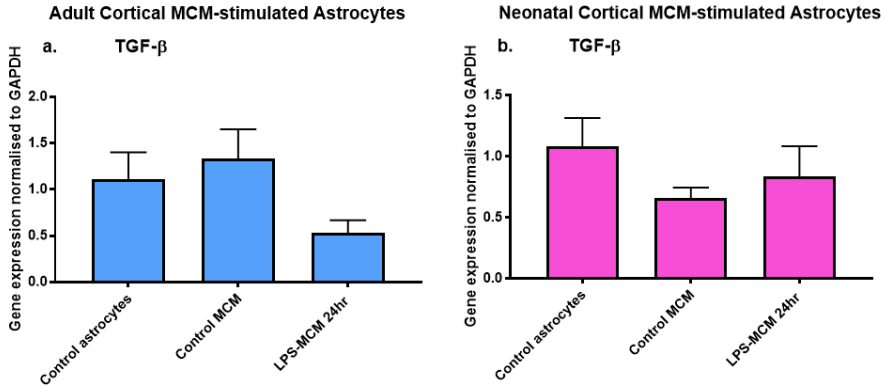

Figure 3-30 Effect of treatment with LPS-stimulated adult (a-b) or neonatal (c-d) cortical MCM on neonatal cortical astrocytes expression of *TGF-β* mRNA. Relative expression of *TGF-β* mRNA (normalised to *GAPDH* following the Livak method) in astrocytes isolated from neonatal rat forebrains. Treatment groups involved control astrocytes (untreated astrocytes), control MCM (1:1; untreated MCM: untreated astrocytes), MCM stimulation for 1, 3, 6 and 24h. Bars represent the mean S.E.M of the values n=4. (one-way ANOVA followed by Bonferroni's multiple comparisons).

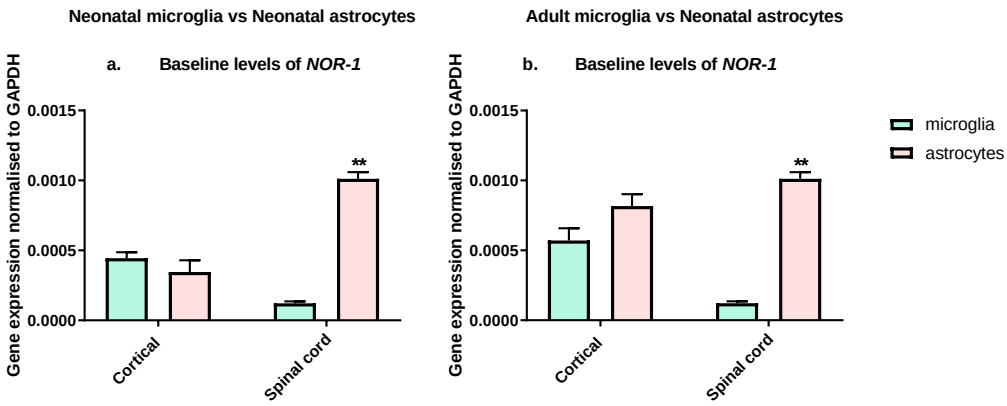

Figure 3-31 Glial regional heterogeneity with respect to *NOR-1 mRNA expression*. A comparison between basal mRNA levels of *NOR-1* (normalised to *GAPDH*) in **(a)** neonatal microglia vs neonatal astrocytes and **(b)** adult microglia vs neonatal astrocytes in different CNS regions. All cells are untreated. Bars represent the standard error mean of the values n=4. Statistically significant differences between microglia and astrocytes: **$p < 0.001$ (Multiple t-tests).

Table 3-4 Summary of relative expression of NR4A subfamily members, IL-1β and TGF-β mRNA in astrocytes in response to MCM treatment (serum-free media)

Region	MCM developmental stage	Gene	Treatment group	Mean relative expression of mRNA	P-value	Statistical test
Cortical Astrocytes	Adult MCM	*Nurr1*	Control-MCM	1.1	>0.9999	One-way ANOVA/Bonferroni
			1 hr	1.0	>0.9999	
			3 hr	4.5	>0.9999	
			6 hr	1.5	>0.9999	
			24 hr	83.4	<0.0001	
	Neonatal MCM		Control-MCM	0.6	>0.9999	
			1 hr	0.9	>0.9999	
			3 hr	1.7	>0.9999	
			6 hr	1.0	>0.9999	
			24 hr	37.8	<0.0001	
Spinal cord Astrocytes	Adult MCM		Control-MCM	0.9	>0.9999	
			1 hr	0.8	>0.9999	
			3 hr	1.9	>0.9999	
			6 hr	1.1	>0.9999	
			24 hr	10.1	<0.0001	
	Neonatal MCM		Control-MCM	2.5	>0.9999	
			1 hr	0.5	>0.9999	
			3 hr	0.5	>0.9999	
			6 hr	0.8	>0.9999	
			24 hr	22.7	0.0095	
Cortical Astrocytes	Adult MCM	*Nur77*	Control-MCM	0.3	>0.9999	
			1 hr	1.3	>0.9999	
			3 hr	8.1	0.7332	
			6 hr	0.3	>0.9999	
			24 hr	69.8	<0.0001	

Region	MCM developmental stage	Gene	Treatment group	Mean relative expression of mRNA	P-value	Statistical test
Spinal cord Astrocytes	Neonatal MCM	*NOR-1*	Control-MCM	3.9	>0.9999	
			1 hr	2.3	>0.9999	
			3 hr	15.6	0.4461	
			6 hr	1.0	>0.9999	
			24 hr	64.9	<0.0001	
	Adult MCM		Control-MCM	1.0	>0.9999	
			1 hr	1.4	>0.9999	
			3 hr	3.4	0.0546	
			6 hr	1.1	>0.9999	
			24 hr	11.3	<0.0001	
	Neonatal MCM		Control-MCM	5.7	>0.9999	
			1 hr	1.2	>0.9999	
			3 hr	3.2	>0.9999	
			6 hr	1.5	>0.9999	
			24 hr	33.0	0.0988	
Cortical Astrocytes	Adult MCM		Control-MCM	1.1	>0.9999	
			1 hr	1.0	>0.9999	
			3 hr	10.8	>0.9999	
			6 hr	2.6	>0.9999	
			24 hr	929.1	<0.0001	
	Neonatal MCM		Control-MCM	0.7	>0.9999	
			1 hr	0.7	>0.9999	
			3 hr	1.8	>0.9999	
			6 hr	0.7	>0.9999	
			24 hr	137.9	<0.0001	

Region	MCM developmental stage	Gene	Treatment group	Mean relative expression of mRNA	P-value	Statistical test
Spinal cord Astrocytes	Adult MCM		Control-MCM	1.0	>0.9999	
			1 hr	1.3	>0.9999	
			3 hr	5.3	<0.0001	
			6 hr	2.1	0.1596	
			24 hr	93.3	<0.0001	
	Neonatal MCM		Control-MCM	2.7	>0.9999	
			1 hr	0.5	>0.9999	
			3 hr	0.9	>0.9999	
			6 hr	1.5	>0.9999	
			24 hr	110.3	<0.0001	
Cortical Astrocytes	Adult MCM	*IL-1b*	Control-MCM	0.7	>0.9999	One-way ANOVA/Bonferroni
			24 hr	59.7	0.0006	
	Neonatal MCM		Control-MCM	0.5	>0.9999	
			24 hr	18.5	0.0178	
Spinal cord Astrocytes	Adult MCM		Control-MCM	1.8	>0.9999	
			24 hr	212.9	<0.0001	
	Neonatal MCM		Control-MCM	3.6	>0.9999	
			24 hr	54.1	0.0041	
Cortical Astrocytes	Adult MCM	*TGF-β*	Control-MCM	1.3	>0.9999	
			24 hr	0.5	0.4100	
	Neonatal MCM		Control-MCM	0.6	0.3900	
			24 hr	0.8	0.8489	
Spinal cord Astrocytes	Adult MCM		Control-MCM	1.2	>0.9999	
			24 hr	2.5	0.1555	
	Neonatal MCM		Control-MCM	1.9	0.3835	
			24 hr	0.8	>0.9999	

3.3.10 Effect of adult or neonatal cortical MCM-stimulated ACM on cortical neurons

Microglia and astrocytes cross-talk consequently affect neurons; therefore, we evaluated the effect of serum-free ACM (previously stimulated with either neonatal or adult MCM) on cortical embryonic neurons. Treating neurons with serum-free media has an advantage over serum-rich media since the latter promote non-neuronal cells proliferation *in vitro*.

Initially, we evaluated the purity of our primary neuronal culture by staining with antibodies against, NeuN (neuron marker), IBA-1 (microglia marker), and GFAP (astrocyte marker). Figure 3-32 shows some contamination with astrocytes, which is expected in a primary neuron culture. The culture was almost devoid of microglia indicated by an absence of IBA-1 immunoreactivity.

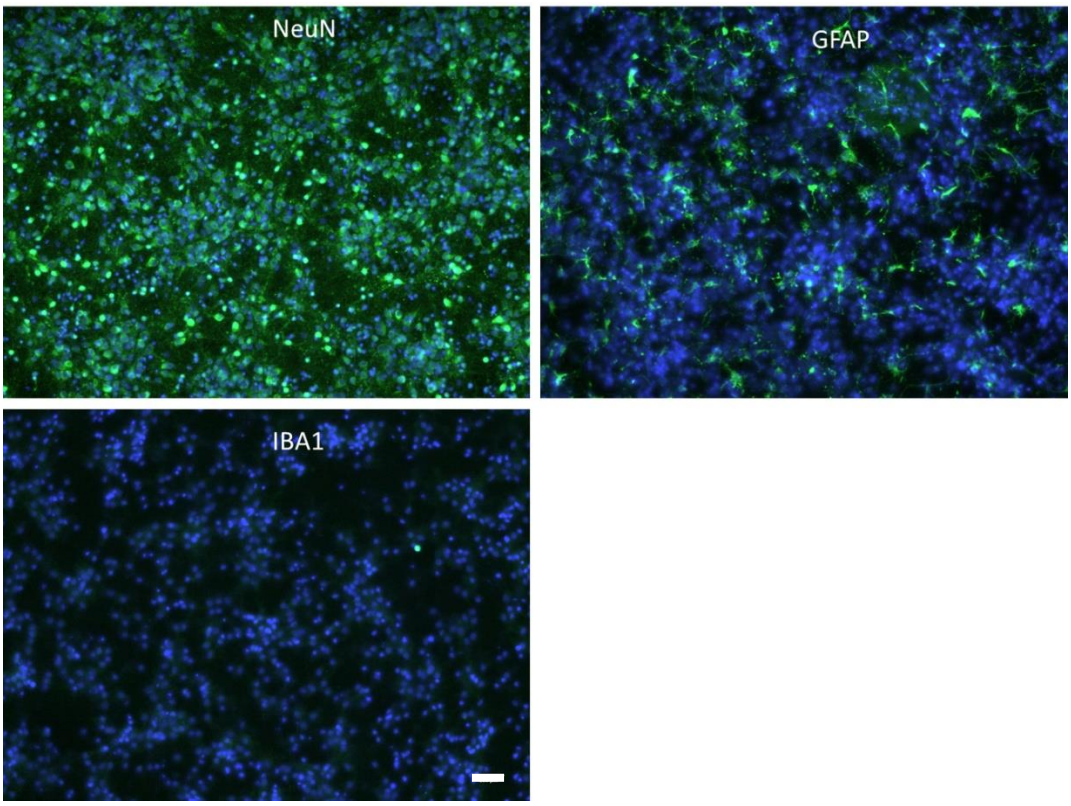

Figure 3-32 Immunocytochemistry of rat embryonic cortical neuron culture (8 days post culture). Immunoreactivity of neuron biomarker (NeuN), Astrocyte biomarker (GFAP) and microglia biomarker (IBA1). Scale bar (200µm).

Neurons were stimulated with MCM-treated ACM. Morphological observations (Figure 3-33) suggested axonal degradation in neurons incubated with 80/20% neurobasal media (NBM)/serum-free media (SFM). On the other hand, neurons incubated with adult or neonatal MCM-stimulated ACM showed enhanced axons. Importantly, neurons treated with neonatal MCM-stimulated ACM showed extended and connected axons.

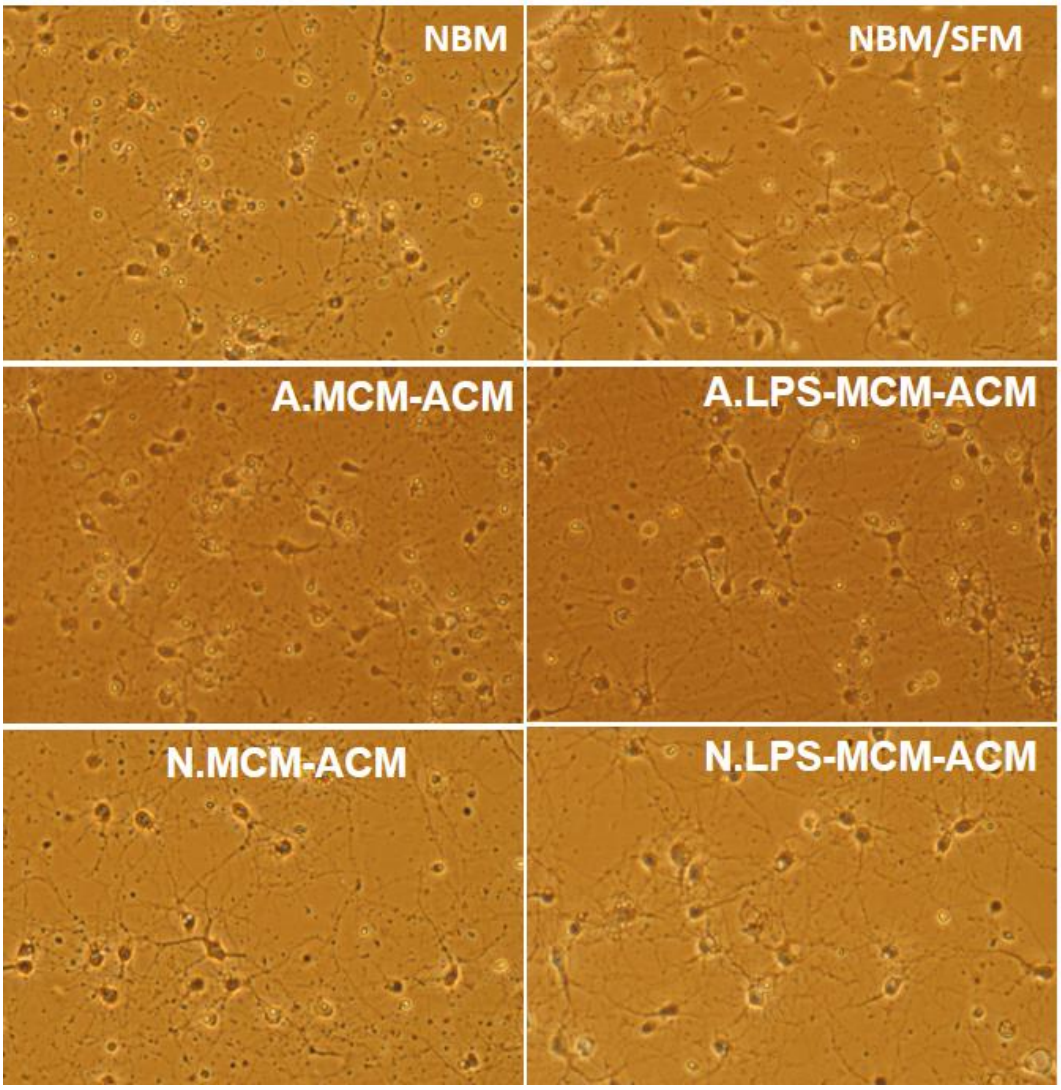

Figure 3-33 Effect of microglia-astrocytes communication on neurons. Data represent ACM-untreated neurons incubated in serum-free/ neurobasal media (SFM/NBM), adult MCM-stimulated ACM (A.MCM-ACM) or neonatal MCM-stimulated ACM (N.MCM-ACM) with or without LPS treatment.

A colourimetric viability assay was used to determine the effect of microglia-astrocyte communication on neurons. Interestingly, neurons viability improved after twenty-four hours of stimulation with MCM-stimulated ACM in comparison to untreated neurons incubated in 80/20% NBM/SFM.

Neonatal MCM-treated ACM significantly increased the viability of neurons regardless of LPS stimulation (153% untreated-MCM-ACM, 154% LPS-stimulated MCM-ACM), as opposed to adult MCM-stimulated ACM that showed a decreased viability in neurons stimulated with LPS treated-MCM (122% (Figure 3-34).

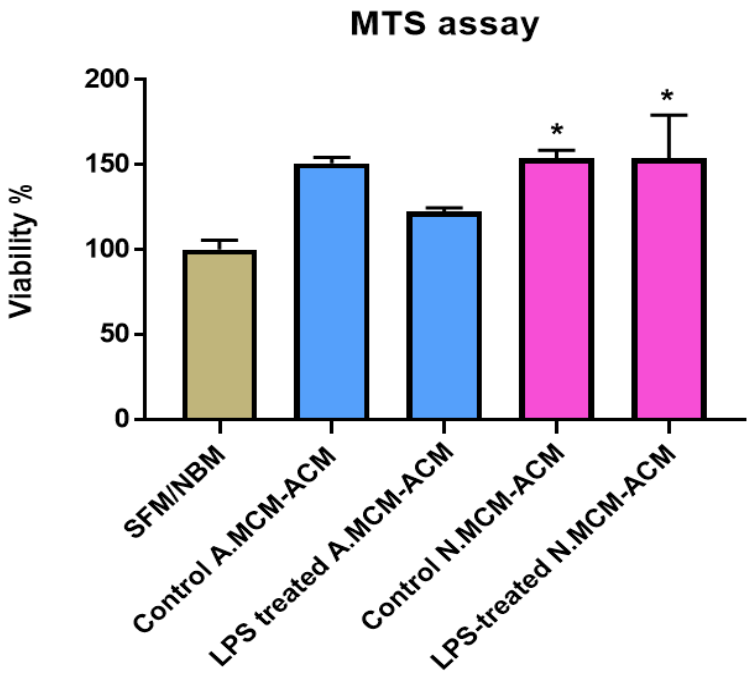

Figure 3-34 MTS assay of cortical neurons stimulated with MCM-stimulated ACM. Data represent ACM-untreated neurons incubated in serum-free/ neurobasal media (SFM/NBM), adult MCM-stimulated ACM (A.MCM-ACM) or neonatal MCM-stimulated ACM (N.MCM-ACM) with or without LPS treatment. Bars represent the mean S.E.M of the values n=4. Statistically significant differences with neurons in SFM/NBM: *****p < 0.05 (one-way ANOVA followed by Bonferroni's multiple comparisons).

3.4 Discussion

In this study, we examined LPS-induced microglia activation and orphan nuclear receptor gene expression in adult or neonatal microglia isolated from rats' forebrains or spinal cords. Our data show that LPS-treated microglia affect astrocyte expression of orphan nuclear receptors and cytokines. Intriguingly, microglia- astrocyte communication enhanced the viability of neurons and showed a potential neuroprotective action.

Glial cells play an important role in CNS maintenance and pathology. Microglia respond to tissue-endangering stimuli that can be either endogenous or exogenous (Kigerl et al., 2014). Upon failure of insult elimination or repair mechanism, chronic activation of microglia can be deleterious to cells and tissues (Ransohoff, 2016). Reported anti-inflammatory properties of orphan nuclear receptors (Liu et al., 2017, Saijo et al., 2009) can be promising in managing neuroinflammation by targeting glial cells polarisation rather than completely inhibiting their activation.

3.4.1 Microglia retain their developmental gene expression profile *in vitro*

Current methods for culturing microglia in serum-rich media have their limitations. It has been reported that microglia exposed to serum show altered morphologies that mimic activated microglia under pathological conditions (Bohlen et al., 2017). Moreover, microglia seem to alter their gene expression profiles *in vitro*, especially upon extended culture periods

(Caldeira et al., 2014). Importantly, microglia are highly reactive, thus they could respond differently to stimuli depending on the chosen method of isolation (Lin et al., 2017). As we are interested in regional and developmental heterogeneity of microglia in response to PAMPs and DAMPs, we ensured that our microglia retain their morphological and transcriptome *in vitro*.

Our isolated microglia mimic their physiological morphologies described in the literature. For instance, our isolated early postnatal microglia acquired an amoeboid phenotype, a characteristic morphology of early developmental microglia (Michell-Robinson et al., 2015). On the other hand, adult microglia isolated from older rats displayed a distinctive ramified morphology (Hammond et al., 2019, Rossi and Lewis, 2018, Lenz and Nelson, 2018). These observations suggest that the isolation protocol and the exposure to serum, to our knowledge, did not alter the developmental microglial morphologies.

Next, we evaluated the expression of developmental biomarkers in our cortical and spinal cord microglia. Our results (Figure 3-6) confirmed that microglia maintain their developmental morphologies and gene expression *in vitro*. The observed correspondent upregulation in adult biomarkers (*MafB* and *Sall1*) and neonatal biomarkers (*Scd2* and *Psat1*) in cortical microglia were consistent with previous findings that utilised RNA-seq technology to screen gene expression in cortical microglia during development (Matcovitch-Natan et al., 2016b).

The role of adult microglia in immune surveillance is essential. An antiviral functional role of the transcription factor MafB was proposed in adult microglia that eventually contributes to tissue homeostasis by interfering with interferon and inflammatory signalling pathways (Matcovitch-Natan et al., 2016b). Ablation of Sall1, on the other hand, was suggested to activate microglia marked by alterations in morphology and hindered neurogenesis (Buttgereit et al., 2016).

Scd2 catalyses desaturation of saturated fats (de Moura et al., 2016) and its expression was suggested to decrease upon LPS stimulation of BV2 microglial cell line (Button et al., 2014). Although Psat1 role in microglia hasn't been explored yet, the enzyme is associated with L-serine synthesis in the CNS by astrocytes (Tabatabaie et al., 2010). L-serine is essential for brain development and function. Moreover, It has been reported that Psat1 deficiency resulted in lethal CNS abnormalities manifested after birth (Hart et al., 2007). These observations indicate that adult microglia biomarkers are involved in maintaining microglial identity and modulating immunity while neonatal microglia biomarkers are associated with regulating metabolism and CNS development. We selected these markers based on a study done on cortical microglia. Perhaps the overlapping in gene expression profiles observed here between adult and neonatal spinal cord microglia is simply because most of the studies are done on cortical microglia and not spinal cord microglia.

3.4.2 LPS-induced pro-inflammatory and anti-inflammatory cytokine mRNA expression in microglia

Persistent activation of NF-kB is a driving force for secondary tissue damage caused by upregulation of adhesion molecules and chemokines leading to increased extravasation of immune cells through the BBB, thus resulting in several CNS pathologies (Engelmann et al., 2014). Prolonged NF-kB activation was observed with LPS or IL-1β (Moynagh et al., 1993, Saijo et al., 2009) stimulation but not with TNF-α (Moynagh et al., 1993). Herein, we also confirm an increase in IL-1β mRNA expression and release as a result of LPS-induced microglial activation. A lower dose of LPS (10ng/ml) has been described to induce IL-1β mRNA after 24 hours in stimulated neonatal microglia (Lively and Schlichter, 2018), however, our data show that LPS-induces loss of viability and cell death after 24 hours of stimulation possibly due to the higher concentration of LPS (100ng/ml) used in the present study. Our chosen concentration of LPS has been previously reported to induce microglial activation leading to neurotoxic astrocytes (Liddelow et al., 2017a). In the present study, we observed a greater response to LPS in terms of IL-1β mRNA expression and release by neonatal microglia in comparison to adult microglia. Not only do adult and neonatal immune cells respond differently to inflammatory stimuli (e.g. TLR ligands) but also differentially secrete pro-inflammatory and anti-inflammatory cytokines at basal levels. Evidently, unstimulated neonatal immune cells (whole blood and mononuclear cells) release higher levels of

IL-10, IL-1β and IL-12p40 in comparison to unstimulated adult immune cells after 18 hours of incubation (Kollmann et al., 2009).

Microglial activation is essential for the process of inflammation to protect tissues against pathogens and damaging agents, however, the right balance is necessary to stop the propagation of pathologies in the CNS that could arise due to persistent pro-inflammatory cytokines and mediator release. Our results show an increase in IL-10 mRNA following LPS stimulation in both adult and neonatal microglia. A similar observation was reported by Seo and colleagues, 2004, who suggested that ATP release from LPS-stimulated microglia induced IL-10 production (Seo et al., 2004).

3.4.3 LPS induces the expression of orphan nuclear receptors in microglia

In the present study, we challenged primary microglia isolated from rat forebrains and spinal cords with LPS as an exogenous stimulus. Different patterns with respect to gene expression were observed. LPS rapidly induced *Nur77* mRNA levels in cortical adult and neonatal microglia. Unlike cortical microglia, spinal cord microglial LPS-induced *Nur77 l*evels were not significantly elevated despite higher basal levels of *Nur77* in adult spinal cord microglia. These findings suggest that adult and neonatal microglia respond to LPS similarly regarding induced- *Nur77* transcript levels in spite of region of origin. LPS-induced gene expression profiles were similar between each

developmental stage suggesting that NR4A subfamily members are induced differently in response to LPS depending on the region of origin or developmental stage of microglia. Interestingly, adult microglia were more resilient than neonatal microglia during longer periods of exposure to LPS marked by a decreased level of housekeeping genes (*GAPDH* mRNA and β-actin protein level) in neonatal microglia. The increased expression of *NOR-1* mRNA after 24 hours of LPS stimulation in adult microglia could be associated with promoting survival. NOR-1 is proposed to have an anti-apoptotic role during hypoxia in endothelial (Martorell et al., 2009) and vascular smooth muscle cells (Alonso et al., 2016).

Although our results showed a resemblance in response to LPS between neonatal and spinal cord microglia, Baskar Jesudasan and colleagues, (2014) reported differences between neonatal brain and spinal cord microglia treated with LPS. Their focus was mainly on the morphological differences that brain and spinal microglia exert. LPS-induced spinal cord microglia displayed a less amoeboid and phagocytic morphology as opposed to brain microglia. Moreover, higher levels of secreted IL-1β, TNF-α and NO have been reported in brain microglia after LPS stimulation (1µg/ml for 24 hours) in comparison to basal levels whereas LPS treatment failed to induce the release of these pro-inflammatory mediators by spinal cord microglia (Baskar Jesudasan et al., 2014).

Nur77 is an important regulator of cell differentiation, growth, apoptosis (Chen et al., 1998) and cortical synaptogenesis (Jeanneteau et al., 2018).

Despite the significant differences in Nur77 mRNA basal levels between adult and neonatal microglia, translation of Nur77 could be restricted to neonatal microglia due to the fact that Nru77 protein expression was not evident in adult microglia samples compared to the endogenous control (β-actin). At earlier stages of development the remodelling of the CNS requires constant removal of dead cells, debris and excess synapse elimination. Protein expression of Nur77 in microglia could be essential during early development. Herein we see region-specific and developmental differential expression of NR4As in microglia. Their differential expression at basal levels as well as in response to activating stimuli is worth exploring in the future. It is less challenging to study the transcriptional profiles as opposed to the proteomic profiles due to the advancements in high throughput mRNA measuring techniques that make them more attractive to be utilised in studies especially in the field of diagnostics; however, quantifying translated proteins is more relevant and more ought to be studied due to their causative interactions in the cell. The availability of more reliable antibodies and more developed techniques is crucial for quantifying proteins (Greenbaum et al., 2003).

The cumulative body of evidence from various studies stresses the importance of microglia and astrocyte cross talk in health and disease. They are the glue that holds CNS tissues together through modulating synaptic plasticity and the process of myelination (Salter and Stevens, 2017, Domingues et al., 2016). Firstly, we evaluated the expression of Nurr1

variants in astrocytes. Secondly, we considered the possibility of altered gene expression in astrocytes due to the addition of serum and utilised a serum-free media to maintain both microglia and astrocytes *in vitro*.

3.4.4 Astrocytes' expression of Nurr1 and splice variants

Nurr1 splice variants have been identified in humans and rats in dopamine neurons (Michelhaugh et al., 2005), however, their expression in microglia and astrocytes have not been extensively studied. Since alternative splicing is essential for development and tissue homeostasis (Blencowe, 2017), we investigated the possibility of alternative splicing of Nurr1 in astrocytes. Our group was able to identify Nurr1 splice variants; TINUR and Nurr1a expression in microglia. Data obtained suggest that their expression and activity differ during different developmental stages of microglia. Here, we were able to highlight that astrocytes do express both variants' mRNA that could potentially carry out anti-inflammatory functions. This would lay down the foundation of the future work to investigate the functional role of potentially translated Nurr1 isoforms in astrocytes during development.

3.4.5 GFAP immunoreactivity of primary Astrocytes cultured in serum/serum-free media

Reports have suggested that microglial functions and morphology can be affected by serum and that current isolation and culturing techniques do not translate to physiological conditions. Moreover, serum-exposed

microglia were reported to phagocytose myelin, unlike microglia grown in serum-free conditions (Bohlen et al., 2017). In addition, astrocytes isolated through immunopanning in serum-free media were reportedly different from astrocytes that were exposed to serum in that serum-free conditioned yielded astrocytes with gene expression profile mimicking physiological astrocytes (Foo et al., 2011). In vitro culturing of microglia in serum-rich conditions can expose them to blood-borne molecules that are excluded from the CNS due to an intact BBB, however depriving microglia from serum resulted in cell death within days of isolation from neonatal rat brains despite the use of a rich culture medium. Microglia maintained in ACM, however showed a more physiologically relevant morphology and response possibly due to astrocytic release of CSF-1 and TGF-β1 (Bohlen et al., 2017). We used a serum-free media supplemented with biotin, basic fibroblast growth factor (FGF), epidermal growth factor (EGF), human transferrin, insulin, hydrocortisone and selenite (Bottenstein G-5 formulation) (Bottenstein and Sato, 1985) designed to promote glial cells' growth in culture. Astrocytes cultured in serum-free media exhibited changes in morphology as opposed to astrocytes in serum-supplemented media. In addition, microglia cultured in serum-free media also displayed morphological changes in comparison to microglia cultures in serum-rich media (data not shown). Astrocyte morphological changes and induced differentiation have been observed formerly upon the addition of the G-5 supplement used in our serum-free media (Goursaud et al., 2009). These changes are believed to be promoted by FGF, EGF and Insulin. Moreover, the same supplement enhanced

glutamate uptake by astrocytes in comparison to astrocytes cultured in the absence of the growth factors included in the supplement. Glutamate is an excitatory neurotransmitter and its regulated uptake by astrocytes is essential to maintain physiological excitatory stimulation in neurons (Vermeiren et al., 2005). Therefore, formulating a serum-free medium that does not induce morphological changes and gene expression alterations might be a better alternative. In the future, avoiding exposing glial cells of serum is key to sustain consistent results by utilising formulated serum-free media proposed to maintain physiological characteristics of astrocytes (Foo et al., 2011) and microglia (Collins and Bohlen, 2018) *in vitro*.

3.4.6 Effect of treatment with LPS-stimulated MCM on astrocyte expression of *Nur77*, *NOR-1*, *Nurr1*, *TINUR*, *Nurr1a*, *IL-1β* and *TGF-β* mRNA

In this study, we evaluated the effect of LPS-stimulated microglial secretome on astrocytes' expression of NR4As, the pro-inflammatory cytokine, *IL-1β* and the anti-inflammatory cytokine *TGF-β*. The current astrocyte isolation method results in about 10% of microglial contamination, however, the stimulus (LPS) was removed from microglial culture and the conditioned media used was devoid of LPS, hence the response couldn't be elicited by microglial contaminated cells. To achieve maximum enrichment of high purity astrocyte culture, cells were treated with L-LME, which is cytotoxic to microglia but not astrocytes (Li et al., 2008). Viability of cells

decreased significantly following treatment with different concentrations of L-LME suggesting that cells were exposed to stress; therefore, LME wasn't used in the current study to achieve microglial depletion. Moreover, the upregulation in astrocytes' NR4As and *IL-1β* mRNA levels can only be linked to microglial activation since astrocytes do not express TLR-4 that conducts LPS signalling cascade (Facci et al., 2014b). Intriguingly, it has been reported that *TLR-4* expression in the brain is higher at the weaning stage (P21 mice) compared to neonatal mice (P2) (Christensen et al., 2014). The results presented here in this study suggest that astrocytes respond to the immunomodulatory factors released by activated microglia. Recent findings indicated that pro-inflammatory astrocytes are triggered when microglia are stimulated with LPS *in vivo*. Moreover, astrocytes acquire a pro-inflammatory status *in vitro* following exposure to TNF-α, IL-1α and c1q. These inflammatory mediators are released primarily by microglia (Liddelow et al., 2017a).

IL-1β transcript levels were higher in both cortical and spinal cord astrocytes stimulated with adult cortical or spinal cord treated-MCM, respectively as opposed to *IL-1β* mRNA levels in response to neonatal treated-MCM. While adult cortical untreated- or LPS-treated-MCM decreased mRNA levels of the anti-inflammatory cytokine *TGF-β* in serum-rich media, this effect was not observed in serum-free media. It has been reported that ageing microglia phenotype is pro-inflammatory skewed and evidently they produce more pro-inflammatory factors and show a lower

production of anti-inflammatory molecules (Perry and Teeling, 2013). This could indicate that adult treated-MCM is shifting the status of neonatal astrocytes towards being more pro-inflammatory rather than anti-inflammatory; hence, this could lead to astrocytes being neurotoxic instead of neuroprotective. However, contrary to Liddelow and colleagues' findings (Liddelow et al., 2017a), our results showed that astrocytes improved the viability of neurons in spite of stimulation with treated-MCM. Importantly, the slight decrease in neurons viability after treatment with adult treated-MCM/ACM suggest that neonatal microglial conditioned media enhanced the neuronal survival through stimulating astrocytes even in the event of an LPS challenge. The discrepancy between our results and Liddelow's could be due to differences in experimental design. In our study, we were interested in physiological responses of microglia rather than induced cytotoxicity with the endotoxin, LPS; therefore, we challenged microglia with LPS for only 6 hours and removed the stimulus from media. On the other hand, Liddelow and colleagues, (2017) stimulated microglia with LPS for 24 hours and used that media to treat astrocytes. Our results showed a decrease in microglial viability with increased exposure to LPS marked by loss of adherence and density. Moreover, 6 hours of stimulation were adequate to elicit a response in microglia displayed by cytokines expression and release. We also used a different media formulation which could contribute to the different outcome of glial cells communication in the event of LPS stimulation.

Our data provide important insights into astrocyte expression of NR4As and their possible neuroprotective role. Neuronal survival is promoted by cAMP response element-binding protein (CREB). It has been reported that NR4As are essential regulators of CREB-induced neuroprotective pathways in neurons (Volakakis et al., 2010). The neuroprotective role of astrocytes observed here could be due to the increased expression of NR4As that act as checkpoints during LPS-induced neuroinflammation potentially by attenuation pro-inflammatory mediators expression and secretion in microglia and astrocytes (Saijo et al., 2009, Saijo et al., 2013).

To summarise, LPS induces microglial activation marked by increased pro-inflammatory and anti-inflammatory mediators' expression. Regional and developmental heterogeneity was observed in microglial response to LPS. LPS-stimulated microglia secrete inflammatory factors that trigger astrocytes activation manifested by NR4As and cytokine altered gene expression. MCM-stimulated ACM is neuroprotective, especially in the case of neonatal cortical microglia.

4) Chapter four:

Developmental differences in microglial responses to ATP

4.1 Introduction

As highlighted earlier, neuropathic pain is a type of chronic pain caused by nerve injury or damage. Microglial activation was observed in various models of neuropathic pain (Tsuda, 2016). Both resting and activated microglia express purinergic receptors. Importantly, P2X receptors are differentially expressed in microglia during development (Crain et al., 2009) ATP released from damaged neurons or nerve endings is a trigger for microglial activation. Such stimulation is mediated by purinergic receptors leading to inflammatory mediators' production by microglia. However, the sensitivity of purinergic receptors is ATP-concentration dependent discussed in (Inoue, 2002). Intrathecal injection of cortical or spinal cord ATP-stimulated microglia in the lumbar spine induced tactile allodynia, a characteristic of neuropathic pain. Importantly, neuropathic pain is mediated by BDNF release from ATP-stimulated microglia affecting TrkB signalling in neurons (Coull et al., 2005). In a PNI mouse model, BDNF release from activated microglia is facilitated by P2X4R (Ulmann et al., 2008). Trang and colleagues, (2009) reported an increase in BDNF expression and release from ATP-stimulated neonatal microglia. They proposed a mechanism for BDNF release that involves the activation of p38 MAPK and increased calcium influx following P2X4R activation (Trang et al., 2009).

Infants' responses to nociceptive stimuli differ from those seen in adults due to the immaturity of the pain-signalling pathway in newborns (Fitzgerald and Walker, 2009). Neuropathic pain is rarely studied in infants primarily

because the incident of neuropathic pain disorders observed in adults is lower in children (Walco et al., 2010). Thus, unravelling the mechanisms behind microglial activation and their contribution to neuropathic pain in new-borns and adults is essential to understanding developmental pain.

4.2 Aim

We aimed to investigate microglial responses to ATP at different developmental stages (neonatal vs adult). We also considered microglial regional heterogeneity; therefore, we aimed to compare between cortical and spinal cord microglia response to ATP, especially in the event of P2X stimulation and BDNF release. The general experimental design is illustrated in Figure 4-1.

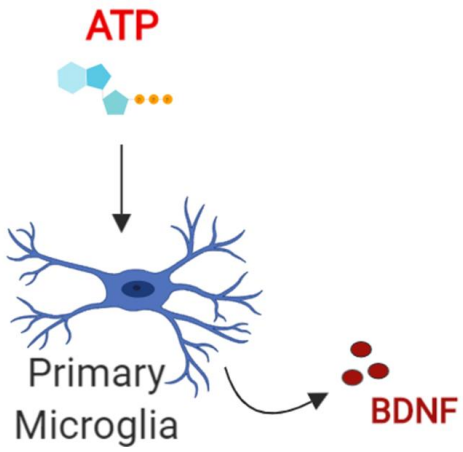

Figure 4-1. Adult or neonatal microglia isolated from rats forebrains or spinal cords were stimulated with ATP. BDNF expression and release with respect to P2X stimulation was investigated. ATP-induced expression of some inflammatory mediators was evaluated.

4.3 Results

4.3.1 ATP-induced NR4A expression in microglia

Extracellular ATP rapidly activates microglia through purinergic receptors in a concentration-dependent manner to trigger the induction of inflammatory mediators' expression and release (Davalos et al., 2005).

4.3.1.1 Different concentrations of ATP induced mRNA expression of *Nur77*, *NOR-1* and *Nurr1* in microglia after 60 min of stimulation

The suggested anti-inflammatory role of Nur77, NOR-1 and Nurr1 makes them an attractive target to study in the event of activated-microglia caused inflammation. In order to identify the appropriate concentration that induces the expression of orphan nuclear receptors, we stimulated adult or neonatal microglia isolated from rats forebrains or spinal cords with different concentrations of ATP ranging from 10µM to 500µM.

In adult cortical microglia, both *Nur77* (7 to 11-fold) and *NOR-1* (9 to 19-fold) mRNA levels significantly increased after ATP stimulation in a concentration-dependent manner (Figure 4-2 a,b). Although these receptors belong to the same family, *Nurr1* transcript levels were not significantly induced with a lower concentration of ATP (10µM), but higher concentrations of ATP (50-500µM) significantly induced *Nurr1* (5 to 15-fold) transcription (Figure 4-2 c).

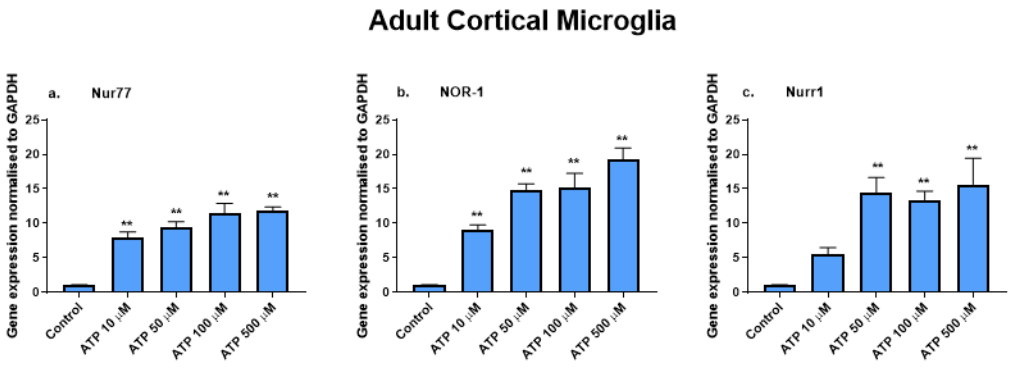

Figure 4-2 Effect of treatment with different concentrations of ATP for 60 minutes on the adult cortical microglial expression of *Nur77*, *NOR-1* and *Nurr1* mRNA. Relative expression of (a) *Nur77*, (b) *NOR-1* and (c) *Nurr1* mRNA (normalised to *GAPDH* as described in methods) in microglia isolated from adult rat forebrains. Treatment groups involved controls (vehicle-treated only), ATP-treated with 10, 50, 100 and 500μM. Bars represent the standard mean of error (SEM) n=4. Statistically significant differences with controls: **p < 0.001. (one-way ANOVA followed by Bonferroni's multiple comparisons).

On the other hand, different mRNA expression patterns were observed in adult spinal cord microglia. For instance, *Nur77* mRNA expression was induced significantly with the lowest concentration of ATP (10μM) by 20 folds, but that induction was downregulated (14 to 10 fold) with higher concentrations of ATP (100-500μM). Although our results suggest that ATP stimulation of adult spinal cord microglia in a concentration of 50-100μM induced *NOR-1* mRNA expression (20-fold) in a higher manner than using 10μM or 500μM ATP (16-fold), all concentrations of ATP resulted in a significant induction of *NOR-1* transcripts. Maximum induction of *Nurr1* mRNA expression was significantly notable with 50μM ATP stimulation (16-fold), yet again all used concentrations of ATP resulted in a significant increase in *Nurr1* mRNA levels in adult spinal cord microglia (Figure 4-3).

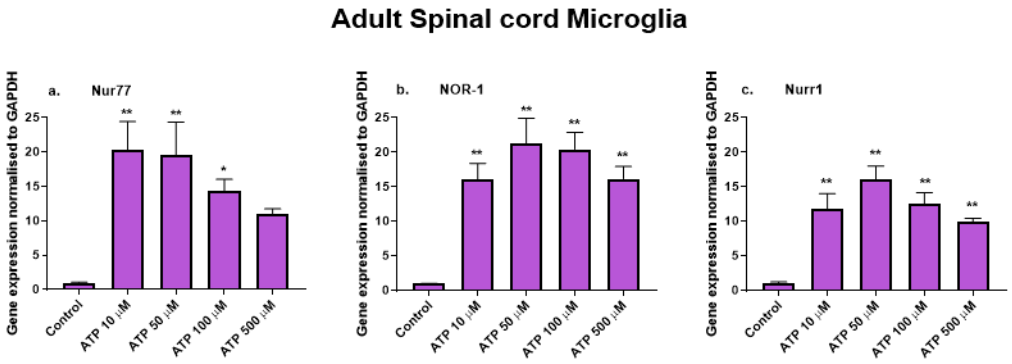

Figure 4-3 Effect of treatment with different concentrations of ATP for 60 minutes on adult spinal cord microglial expression of *Nur77*, *NOR-1* and *Nurr1* mRNA. Relative expression of (a) *Nur77*, (b) *NOR-1* and (c) *Nurr1* mRNA (normalised to *GAPDH* as described in methods) in microglia isolated from adult rat spinal cords. Treatment groups involved controls (vehicle-treated only), ATP-treated with 10, 50, 100 and 500μM. Bars represent the standard mean of error (SEM) n=5. Statistically significant differences with controls: *p < 0.05, **p < 0.001. (one-way ANOVA followed by Bonferroni's multiple comparisons).

In contrast to adult cortical microglia, higher concentrations of ATP (100-500μM) were needed to induce *Nur77* (5-fold) and *NOR-1* (4 to 5 fold change) mRNA levels significantly in neonatal microglia (Figure 4-4 a,b). Alternatively, concentrations of 50-500μM of ATP were sufficient to induce a significant increase in Nurr1 (6-fold) transcript levels in neonatal cortical microglia (Figure 4-4 c).

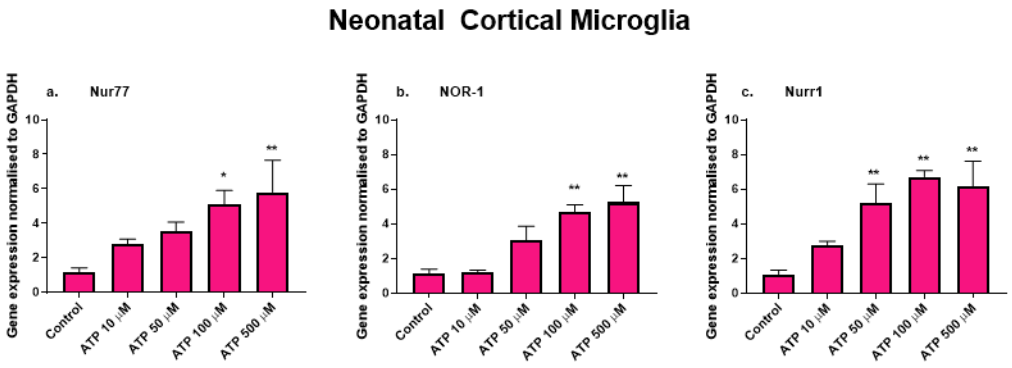

Figure 4-4 Effect of treatment with different concentrations of ATP for 60 minutes on the neonatal cortical microglial expression of *Nur77*, *NOR-1* and *Nurr1* mRNA. Relative expression of (a) *Nur77*, (b) *NOR-1* and (c) *Nurr1* mRNA (normalised to *GAPDH* as described in methods) in microglia isolated from neonatal rat forebrains. Treatment groups involved controls (vehicle-treated only), ATP-treated with 10, 50, 100 and 500μM. Bars represent the standard mean of error (SEM) n=5. Statistically significant differences with controls: *p < 0.05, **p < 0.001. (one-way ANOVA followed by Bonferroni's multiple comparisons).

In Figure 4-5, Baseline levels of *Nurr1* mRNA appeared to be significantly higher in neonatal cortical in comparison to adult cortical microglia. In addition, basal levels of *Nur77* mRNA seemed to be higher in adult in comparison to neonatal cortical microglia, the difference was not statistically significant. However, the different concentrations of ATP triggered a significant increase in all NR4As mRNA expression.

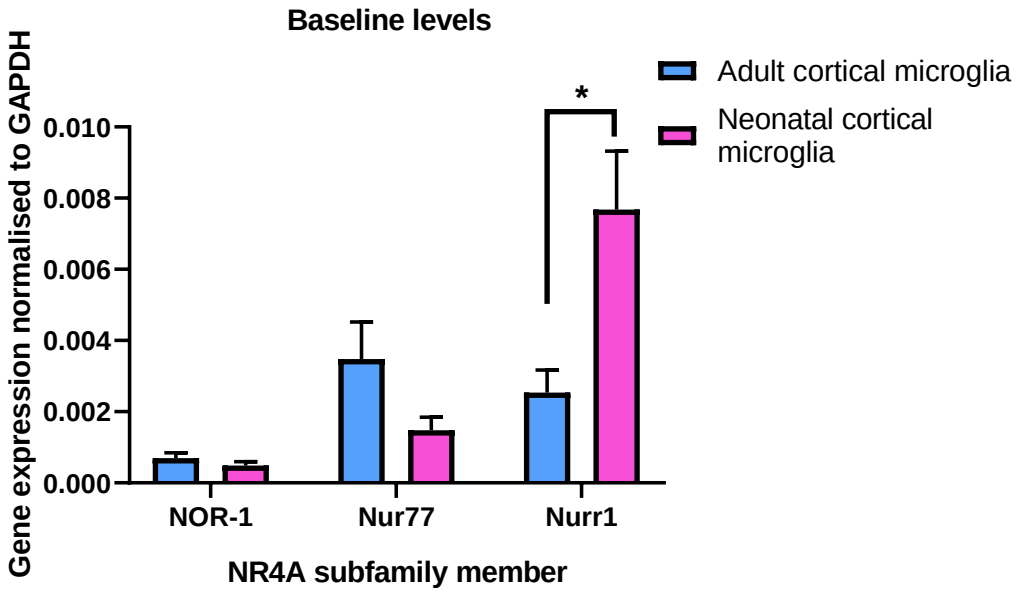

Figure 4-5 Baseline levels of *Nur77, NOR-1* and *Nurr1* mRNA in untreated adult or neonatal cortical microglia. Relative expression of *Nur77, NOR-1* and *Nurr1* mRNA (normalised to *GAPDH* as described in methods) in microglia isolated from adult or neonatal rat forebrains. Bars represent the standard mean of error (SEM) n=4 Adult cortical and n=5 neonatal cortical microglia. (Multiple t-tests).

ATP-induced *Nur77* and *NOR-1* expression fluctuated where *Nur77* mRNA appeared to decrease when neonatal spinal cord microglia were treated with 100µM ATP (8-fold) whereas the same concentration of ATP failed to induce a significant increase in *NOR-1* mRNA (Figure 4-6). Moreover, all ATP concentrations stimulated neonatal spinal cord microglia to increase the expression of *Nurr1* mRNA in a similar fashion despite increased concentrations (6-, 9-, 5- and 7-fold respectively) (Figure 4-6 c).

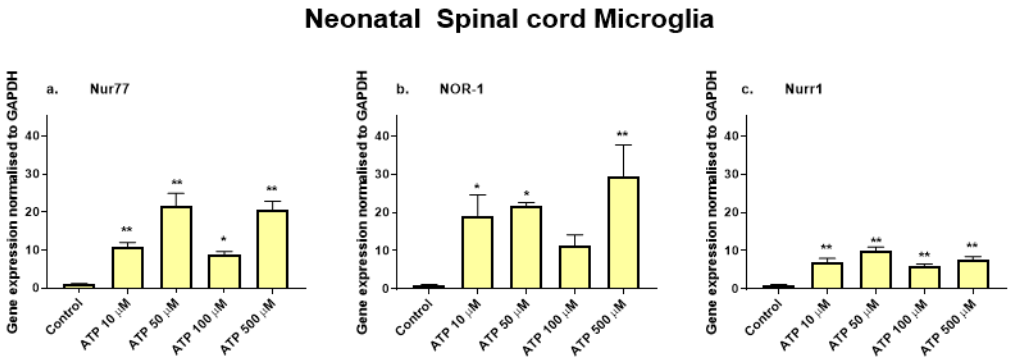

Figure 4-6 Effect of treatment with different concentrations of ATP for 60 minutes on neonatal spinal cord microglial expression of *Nur77*, *NOR-1* and *Nurr1* mRNA. Relative expression of (a) *Nur77*, (b) *NOR-1* and (c) *Nurr1* mRNA (normalised to *GAPDH* as described in methods) in microglia isolated from neonatal rat spinal cords. Treatment groups involved controls (vehicle-treated only), ATP-treated with 10, 50, 100 and 500μM. Bars represent the standard mean of error (SEM) n=5. Statistically significant differences with controls: *p < 0.05, **p < 0.001. (one-way ANOVA followed by Bonferroni's multiple comparisons).

Unlike basal level expression profiles in cortical microglia, In spinal cord microglia NR4A subfamily member transcript levels were statistically significant (Figure 4-7). In unstimulated neonatal spinal cord microglia, *Nurr1* transcript levels were higher than unstimulated adult spinal cord microglia, similar to cortical microglia. On the other hand, *NOR-1* and *Nur77* mRNA levels were higher in adult than neonatal spinal cord microglia.

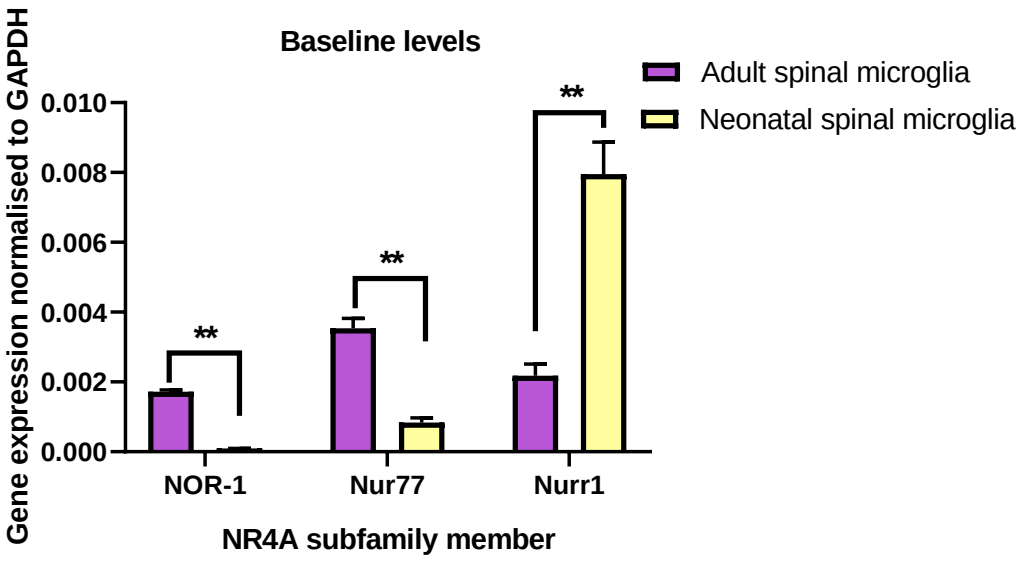

Figure 4-7 Baseline levels of *Nur77, NOR-1* and *Nurr1* mRNA in untreated adult or neonatal spinal cord microglia. Relative expression of *Nur77, NOR-1* and *Nurr1* mRNA (normalised to *GAPDH* as described in methods) in microglia isolated from adult or neonatal rat spinal cords. Bars represent the standard mean of error (SEM) n=5. Significant differences: **p < 0.0003 (Multiple t-tests).

Table 4-1 Summary of relative mRNA expression of *Nurr1*, *Nur77* and *NOR-1* in microglia after treatment with different concentrations of ATP for 60 minutes.

Region	Developmental stage	Gene	Treatment group (ATP)	Mean relative expression of mRNA	P-value	Statistical test
Cortical microglia	Adult	*Nurr1*	10 µM	5.5	0.3604	One-way ANOVA/Bonferroni
			50 µM	14.5	0.0002	
			100 µM	13.4	0.0005	
			500 µM	15.6	0.0001	
	Neonatal		10 µM	6.9	0.7371	
			50 µM	9.8	0.0088	
			100 µM	5.9	0.0009	
			500 µM	7.5	0.0025	
Spinal cord microglia	Adult		10 µM	11.7	0.0004	
			50 µM	16.0	<0.0001	
			100 µM	12.5	0.0002	
			500 µM	9.8	0.0096	
	Neonatal		10 µM	2.7	0.0001	
			50 µM	5.1	<0.0001	
			100 µM	6.7	0.0010	
			500 µM	6.1	<0.0001	
Cortical microglia	Adult	*Nur77*	10 µM	7.8	0.0001	
			50 µM	9.4	<0.0001	
			100 µM	11.4	<0.0001	
			500 µM	11.7	<0.0001	
	Neonatal		10 µM	2.7	0.8080	
			50 µM	3.5	0.2232	
			100 µM	5.1	0.0142	

			500 µM	5.8	0.0061
Spinal cord microglia	**Adult**	*NOR-1*	10 µM	20.2	0.0007
			50 µM	19.5	0.0018
			100 µM	14.3	0.0166
			500 µM	10.9	0.1888
	Neonatal		10 µM	10.8	0.0021
			50 µM	21.5	<0.0001
			100 µM	8.8	0.0146
			500 µM	20.4	<0.0001
Cortical microglia	**Adult**		10 µM	9.0	0.0004
			50 µM	14.8	<0.0001
			100 µM	15.2	<0.0001
			500 µM	19.2	<0.0001
	Neonatal		10 µM	1.2	>0.9999
			50 µM	3.1	0.1087
			100 µM	4.6	0.0014
			500 µM	5.2	0.0006
Spinal cord microglia	**Adult**		10 µM	16.1	0.0005
			50 µM	21.2	<0.0001
			100 µM	20.4	<0.0001
			500 µM	16.1	0.0008
	Neonatal		10 µM	19.1	0.0315
			50 µM	21.7	0.0342
			100 µM	11.3	0.4210
			500 µM	29.5	0.0014

4.3.1.2 Induced transcript levels of *Nur77* and *NOR-1* in microglia stimulated with 100μM ATP at different time points

Preliminary studies led to a chosen concentration of 100μM to stimulate microglia and evaluate the mRNA expression of *Nur77* and *NOR-1*. Firstly, In adult cortical microglia, ATP-induced an increase in *Nur77* (50-fold) and *NOR-1* (35-fold) mRNA significantly after treatment for one hour. While *Nur77* transcript levels decreased after one hour of ATP stimulation, *NOR-1* mRNA expression remained significantly up-regulated until three hours of ATP treatment in adult cortical microglia (30-fold up). ATP-induced *Nur77* (37-fold) and *NOR-1* (97-fold) expression significantly increased again after twelve hours of ATP stimulation (Figure 4-8 a,b).

Similarly, ATP induced an increase in both *Nur77* (17-fold) and *NOR-1* (25-fold) transcript levels significantly after one hour of treatment in neonatal cortical microglia, however, unlike adult cortical microglia a significant up-regulation in *Nur77* and *NOR-1* mRNA levels was not shown after twelve hours of ATP stimulation (Figure 4-8 c,d).

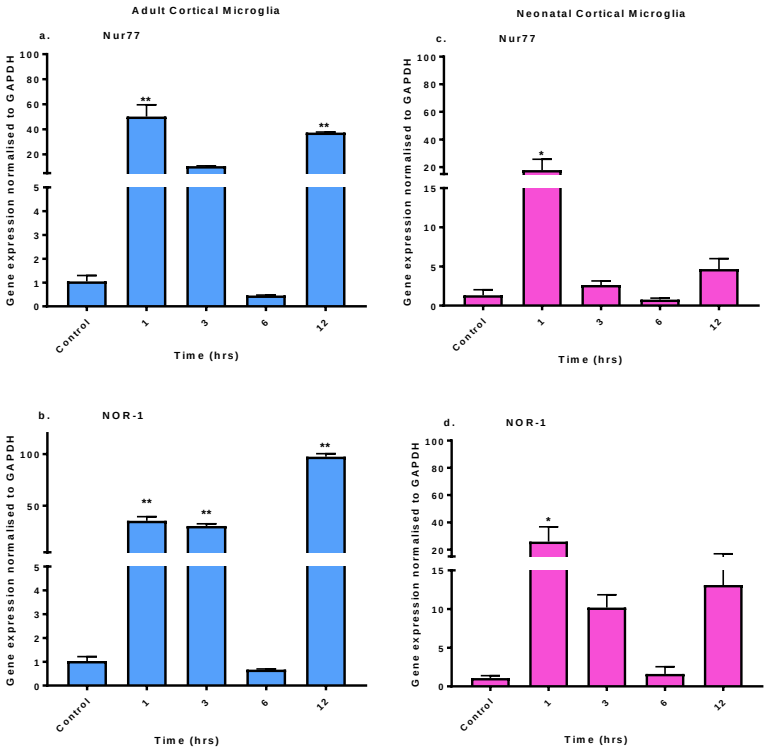

Figure 4-8 Effect of treatment with ATP on the cortical microglial expression of *Nur77* and *NOR-1* mRNA. Relative expression of *Nur77* and *NOR-1* mRNA (normalised to *GAPDH* as described in methods) in microglia isolated from adult (a and b) or neonatal (c and d) rat forebrains. Treatment groups involved controls (vehicle-treated only), ATP-treated for 1, 3, 6 and 12 hours. Bars represent the standard mean of error (SEM) n=3. Statistically significant differences with controls: *****$p < 0.05$, ******$p < 0.001$ (one-way ANOVA followed by Bonferroni's multiple comparisons).

In spite of the similarity in the significant ATP-induced *Nur77* (28-fold) and *NOR-1* (29-fold) transcript levels increase in adult spinal cord microglia, unlike adult cortical microglia, ATP stimulation did not result in an increase in *Nur77* and *NOR-1* mRNA levels after twelve hours (Figure 4-9 a,b). A similar pattern to adult spinal cord microglia was observed when neonatal spinal cord microglia were stimulated with ATP as shown in Figure 4-9 c,d where ATP stimulation elevated *Nur77* mRNA expression by 15 folds and *NOR-1* mRNA by 38 folds.

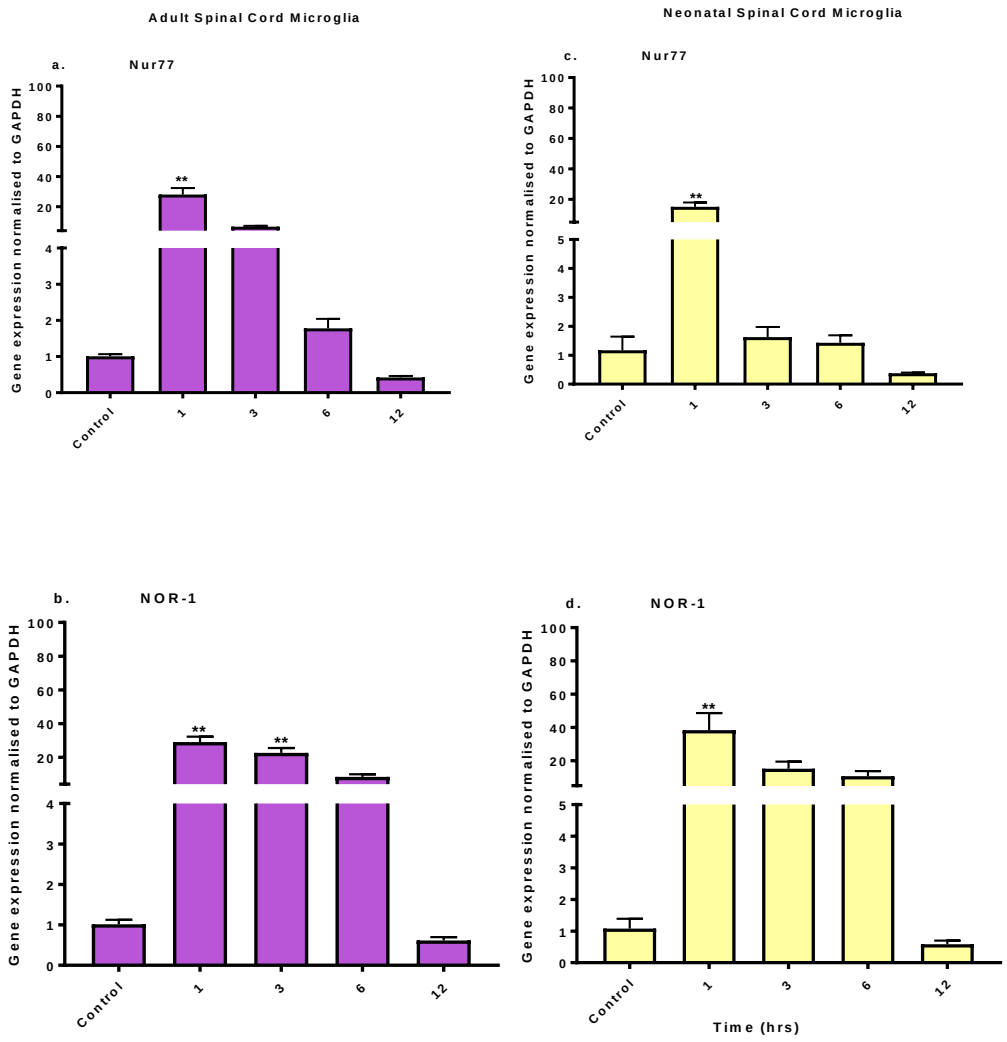

Figure 4-9 Effect of treatment with ATP on spinal cord microglial expression of *Nur77* and *NOR-1* mRNA. Relative expression of *Nur77* and *NOR-1* mRNA (normalised to *GAPDH* as described in methods) in microglia isolated from adult (a and b) or neonatal (c and d) rat spinal cords. Treatment groups involved controls (vehicle-treated only), ATP-treated for 1, 3, 6 and 12 hours. Bars represent the standard mean of error (SEM) n=3. Statistically significant differences with controls: **$p < 0.001$ (one-way ANOVA followed by Bonferroni's multiple comparisons).

Table 4-2 Summary of relative mRNA expression of *Nur77* and *NOR-1* in microglia following stimulation with 100μM ATP at different time points.

Region	developmental stage	Gene	Treatment group (ATP)	Mean relative expression of mRNA	P-value	Statistical test
Cortical microglia	**Adult**	*Nur77*	1 hr	50.1	<0.0001	One-way ANOVA/Bonferroni
			3 hr	10.5	0.5599	
			6 hr	0.4	>0.9999	
			12 hr	37.3	0.0005	
	Neonatal		1 hr	17.9	0.0336	
			3 hr	2.6	>0.9999	
			6 hr	0.7	>0.9999	
			12 hr	4.6	>0.9999	
Spinal cord microglia	**Adult**		1 hr	28.0	<0.0001	
			3 hr	6.7	0.2615	
			6 hr	1.7	>0.9999	
			12 hr	0.4	>0.9999	
	Neonatal		1 hr	15.1	<0.0001	
			3 hr	1.6	>0.9999	
			6 hr	1.4	>0.9999	
			12 hr	0.3	>0.9999	
Cortical microglia	**Adult**	*NOR-1*	1 hr	35.5	<0.0001	
			3 hr	30.5	<0.0001	
			6 hr	0.6	>0.9999	
			12 hr	97.4	<0.0001	
	Neonatal		1 hr	25.8	0.0287	
			3 hr	10.1	0.9793	
			6 hr	1.6	>0.9999	

		12 hr	13.1	0.5365
Spinal cord microglia	Adult	1 hr	29.0	<0.0001
		3 hr	22.5	<0.0001
		6 hr	8.3	0.0830
		12 hr	0.6	0.9998
	Neonatal	10 µM	38.4	0.0018
		50 µM	15.2	0.3192
		100 µM	10.7	0.8565
		500 µM	0.5	>0.9999

4.3.1.3 ATP-induced Nur77 protein expression in microglia in a time-dependent manner

We evaluated the protein expression of Nur77 in response to ATP stimulation in microglia. Surprisingly, unlike mRNA expression of *Nur77*, Nur77 protein levels continued to increase in a time-dependent manner when both neonatal cortical (Figure 4-10) or spinal cord (Figure 4-11) microglia were treated with 100µM ATP. Nur77 protein expression from adult cortical (Figure 4-10) or spinal cord (Figure 4-11) microglia wasn't detectable on the blot, whereas corresponding bands for the control which is β-actin were detectable.

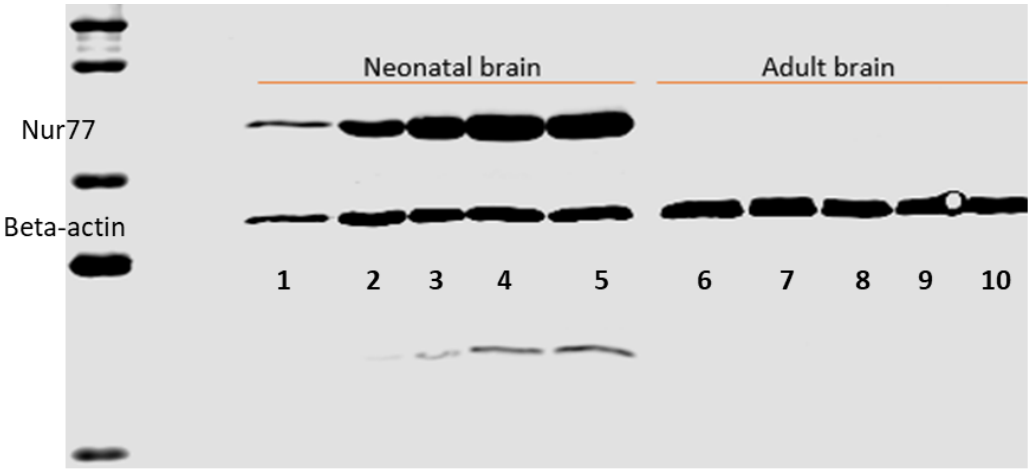

1. Neonatal brain control microglia
2. Neonatal brain microglia treated with 100µM ATP for 1 hr
3. Neonatal brain microglia treated with 100µM ATP for 3 hrs
4. Neonatal brain microglia treated with 100µM ATP for 6 hrs
5. Neonatal brain microglia treated with 100µM ATP for 12 hrs
6. Adult brain control microglia
7. Adult brain microglia treated with 100µM ATP for 1 hrs
8. Adult brain microglia treated with 100µM ATP for 3 hrs
9. Adult brain microglia treated with 100µM ATP for 6 hrs
10. Adult brain microglia treated with 100µM ATP for 12 hrs

Figure 4-10 Effect of ATP treatment on neonatal and adult rat cortical microglial protein expression of Nur77 represented by Western blot. The blot displays cortical microglia treated with ATP for 1, 3, 6 and 12 hours. The upper bands correspond to Nur77 protein (~64kDa). The lower bands correspond to the housekeeping gene, beta-actin (~43 kDa).

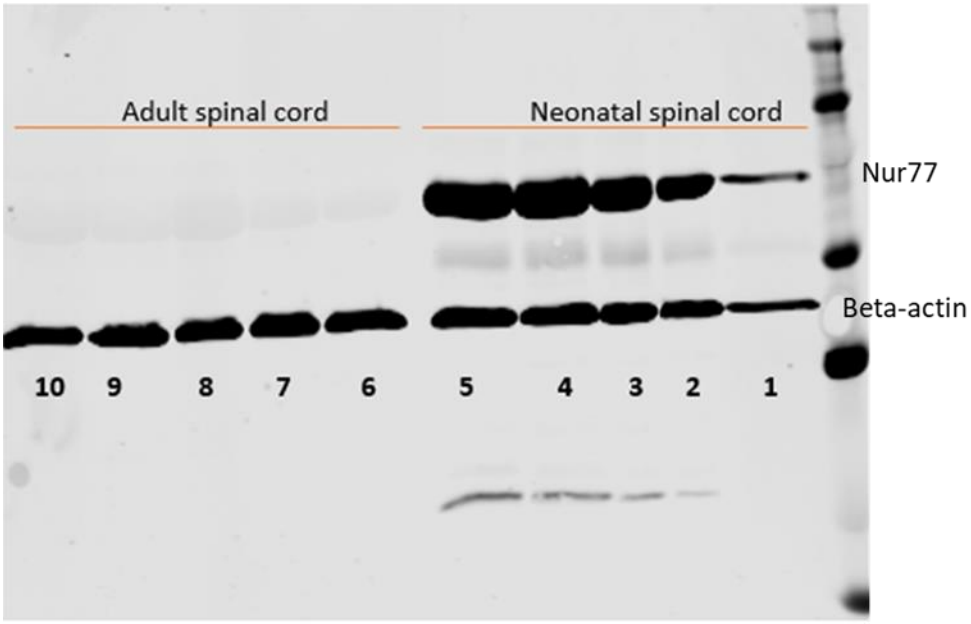

1. Neonatal spinal cord control microglia
2. Neonatal spinal cord microglia treated with 100µM ATP for 1 hr
3. Neonatal spinal cord microglia treated with 100µM ATP for 3 hrs
4. Neonatal spinal cord microglia treated with 100µM ATP for 6 hrs
5. Neonatal spinal cord microglia treated with 100µM ATP for 12 hrs
6. Adult spinal cord control microglia
7. Adult spinal cord microglia treated with 100µM ATP for 1 hrs
8. Adult spinal cord microglia treated with 100µM ATP for 3 hrs
9. Adult spinal cord microglia treated with 100µM ATP for 6 hrs
10. Adult spinal cord microglia treated with 100µM ATP for 12 hrs

Figure 4-11 Effect of ATP treatment on neonatal and adult rat spinal cord microglial protein expression of Nur77 represented by Western blot. The blot displays spinal cord microglia treated with ATP for 1, 3, 6 and 12 hours. The upper bands correspond to Nur77 protein (~64kDa). The lower bands correspond to the housekeeping gene, beta-actin (~43 kDa).

4.3.2 P2X4R protein expression and localisation in neonatal or adult microglia

As mentioned earlier, it has been reported that ATP triggers the release of BDNF from neonatal microglia through activating P2X4R

signalling pathway (Trang et al., 2009). In the present study, we compared the expression of P2X4R in resting adult and neonatal microglia. As shown in the blot in Figure 4-12, P2X4R protein expression was higher in neonatal microglia and almost undetectable in adult microglia. Moreover, the expression of P2X4R protein was higher in neonatal cortical microglia as opposed to neonatal spinal cord microglia.

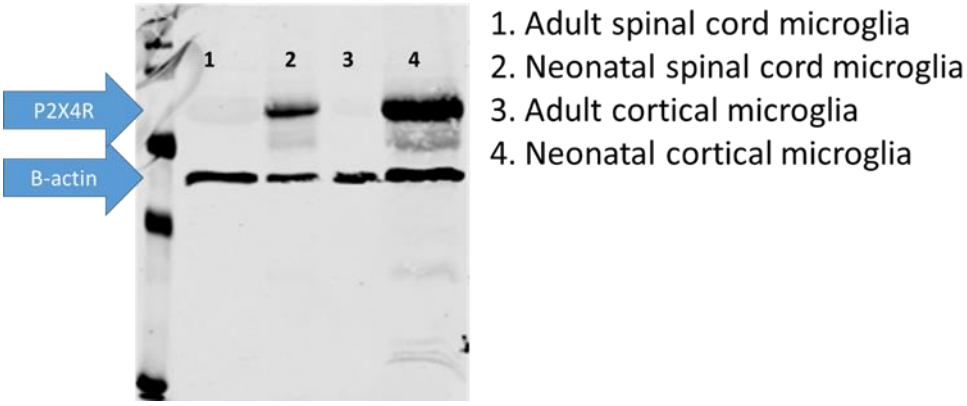

Figure 4-12 Protein expression of P2X4R in microglia. The western blot represents the difference in P2X4R protein expression in untreated adult (1,3) or neonatal microglia (2,4). The upper bands correspond to P2X4R protein (~65 kDa) while the lower bands correspond to the housekeeping gene beta-actin (~43 kDa).

These observations were confirmed when we used epifluorescence microscopy. P2X4R immunoreactivity appeared to be higher in neonatal cortical and spinal cord microglia in comparison to adult cortical and spinal cord microglia (Figure 4-13).

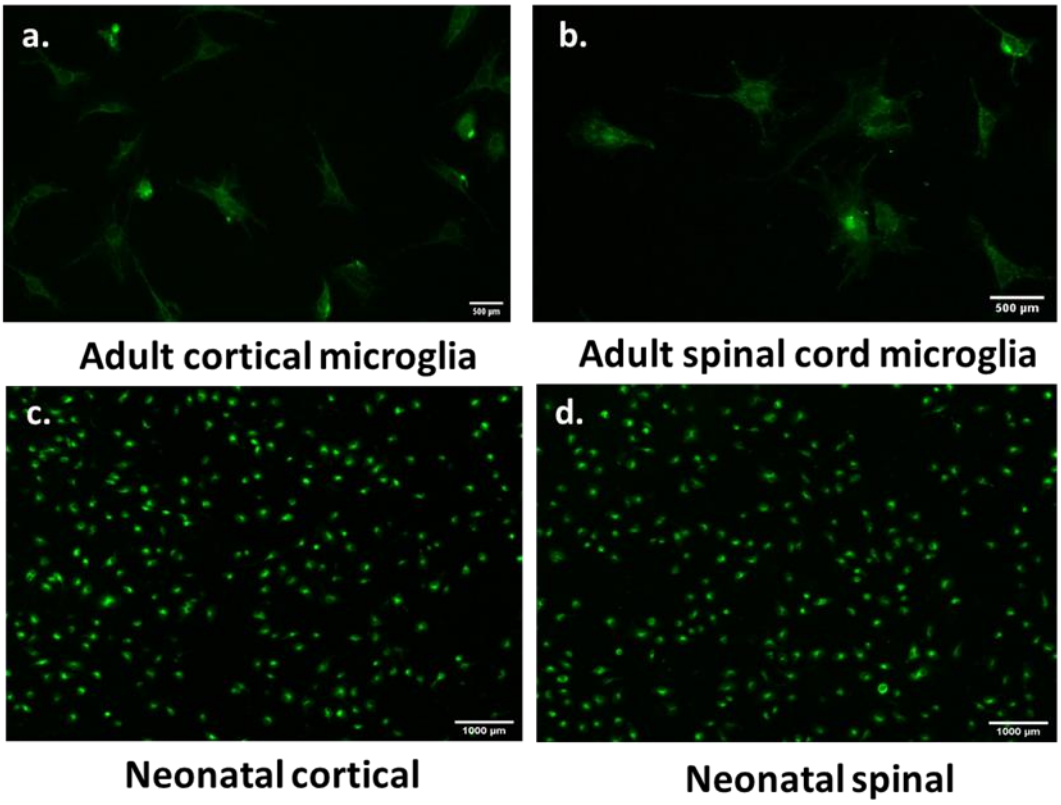

Figure 4-13 Immunoreactivity of P2XR4 in rat primary untreated microglia. The localisation of P2X4R protein in adult (a) cortical or (b) spinal cord microglia (scale bar 500µm) and in neonatal (c) cortical or (d) spinal cord microglia (scale bar 1000 µm) using an epifluorescent microscope. Magnification 4x neonatal microglia and 10x adult microglia.

Intriguingly, the expression of P2X4R in resting microglia seemed to be more in the cytoplasm rather than on the cell membrane. These findings were obtained through a confocal microscope. Once more, the expression of P2X4R seemed to be qualitatively higher in neonatal microglia compared to adult microglia (Figure 4-14).

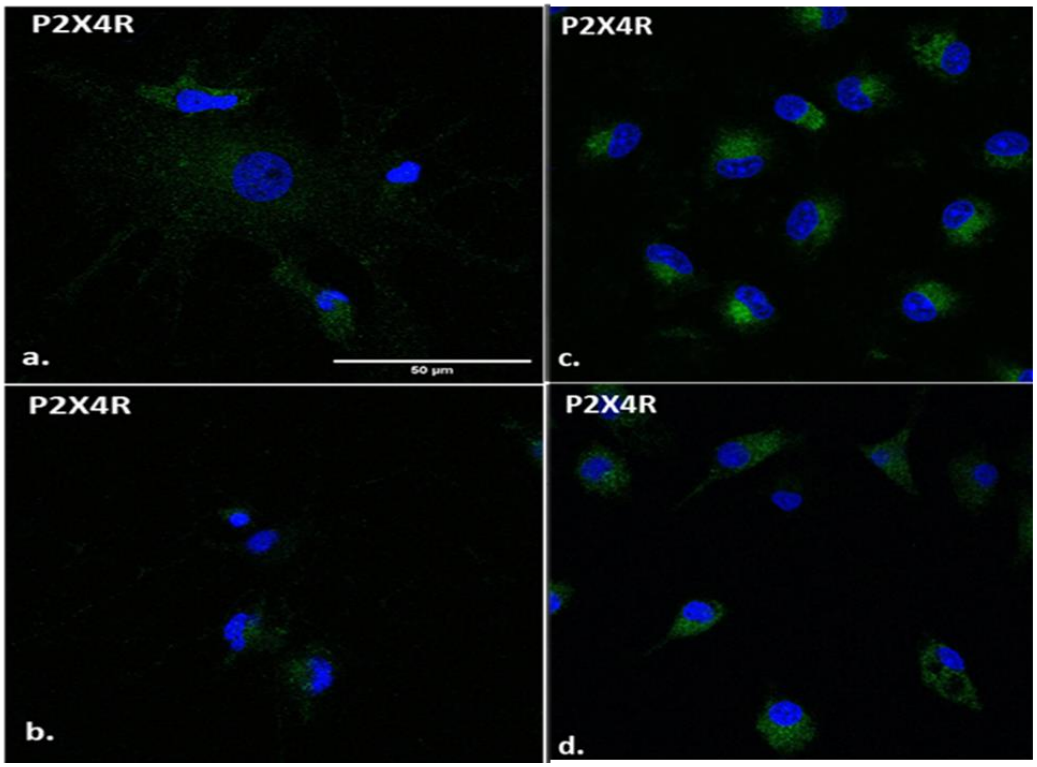

Figure 4-14 Immunoreactivity of P2XR4 in rat primary untreated microglia. The localisation of P2X4R protein in adult (a) cortical or (b) spinal cord microglia and in neonatal (c) cortical or (d) spinal cord microglia using a confocal microscope. Nuclei are stained with DAPI. Magnification 60x (scale bar 50µm).

4.3.3 *BDNF* mRNA expression in response to ATP stimulation of microglia

In order to evaluate BDNF expression in adult compared to neonatal microglia, different concentrations of ATP were used to induce microglial activation. Trang and colleagues, 2009 reported an increase in BDNF release after 5 minutes and 60 minutes of ATP stimulation (Trang et al., 2009); therefore, we stimulated both adult and neonatal microglia for 60 min with ATP. Our results showed a significant increase in *BDNF* mRNA

expression in adult cortical microglia (Figure 4-15 a) after stimulation with 50µM (2.7-fold) or 100µM (2.4-fold) ATP, though the lower concentration resulted in a greater fold change compared to untreated microglia (controls). Moreover, *IL-1β* transcript level was not significantly affected by ATP treatment (Figure 4-15 b).

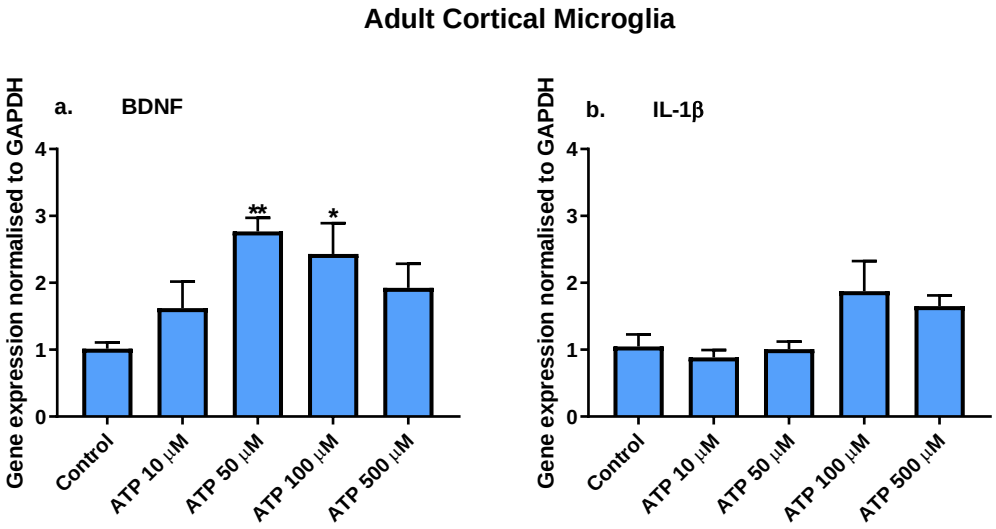

Figure 4-15 Effect of treatment with different concentrations of ATP on the adult cortical microglial expression of BDNF and IL-1β mRNA. Relative expression of (a) *BDNF* and (b) *IL-1β* mRNA (normalised to *GAPDH* as described in methods) in microglia isolated from adult rat forebrains. Treatment groups involved controls (vehicle-treated only), ATP-treated with 10, 50, 100 and 500µM. Bars represent the standard mean of error (SEM) n=4. Statistically significant differences with controls:*p < 0.05 **p < 0.001. (one-way ANOVA followed by Bonferroni's multiple comparisons).

On the other hand, neither *BDNF* nor *IL-1β* mRNA expression was affected with ATP stimulation in adult spinal cord microglia, as shown in Figure 4-16 a,b.

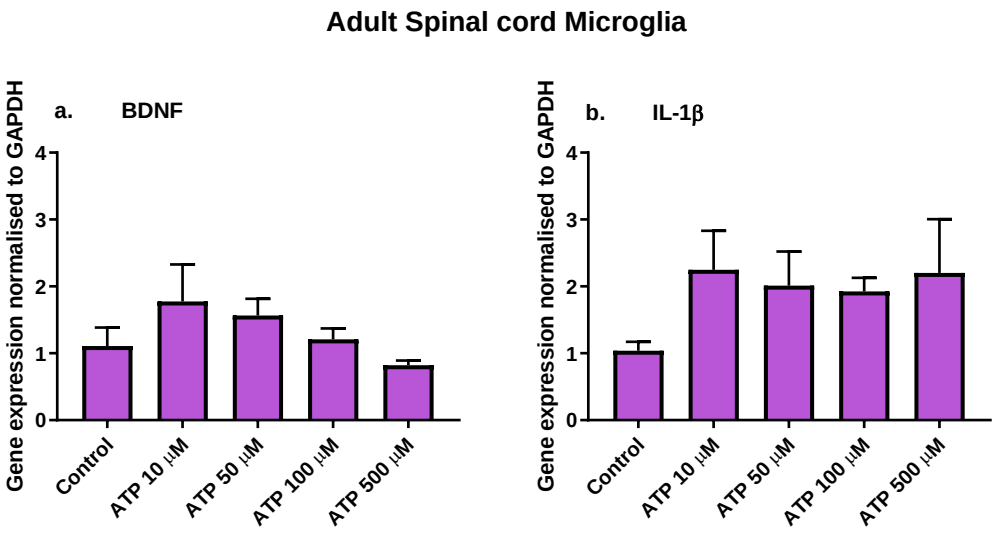

Figure 4-16 Effect of treatment with different concentrations of ATP on the adult spinal cord microglial expression of *BDNF* and *IL-1β* mRNA. Relative expression of (a) *BDNF* and (b) *IL-1β* mRNA (normalised to *GAPDH* as described in methods) in microglia isolated from adult rat spinal cords. Treatment groups involved controls (vehicle-treated only), ATP-treated with 10, 50, 100 and 500μM. Bars represent the standard mean of error (SEM) n=5. (one-way ANOVA followed by Bonferroni's multiple comparisons).

When neonatal cortical microglia were treated with 100μM ATP, a significant increase in *BDNF* mRNA expression was noticeable (3-fold) (Figure 4-17 a); however, ATP stimulation failed to induce a substantial up-regulation in *IL-1β* mRNA (Figure 4-17 b).

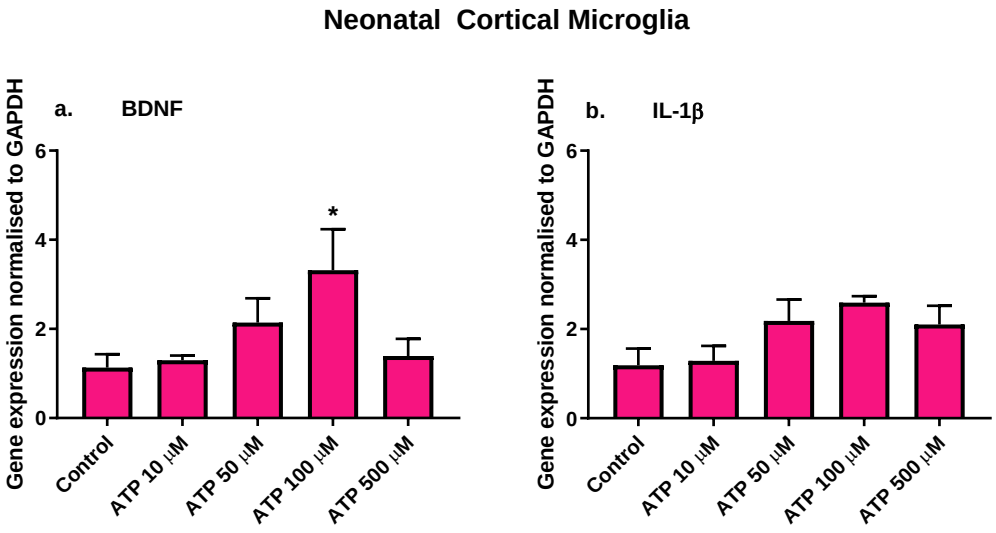

Figure 4-17 Effect of treatment with different concentrations of ATP on neonatal cortical microglial expression of *BDNF* and *IL-1β* mRNA. Relative expression of (a) *BDNF* and (b) *IL-1β* mRNA (normalised to *GAPDH* as described in methods) in microglia isolated from neonatal rat forebrains. Treatment groups involved controls (vehicle-treated only), ATP-treated with 10, 50, 100 and 500μM. Bars represent the standard mean of error (SEM) n=5. Statistically significant differences with controls:*$p < 0.05$ (one-way ANOVA followed by Bonferroni's multiple comparisons).

Surprisingly, *IL-1β* transcript levels were significantly elevated in neonatal spinal cord microglia by 2 folds when a high concentration of ATP (500μM) was used for activation (Figure 4-18 b). Nevertheless, BDNF mRNA levels were not affected by ATP treatment (Figure 4-19 a)

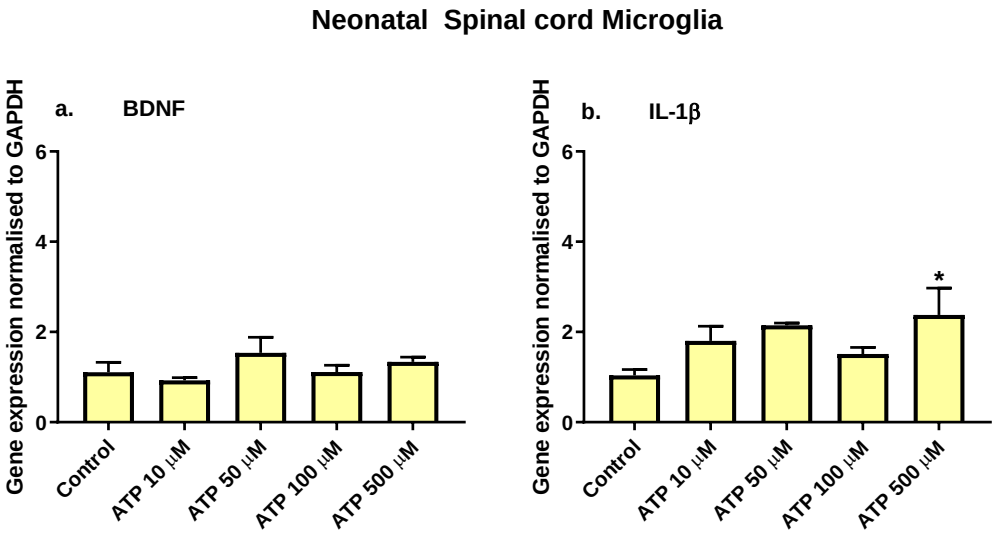

Figure 4-18 Effect of treatment with different concentrations of ATP on neonatal spinal cord microglial expression of *BDNF* and *IL-1β* mRNA. Relative expression of (a) *BDNF* and (b) *IL-1β* mRNA (normalised to *GAPDH* as described in methods) in microglia isolated from neonatal rat spinal cords. Treatment groups involved controls (vehicle-treated only), ATP-treated with 10, 50, 100 and 500μM. Bars represent the standard mean of error (SEM) =5. Statistically significant differences with controls:*p < 0.05 (one-way ANOVA followed by Bonferroni's multiple comparisons).

Table 4-3 Summary of relative mRNA expression of *BDNF* and *IL-1β* in microglia after stimulation with different concentrations of ATP for 60 minutes.

Region	Developmental stage	Gene	Treatment group (ATP)	Mean relative expression of mRNA	P-value	Statistical test
Cortical microglia	Adult	*BDNF*	10 µM	1.6	0.8037	One-way ANOVA/Bonferroni
			50 µM	2.7	0.0045	
			100 µM	2.4	0.0237	
			500 µM	1.9	0.3059	
	Neonatal		10 µM	1.2	>0.9999	
			50 µM	2.1	0.8139	
			100 µM	3.3	0.0430	
			500 µM	1.3	>0.9999	
Spinal cord microglia	Adult		10 µM	1.7	0.6689	
			50 µM	1.5	>0.9999	
			100 µM	1.2	>0.9999	
			500 µM	0.8	>0.9999	
	Neonatal		10 µM	0.9	>0.9999	
			50 µM	1.5	0.5783	
			100 µM	1.1	>0.9999	
			500 µM	1.3	>0.9999	
Cortical microglia	Adult	*IL-1β*	10 µM	0.8	>0.9999	
			50 µM	1.0	>0.9999	
			100 µM	1.8	0.1019	
			500 µM	1.6	0.4440	
	Neonatal		10 µM	1.2	>0.9999	
			50 µM	2.1	0.2774	
			100 µM	2.5	0.0772	
			500 µM	2.1	0.4430	

Spinal cord microglia	Adult	10 µM	1.7	0.3086
		50 µM	2.0	0.6924
		100 µM	1.9	0.7450
		500 µM	2.2	0.4261
	Neonatal	10 µM	1.8	0.3205
		50 µM	2.1	0.1265
		100 µM	1.5	>0.9999
		500 µM	2.3	0.0271

4.3.3.1 ATP-induced BDNF expression and release was changed in adult microglia upon interference with P2X or P38 MAPK pathways in a time-dependent manner

As mentioned earlier in chapter one, ATP activates P2X receptors in a concentration-dependent way; therefore, we used a concentration of 50µM ATP to induce microglial activation targetting P2X4R as previously reported (Trang et al., 2009). It has been suggested that 5-BDBD is a selective antagonist for P2X4R (Coddou et al., 2019); hence we evaluated its effect in inhibiting P2X4R signalling pathway by focusing on the activation of p38 MAPK. We only used adult cortical microglia to investigate the phosphorylation of p38 MAPK since our results showed an increase in BDNF mRNA expression after stimulation with 50µM of ATP. ATP stimulation resulted in increased phosphorylation of p38 MAPK after stimulation with ATP for 5 minutes. Phosphorylation of p38 MAPK decreased after ATP stimulation for 10 or 20 minutes, however, increased again after 60 min of

ATP stimulation. Despite the increased in p38 phosphorylation, 5-BDBD did not affect p38 phosphorylation, as shown in Figure 4-19.

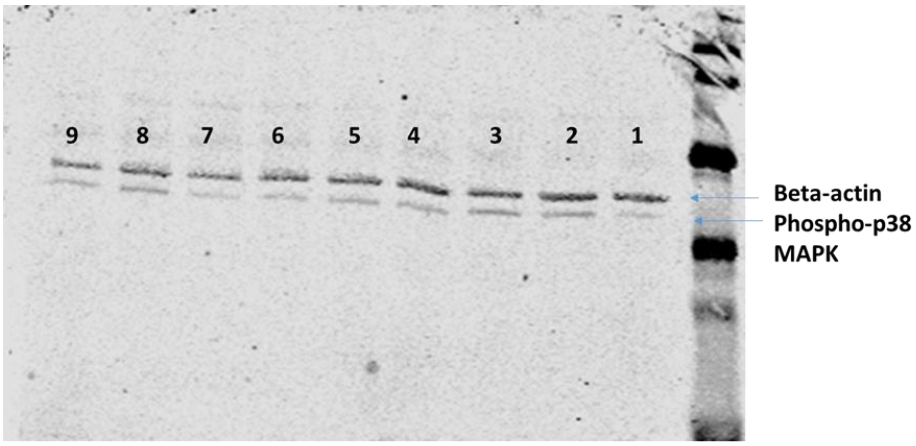

1. Control
2. ATP 50µM, 5 min
3. ATP 50µM 5 min +20µM 5-BDBD
4. ATP 50µM, 10 min
5. ATP 50µM 10 min +20µM 5-BDBD
6. ATP 50µM, 20 min
7. ATP 50µM 20 min +20µM 5-BDBD
8. ATP 50µM, 60 min
9. ATP 50µM 60 min +20µM 5-BDBD

Figure 4-19 Immunoblotting of Pohsopho-p38 (pp38) MAPK protein expression in adult cortical microglia. Microglia were treated with vehicle-only (control) or with a dose of 50µM of ATP was used to stimulate adult cortical microglia for different time points (5, 10, 20 and 60 minutes). Pretreatment of 5-BDBD (P2X4R selective antagonist) at a concentration of 20µM for 30 minutes before ATP stimulation showed no difference in P-p38 MAPK expression. Upper band corresponds to beta-actin (~43 kDa) as an endogenous control while the lower bands correspond to P-p38 MAPK (~41 kDa).

A preliminary experiment showed an increase in *BDNF* mRNA expression after 12 hours of ATP stimulation; therefore, we evaluated *BDNF* mRNA expression in response to 50µM of ATP stimulation in adult and neonatal microglia. We also used inhibitors for p38 MAPK (SB202190) and P2X7R (A438079). Although ATP-induced p38 phosphorylation was inhibited with SB202190 pre-treatment and not affected by A438079 in adult cortical microglia (Figure 4-21), the same treatment did not have any effect

on *BDNF* mRNA expression in adult or neonatal microglia (Figure 4-20 and Figure 4-22, respectively). Figure 4-21 display preliminary studies using a lower concentration of ATP (see Figure 4-31 for the effect of inhibiting p38 MAPK on Pp38 and housekeeping gene).

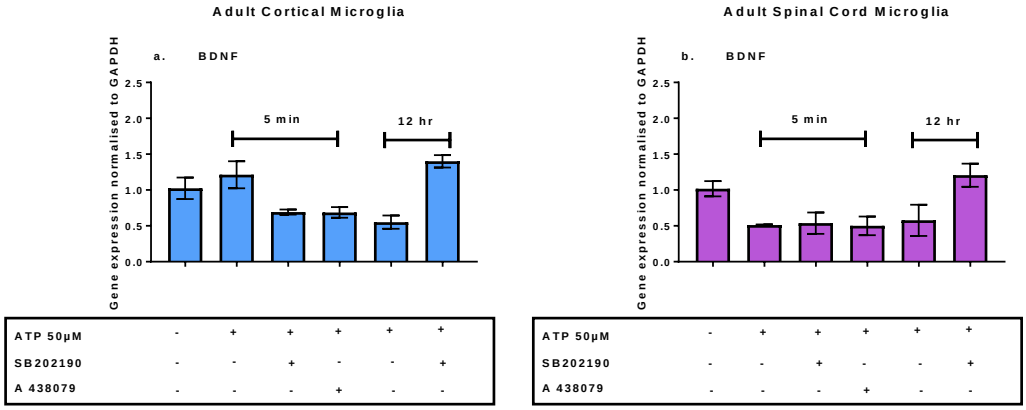

Figure 4-20 Effect of treatment with 50µM ATP on adult cortical or spinal cord microglial expression of *BDNF* mRNA. Relative expression of *BDNF* mRNA (normalised to *GAPDH* as described in methods) in microglia isolated from adult rat (a) forebrains or (b) spinal cords. Treatment groups involved controls (vehicle-treated only), ATP-treated with 50µM for 5 min or 12 hours with or without pretreatment with 10µM p38 MAPK inhibitor (SB202190) or 10µM P2X7R inhibitor (A438079) Bars represent the standard mean of error (SEM) n=4. (one-way ANOVA followed by Bonferroni's multiple comparisons).

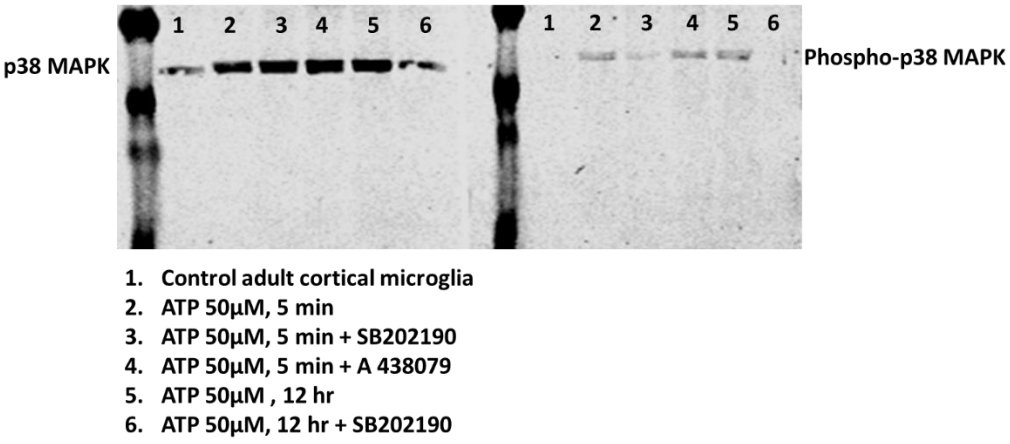

Figure 4-21 Immunoblotting of total or P-p38 MAPK protein expression in adult cortical microglia. A dose of 50µM of ATP was used to stimulate adult cortical microglia for different time points (5 minutes and 12 hours). Microglia were pretreated with 10µM p38 MAPK inhibitor (SB202190) or 10µM P2X7R inhibitor (A438079). The blot on the left shows the protein expression of total p38 MAPK as a control while the blot on the right shows the protein expression of P-p38 MAPK.

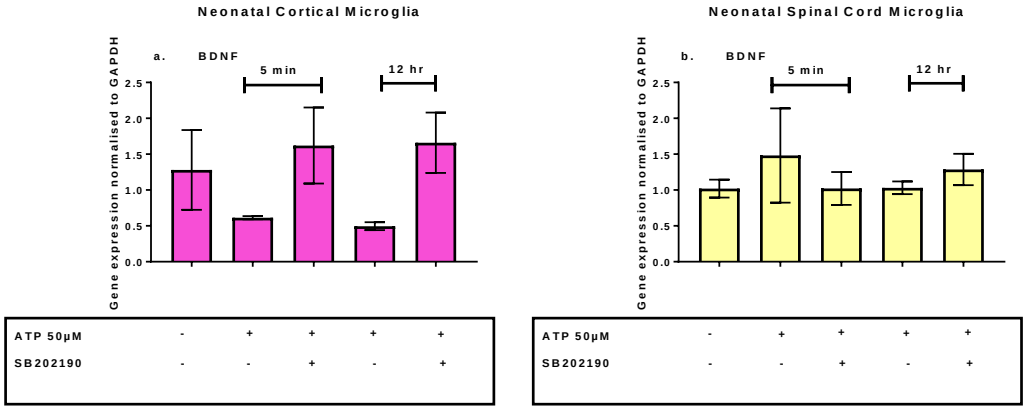

Figure 4-22 Effect of treatment with 50µM ATP on neonatal cortical or spinal cord microglial expression of *BDNF* mRNA. Relative expression of *BDNF* mRNA (normalised to *GAPDH* as described in methods) in microglia isolated from neonatal rat (a) forebrains or (b) spinal cords. Treatment groups involved controls (vehicle-treated only), ATP-treated with 50µM for 5 min or 12 hours with or without pretreatment with 10µM p38 MAPK inhibitor (SB202190). Bars represent the standard mean of error (SEM) n=4. (one-way ANOVA followed by Bonferroni's multiple comparisons).

We treated adult microglia again with 50µM of ATP for 60 minutes to evaluate *BDNF* expression in response to both ATP or pretreatment with SB202190. Our results showed a significant up-regulation in *BDNF* mRNA expression in adult cortical microglia after 60 minutes of stimulation (3-fold). A lower fold change of *BDNF* was evident when cells were pretreated with SB202190 (2.7-fold) (Figure 4-23 a). Once more, IL-1β transcript levels were not significantly affected by the treatment (Figure 4-23 b).

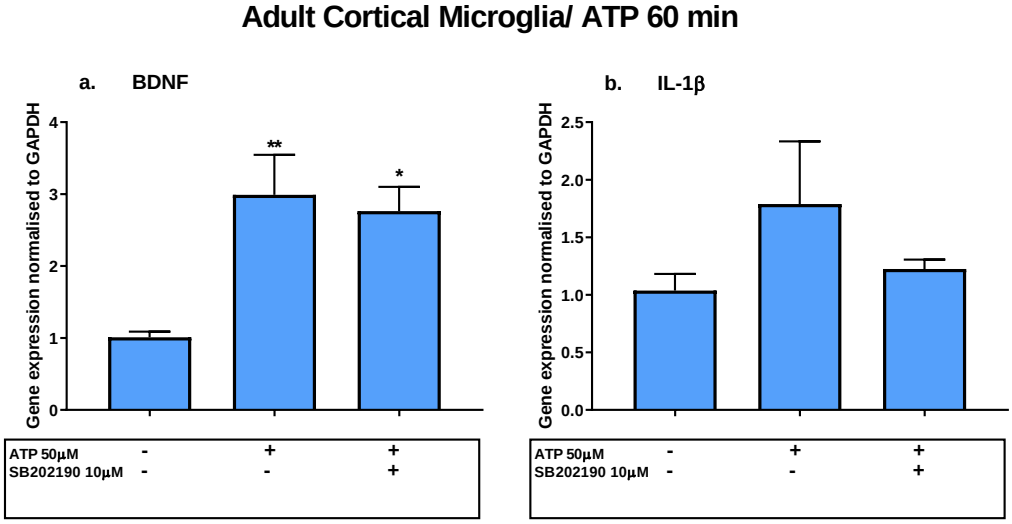

Figure 4-23 Effect of treatment with 50µM ATP with or without p38 MAPK inhibitor on the adult cortical microglial expression of BDNF and IL-1β mRNA. Relative expression of (a) *BDNF* and (b) *IL-1β* mRNA (normalised to *GAPDH* as described in methods) in microglia isolated from adult rat forebrains. Treatment groups involved controls (vehicle-treated only), ATP-treated with 50µM and pre-treatment with 10µM p38 MAPk inhibitor (SB202190). Bars represent the standard mean of error (SEM) n=4. Statistically significant differences with controls:*p < 0.05 **p < 0.001. (one-way ANOVA followed by Bonferroni's multiple comparisons).

On the other hand, the same treatment failed to induce a response concerning *BDNF* (Figure 4-24 a) or *IL-1β* (Figure 4-24) mRNA expression in adult spinal cord microglia.

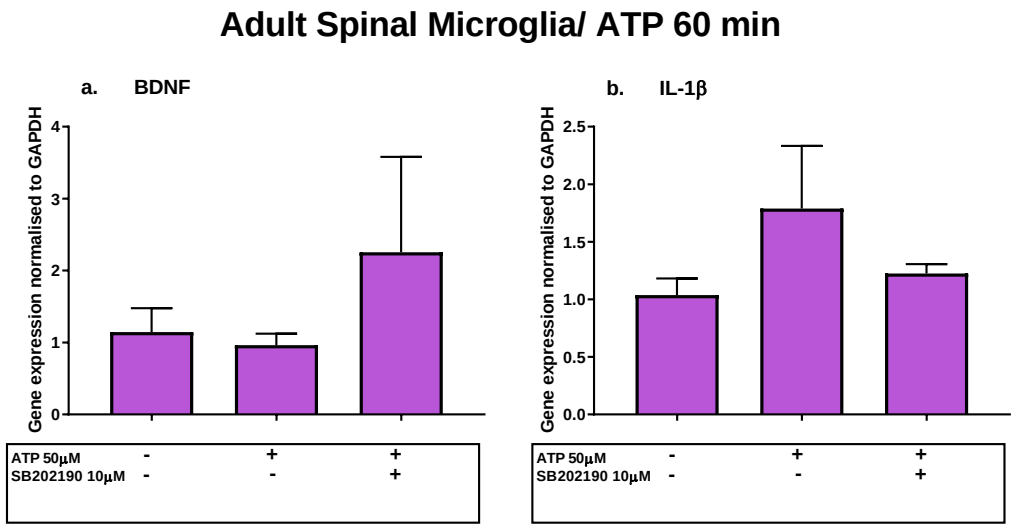

Figure 4-24 Effect of treatment with 50µM ATP with or without p38 MAPK inhibitor on the adult spinal cord microglial expression of BDNF and IL-1β mRNA. Relative expression of (a) *BDNF* and (b) *IL-1β* mRNA (normalised to *GAPDH* as described in methods) in microglia isolated from adult rat spinal cords. Treatment groups involved controls (vehicle-treated only), ATP-treated with 50µM and pre-treatment with 10µM p38 MAPk inhibitor (SB202190). Bars represent the standard mean of error (SEM) n=4. (one-way ANOVA followed by Bonferroni's multiple comparisons).

For the reason that a lower dose of ATP (50µM) failed to induce *BDNF* expression In adult spinal cord microglia as mentioned above, we evaluated *BDNF* mRNA expression in both adult cortical and spinal cord microglia after treatment with 100µM of ATP at different time points. Consistent with previous results, ATP induced BDNF mRNA expression after 60 minutes of stimulation in adult cortical microglia (Figure 4-25 a). Although the same concentration of ATP failed to elevate *BDNF* mRNA expression significantly as mentioned earlier in the ATP concentration graph, these results showed a significant increase in *BDNF* mRNA expression after 60 minutes of ATP stimulation in adult spinal cord microglia (2-fold) (Figure 4-25 b), a similar effect to adult cortical microglia (4-fold).

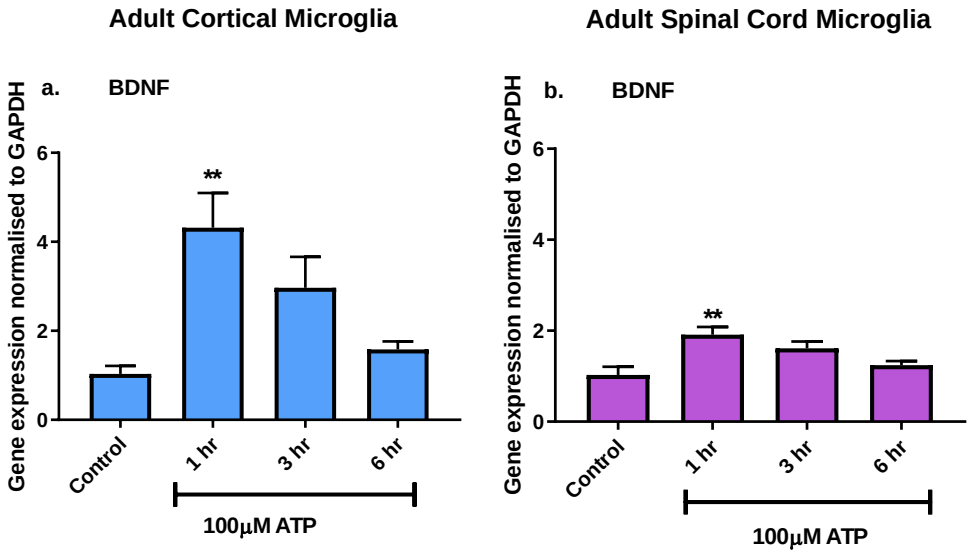

Figure 4-25 Effect of treatment with 100µM ATP on the adult microglial expression of *BDNF* mRNA. Relative expression of *BDNF* mRNA (normalised to *GAPDH* as described in methods) in microglia isolated from adult rat (a) forebrains or (b) spinal cords. Treatment groups involved controls (vehicle-treated only), ATP-treated for 1, 3 and 6 hours. Bars represent the standard mean of error (SEM) n=3. Statistically significant differences with controls: **p < 0.001 (one-way ANOVA followed by Bonferroni's multiple comparisons).

Due to the lack of a potent, selective antagonist for P2X4R, we used TNP-ATP [2',3'-O-(2,4,6-Trinitrophenyl)adenosine-5'-triphosphate tetra(triethylammonium) salt] as a general P2X inhibitor to evaluate the effect of inhibiting purinergic receptors on ATP-induced *BDNF* mRNA expression. We also pretreated microglia with SB202190 that proved to be effective in inhibiting p38 phosphorylation triggered by ATP stimulation. Interestingly, ATP-induced *BDNF* transcript levels were significantly down-regulated when adult cortical microglia were pretreated with either TNP-ATP (2-fold down) or SB202190 (2.8-fold) (Figure 4-26) compared to ATP-treated cells.

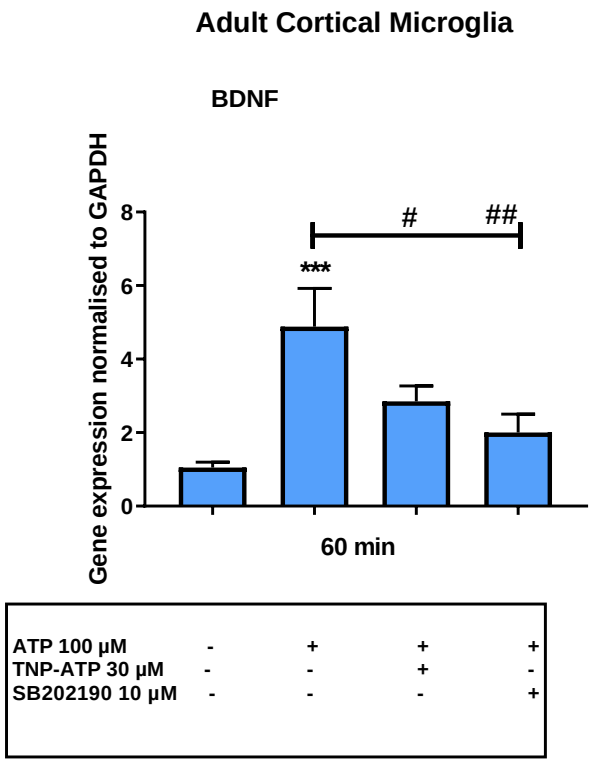

Figure 4-26 Effect of treatment with100µM ATP with or without P2X and p38 MAPK inhibitor on adult cortical microglial expression of *BDNF* mRNA. Relative expression of *BDNF* mRNA (normalised to *GAPDH* as described in methods) in microglia isolated from adult rat forebrains. Treatment groups involved controls (vehicle-treated only), ATP-treated with 100µM and pre-treatment with 30µM P2X inhibitor (TNP-ATP) or 10µM p38 MAPk inhibitor (SB202190). Bars represent the standard mean of error (SEM) n=8. Statistically significant differences with untreated controls: ***p < 0.002; statistical differences with ATP-treated: #p < 0.05, ##p < 0.001. (one-way ANOVA followed by Bonferroni's multiple comparisons).

The same effect of the inhibitors was observed in adult spinal cord microglia. Following an increase in *BDNF* expression after ATP treatment (4-fold), TNP-ATP and SB202190 significantly decreased *BDNF* mRNA levels (3-fold and 3.4-fold respectively) compared to ATP-stimulated microglia as shown in Figure 4-27.

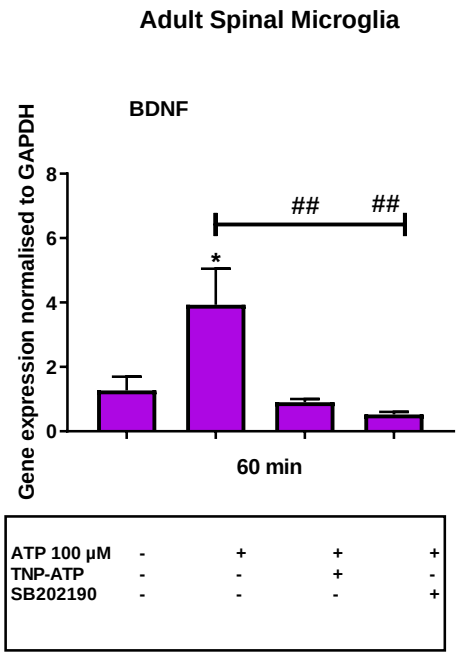

Figure 4-27 Effect of treatment with100µM ATP with or without P2X and p38 MAPK inhibitor on adult spinal cord microglial expression of *BDNF* mRNA. Relative expression of *BDNF* mRNA (normalised to *GAPDH* as described in methods) in microglia isolated from adult rat spinal cords. Treatment groups involved controls (vehicle-treated only), ATP-treated with 100µM and pre-treatment with 30µM P2X inhibitor (TNP-ATP) or 10µM p38 MAPk inhibitor (SB202190). Bars represent the standard mean of error (SEM) n=5. Statistically significant differences with untreated controls: *****$p < 0.05$; statistical differences with ATP-treated: ##$p < 0.001$. (one-way ANOVA followed by Bonferroni's multiple comparisons).

BDNF mRNA basal levels were compared between adult and neonatal microglia. Our data showed a significantly higher level of *BDNF* mRNA expression in resting adult cortical microglia (0.001) in comparison to untreated neonatal cortical microglia ($4x10^{-5}$). Although it appeared that *BDNF* basal transcript levels were higher in adult spinal cord microglia (0.008) as opposed to neonatal spinal cord microglia (0.0007), that difference was not significant. Notably, our results suggested that baseline *BDNF* mRNA levels were significantly higher in adult spinal cord microglia compared to adult cortical microglia (Figure 4-28).

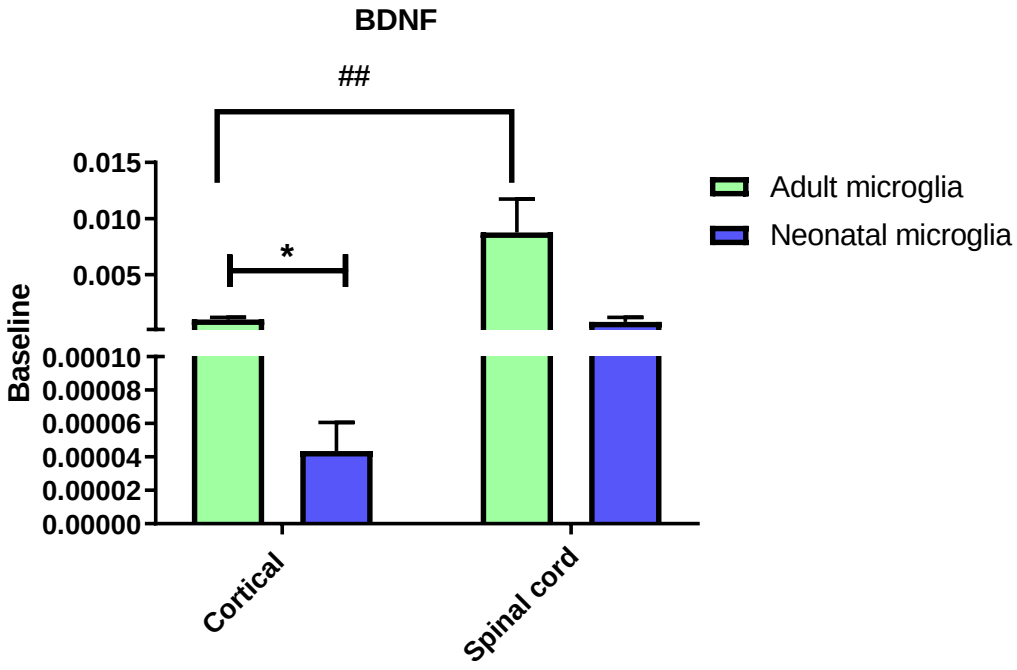

Figure 4-28 Regional and developmental heterogeneity concerning *BDNF* transcript levels. Basal mRNA levels of *BDNF* (normalised to *GAPDH*) in untreated microglia isolated from adult or neonatal rat forebrains and spinal cords. Bars represent the standard error mean of the values n=4. Statistically significant differences between adult and neonatal microglia: *****$p < 0.05$. Statistical significance between adult spinal cord and adult cortical microglia ##$p < 0.001$. (Multiple t-tests).

The next step was to evaluate BDNF release from adult microglia in response to ATP and pretreatment with inhibitors. Similar patterns were observed in adult cortical and spinal cord microglia. In fact, ATP stimulation increased BDNF release from adult microglia significantly. When adult microglia were pretreated with TNP-ATP, BDNF release significantly decreased to below baseline levels. Despite the decrease in *BDNF* mRNA expression In response to pretreatment with SB202190 as mentioned earlier, SB202190 failed to significantly decrease BDNF release from adult microglia in comparison to ATP-induced BDNF release. Notably, ATP-

induced BDNF release from SB202190-pretreated cells was not significant compared to untreated cells (Figure 4-29).

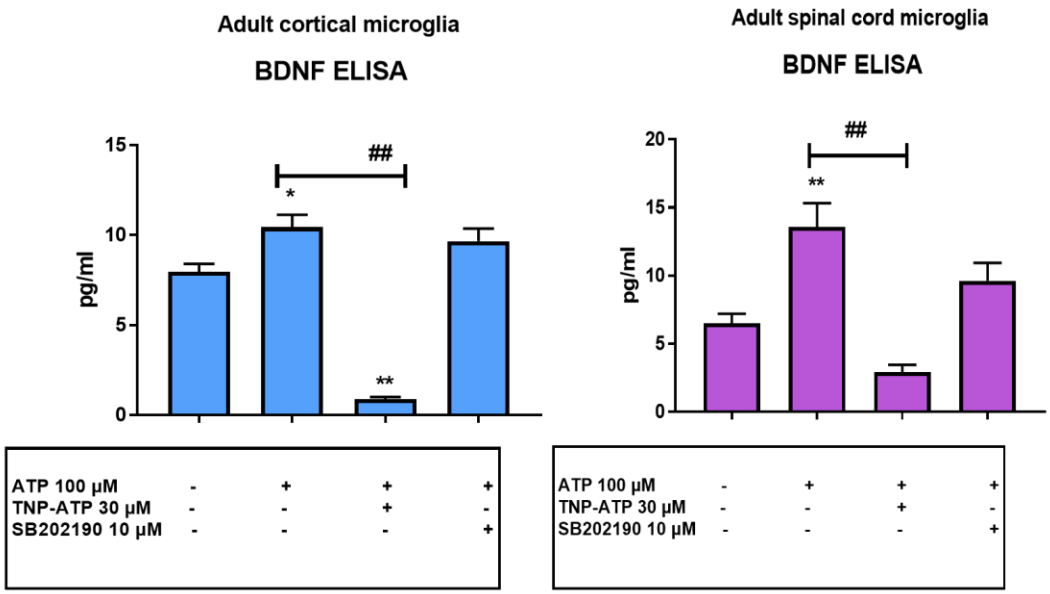

Figure 4-29 Effect of treatment with100µM ATP with or without P2X and p38 MAPK inhibitor on adult cortical or spinal cord microglial release of BDNF. The concentration of BDNF released into the supernatant of cultured adult cortical (left) or spinal cord (right) microglia in response to ATP or inhibitors treatment. Treatment groups involved controls (vehicle-treated only), ATP-treated with 100µM and pre-treatment with 30µM P2X inhibitor (TNP-ATP) or 10µM p38 MAPk inhibitor (SB202190). Bars represent the standard mean of error (SEM) n=3. Statistically significant differences with untreated controls: *****$p < 0.05$; statistical differences with ATP-treated: ##$p < 0.001$. (one-way ANOVA followed by Bonferroni's multiple comparisons).

Contrary to previous reports (Trang et al., 2009) and our reported results mentioned earlier (Figure 4-17), ATP and inhibitors treatment did not affect BDNF mRNA expression in neonatal microglia (Figure 4-30).

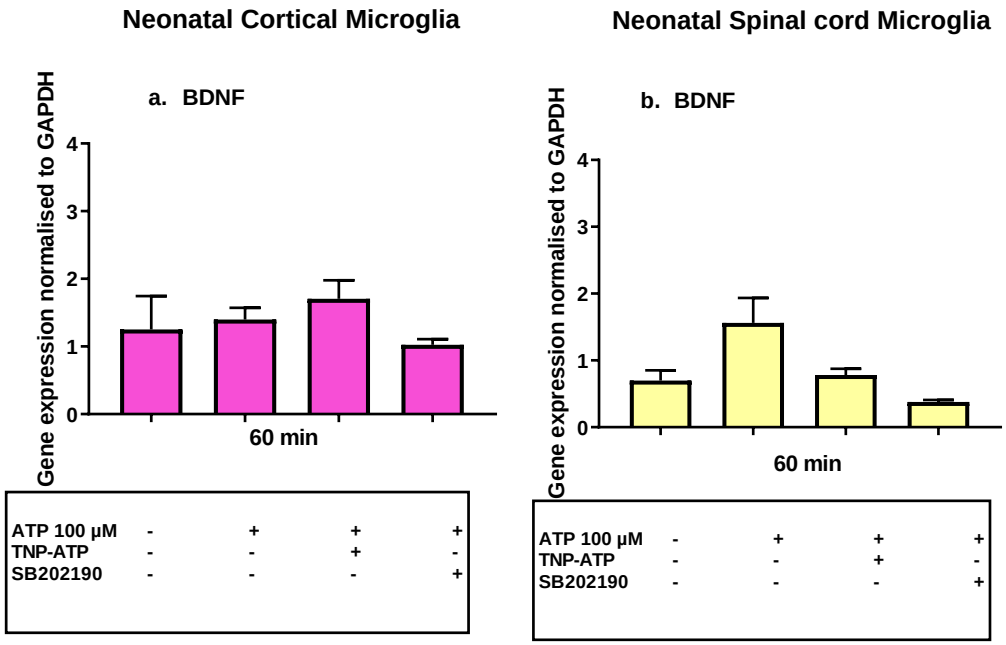

Figure 4-30 Effect of treatment with100µM ATP with or without P2X and p38 MAPK inhibitor on neonatal cortical or spinal cord microglial expression of *BDNF* mRNA. Relative expression of *BDNF* mRNA (normalised to *GAPDH* as described in methods) in microglia isolated from neonatal rat (a) forebrains or (b) spinal cords. Treatment groups involved controls (vehicle-treated only), ATP-treated with 100µM and pre-treatment with 30µM P2X inhibitor (TNP-ATP) or 10µM p38 MAPk inhibitor (SB202190). Bars represent the standard mean of error (SEM) n=5. (one-way ANOVA followed by Bonferroni's multiple comparisons).

Table 4-4 Summary of relative expression of mRNA of *BDNF* in microglia after stimulating with 100μM ATP with or without pre-treatment with P2X (TNP-ATP) and P38 MAPK inhibitors (SB202190).

Region	Developmental stage	Gene	Treatment group	Mean relative expression of mRNA	P-value	Statistical test
Cortical microglia	Adult	*BDNF*	ATP	4.8	0.0005	One-way ANOVA/Bonferroni
			ATP + TNP-ATP	2.8	0.1333	
			ATP+ SB202190	2.0	0.8264	
	Neonatal		ATP	1.3	>0.9999	
			ATP + TNP-ATP	1.7	0.9418	
			ATP+ SB202190	1.0	>0.9999	
Spinal cordmicroglia	Adult		ATP	3.9	0.0202	
			ATP + TNP-ATP	0.9	>0.9999	
			ATP+ SB202190	0.5	>0.9999	
	Neonatal		ATP	1.5	0.1091	
			ATP + TNP-ATP	0.7	>0.9999	
			ATP+ SB202190	0.3	>0.9999	

We evaluated ATP-induced P2X4R activation through investigating the effect of TNP-ATP and SB202190 on adult and neonatal microglia phosphorylation of p38 MAPK. We also examined BDNF protein expression in response to ATP and pre-treatment with inhibitors. Although ATP triggered p38 phosphorylation in neonatal cortical microglia, treatment with inhibitors did not affect p38 MAPK activation demonstrated by p38

phosphorylation (Figure 4-31, 1-4). On the other hand, ATP-induced p38 phosphorylation was decreased when adult cortical microglia were pre-treated with SB202190; however, TNP-ATP pre-treatment did not inhibit p38 MAPK activation (Figure 4-31, 5-8). Surprisingly, BDNF protein was not detected in both neonatal and adult cortical microglia, but the immature protein, pro-BDNF, was detectable. It appeared that the expression of the pro-BDNF protein was not changed in neonatal cortical microglia (Figure 4-31,1-4 bottom blot). Contrary, untreated adult cortical microglial pro-BDNF levels were lower than those induced with ATP treatment. Nonetheless, pre-treatment with inhibitors did not alter the levels of ATP-induced pro-BDNF protein (Figure 4-31,5-8 bottom blot).

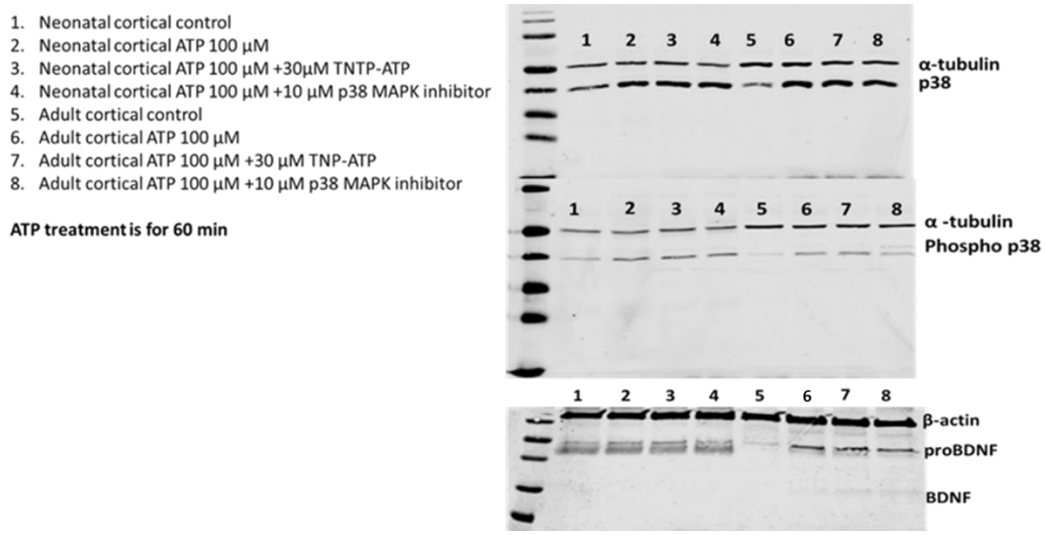

Figure 4-31 Immunoblots of total p38 MAPK, P-p38 MAPK and pro-BDNF. The western blots show total p38 MAPK (top blot) and P-p38 MAPK (middle blot) in response to ATP stimulation of microglia with or without the addition of 10µM p38 MAPK (SB202190) or 30µM P2X inhibitor (TNP-ATP), using α-tubulin or β-actin as controls. The bottom blot shows Pro-BDNF protein expression in microglia in response to stimulation with ATP and inhibitors.

Similarly, p38 MAPK activation was suggested by the increase in p38 phosphorylation in adult spinal cord microglia. As observed in adult cortical microglia, only SB202190 pretreatment was effective in inhibiting p38 MAPK activation in adult spinal cord microglia (Figure 4-32, top panel, left 5-8). Like neonatal cortical microglia, phosphorylation of p38 was not affected by pretreatment with inhibitors (Figure 4-32, top panel, right 1-4). Unlike adult cortical microglia, neither pro-BDNF nor BDNF proteins were detectable on the blot (Figure 4-32, bottom panel 5-8), yet neonatal pro-BDNF protein expression seemed to be similar to neonatal cortical microglia's (Figure 4-32, bottom panel, 1-4).

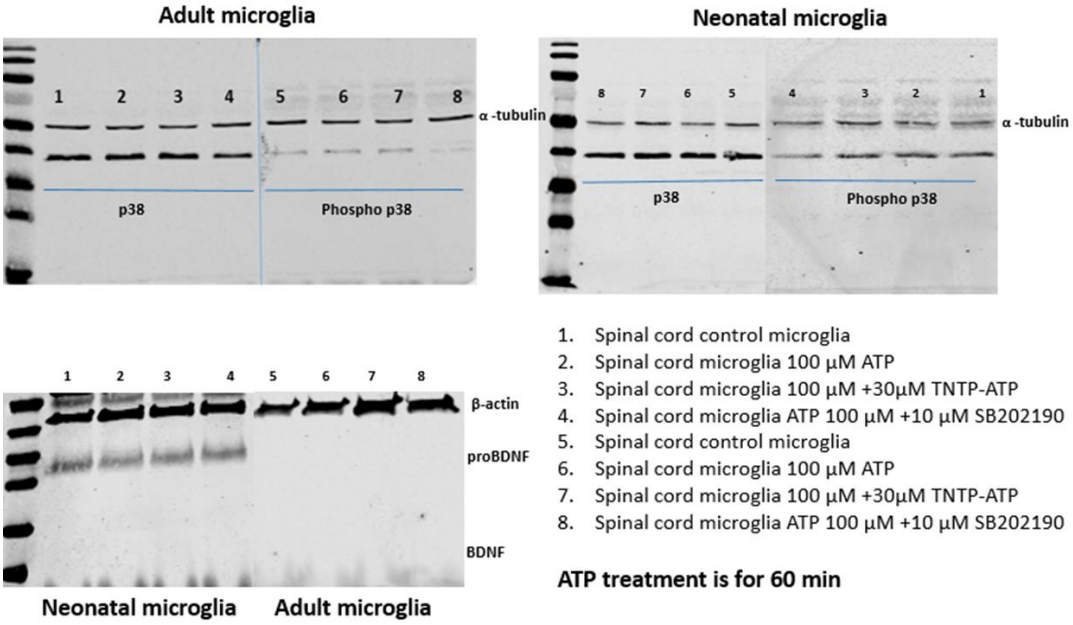

Figure 4-32 Immunoblots of total p38 MAPK, P-p38 MAPK and pro-BDNF. The western blots show the following) in response to ATP stimulation of microglia with or without the addition of 10µM p38 MAPK (SB202190) or 30µM P2X inhibitor (TNP-ATP): total p38 MAPK protein expression in adult spinal cord microglia (1-4;top left) and neonatal spinal cord microglia (5-8, top right), P-p38 MAPK protein expression in adult (5-8; top left) or neonatal (1-4; top right) spinal cord microglia and finally Pro-BDNF expression in adult (1-4) or neonatal (5-8) spinal cord microglia (bottom blot). α-tubulin or β-actin were used as controls.

4.3.4 ATP-induced anti-inflammatory mediators' expression is altered in adult microglia upon inhibition with P2X or P38 MAPK pathways in a concentration-dependent manner

Here, we evaluated the expression of *NR4As* and *IL-10* In response to ATP and inhibitors.

4.3.4.1 ATP-induced *Nurr1* mRNA expression decreased with p38 MAPK inhibitor In adult spinal cord microglia

Herein, we evaluated the expression of *Nur77*, *NOR-1* and *Nurr1* in adult microglia. Our data suggested a regional heterogeneity in response to a lower concentration of ATP (50µM). For instance, ATP stimulation significantly induced *NOR-1* and *Nurr1* in adult spinal cord microglia. Although *Nur77* mRNA levels appeared to increase in adult spinal cord microglia, such up-regulation was not significant. Interestingly, interfering with the p38 MAPK pathway using SB202190 significantly decreased Nurr1 induced mRNA levels (Figure 4-33 c).

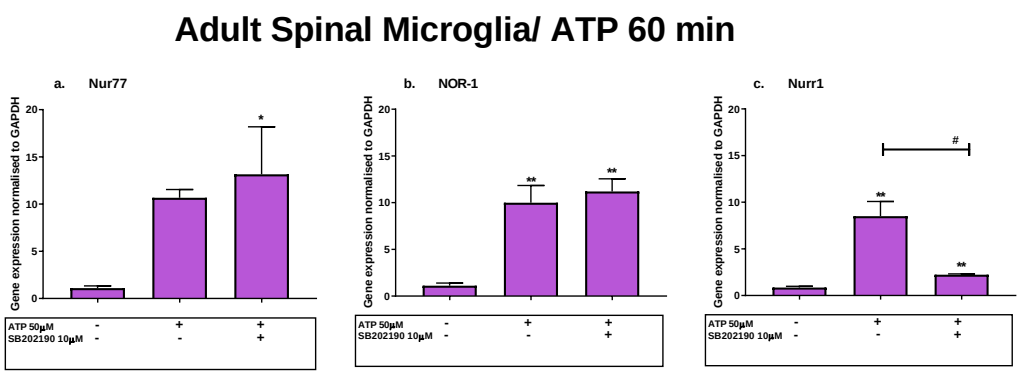

Figure 4-33 Effect of treatment with 50µM ATP with or without p38 MAPK inhibitor on adult spinal cord microglial expression of *Nur77, NOR-1* and *Nurr1* mRNA. Relative expression of (a) *Nur77*, (b) *NOR-1* and (c) *Nurr1* mRNA (normalised to *GAPDH* as described in methods) in microglia isolated from adult rat spinal cords. Treatment groups involved controls (vehicle-treated only), ATP-treated with 50µM and pre-treatment with 10µM p38 MAPk inhibitor (SB202190). Bars represent the standard mean of error (SEM) n=5. Statistically significant differences with untreated controls: *p < 0.05, **p < 0.001; statistical differences with ATP-treated: #p < 0.05. (one-way ANOVA followed by Bonferroni's multiple comparisons).

On the other hand, 50µM of ATP induced the expression of all NR4As mRNA despite SB202190 pretreatment in adult cortical microglia (Figure 4-34).

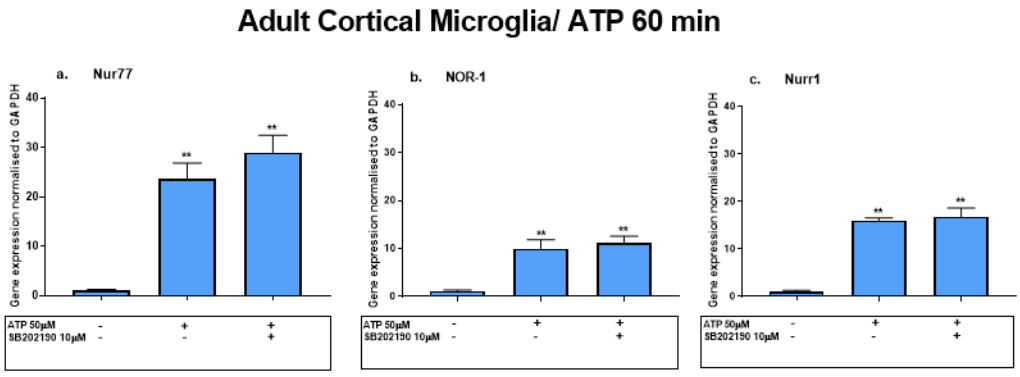

Figure 4-34 Effect of treatment with 50µM ATP with or without p38 MAPK inhibitor on adult cortical microglial expression of *Nur77, NOR-1* and *Nurr1* mRNA. Relative expression of (a) *Nur77*, (b) *NOR-1* and (c) *Nurr1* mRNA (normalised to *GAPDH* as described in methods) in microglia isolated from adult rat forebrains. Treatment groups involved controls (vehicle-treated only), ATP-treated with 50µM and pre-treatment with 10µM p38 MAPk inhibitor (SB202190). Bars represent the standard mean of error (SEM) n=5. Statistically significant differences with untreated controls: **p < 0.001. (one-way ANOVA followed by Bonferroni's multiple comparisons).

Table 4-5 Summary of relative mRNA expression of NR4A subfamily members in microglia after stimulating with 50μM ATP with or without pre-treatment with p38 MAPK inhibitor (SB202190).

Region/ Developmental stage	Gene	Treatment group ATP	Mean relative expression of mRNA	P-value	Statistical test
Adult cortical microglia	*Nur77*	ATP 50 μM	23.6	0.0002	One-way ANOVA/Bonferroni
		ATP+ SB202190	29.0	<0.0001	
Adult spinal cord microglia		ATP	10.6	0.0579	
		ATP+ SB202190	13.1	0.0187	
Adult cortical microglia	*NOR-1*	ATP 50 μM	9.9	0.0024	
		ATP+ SB202190	11.1	0.0006	
Adult spinal cord microglia		ATP	9.9	0.0024	
		ATP+ SB202190	11.1	0.0006	
Adult cortical microglia	*Nurr1*	ATP 50 μM	16.0	<0.0001	
		ATP+ SB202190	16.7	<0.0001	
Adult spinal cord microglia		ATP	8.509914	0.0010	
		ATP+ SB202190	2.22681	0.7588	

4.3.4.2 100μM ATP-induced *Nurr1* and *IL-10* mRNA expression was decreased with TNP-ATP and SB202190 pretreatment

A higher concentration of ATP (100μM) was used to compare the effect seen on *BDNF* mRNA expression and the expression of *Nurr1* and *IL-10*. The same pattern was observed in adult and neonatal microglia.

ATP significantly induced *Nurr1* upregulation in adult (cortical by 77 folds and spinal cord by 33 folds) and neonatal (cortical by 9 folds and spinal cord by 14 folds) microglia. (Figure 4-35). Inhibiting P2X receptors by pre-treatment with TNP-ATP downregulated Nurr1 mRNA expression in adult cortical (37-fold) and spinal cord (7-fold) microglia. The same effect was observed in neonatal cortical and spinal cord microglia (5-fold), however the downregulation In *Nurr1* transcript levels was not statistically significant in cortical microglia. Similarly, inhibiting p38 MAPK by pre-treatment with SB202190 downregulated Nurr1 mRNA expression in adult cortical (38-fold) or spinal cord (5-fold) (Figure 4-35 a,b)and neonatal cortical or spinal cord microglia (4-fold) (Figure 4-35 c,d).

A comparable pattern to *Nurr1* was noticed when *IL-10* mRNA expression was evaluated. ATP stimulation resulted in a significant increase in *IL-10* transcript levels in adult cortical (by 4.8 folds) and neonatal cortical (by 5 folds) or spinal cord microglia (3-fold), but the resultant increase was not statistically significant in adult spinal cord microglia. Moreover, SB202190 pretreatment lowered *IL-10* transcript levels in both adult and

neonatal cortical microglia by 3 folds down and in adult and neonatal microglia by 2 folds down. Interestingly, TNP-ATP pretreatment significantly lowered the elevated mRNA levels of *IL-10* in adult microglia by 2 folds. P2X inhibiting also downregulated IL-10 mRNA expression in neonatal cortical and spinal cord microglia by about 2 folds (Figure 4-36).

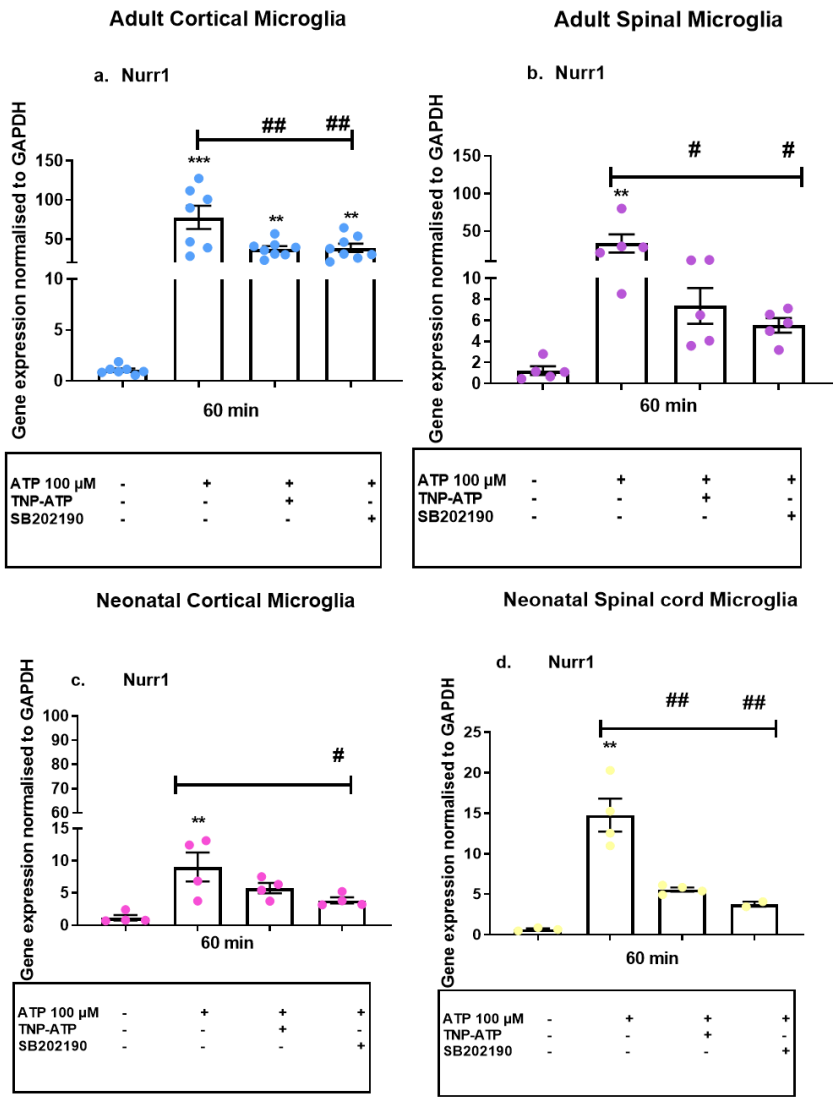

Figure 4-35 Effect of treatment with 100µM ATP with or without P2X and p38 MAPK inhibitor on the adult or neonatal microglial expression of *Nurr1* mRNA. Relative expression of *Nurr1* mRNA (normalised to *GAPDH* as described in methods) in microglia isolated from (a,b) adult or neonatal (c,d) rat (a,c) forebrains or (b,d) spinal cords. Treatment groups involved controls (vehicle-treated only), ATP-treated with 100µM and pre-treatment with 30µM P2X inhibitor (TNP-ATP) or 10µM p38 MAPk inhibitor (SB202190). Bars represent the standard mean of error. Statistically significant differences with untreated controls: **p < 0.001, ***p < 0.002; statistical differences with ATP-treated: #p < 0.05, ##p < 0.001. (one-way ANOVA followed by Bonferroni's multiple comparisons).

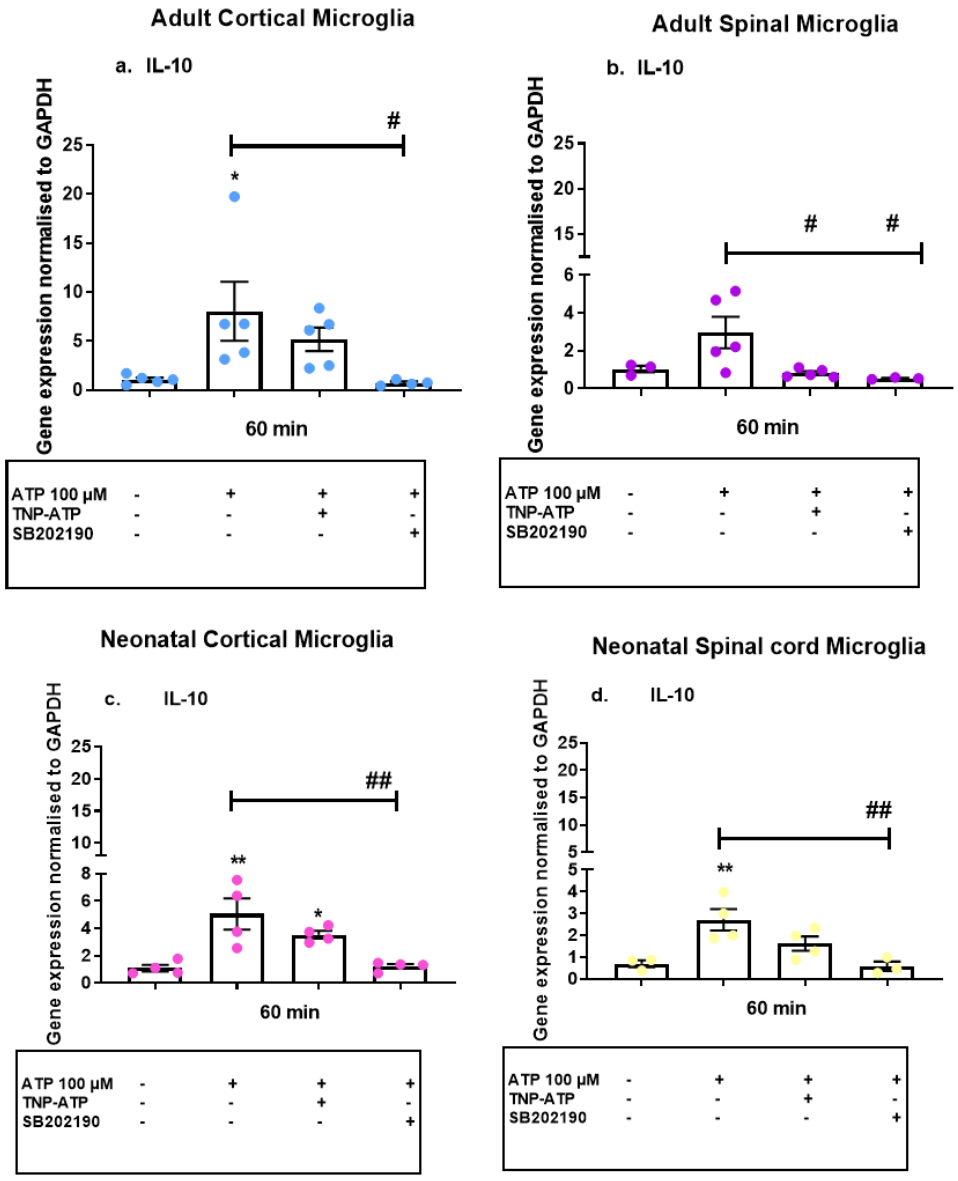

Figure 4-36 Effect of treatment with 100µM ATP with or without P2X and p38 MAPK inhibitor on the adult or neonatal microglial expression of *IL-10* mRNA. Relative expression of *IL-10* mRNA (normalised to *GAPDH* as described in methods) in microglia isolated from (a,b) adult or neonatal (c,d) rat (a,c) forebrains or (b,d) spinal cords. Treatment groups involved controls (vehicle-treated only), ATP-treated with 100µM and pre-treatment with 30µM P2X inhibitor (TNP-ATP) or 10µM p38 MAPk inhibitor (SB202190). Bars represent the standard mean of error. Statistically significant differences with untreated controls: *****p < 0.05, **p < 0.001; statistical differences with ATP-treated: #p < 0.05, ##p < 0.001. (one-way ANOVA followed by Bonferroni's multiple comparisons).

Table 4-6 Summary of relative mRNA expression of *Nurr1* and *IL-10* in microglia after treatment with 100μM ATP for 60 minutes with or without pre-treatment with P2X (TNP ATP) and p38 MAPK (SB202190) inhibitors.

Region	Developmental stage	Gene	Treatment group	Mean relative expression of mRNA	P-value	Statistical test
Cortical microglia	Adult	*Nurr1*	ATP	77.7	<0.0001	One-way ANOVA/Bonferroni
			ATP + TNP-ATP	37.5	0.0076	
			ATP+ SB202190	38.9	0.0055	
	Neonatal		ATP	9.0	0.0021	
			ATP + TNP-ATP	5.7	0.0655	
			ATP+ SB202190	3.8	0.4458	
Spinal cord microglia	Adult		ATP	33.5	0.0056	
			ATP + TNP-ATP	7.3	>0.9999	
			ATP+ SB202190	5.5	>0.9999	
	Neonatal		ATP	14.7	<0.0001	
			ATP + TNP-ATP	5.5	0.0740	
			ATP+ SB202190	3.7	0.5631	
Cortical microglia	Adult	*IL-10*	ATP	8.0	0.0309	
			ATP + TNP-ATP	5.1	0.3131	
			ATP+ SB202190	0.7	>0.9999	
	Neonatal		ATP	5.0	0.0018	
			ATP + TNP-ATP	3.5	0.0445	
			ATP+ SB202190	1.2	>0.9999	
Spinal cord microglia	Adult		ATP	2.9	0.0950	
			ATP + TNP-ATP	0.8	>0.9999	
			ATP+ SB202190	0.5	>0.9999	
	Neonatal		ATP	2.7	0.0094	
			ATP + TNP-ATP	1.6	0.3210	
			ATP+ SB202190	0.5	>0.9999	

4.4 Discussion

Microglia are the resident immune cells in the CNS, and their roles are critical in health and disease (Pocock and Piers, 2018). Microglia express functional purinergic receptors that respond to ATP signalling (Inoue, 2002). In the CNS, ATP acts as an intercellular neurotransmitter that regulates neuron-glia or glia-glia communication under physiological and pathological conditions (Verkhratsky et al., 2012). Although both P2X4R and P2X7R have been associated with neuropathic pain (Ulmann et al., 2008), ATP-induced BDNF secretion from microglia was reported to induce tactile allodynia and nociception through P2X4R signalling (Trang et al., 2009). In the present study, we compared developmental and regional microglial responses to ATP *in vitro*. To our knowledge, this is the first study to compare adult and neonatal microglial BDNF expression and release in response to ATP stimulation.

Moreover, because orphan nuclear receptors possess anti-inflammatory roles in modulating inflammation and microglial polarisation, we evaluated their expression in developmental microglia isolated from different CNS regions in response to ATP stimulation since the latter activates NF-kB pathway and triggers cytokine expression and release (Hide et al., 2000).

4.4.1 ATP stimulation rapidly induces NR4A subfamily members of nuclear receptors expression in microglia

Here, we report a transient up-regulation in NR4A subfamily members in response to different concentrations of ATP. The observed rapid induction in their mRNA levels in response to ATP is consistent with previous studies reporting an immediate increase in their levels in response to various stimuli including neurotransmitters, calcium, mechanical agitation and inflammatory cytokines reviewed in (Maxwell and Muscat, 2006). Therefore, they are classified as immediate-early response genes due to their rapidly-induced expression (Pearen and Muscat, 2010). Developmental heterogeneity was observed in this study in which NR4A subfamily members showed different expression profiles in neonatal microglia compared to adult microglia. For instance, *Nur77* mRNA expression was higher than the other two members of the orphan nuclear receptor family, whereas in neonatal microglia *Nurr1* mRNA expression was higher than *Nur77* and *NOR-1*. Moreover, adult cortical microglia were more sensitive to lower concentrations of ATP where NR4A subfamily members were induced rapidly, while in neonatal cortical microglia higher concentrations of ATP were needed to induce a rapid induction of NR4As. Nevertheless, treatment with a higher concentration of ATP (100µM) resulted in consistent increase in NR4As transcript levels in microglia while using a lower concentration (50µM) resulted in variable and inconsistent results. Moreover, regional heterogeneity was also observed in response to ATP stimulation. Evidently, neonatal spinal cord microglia were

more sensitive than neonatal cortical microglia to treatment with lower concentrations of ATP. Furthermore, *Nur77* transcript levels significantly increased after 12 hours of ATP stimulation in adult cortical microglia, but the same effect was not observed in adult spinal cord microglia.

Our results showed that the continuous increase in Nur77 protein in response to ATP stimulation did not correspond to the rapidly-induced *Nur77* mRNA expression that decreased after one hour of the challenge. Transcript levels may or may not correlate with relative protein abundances, that is mRNA can be expressed relatively at a lower level than its corresponding protein or vice versa. This could be due to the fact that mRNA is easily degraded (within 2-7 hours) and less stable while proteins have an average half-life of 46 hours. The importance of the protein to the cell and its functions can result in its prolonged half-life (Vogel and Marcotte, 2012). Surprisingly, the increase in Nur77 protein expression was detected in neonatal microglia but not in adult microglia despite loading similar protein concentrations as confirmed by β-actin. This could suggest that translation of Nur77 could occur in neonates and not adults especially that Nur77 protein expression was not visible in adult microglia (cortical and spinal) in response to LPS (chapter 3) or ATP. Overall, the acute increase in NR4A subfamily members in ATP-stimulated microglia could regulate microglial polarisation and prevent overactivation.

4.4.2 P2X4R expression and localisation in microglia

P2X4R gene expression is enhanced upon microglial activation (Qureshi et al., 2007). Indeed, neonatal microglia acquire an ameboid activated phenotype due to the requirement in the developing CNS for removal of redundant synapses and dead cells (Matcovitch-Natan et al., 2016b). Our observations are consistent with previous reports showing an up-regulated P2X4R expression at earlier stages of development in P3 mice compared to P21 mice (Crain et al., 2009). ATP stimulates P2X4R expressed on the cell membrane of microglia; however, our results show that the abundance of P2X4R protein expression is localised in the cytoplasm rather than on the cell membrane in both adult and neonatal microglia. Evidently, P2X4R is encapsulated in lysosomes within rat microglia, yet retain their function to regulate cellular responses to extracellular ATP. Increased intracellular Ca^{2+} levels trigger lysosomal excocytosis that in turn up-regulate surface expression of P2X4R (Qureshi et al., 2007).

4.4.3 ATP-induces BDNF expression and release in adult microglia only

Neuropathic pain has been described to be induced when neonatal microglia were stimulated with ATP. Such stimulation was reported to be a resultant of P2X4R activation (Tsuda et al., 2003). P2X4R signalling cascade was proposed to lead to the phosphorylation of p38 MAPK and eventually result in the microglial release of BDNF that promotes

neuropathic pain (Trang et al., 2009). Despite the higher level of lysosomal P2X4R in neonatal microglia as opposed to adult microglia, our results showed an increase in BDNF release and mRNA expression after 60 minutes of ATP stimulation solely by adult microglia and not neonatal microglia. In the present study, replicating the results reported by Trang and colleagues (2009) has not been successful possibly due to the differences in experimental design used when treating microglia. For instance, Trang and colleagues (2009) explained in their methodology that they collect microglia in saline in an Eppendorf tube and treat them immediately with ATP. One the other hand, we allow microglia to adhere to the culture plate for a minimum of 14 hours in a similar density between independent samples. Microglia can be easily activated; therefore; we took caution in treating microglia to avoid misinterpretation of results. We also attempted to stimulate microglia with ATP in serum-free media (no growth factors added) for one hour; however the viability rate was very low, hence treating microglia in PBS with ATP was avoided.

4.4.3.1 P2X and p38 MAPK inhibitors affect BDNF mRNA and release

As mentioned earlier, p38 MAPK activation was suggested as a downstream signalling pathway of P2X4R activation as a result of ATP stimulation. Our results show a decrease in *BDNF* mRNA levels in both adult cortical and spinal cord microglia when pretreated with P2X (TNP-ATP) or p38 MAPK (SB202190) inhibitors, however, only P2X inhibition resulted in a

significant reduction in BDNF released by microglia. ATP stimulation activates P2X receptors differentially based on the concentration used as reviewed in (Inoue, 2002). Here, we used a higher level of ATP (100μM) to stimulate microglia as opposed to the concentration (50μM) used by Trang and colleagues (2009). Higher levels of ATP (1mM) induces TNF-α release from neonatal coritcal microglia mediated by p38 MAPK and ERK1/2 signalling pathways (Hide et al., 2000). Our results showed that the p38 MAPK inhibitor (SB202190) inhibited p38 MAPK activation after 5 minutes of ATP stimulation while P2X7R inhibition had no effect on the activated p38 MAPK pathway. Moreover, functional interaction of P2X4R with P2X7R has been previously reported (Boumechache et al., 2009). Therefore, due to the involvement of both P2X4R and P2X7R in the development of neuropathic pain (Tsuda et al., 2012), and the fact that different ATP concentrations and duration of stimulation trigger each receptor differently, more studies are required to single out the role of each receptor in mediating BDNF-mediated neuropathic pain.

4.4.3.2 P2X and p38 MAPK inhibitors regulate ATP-induced *Nurr1* and *IL-10* mRNA expression

Here we reported the up-regulation of the anti-inflammatory mediators *Nurr1* and *IL-10* mRNA expression after stimulation with ATP. Surprisingly, their induced transcript levels were down-regulated when cells were pretreated with TNP-ATP and SB202190. Despite the similarity in the expression profile between these mediators and *BDNF* with respect to ATP

stimulation and inhibitors, in neonatal microglia, significantly decreased mRNA levels were observed with pretreatment with inhibitors unlike unaffected BDNF transcript levels in neonatal microglia.

In neonatal rat cortical microglia, IL-10 release was induced in a dose-dependent manner and peaked with ATP concentration of 100μM. As Intracellular release of Ca^{2+} induces the expression of *IL-10 (Seo et al., 2008),* interfering with p38 MAPK could potentially contribute to the observed down-regulation in *IL-10* mRNA due to lower levels of intracellular Ca^{2+}. Contrary to our findings, Seo and colleagues (2008) reported an increase in ATP-induced IL-10 secretion when microglia were treated with TNP-ATP (Seo et al., 2008). It has been proposed that exposure to constituent lower doses of ATP induced IL-10 secretion in macrophages suggesting an anti-inflammatory action of ATP (la Sala et al., 2003). Overexpression of Nurr1 in macrophages enhanced the release of IL-10 (Mahajan et al., 2015).

Intriguingly, stimulation of microglia with LPS induces the release of BDNF. Although microglial BDNF release could be neuroprotective, dysregulated p38 MAPK activation is often associated with causing harm to tissues due to the subsequent production of pro-inflammatory mediators (Nakajima and Kohsaka, 2004).

In this chapter, we showed an immediate increase in NR4A subfamily members mRNA expression after ATP treatment. Moreover, our data suggest a differential expression in P2X4R during development in which neonatal microglia express more P2X4R as opposed to adult microglia.

Stimulating microglia with ATP led to the expression and release of BDNF from adult microglia but not neonatal microglia indicating that microglia may respond differently to the same stimulus depending on their developmental stage. In summary, tissue injury can result In the release of extracellular ATP that activate microglia. ATP-induced microglial activation can be either neuroprotective or neurotoxic depending on the concentration and duration of ATP. The rapid increase in NR4A subfamily members indicates an important role of these receptors in modulating microglial activation. BDNF release from ATP-stimulated microglia can be as a result of P2X4R activation due to the fact that interfering with P2X receptors leads to the inhibition of BDNF release and expression. A selective P2X4R inhibitor can give us better insight into the mechanism behind ATP-induced BDNF expression and secretion from adult microglia.

5) Chapter Five:

General Discussion and future directions

5.1 Summary of findings

In the present study, we aimed to investigate the extent of microglial regional and developmental heterogeneity. Although a comparison between early postnatal and adult microglia heterogeneity under physiological conditions has been recently reported (Li et al., 2019, Matcovitch-Natan et al., 2016b), we focused mainly on regional-specific differences in microglial responses to PAMPs and DAMPs during development. Firstly, we confirmed that our adult and neonatal microglia retain their phenotypes *in vitro* by evaluating transcriptomic profiles of microglial developmental markers. Secondly, microglia displayed regional and developmental heterogeneity in the event of an LPS challenge. The rapid increase in both pro-inflammatory and anti-inflammatory mediators' expression suggest a mixed state of microglia (M1/M2), potentially skewed in an M1 phenotype marked by the release of IL-1β. Interestingly, LPS-activated microglial secretome stimulated astrocytes to enhance the viability of neurons, especially when astrocytes were treated with neonatal LPS-stimulated MCM. The up-regulation of pro-inflammatory and anti-inflammatory factors in astrocytes after MCM stimulation suggests a mixed state of A1/A2 in astrocytes.

Thirdly, we evaluated the response to DAMPs by stimulating microglia with ATP. NR4A subfamily members transcript levels were rapidly up-regulated in stimulated microglia. Once more, regional and developmental heterogeneity was observed in the event of an ATP challenge. We evaluated BDNF expression and secretion from microglia after ATP stimulation and

activation of P2X receptors. Surprisingly, BDNF mRNA expression and release was only induced in adult microglia and not in neonatal microglia. P2X activation resulted in the observed BDNF mRNA expression and secretion. Intriguingly, inhibiting P2X signalling pathway affected *IL-10* and *Nurr1* mRNA expression in a similar way *BDNF* was affected.

5.2 Markers for developmental microglia

Gene expression in microglia is tightly regulated during development to respond to certain environmental stimuli during a specific developmental stage to sustain tissue homeostasis (Matcovitch-Natan et al., 2016b). Recent findings suggest that female and male microglial transcriptomes are similar during early developmental stages but male microglial development plateaus at P60 whereas adult female microglia does not. Interestingly, a developmental response to LPS was observed In male microglia in that LPS induced male microglia maturation to a similar level of female maturation; however the same was not observed in female microglia (Hanamsagar et al., 2017). Herein we used adult male rats to avoid the possibility of sexual dimorphism; however, mixed-gender postnatal pups were used for neonatal microglia culture. In light of our results, microglia isolated from both adult and neonates showed an up-regulation in developmental markers, *Sal1* and *MafB* for adult microglia and *Psat1* and *Scd2* for early postnatal microglia. Although spinal cord microglia displayed variation with respect to developmental markers gene expression, most studies have reported these

markers to be expressed in brain microglia (Matcovitch-Natan et al., 2016a, Hanamsagar et al., 2017).

5.3 Microglia-astrocyte communication after LPS stimulation

In chapter three, stimulating microglia with a PAMP (LPS) and the consequent effect on astrocytes and neurons was evaluated. The resolution of acute LPS-induced microglial activation is vital for modulating inflammation (Norden et al., 2016) that is tightly regulated by glial cells communication (Norden et al., 2014). Indeed, microglial activation was marked by the rapid up-regulation of *IL-1β* transcripts in both adult and neonatal microglia after stimulation with LPS. A slightly delayed up-regulation in *IL-10* mRNA expression indicates a regulatory mechanism for the resolution of neuroinflammation. In addition, orphan nuclear receptors attenuate the expression and release of pro-inflammatory cytokines, thus regulating inflammation in microglia and astrocytes (Saijo et al., 2009). Their rapidly induced-mRNA expression following LPS stimulation suggests a coordinated microglial acute phase response to prevent overactivation and chronic neuroinflammation. The differential up-regulation in NR4As basal levels during development might be linked to their physiological roles responding to developmental stimuli.

Microglia-astrocyte communication is essential for maintaining a healthy CNS. In our study, microglia could be producing factors that induce neuroprotective astrocytes marked by the up-regulated NR4As in astrocytes. In contrast, Liddelow and colleagues (2017) reported that LPS-stimulated MCM triggered neurotoxic astrocytes (A1) and promoted neuronal death. Astrocytes showed a neuroprotective role when they were stimulated with anti-inflammatory cytokines, IL-10 or IL-4, whereas LPS+IFNγ-stimulated ACM decreased neuronal viability (Jang et al., 2013), however microglial secretome can contain both pro-inflammatory and anti-inflammatory cytokines in response to LPS as our data suggested. Moreover, due to the lack of TLR-4 expression in astrocytes, LPS could potentially activate contaminating microglia or the effect seen was due to IFN-γ. Indeed, Stimulating human astrocytes with IFN-γ, but not LPS, led to neurotoxicity. On the other hand, astrocytes stimulated with both IFN-γ+ LPS resulted in neuronal death (Hashioka et al., 2009). Herein, we acutely stimulated microglia for only 6 hours followed by removal of LPS from MCM which could contribute to a less pro-inflammatory phenotype in comparison to microglia stimulated for 24 hours with LPS. Notably, we observed that LPS stimulation for 24 hours affected RNA and protein levels marked by a decrease in *GAPDH* mRNA and β–actin protein; therefore, the discrepancies between our findings and previously reported ones could be due to the different approaches. The extent of microglial activation and their production of inflammatory mediators depend on the duration of LPS stimulation. For instance, LPS-stimulated microglia reportedly release IL-1α,

TNF-α and c1q after 24 hours of stimulation and these inflammatory mediators collectively trigger neuronal death (Liddelow et al., 2017b).

Similarly, maximum induction of IL-1α release from LPS-stimulated microglia was reported after 24 hours, whereas 6 hours of stimulation did not induce IL-1α secretion. Furthermore, prolonged microglial stimulation with LPS (14 or 24 hours) triggered neuronal death (Dean et al., 2010). LPS-stimulated microglia release IL-6 that in turn activates astrocytes upregulation of hepcidin (a regulator of iron homeostasis) that leads to neuronal death. The proposed neurotoxic effect is maybe due to the accumulation of iron in neurons (You et al., 2017).

Similar to our findings, previous reports showed regional and developmental heterogeneity in response to LPS stimulation. Systemic administration of low doses of LPS induced up-regulation of apoptotic and immune-related genes in response to external stimuli in rat pups, the alternation in gene expression was suggested to be region-specific in the brain (Eklind et al., 2006). Changes in gene expression were region-specific with ageing in microglia (Grabert et al., 2016) and astrocytes (Clarke et al., 2018). In cerebellar and cortical microglia, gene expression profiles relatively changed during earlier stages of ageing (4-12 months) and late stages (12-22 months) in mice whereas noticeable gene expression changes in striatal microglia occurred at early ageing and in the hippocampus at late ageing (Grabert et al., 2016). Moreover, genes associated with reactive A1 astrocytes were upregulated in mice striatum

and hippocampus as opposed to the cortex during ageing (Clarke et al., 2018) Furthermore, minocycline (a second-generation tetracycline) attenuated LPS-stimulated microglial induced cytotoxicity in human fetal microglia-neuron co-cultures (Filipovic and Zecevic, 2008) and rat brain microglia (Fan et al., 2005). Moreover, differential responses between the brain and spinal cord microglial to LPS were also reported in neonatal rat microglia as discussed earlier in chapter 3 in which LPS stimulation increased pro-inflammatory markers in brain microglia as opposed to spinal cord microglia (Baskar Jesudasan et al., 2014). Therefore, localisation of microglia influences their transcriptomes suggesting that their gene expression depends on signals received from their extracellular milieu. Nevertheless, emerging evidence indicates that microglia retain their sex following transplantation and their wiring at early developmental stages is not altered when they are transplanted to a foreign environment (Villa et al., 2018). This suggests that microglia potentially retain their regional and developmental identity in culture. Systemic injection of aged mice with LPS resulted in a higher level of IL-1β in comparison to younger animals (adult mice) (Godbout et al., 2005). Likewise, the decrease In anti-inflammatory cytokine and an increase in pro-inflammatory cytokine expression in adult cortical MCM-stimulated astrocytes suggest that adult microglia affect neonatal astrocytes to acquire a more pro-inflammatory phenotype in comparison to neonatal cortical microglia.

5.4 Microglial responses to ATP stimulation

In chapter four, we stimulated microglia with ATP. All NR4A subfamily members transcript levels rapidly increased following ATP stimulation. This transient up-regulation suggests a critical role of these orphan nuclear receptors in regulating microglial responses to extracellular danger signals under physiological and pathological conditions. Our findings indicate a differential response to ATP in adult microglia compared to neonatal microglia, especially in the event of BDNF expression and secretion.

Interestingly, ablation of microglia contributed to learning impairments and reduced learning dependent-synaptic plasticity. A similar effect was observed when BDNF was conditionally removed from microglia (Parkhurst et al., 2013). Although microglial BDNF promotes survival and synaptic plasticity (Paolicelli and Ferretti, 2017), it is proposed that BDNF can prolong microglial activation through an autocrine mechanism, meaning that BDNF secreted from ATP-stimulated microglia can promote migration and a further secretion of TNF-α from microglia (Zhang et al., 2014). A concentration of 100μM of ATP, like the one used for the current study, stimulated rat microglia to release BDNF through P2X4R (Ulmann et al., 2008). Inflammation in microglia may be regulated by p38α MAPK activation after inducing traumatic brain injury In the cortex of mice (Bachstetter et al., 2013), which can be correlated to an ATP stimulation. Moreover, an up-regulation in P2X4R expression was observed in microglia/macrophages in rat cortices following traumatic brain injury (Zhang et al., 2006). Our results indicate a

P2X-mediated BDNF release from adult microglia after stimulation with ATP. Intriguingly, inhibiting p38 MAPK significantly affected mRNA expression of *BDNF* but not its secretion from adult microglia. Trang et al (2009) suggested a 20% decrease in ATP-induced BDNF secretion from microglia upon inhibiting p38 MAPK (Trang et al., 2009) however, the decrease in BDNF release from microglia was not statistically significant compared to ATP – treated. Our result indicated a slight decrease in BDNF release from adult microglia pre-treated with p38 MAPK inhibitor, however that effect was not statistically significant. Nevertheless, our percentage of ATP-induced BDNF decreases upon pre-treatment with p38 MAPK was 29% in adult spinal cord microglia, similar to the decrease in BDNF reported by Trang and colleagues (2009). Moreover, TNP-ATP treatment did not affect the activation of p38 MAPK yet downregulated BDNF mRNA expression and release from microglia, suggesting the involvement of another pathway downstream to P2X activation by ATP other than p38 MAPK.

Indeed, microglial developmental heterogeneity in response to ATP was noted. A physiological function of microglia is to respond to ATP leased from various cell types or upon necrosis and apoptosis during development (Del Puerto et al., 2013). This could explain the reduced response to ATP and the lack of BDNF release from neonatal microglia in the present study. On the other hand, ageing microglia undergo several morphological and functional changes. In fact, brain adult microglia show a higher activated basal state marked by up-regulated pro-inflammatory and MHC-II mRNA

expression (Frank et al., 2006). The CNS developmental stage determines the functional interaction of microglia and neurons (Parkhurst et al., 2013). Perhaps this is the reason behind the higher levels of BDNF basal expression in adult microglia compared to neonatal microglia. Evidently, the development of neuropathic pain is influenced by immune responses in different age groups. For instance, inducing nerve injury (SNI) in young rat pups (P10) triggered an anti-inflammatory response in the dorsal horn marked by an increase in *IL-10* and *IL-4* expression and low transcript levels of *Iba-1*. On the other hand, SNI induced in adults (P33) resulted in an increase in the mRNA expression of pro-inflammatory mediators like *TNF-α* or *BDNF* and *Iba-1* transcripts (McKelvey et al., 2015). In the present study, we also showed differential expression and release of BDNF from ATP-stimulated neonatal or adult microglia. In this context, differential age-related immunological responses must be taken into consideration when using microglia In pain research; thus intrathecal injection of ATP-stimulated neonatal microglia in adult rats (Tsuda et al., 2003) may not appropriately elucidate the mechanisms behind microglial contribution to pain.

Researchers have reported microglial regional-heterogeneity in response to injury. For instance, following inducing PNI In adult mice, prefrontal cortex microglia showed a more pro-inflammatory phenotype in comparison to spinal cord microglia. On the other hand, in a mouse model of neuropathic pain, activated microglia were reportedly limited to the spinal cord and not other supraspinal regions (Zhang et al., 2008). Moreover, basal

states of spinal cord microglia showed a higher pro-inflammatory subtype compared to cortical microglia (Li et al., 2016b). Differences in the baseline of *BDNF* expression, displaying a higher *BDNF* expression level in spinal cord microglia as opposed to cortical microglia could indicate to their differential responses to the inflammatory milieu.

In conclusion, microglial activation and the resultant response is dependent on their microenvironment; thus, they respond differently to certain stimuli based on their developmental stage and region. Glia-neuron cross-talk is tightly regulated, and any slight dysregulation can be detrimental to the CNS.

5.5 Future directions

In this thesis, although ACM improved the viability of neurons possibly due to growth and neuroprotective factors produced by astrocytes, the increase in NR4A subfamily members in astrocytes might have a potential role in improving neuronal viability. It is worth overexpressing each NR4A subfamily member in microglia to investigate that effect on microglial activation and polarisation and consequently the fate of neurons as a result of glial cells communication.

To our knowledge, this is the first study that compares ATP-induced BDNF expression and release in two different stages of developmental microglia. The lack of an effective selective P2X4R inhibitor is challenging to investigate the signalling pathway behind ATP-activated microglia. Knocking

down P2X4R and P2X7R expression can give us better insight into the mechanism of *BDNF* expression. Overexpression of Nurr1 or IL-10 can potentially affect BDNF expression and release because as our results showed, their mRNA expression profiles are nearly comparable.

Appendix

Data presented at conferences

A poster was presented at The XIV European Meeting on Glial Cells in Health and Disease, Porto July 2019

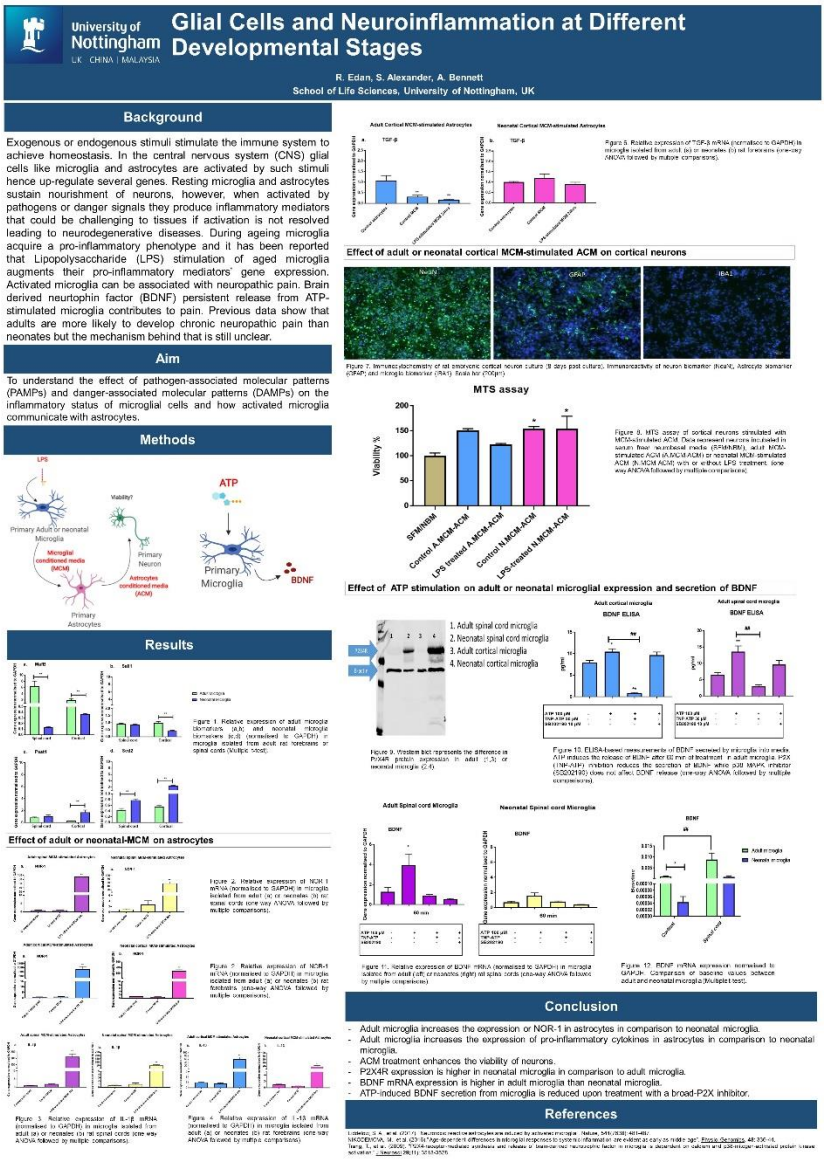

6) Chapter six:

Bibliography

AARNISALO, P., KIM, C. H., LEE, J. W. & PERLMANN, T. 2002. Defining requirements for heterodimerization between the retinoid X receptor and the orphan nuclear receptor Nurr1. *J Biol Chem,* 277**,** 35118-23.

AARUM, J., SANDBERG, K., HAEBERLEIN, S. L. & PERSSON, M. A. 2003. Migration and differentiation of neural precursor cells can be directed by microglia. *Proc Natl Acad Sci U S A,* 100**,** 15983-8.

AGULHON, C., PETRAVICZ, J., MCMULLEN, A. B., SWEGER, E. J., MINTON, S. K., TAVES, S. R., CASPER, K. B., FIACCO, T. A. & MCCARTHY, K. D. 2008. What is the role of astrocyte calcium in neurophysiology? *Neuron,* 59**,** 932-46.

AJAMI, B., BENNETT, J. L., KRIEGER, C., TETZLAFF, W. & ROSSI, F. M. 2007. Local self-renewal can sustain CNS microglia maintenance and function throughout adult life. *Nat Neurosci,* 10**,** 1538-43.

AKIRA, S., UEMATSU, S. & TAKEUCHI, O. 2006. Pathogen recognition and innate immunity. *Cell,* 124**,** 783-801.

ALONSO, J., GALAN, M., MARTI-PAMIES, I., ROMERO, J. M., CAMACHO, M., RODRIGUEZ, C. & MARTINEZ-GONZALEZ, J. 2016. NOR-1/NR4A3 regulates the cellular inhibitor of apoptosis 2 (cIAP2) in vascular cells: role in the survival response to hypoxic stress. *Sci Rep,* 6**,** 34056.

ARCURI, C., MECCA, C., BIANCHI, R., GIAMBANCO, I. & DONATO, R. 2017. The Pathophysiological Role of Microglia in Dynamic Surveillance, Phagocytosis and Structural Remodeling of the Developing CNS. *Front Mol Neurosci,* 10**,** 191.

BACHSTETTER, A. D., ROWE, R. K., KANEKO, M., GOULDING, D., LIFSHITZ, J. & VAN ELDIK, L. J. 2013. The p38alpha MAPK regulates microglial responsiveness to diffuse traumatic brain injury. *J Neurosci,* 33**,** 6143-53.

BACHSTETTER, A. D., VAN ELDIK, L. J., SCHMITT, F. A., NELTNER, J. H., IGHODARO, E. T., WEBSTER, S. J., PATEL, E., ABNER, E. L., KRYSCIO, R. J. & NELSON, P. T. 2015. Disease-related microglia heterogeneity in the hippocampus of Alzheimer's disease, dementia with Lewy bodies, and hippocampal sclerosis of aging. *Acta Neuropathol Commun,* 3**,** 32.

BALOYANNIS, S. J. 2015. Staining neurons with Golgi techniques in degenerative diseases of the brain. *Neural Regen Res,* 10**,** 693-5.

BANKS, W. A., GRAY, A. M., ERICKSON, M. A., SALAMEH, T. S., DAMODARASAMY, M., SHEIBANI, N., MEABON, J. S., WING, E. E., MOROFUJI, Y., COOK, D. G. & REED, M. J. 2015. Lipopolysaccharide-induced blood-brain barrier disruption: roles of cyclooxygenase, oxidative stress, neuroinflammation, and elements of the neurovascular unit. *J Neuroinflammation,* 12**,** 223.

BARGER, S. W., MOERMAN, A. M. & MAO, X. 2005. Molecular mechanisms of cytokine-induced neuroprotection: NFkappaB and neuroplasticity. *Curr Pharm Des,* 11**,** 985-98.

BASKAR JESUDASAN, S. J., TODD, K. G. & WINSHIP, I. R. 2014. Reduced inflammatory phenotype in microglia derived from neonatal rat spinal cord versus brain. *PLoS One,* 9**,** e99443.

BENNETT, M. L., BENNETT, F. C., LIDDELOW, S. A., AJAMI, B., ZAMANIAN, J. L., FERNHOFF, N. B., MULINYAWE, S. B., BOHLEN, C. J., ADIL, A., TUCKER, A., WEISSMAN, I. L., CHANG, E. F., LI, G., GRANT, G. A., HAYDEN GEPHART, M. G. & BARRES, B. A. 2016. New tools for studying microglia in the mouse and human CNS. *Proc Natl Acad Sci U S A,* 113**,** E1738-46.

BERNIER, L. P. 2012. Purinergic regulation of inflammasome activation after central nervous system injury. *J Gen Physiol,* 140**,** 571-5.

BIANCHI, M. E. 2007. DAMPs, PAMPs and alarmins: all we need to know about danger. *J Leukoc Biol,* 81**,** 1-5.

BLENCOWE, B. J. 2017. The Relationship between Alternative Splicing and Proteomic Complexity. *Trends Biochem Sci,* 42**,** 407-408.

BLOCK, M. L., ZECCA, L. & HONG, J. S. 2007. Microglia-mediated neurotoxicity: uncovering the molecular mechanisms. *Nat Rev Neurosci,* 8**,** 57-69.

BOEHME, S. A., LIO, F. M., MACIEJEWSKI-LENOIR, D., BACON, K. B. & CONLON, P. J. 2000. The chemokine fractalkine inhibits Fas-mediated cell death of brain microglia. *J Immunol,* 165**,** 397-403.

BOHLEN, C. J., BENNETT, F. C., TUCKER, A. F., COLLINS, H. Y., MULINYAWE, S. B. & BARRES, B. A. 2017. Diverse Requirements for Microglial Survival, Specification, and Function Revealed by Defined-Medium Cultures. *Neuron,* 94**,** 759-773.e8.

BOTTCHER, C., SCHLICKEISER, S., SNEEBOER, M. A. M., KUNKEL, D., KNOP, A., PAZA, E., FIDZINSKI, P., KRAUS, L., SNIJDERS, G. J. L., KAHN, R. S., SCHULZ, A. R., MEI, H. E., PSY, N. B. B., HOL, E. M., SIEGMUND, B., GLAUBEN, R., SPRUTH, E. J., DE WITTE, L. D. & PRILLER, J. 2019. Human microglia regional heterogeneity and phenotypes determined by multiplexed single-cell mass cytometry. *Nat Neurosci,* 22**,** 78-90.

BOTTENSTEIN, J. E. & SATO, G. 1985. *Cell Culture in the Neurosciences*, Plenum Press: New York and London.

BOUMECHACHE, M., MASIN, M., EDWARDSON, J. M., GORECKI, D. C. & MURRELL-LAGNADO, R. 2009. Analysis of assembly and trafficking of native P2X4 and P2X7 receptor complexes in rodent immune cells. *J Biol Chem,* 284**,** 13446-54.

BRAMBILLA, R., BRACCHI-RICARD, V., HU, W. H., FRYDEL, B., BRAMWELL, A., KARMALLY, S., GREEN, E. J. & BETHEA, J. R. 2005. Inhibition of astroglial nuclear factor kappaB reduces inflammation and improves functional recovery after spinal cord injury. *J Exp Med,* 202**,** 145-56.

BUTOVSKY, O., JEDRYCHOWSKI, M. P., MOORE, C. S., CIALIC, R., LANSER, A. J., GABRIELY, G., KOEGLSPERGER, T., DAKE, B., WU, P. M., DOYKAN, C. E., FANEK, Z., LIU, L., CHEN, Z., ROTHSTEIN, J. D., RANSOHOFF, R. M., GYGI, S. P., ANTEL, J. P. & WEINER, H. L. 2014. Identification of a unique TGF-beta-dependent molecular and functional signature in microglia. *Nat Neurosci,* 17**,** 131-43.

BUTTGEREIT, A., LELIOS, I., YU, X., VROHLINGS, M., KRAKOSKI, N. R., GAUTIER, E. L., NISHINAKAMURA, R., BECHER, B. & GRETER, M. 2016. Sall1 is a transcriptional regulator defining microglia identity and function. *Nat Immunol,* 17**,** 1397-1406.

BUTTON, E. B., MITCHELL, A. S., DOMINGOS, M. M., CHUNG, J. H., BRADLEY, R. M., HASHEMI, A., MARVYN, P. M., PATTERSON, A. C., STARK, K. D., QUADRILATERO, J. & DUNCAN, R. E. 2014. Microglial cell activation increases saturated and decreases monounsaturated fatty acid content, but both lipid species are proinflammatory. *Lipids,* 49**,** 305-16.

CAJAL, S. R. Y. 1913. Un nuevo proceder para la impregnacio´n de la neurogli´a. *Bol. Soc. Esp,* Biol. **,** 104–108.

CALDEIRA, C., OLIVEIRA, A. F., CUNHA, C., VAZ, A. R., FALCAO, A. S., FERNANDES, A. & BRITES, D. 2014. Microglia change from a reactive to an age-like phenotype with the time in culture. *Front Cell Neurosci,* 8**,** 152.

CALNAN, B. J., SZYCHOWSKI, S., CHAN, F. K., CADO, D. & WINOTO, A. 1995. A role for the orphan steroid receptor Nur77 in apoptosis accompanying antigen-induced negative selection. *Immunity,* 3**,** 273-82.

CARDONA, A. E., PIORO, E. P., SASSE, M. E., KOSTENKO, V., CARDONA, S. M., DIJKSTRA, I. M., HUANG, D., KIDD, G., DOMBROWSKI, S., DUTTA, R., LEE, J. C., COOK, D. N., JUNG, S., LIRA, S. A., LITTMAN, D. R. & RANSOHOFF, R. M. 2006. Control of microglial neurotoxicity by the fractalkine receptor. *Nat Neurosci,* 9**,** 917-24.

CAROFF, M., KARIBIAN, D., CAVAILLON, J. M. & HAEFFNER-CAVAILLON, N. 2002. Structural and functional analyses of bacterial lipopolysaccharides. *Microbes Infect,* 4**,** 915-26.

CARSON, M. J., THRASH, J. C. & WALTER, B. 2006. The cellular response in neuroinflammation: The role of leukocytes, microglia and astrocytes in neuronal death and survival. *Clin Neurosci Res,* 6**,** 237-245.

CASTRO, D. S., ARVIDSSON, M., BONDESSON BOLIN, M. & PERLMANN, T. 1999. Activity of the Nurr1 carboxyl-terminal domain depends on cell type and integrity of the activation function 2. *J Biol Chem,* 274**,** 37483-90.

CHEEPSUNTHORN, P., RADOV, L., MENZIES, S., REID, J. & CONNOR, J. R. 2001. Characterization of a novel brain-derived microglial cell line isolated from neonatal rat brain. *Glia,* 35**,** 53-62.

CHEN, X., ZACHAR, V., CHANG, C., EBBESEN, P. & LIU, X. 1998. Differential expression of Nur77 family members in human T-lymphotropic virus type 1-infected cells: transactivation of the TR3/nur77 gene by Tax protein. *J Virol,* 72**,** 6902-6.

CHEN, Y., JIN, Y., ZHAN, H., CHEN, J., CHEN, Y., MENG, H., JIN, J., YU, L., CAO, X. & XU, Y. 2017. Proteomic analysis of the effects of Nur77 on lipopolysaccharide-induced microglial activation. *Neurosci Lett,* 659**,** 33-43.

CHHOR, V., LE CHARPENTIER, T., LEBON, S., ORE, M. V., CELADOR, I. L., JOSSERAND, J., DEGOS, V., JACOTOT, E., HAGBERG, H., SAVMAN, K., MALLARD, C., GRESSENS, P. & FLEISS, B. 2013. Characterization of phenotype markers and neuronotoxic potential of polarised primary microglia in vitro. *Brain Behav Immun,* 32**,** 70-85.

CHO, C. E., DAMLE, S. S., WANCEWICZ, E. V., MUKHOPADHYAY, S., HART, C. E., MAZUR, C., SWAYZE, E. E. & KAMME, F. 2019. A modular analysis of microglia gene expression, insights into the aged phenotype. *BMC Genomics,* 20**,** 164.

CHRISTENSEN, L. B., WOODS, T. A., CARMODY, A. B., CAUGHEY, B. & PETERSON, K. E. 2014. Age-related differences in neuroinflammatory responses associated with a distinct profile of regulatory markers on neonatal microglia. *J Neuroinflammation,* 11**,** 70.

CLARK, A. K., YIP, P. K., GRIST, J., GENTRY, C., STANILAND, A. A., MARCHAND, F., DEHVARI, M., WOTHERSPOON, G., WINTER, J., ULLAH, J., BEVAN, S. & MALCANGIO, M. 2007.

Inhibition of spinal microglial cathepsin S for the reversal of neuropathic pain. *Proc Natl Acad Sci U S A,* 104**,** 10655-60.

CLARKE, L. E., LIDDELOW, S. A., CHAKRABORTY, C., MUNCH, A. E., HEIMAN, M. & BARRES, B. A. 2018. Normal aging induces A1-like astrocyte reactivity. *Proc Natl Acad Sci U S A,* 115**,** E1896-E1905.

CODDOU, C., SANDOVAL, R., HEVIA, M. J. & STOJILKOVIC, S. S. 2019. Characterization of the antagonist actions of 5-BDBD at the rat P2X4 receptor. *Neurosci Lett,* 690**,** 219-224.

COLLINS, H. Y. & BOHLEN, C. J. 2018. Isolation and Culture of Rodent Microglia to Promote a Dynamic Ramified Morphology in Serum-free Medium. *J Vis Exp*.

COLONNA, M. & BUTOVSKY, O. 2017. Microglia Function in the Central Nervous System During Health and Neurodegeneration. *Annu Rev Immunol*.

COULL, J. A., BEGGS, S., BOUDREAU, D., BOIVIN, D., TSUDA, M., INOUE, K., GRAVEL, C., SALTER, M. W. & DE KONINCK, Y. 2005. BDNF from microglia causes the shift in neuronal anion gradient underlying neuropathic pain. *Nature,* 438**,** 1017-21.

CRAIN, J. M., NIKODEMOVA, M. & WATTERS, J. J. 2009. Expression of P2 nucleotide receptors varies with age and sex in murine brain microglia. *J Neuroinflammation,* 6**,** 24.

CREAN, D., CUMMINS, E. P., BAHAR, B., MOHAN, H., MCMORROW, J. P. & MURPHY, E. P. 2015. Adenosine Modulates NR4A Orphan Nuclear Receptors To Attenuate Hyperinflammatory Responses in Monocytic Cells. *J Immunol,* 195**,** 1436-48.

DA FONSECA, A. C., MATIAS, D., GARCIA, C., AMARAL, R., GERALDO, L. H., FREITAS, C. & LIMA, F. R. 2014. The impact of microglial activation on blood-brain barrier in brain diseases. *Front Cell Neurosci,* 8**,** 362.

DAMANI, M. R., ZHAO, L., FONTAINHAS, A. M., AMARAL, J., FARISS, R. N. & WONG, W. T. 2011. Age-related alterations in the dynamic behavior of microglia. *Aging Cell,* 10**,** 263-76.

DANEMAN, R. & PRAT, A. 2015. The blood-brain barrier. *Cold Spring Harb Perspect Biol,* 7**,** a020412.

DAS, A., KIM, S. H., ARIFUZZAMAN, S., YOON, T., CHAI, J. C., LEE, Y. S., PARK, K. S., JUNG, K. H. & CHAI, Y. G. 2016. Transcriptome sequencing reveals that LPS-triggered transcriptional responses in established microglia BV2 cell lines are poorly representative of primary microglia. *J Neuroinflammation,* 13**,** 182.

DAVALOS, D., GRUTZENDLER, J., YANG, G., KIM, J. V., ZUO, Y., JUNG, S., LITTMAN, D. R., DUSTIN, M. L. & GAN, W. B. 2005. ATP mediates rapid microglial response to local brain injury in vivo. *Nat Neurosci,* 8**,** 752-8.

DE MOURA, R. F., NASCIMENTO, L. F., IGNACIO-SOUZA, L. M., MORARI, J., RAZOLLI, D. S., SOLON, C., DE SOUZA, G. F., FESTUCCIA, W. T. & VELLOSO, L. A. 2016. Hypothalamic stearoyl-CoA desaturase-2 (SCD2) controls whole-body energy expenditure. *Int J Obes (Lond),* 40**,** 471-8.

DE PAOLI, F., EECKHOUTE, J., COPIN, C., VANHOUTTE, J., DUHEM, C., DERUDAS, B., DUBOIS-CHEVALIER, J., COLIN, S., ZAWADZKI, C., JUDE, B., HAULON, S., LEFEBVRE, P., STAELS, B. & CHINETTI-GBAGUIDI, G. 2015. The neuron-derived orphan receptor 1 (NOR1) is induced upon human alternative macrophage polarization and stimulates the expression of markers of the M2 phenotype. *Atherosclerosis,* 241**,** 18-26.

DEAN, J. M., WANG, X., KAINDL, A. M., GRESSENS, P., FLEISS, B., HAGBERG, H. & MALLARD, C. 2010. Microglial MyD88 signaling regulates acute neuronal toxicity of LPS-stimulated microglia in vitro. *Brain Behav Immun,* 24**,** 776-83.

DEL PUERTO, A., WANDOSELL, F. & GARRIDO, J. J. 2013. Neuronal and glial purinergic receptors functions in neuron development and brain disease. *Front Cell Neurosci,* 7**,** 197.

DEL RIO-HORTEGA, P. 1939. The Microglia. *The Lancet***,** 1023-1026.

DELERIVE, P., DE BOSSCHER, K., BESNARD, S., VANDEN BERGHE, W., PETERS, J. M., GONZALEZ, F. J., FRUCHART, J. C., TEDGUI, A., HAEGEMAN, G. & STAELS, B. 1999. Peroxisome proliferator-activated receptor alpha negatively regulates the vascular inflammatory gene response by negative cross-talk with transcription factors NF-kappaB and AP-1. *J Biol Chem,* 274**,** 32048-54.

DEPAULA-SILVA, A. B., GORBEA, C., DOTY, D. J., LIBBEY, J. E., SANCHEZ, J. M. S., HANAK, T. J., CAZALLA, D. & FUJINAMI, R. S. 2019. Differential transcriptional profiles identify microglial- and macrophage-specific gene markers expressed during virus-induced neuroinflammation. *J Neuroinflammation,* 16**,** 152.

DHEEN, S. T., KAUR, C. & LING, E. A. 2007. Microglial activation and its implications in the brain diseases. *Curr Med Chem,* 14**,** 1189-97.

DING, S. 2014. Ca(2+) signaling in astrocytes and its role in ischemic stroke. *Adv Neurobiol,* 11**,** 189-211.

DOBROVOLSKAIA, M. A. & VOGEL, S. N. 2002. Toll receptors, CD14, and macrophage activation and deactivation by LPS. *Microbes Infect,* 4**,** 903-14.

DOMINGUES, H. S., PORTUGAL, C. C., SOCODATO, R. & RELVAS, J. B. 2016. Oligodendrocyte, Astrocyte, and Microglia Crosstalk in Myelin Development, Damage, and Repair. *Front Cell Dev Biol,* 4**,** 71.

DUTTA, G., ZHANG, P. & LIU, B. 2008. The lipopolysaccharide Parkinson's disease animal model: mechanistic studies and drug discovery. *Fundam Clin Pharmacol,* 22**,** 453-64.

EDAN, R. A., LUQMANI, Y. A. & MASOCHA, W. 2013. COL-3, a chemically modified tetracycline, inhibits lipopolysaccharide-induced microglia activation and cytokine expression in the brain. *PLoS One,* 8**,** e57827.

EHRLICH, L. C., HU, S., SHENG, W. S., SUTTON, R. L., ROCKSWOLD, G. L., PETERSON, P. K. & CHAO, C. C. 1998. Cytokine regulation of human microglial cell IL-8 production. *J Immunol,* 160**,** 1944-8.

EKLIND, S., HAGBERG, H., WANG, X., SAVMAN, K., LEVERIN, A. L., HEDTJARN, M. & MALLARD, C. 2006. Effect of lipopolysaccharide on global gene expression in the immature rat brain. *Pediatr Res,* 60**,** 161-8.

ENGELMANN, C., WEIH, F. & HAENOLD, R. 2014. Role of nuclear factor kappa B in central nervous system regeneration. *Neural Regen Res,* 9**,** 707-11.

ERICKSON, M. A., DOHI, K. & BANKS, W. A. 2012. Neuroinflammation: a common pathway in CNS diseases as mediated at the blood-brain barrier. *Neuroimmunomodulation,* 19**,** 121-30.

FACCI, L., BARBIERATO, M., MARINELLI, C., ARGENTINI, C., SKAPER, S. D. & GIUSTI, P. 2014a. Toll-like receptors 2, -3 and -4 prime microglia but not astrocytes across central nervous system regions for ATP-dependent interleukin-1beta release. *Sci Rep,* 4**,** 6824.

FACCI, L., BARBIERATO, M., MARINELLI, C., ARGENTINI, C., SKAPER, S. D. & GIUSTI, P. 2014b. Toll-like receptors 2, -3 and -4 prime microglia but not astrocytes across

central nervous system regions for ATP-dependent interleukin-1β release. *Sci Rep,* 4**,** 6824.

FAN, L. W., PANG, Y., LIN, S., TIEN, L. T., MA, T., RHODES, P. G. & CAI, Z. 2005. Minocycline reduces lipopolysaccharide-induced neurological dysfunction and brain injury in the neonatal rat. *J Neurosci Res,* 82**,** 71-82.

FENTON, M. J. & GOLENBOCK, D. T. 1998. LPS-binding proteins and receptors. *J Leukoc Biol,* 64**,** 25-32.

FERNANDEZ, J. R., BYRNE, B. & FIRESTEIN, B. L. 2009. Phylogenetic analysis and molecular evolution of guanine deaminases: from guanine to dendrites. *J Mol Evol,* 68**,** 227-35.

FILIPOVIC, R. & ZECEVIC, N. 2008. Neuroprotective role of minocycline in co-cultures of human fetal neurons and microglia. *Exp Neurol,* 211**,** 41-51.

FITZGERALD, M. & WALKER, S. M. 2009. Infant pain management: a developmental neurobiological approach. *Nat Clin Pract Neurol,* 5**,** 35-50.

FLANARY, B. E., SAMMONS, N. W., NGUYEN, C., WALKER, D. & STREIT, W. J. 2007. Evidence that aging and amyloid promote microglial cell senescence. *Rejuvenation Res,* 10**,** 61-74.

FOO, L. C., ALLEN, N. J., BUSHONG, E. A., VENTURA, P. B., CHUNG, W. S., ZHOU, L., CAHOY, J. D., DANEMAN, R., ZONG, H., ELLISMAN, M. H. & BARRES, B. A. 2011. Development of a method for the purification and culture of rodent astrocytes. *Neuron,* 71**,** 799-811.

FRANCESCHI, C. & CAMPISI, J. 2014. Chronic inflammation (inflammaging) and its potential contribution to age-associated diseases. *J Gerontol A Biol Sci Med Sci,* 69 Suppl 1**,** S4-9.

FRANK, M. G., BARRIENTOS, R. M., BIEDENKAPP, J. C., RUDY, J. W., WATKINS, L. R. & MAIER, S. F. 2006. mRNA up-regulation of MHC II and pivotal pro-inflammatory genes in normal brain aging. *Neurobiol Aging,* 27**,** 717-22.

GALATRO, T. F., HOLTMAN, I. R., LERARIO, A. M., VAINCHTEIN, I. D., BROUWER, N., SOLA, P. R., VERAS, M. M., PEREIRA, T. F., LEITE, R. E. P., MOLLER, T., WES, P. D., SOGAYAR, M. C., LAMAN, J. D., DEN DUNNEN, W., PASQUALUCCI, C. A., OBA-SHINJO, S. M., BODDEKE, E., MARIE, S. K. N. & EGGEN, B. J. L. 2017. Transcriptomic analysis of purified human cortical microglia reveals age-associated changes. *Nat Neurosci,* 20**,** 1162-1171.

GARCIA-MESA, Y., JAY, T. R., CHECKLEY, M. A., LUTTGE, B., DOBROWOLSKI, C., VALADKHAN, S., LANDRETH, G. E., KARN, J. & ALVAREZ-CARBONELL, D. 2017. Immortalization of primary microglia: a new platform to study HIV regulation in the central nervous system. *J Neurovirol,* 23**,** 47-66.

GHISLETTI, S., HUANG, W., OGAWA, S., PASCUAL, G., LIN, M. E., WILLSON, T. M., ROSENFELD, M. G. & GLASS, C. K. 2007. Parallel SUMOylation-dependent pathways mediate gene- and signal-specific transrepression by LXRs and PPARgamma. *Mol Cell,* 25**,** 57-70.

GIULIAN, D. & BAKER, T. J. 1986. Characterization of ameboid microglia isolated from developing mammalian brain. *J Neurosci,* 6**,** 2163-78.

GIULIAN, D., LI, J., BARTEL, S., BROKER, J., LI, X. & KIRKPATRICK, J. B. 1995. Cell surface morphology identifies microglia as a distinct class of mononuclear phagocyte. *J Neurosci,* 15**,** 7712-26.

GODBOUT, J. P., CHEN, J., ABRAHAM, J., RICHWINE, A. F., BERG, B. M., KELLEY, K. W. & JOHNSON, R. W. 2005. Exaggerated neuroinflammation and sickness behavior in

aged mice following activation of the peripheral innate immune system. *FASEB J,* 19**,** 1329-31.

GOLGI, C. 1873. Sulla struttura della sostanza grigia del cervello. *Gazzetta Medica Italiana,* Lombardia 6**,** 244–246.

GORINA, R., FONT-NIEVES, M., MARQUEZ-KISINOUSKY, L., SANTALUCIA, T. & PLANAS, A. M. 2011. Astrocyte TLR4 activation induces a proinflammatory environment through the interplay between MyD88-dependent NFkappaB signaling, MAPK, and Jak1/Stat1 pathways. *Glia,* 59**,** 242-55.

GOSSELIN, D., LINK, V. M., ROMANOSKI, C. E., FONSECA, G. J., EICHENFIELD, D. Z., SPANN, N. J., STENDER, J. D., CHUN, H. B., GARNER, H., GEISSMANN, F. & GLASS, C. K. 2014. Environment drives selection and function of enhancers controlling tissue-specific macrophage identities. *Cell,* 159**,** 1327-40.

GOSSELIN, D., SKOLA, D., COUFAL, N. G., HOLTMAN, I. R., SCHLACHETZKI, J. C. M., SAJTI, E., JAEGER, B. N., O'CONNOR, C., FITZPATRICK, C., PASILLAS, M. P., PENA, M., ADAIR, A., GONDA, D. D., LEVY, M. L., RANSOHOFF, R. M., GAGE, F. H. & GLASS, C. K. 2017. An environment-dependent transcriptional network specifies human microglia identity. *Science,* 356.

GOURSAUD, S., KOZLOVA, E. N., MALOTEAUX, J. M. & HERMANS, E. 2009. Cultured astrocytes derived from corpus callosum or cortical grey matter show distinct glutamate handling properties. *J Neurochem,* 108**,** 1442-52.

GRABERT, K., MICHOEL, T., KARAVOLOS, M. H., CLOHISEY, S., BAILLIE, J. K., STEVENS, M. P., FREEMAN, T. C., SUMMERS, K. M. & MCCOLL, B. W. 2016. Microglial brain region-dependent diversity and selective regional sensitivities to aging. *Nat Neurosci,* 19**,** 504-16.

GREENBAUM, D., COLANGELO, C., WILLIAMS, K. & GERSTEIN, M. 2003. Comparing protein abundance and mRNA expression levels on a genomic scale. *Genome Biol,* 4**,** 117.

GROSS, O., THOMAS, C. J., GUARDA, G. & TSCHOPP, J. 2011. The inflammasome: an integrated view. *Immunol Rev,* 243**,** 136-51.

GUO, H., CALLAWAY, J. B. & TING, J. P. 2015. Inflammasomes: mechanism of action, role in disease, and therapeutics. *Nat Med,* 21**,** 677-87.

GUTTENPLAN, K. A. & LIDDELOW, S. A. 2019. Astrocytes and microglia: Models and tools. *J Exp Med,* 216**,** 71-83.

HAAGE, V., SEMTNER, M., VIDAL, R. O., HERNANDEZ, D. P., PONG, W. W., CHEN, Z., HAMBARDZUMYAN, D., MAGRINI, V., LY, A., WALKER, J., MARDIS, E., MERTINS, P., SAUER, S., KETTENMANN, H. & GUTMANN, D. H. 2019. Comprehensive gene expression meta-analysis identifies signature genes that distinguish microglia from peripheral monocytes/macrophages in health and glioma. *Acta Neuropathol Commun,* 7**,** 20.

HAMMOND, T. R., DUFORT, C., DISSING-OLESEN, L., GIERA, S., YOUNG, A., WYSOKER, A., WALKER, A. J., GERGITS, F., SEGEL, M., NEMESH, J., MARSH, S. E., SAUNDERS, A., MACOSKO, E., GINHOUX, F., CHEN, J., FRANKLIN, R. J. M., PIAO, X., MCCARROLL, S. A. & STEVENS, B. 2019. Single-Cell RNA Sequencing of Microglia throughout the Mouse Lifespan and in the Injured Brain Reveals Complex Cell-State Changes. *Immunity,* 50**,** 253-271 e6.

HANAMSAGAR, R., ALTER, M. D., BLOCK, C. S., SULLIVAN, H., BOLTON, J. L. & BILBO, S. D. 2017. Generation of a microglial developmental index in mice and in humans reveals a sex difference in maturation and immune reactivity. *Glia,* 65**,** 1504-1520.

HANISCH, U. K. 2002. Microglia as a source and target of cytokines. *Glia,* 40**,** 140-55.

HANNA, R. N., SHAKED, I., HUBBELING, H. G., PUNT, J. A., WU, R., HERRLEY, E., ZAUGG, C., PEI, H., GEISSMANN, F., LEY, K. & HEDRICK, C. C. 2012. NR4A1 (Nur77) deletion polarizes macrophages toward an inflammatory phenotype and increases atherosclerosis. *Circ Res,* 110**,** 416-27.

HARRY, G. J. 2013. Microglia during development and aging. *Pharmacol Ther,* 139**,** 313-26.

HARRY, G. J. & KRAFT, A. D. 2008. Neuroinflammation and microglia: considerations and approaches for neurotoxicity assessment. *Expert Opin Drug Metab Toxicol,* 4**,** 1265-77.

HARRY, G. J. & KRAFT, A. D. 2012. Microglia in the developing brain: a potential target with lifetime effects. *Neurotoxicology,* 33**,** 191-206.

HART, C. E., RACE, V., ACHOURI, Y., WIAME, E., SHARRARD, M., OLPIN, S. E., WATKINSON, J., BONHAM, J. R., JAEKEN, J., MATTHIJS, G. & VAN SCHAFTINGEN, E. 2007. Phosphoserine aminotransferase deficiency: a novel disorder of the serine biosynthesis pathway. *Am J Hum Genet,* 80**,** 931-7.

HASHIOKA, S., KLEGERIS, A., SCHWAB, C. & MCGEER, P. L. 2009. Interferon-gamma-dependent cytotoxic activation of human astrocytes and astrocytoma cells. *Neurobiol Aging,* 30**,** 1924-35.

HICKEY, W. F. & KIMURA, H. 1988. Perivascular microglial cells of the CNS are bone marrow-derived and present antigen in vivo. *Science,* 239**,** 290-2.

HIDANO, S., RANDALL, L. M., DAWSON, L., DIETRICH, H. K., KONRADT, C., KLOVER, P. J., JOHN, B., HARRIS, T. H., FANG, Q., TUREK, B., KOBAYASHI, T., HENNIGHAUSEN, L., BEITING, D. P., KOSHY, A. A. & HUNTER, C. A. 2016. STAT1 Signaling in Astrocytes Is Essential for Control of Infection in the Central Nervous System. *MBio,* 7.

HIDE, I., TANAKA, M., INOUE, A., NAKAJIMA, K., KOHSAKA, S., INOUE, K. & NAKATA, Y. 2000. Extracellular ATP triggers tumor necrosis factor-alpha release from rat microglia. *J Neurochem,* 75**,** 965-72.

HINES, D. J., CHOI, H. B., HINES, R. M., PHILLIPS, A. G. & MACVICAR, B. A. 2013. Prevention of LPS-induced microglia activation, cytokine production and sickness behavior with TLR4 receptor interfering peptides. *PLoS One,* 8**,** e60388.

HU, S., CHAO, C. C., EHRLICH, L. C., SHENG, W. S., SUTTON, R. L., ROCKSWOLD, G. L. & PETERSON, P. K. 1999. Inhibition of microglial cell RANTES production by IL-10 and TGF-beta. *J Leukoc Biol,* 65**,** 815-21.

HUANG, H. Y., CHANG, H. F., TSAI, M. J., CHEN, J. S. & WANG, M. J. 2016. 6-Mercaptopurine attenuates tumor necrosis factor-alpha production in microglia through Nur77-mediated transrepression and PI3K/Akt/mTOR signaling-mediated translational regulation. *J Neuroinflammation,* 13**,** 78.

HUANG, W. & GLASS, C. K. 2010. Nuclear receptors and inflammation control: molecular mechanisms and pathophysiological relevance. *Arterioscler Thromb Vasc Biol,* 30**,** 1542-9.

IMRAISH, A. 2018. Age-related changes in the phenotype of microglia. *PhD thesis,* University of Nottingham.

INOUE, K. 2002. Microglial activation by purines and pyrimidines. *Glia,* 40**,** 156-63.

IRNICH, D., TRACEY, D. J., POLTEN, J., BURGSTAHLER, R. & GRAFE, P. 2002. ATP stimulates peripheral axons in human, rat and mouse--differential involvement of A(2B) adenosine and P2X purinergic receptors. *Neuroscience,* 110**,** 123-9.

IVETIC, A., HOSKINS GREEN, H. L. & HART, S. J. 2019. L-selectin: A Major Regulator of Leukocyte Adhesion, Migration and Signaling. *Front Immunol,* 10**,** 1068.

JAEGER, L. B., DOHGU, S., SULTANA, R., LYNCH, J. L., OWEN, J. B., ERICKSON, M. A., SHAH, G. N., PRICE, T. O., FLEEGAL-DEMOTTA, M. A., BUTTERFIELD, D. A., BUTTERFILED, D. A. & BANKS, W. A. 2009. Lipopolysaccharide alters the blood-brain barrier transport of amyloid beta protein: a mechanism for inflammation in the progression of Alzheimer's disease. *Brain Behav Immun,* 23**,** 507-17.

JANG, E., KIM, J. H., LEE, S., KIM, J. H., SEO, J. W., JIN, M., LEE, M. G., JANG, I. S., LEE, W. H. & SUK, K. 2013. Phenotypic polarization of activated astrocytes: the critical role of lipocalin-2 in the classical inflammatory activation of astrocytes. *J Immunol,* 191**,** 5204-19.

JEANNETEAU, F., BARRERE, C., VOS, M., DE VRIES, C. J. M., ROUILLARD, C., LEVESQUE, D., DROMARD, Y., MOISAN, M. P., DURIC, V., FRANKLIN, T. C., DUMAN, R. S., LEWIS, D. A., GINSBERG, S. D. & ARANGO-LIEVANO, M. 2018. The Stress-Induced Transcription Factor NR4A1 Adjusts Mitochondrial Function and Synapse Number in Prefrontal Cortex. *J Neurosci,* 38**,** 1335-1350.

JEBELLI, J., PIERS, T. & POCOCK, J. 2015. Selective Depletion of Microglia from Cerebellar Granule Cell Cultures Using L-leucine Methyl Ester. *J Vis Exp***,** e52983.

JHA, M. K., JO, M., KIM, J. H. & SUK, K. 2019. Microglia-Astrocyte Crosstalk: An Intimate Molecular Conversation. *Neuroscientist,* 25**,** 227-240.

JURGA, A. M., PIOTROWSKA, A., MAKUCH, W., PRZEWLOCKA, B. & MIKA, J. 2017. Blockade of P2X4 Receptors Inhibits Neuropathic Pain-Related Behavior by Preventing MMP-9 Activation and, Consequently, Pronociceptive Interleukin Release in a Rat Model. *Front Pharmacol,* 8**,** 48.

KIELIAN, T. 2004. Microglia and chemokines in infectious diseases of the nervous system: views and reviews. *Front Biosci,* 9**,** 732-50.

KIELIAN, T. 2006. Toll-like receptors in central nervous system glial inflammation and homeostasis. *J Neurosci Res,* 83**,** 711-30.

KIGERL, K. A., DE RIVERO VACCARI, J. P., DIETRICH, W. D., POPOVICH, P. G. & KEANE, R. W. 2014. Pattern recognition receptors and central nervous system repair. *Exp Neurol,* 258**,** 5-16.

KINOSHITA, K., MATSUMOTO, K., KURAUCHI, Y., HISATSUNE, A., SEKI, T. & KATSUKI, H. 2019. A Nurr1 agonist amodiaquine attenuates inflammatory events and neurological deficits in a mouse model of intracerebral hemorrhage. *J Neuroimmunol,* 330**,** 48-54.

KIRIKAE, T., KIRIKAE, F., SAITO, S., TOMINAGA, K., TAMURA, H., UEMURA, Y., YOKOCHI, T. & NAKANO, M. 1998. Biological characterization of endotoxins released from antibiotic-treated Pseudomonas aeruginosa and Escherichia coli. *Antimicrob Agents Chemother,* 42**,** 1015-21.

KLOSS, C. U., BOHATSCHEK, M., KREUTZBERG, G. W. & RAIVICH, G. 2001. Effect of lipopolysaccharide on the morphology and integrin immunoreactivity of ramified microglia in the mouse brain and in cell culture. *Exp Neurol,* 168**,** 32-46.

KOIZUMI, S., OHSAWA, K., INOUE, K. & KOHSAKA, S. 2013. Purinergic receptors in microglia: functional modal shifts of microglia mediated by P2 and P1 receptors. *Glia,* 61**,** 47-54.

KOLACZKOWSKA, E. & KUBES, P. 2013. Neutrophil recruitment and function in health and inflammation. *Nat Rev Immunol,* 13**,** 159-75.

KOLLMANN, T. R., CRABTREE, J., REIN-WESTON, A., BLIMKIE, D., THOMMAI, F., WANG, X. Y., LAVOIE, P. M., FURLONG, J., FORTUNO, E. S., 3RD, HAJJAR, A. M., HAWKINS, N.

R., SELF, S. G. & WILSON, C. B. 2009. Neonatal innate TLR-mediated responses are distinct from those of adults. *J Immunol,* 183**,** 7150-60.

LA SALA, A., FERRARI, D., DI VIRGILIO, F., IDZKO, M., NORGAUER, J. & GIROLOMONI, G. 2003. Alerting and tuning the immune response by extracellular nucleotides. *J Leukoc Biol,* 73**,** 339-43.

LAI, S. W., CHEN, J. H., LIN, H. Y., LIU, Y. S., TSAI, C. F., CHANG, P. C., LU, D. Y. & LIN, C. 2018. Regulatory Effects of Neuroinflammatory Responses Through Brain-Derived Neurotrophic Factor Signaling in Microglial Cells. *Mol Neurobiol,* 55**,** 7487-7499.

LALLIER, S. W., GRAF, A. E., WAIDYARANTE, G. R. & ROGERS, L. K. 2016. Nurr1 expression is modified by inflammation in microglia. *Neuroreport,* 27**,** 1120-7.

LEDEBOER, A., BREVÉ, J. J., WIERINCKX, A., VAN DER JAGT, S., BRISTOW, A. F., LEYSEN, J. E., TILDERS, F. J. & VAN DAM, A. M. 2002. Expression and regulation of interleukin-10 and interleukin-10 receptor in rat astroglial and microglial cells. *Eur J Neurosci,* 16**,** 1175-85.

LEE, S. C., LIU, W., DICKSON, D. W., BROSNAN, C. F. & BERMAN, J. W. 1993. Cytokine production by human fetal microglia and astrocytes. Differential induction by lipopolysaccharide and IL-1 beta. *J Immunol,* 150**,** 2659-67.

LEE, S. O., LI, X., KHAN, S. & SAFE, S. 2011. Targeting NR4A1 (TR3) in cancer cells and tumors. *Expert Opin Ther Targets,* 15**,** 195-206.

LEHNARDT, S. 2010. Innate immunity and neuroinflammation in the CNS: the role of microglia in Toll-like receptor-mediated neuronal injury. *Glia,* 58**,** 253-63.

LENZ, K. M. & NELSON, L. H. 2018. Microglia and Beyond: Innate Immune Cells As Regulators of Brain Development and Behavioral Function. *Front Immunol,* 9**,** 698.

LI, J., RAMENADEN, E. R., PENG, J., KOITO, H., VOLPE, J. J. & ROSENBERG, P. A. 2008. Tumor necrosis factor alpha mediates lipopolysaccharide-induced microglial toxicity to developing oligodendrocytes when astrocytes are present. *J Neurosci,* 28**,** 5321-30.

LI, N., ZHANG, X., DONG, H., ZHANG, S., SUN, J. & QIAN, Y. 2016a. Lithium Ameliorates LPS-Induced Astrocytes Activation Partly via Inhibition of Toll-Like Receptor 4 Expression. *Cell Physiol Biochem,* 38**,** 714-25.

LI, Q., CHENG, Z., ZHOU, L., DARMANIS, S., NEFF, N. F., OKAMOTO, J., GULATI, G., BENNETT, M. L., SUN, L. O., CLARKE, L. E., MARSCHALLINGER, J., YU, G., QUAKE, S. R., WYSS-CORAY, T. & BARRES, B. A. 2019. Developmental Heterogeneity of Microglia and Brain Myeloid Cells Revealed by Deep Single-Cell RNA Sequencing. *Neuron,* 101**,** 207-223 e10.

LI, Y., LIU, L., BARGER, S. W. & GRIFFIN, W. S. 2003. Interleukin-1 mediates pathological effects of microglia on tau phosphorylation and on synaptophysin synthesis in cortical neurons through a p38-MAPK pathway. *J Neurosci,* 23**,** 1605-11.

LI, Y., POWELL, D. A., SHAFFER, S. A., RASKO, D. A., PELLETIER, M. R., LESZYK, J. D., SCOTT, A. J., MASOUDI, A., GOODLETT, D. R., WANG, X., RAETZ, C. R. & ERNST, R. K. 2012. LPS remodeling is an evolved survival strategy for bacteria. *Proc Natl Acad Sci U S A,* 109**,** 8716-21.

LI, Z., WEI, H., PIIRAINEN, S., CHEN, Z., KALSO, E., PERTOVAARA, A. & TIAN, L. 2016b. Spinal versus brain microglial and macrophage activation traits determine the differential neuroinflammatory responses and analgesic effect of minocycline in chronic neuropathic pain. *Brain Behav Immun,* 58**,** 107-117.

LIDDELOW, S. A. & BARRES, B. A. 2017. Reactive Astrocytes: Production, Function, and Therapeutic Potential. *Immunity,* 46**,** 957-967.

LIDDELOW, S. A., GUTTENPLAN, K. A., CLARKE, L. E., BENNETT, F. C., BOHLEN, C. J., SCHIRMER, L., BENNETT, M. L., MUNCH, A. E., CHUNG, W. S., PETERSON, T. C., WILTON, D. K., FROUIN, A., NAPIER, B. A., PANICKER, N., KUMAR, M., BUCKWALTER, M. S., ROWITCH, D. H., DAWSON, V. L., DAWSON, T. M., STEVENS, B. & BARRES, B. A. 2017a. Neurotoxic reactive astrocytes are induced by activated microglia. *Nature,* 541**,** 481-487.

LIDDELOW, S. A., GUTTENPLAN, K. A., CLARKE, L. E., BENNETT, F. C., BOHLEN, C. J., SCHIRMER, L., BENNETT, M. L., MÜNCH, A. E., CHUNG, W. S., PETERSON, T. C., WILTON, D. K., FROUIN, A., NAPIER, B. A., PANICKER, N., KUMAR, M., BUCKWALTER, M. S., ROWITCH, D. H., DAWSON, V. L., DAWSON, T. M., STEVENS, B. & BARRES, B. A. 2017b. Neurotoxic reactive astrocytes are induced by activated microglia. *Nature,* 541**,** 481-487.

LIN, L., DESAI, R., WANG, X., LO, E. H. & XING, C. 2017. Characteristics of primary rat microglia isolated from mixed cultures using two different methods. *J Neuroinflammation,* 14**,** 101.

LIU, T. Y., YANG, X. Y., ZHENG, L. T., WANG, G. H. & ZHEN, X. C. 2017. Activation of Nur77 in microglia attenuates proinflammatory mediators production and protects dopaminergic neurons from inflammation-induced cell death. *J Neurochem,* 140**,** 589-604.

LIU, W., TANG, Y. & FENG, J. 2011. Cross talk between activation of microglia and astrocytes in pathological conditions in the central nervous system. *Life Sci,* 89**,** 141-6.

LIVAK, K. J. & SCHMITTGEN, T. D. 2001. Analysis of relative gene expression data using real-time quantitative PCR and the 2(-Delta Delta C(T)) Method. *Methods,* 25**,** 402-8.

LIVELY, S. & SCHLICHTER, L. C. 2018. Microglia Responses to Pro-inflammatory Stimuli (LPS, IFNgamma+TNFalpha) and Reprogramming by Resolving Cytokines (IL-4, IL-10). *Front Cell Neurosci,* 12**,** 215.

LOU, N., TAKANO, T., PEI, Y., XAVIER, A. L., GOLDMAN, S. A. & NEDERGAARD, M. 2016. Purinergic receptor P2RY12-dependent microglial closure of the injured blood-brain barrier. *Proc Natl Acad Sci U S A,* 113**,** 1074-9.

LUCAS, S. M., ROTHWELL, N. J. & GIBSON, R. M. 2006. The role of inflammation in CNS injury and disease. *Br J Pharmacol,* 147 Suppl 1**,** S232-40.

LULL, M. E. & BLOCK, M. L. 2010. Microglial activation and chronic neurodegeneration. *Neurotherapeutics,* 7**,** 354-65.

LUO, X. G., DING, J. Q. & CHEN, S. D. 2010. Microglia in the aging brain: relevance to neurodegeneration. *Mol Neurodegener,* 5**,** 12.

MA, Q., CHEN, S., KLEBE, D., ZHANG, J. H. & TANG, J. 2013. Adhesion molecules in CNS disorders: biomarker and therapeutic targets. *CNS Neurol Disord Drug Targets,* 12**,** 392-404.

MACIEJEWSKI-LENOIR, D., CHEN, S., FENG, L., MAKI, R. & BACON, K. B. 1999. Characterization of fractalkine in rat brain cells: migratory and activation signals for CX3CR-1-expressing microglia. *J Immunol,* 163**,** 1628-35.

MAHAJAN, S., SAINI, A., CHANDRA, V., NANDURI, R., KALRA, R., BHAGYARAJ, E., KHATRI, N. & GUPTA, P. 2015. Nuclear Receptor Nr4a2 Promotes Alternative Polarization of Macrophages and Confers Protection in Sepsis. *J Biol Chem,* 290**,** 18304-14.

MAPPLEBECK, J. C. S., DALGARNO, R., TU, Y., MORIARTY, O., BEGGS, S., KWOK, C. H. T., HALIEVSKI, K., ASSI, S., MOGIL, J. S., TRANG, T. & SALTER, M. W. 2018. Microglial

P2X4R-evoked pain hypersensitivity is sexually dimorphic in rats. *Pain,* 159**,** 1752-1763.

MARINELLI, C., DI LIDDO, R., FACCI, L., BERTALOT, T., CONCONI, M. T., ZUSSO, M., SKAPER, S. D. & GIUSTI, P. 2015. Ligand engagement of Toll-like receptors regulates their expression in cortical microglia and astrocytes. *J Neuroinflammation,* 12**,** 244.

MARTORELL, L., GENTILE, M., RIUS, J., RODRIGUEZ, C., CRESPO, J., BADIMON, L. & MARTINEZ-GONZALEZ, J. 2009. The hypoxia-inducible factor 1/NOR-1 axis regulates the survival response of endothelial cells to hypoxia. *Mol Cell Biol,* 29**,** 5828-42.

MATCOVITCH-NATAN, O., WINTER, D. R., GILADI, A., VARGAS AGUILAR, S., SPINRAD, A., SARRAZIN, S., BEN-YEHUDA, H., DAVID, E., ZELADA GONZALEZ, F., PERRIN, P., KEREN-SHAUL, H., GURY, M., LARA-ASTAISO, D., THAISS, C. A., COHEN, M., BAHAR HALPERN, K., BARUCH, K., DECZKOWSKA, A., LORENZO-VIVAS, E., ITZKOVITZ, S., ELINAV, E., SIEWEKE, M. H., SCHWARTZ, M. & AMIT, I. 2016a. Microglia development follows a stepwise program to regulate brain homeostasis. *Science,* 353**,** aad8670.

MATCOVITCH-NATAN, O., WINTER, D. R., GILADI, A., VARGAS AGUILAR, S., SPINRAD, A., SARRAZIN, S., BEN-YEHUDA, H., DAVID, E., ZELADA GONZÁLEZ, F., PERRIN, P., KEREN-SHAUL, H., GURY, M., LARA-ASTAISO, D., THAISS, C. A., COHEN, M., BAHAR HALPERN, K., BARUCH, K., DECZKOWSKA, A., LORENZO-VIVAS, E., ITZKOVITZ, S., ELINAV, E., SIEWEKE, M. H., SCHWARTZ, M. & AMIT, I. 2016b. Microglia development follows a stepwise program to regulate brain homeostasis. *Science,* 353**,** aad8670.

MATIAS, I., MORGADO, J. & GOMES, F. C. A. 2019. Astrocyte Heterogeneity: Impact to Brain Aging and Disease. *Front Aging Neurosci,* 11**,** 59.

MATSUMURA, Y., YAMASHITA, T., SASAKI, A., NAKATA, E., KOHNO, K., MASUDA, T., TOZAKI-SAITOH, H., IMAI, T., KURAISHI, Y., TSUDA, M. & INOUE, K. 2016. A novel P2X4 receptor-selective antagonist produces anti-allodynic effect in a mouse model of herpetic pain. *Sci Rep,* 6**,** 32461.

MAXWELL, M. A. & MUSCAT, G. E. 2006. The NR4A subgroup: immediate early response genes with pleiotropic physiological roles. *Nucl Recept Signal,* 4**,** e002.

MCKAY, S. M., BROOKS, D. J., HU, P. & MCLACHLAN, E. M. 2007. Distinct types of microglial activation in white and grey matter of rat lumbosacral cord after mid-thoracic spinal transection. *J Neuropathol Exp Neurol,* 66**,** 698-710.

MCKELVEY, R., BERTA, T., OLD, E., JI, R. R. & FITZGERALD, M. 2015. Neuropathic pain is constitutively suppressed in early life by anti-inflammatory neuroimmune regulation. *J Neurosci,* 35**,** 457-66.

MCMORROW, J. P. & MURPHY, E. P. 2011. Inflammation: a role for NR4A orphan nuclear receptors? *Biochem Soc Trans,* 39**,** 688-93.

MCPHERSON, C. A., KRAFT, A. D. & HARRY, G. J. 2011. Injury-induced neurogenesis: consideration of resident microglia as supportive of neural progenitor cells. *Neurotox Res,* 19**,** 341-52.

MICHELHAUGH, S. K., VAITKEVICIUS, H., WANG, J., BOUHAMDAN, M., KRIEG, A. R., WALKER, J. L., MENDIRATTA, V. & BANNON, M. J. 2005. Dopamine neurons express multiple isoforms of the nuclear receptor nurr1 with diminished transcriptional activity. *J Neurochem,* 95**,** 1342-50.

MICHELL-ROBINSON, M. A., TOUIL, H., HEALY, L. M., OWEN, D. R., DURAFOURT, B. A., BAR-OR, A., ANTEL, J. P. & MOORE, C. S. 2015. Roles of microglia in brain development, tissue maintenance and repair. *Brain,* 138**,** 1138-59.

MILLER, R. H. & RAFF, M. C. 1984. Fibrous and protoplasmic astrocytes are biochemically and developmentally distinct. *J Neurosci,* 4**,** 585-92.

MILLIGAN, E. D., ZAPATA, V., CHACUR, M., SCHOENIGER, D., BIEDENKAPP, J., O'CONNOR, K. A., VERGE, G. M., CHAPMAN, G., GREEN, P., FOSTER, A. C., NAEVE, G. S., MAIER, S. F. & WATKINS, L. R. 2004. Evidence that exogenous and endogenous fractalkine can induce spinal nociceptive facilitation in rats. *Eur J Neurosci,* 20**,** 2294-302.

MILLS, C. D., KINCAID, K., ALT, J. M., HEILMAN, M. J. & HILL, A. M. 2000. M-1/M-2 macrophages and the Th1/Th2 paradigm. *J Immunol,* 164**,** 6166-73.

MINKIEWICZ, J., DE RIVERO VACCARI, J. P. & KEANE, R. W. 2013. Human astrocytes express a novel NLRP2 inflammasome. *Glia,* 61**,** 1113-21.

MIWA, T., FURUKAWA, S., NAKAJIMA, K., FURUKAWA, Y. & KOHSAKA, S. 1997. Lipopolysaccharide enhances synthesis of brain-derived neurotrophic factor in cultured rat microglia. *J Neurosci Res,* 50**,** 1023-9.

MIZEE, M. R., MIEDEMA, S. S., VAN DER POEL, M., ADELIA, SCHUURMAN, K. G., VAN STRIEN, M. E., MELIEF, J., SMOLDERS, J., HENDRICKX, D. A., HEUTINCK, K. M., HAMANN, J. & HUITINGA, I. 2017. Isolation of primary microglia from the human post-mortem brain: effects of ante- and post-mortem variables. *Acta Neuropathol Commun,* 5**,** 16.

MOLOFSKY, A. V., KRENCIK, R., ULLIAN, E. M., TSAI, H. H., DENEEN, B., RICHARDSON, W. D., BARRES, B. A. & ROWITCH, D. H. 2012. Astrocytes and disease: a neurodevelopmental perspective. *Genes Dev,* 26**,** 891-907.

MONTAROLO, F., RAFFAELE, C., PERGA, S., MARTIRE, S., FINARDI, A., FURLAN, R., HINTERMANN, S. & BERTOLOTTO, A. 2014. Effects of isoxazolo-pyridinone 7e, a potent activator of the Nurr1 signaling pathway, on experimental autoimmune encephalomyelitis in mice. *PLoS One,* 9**,** e108791.

MOYNAGH, P. N., WILLIAMS, D. C. & O'NEILL, L. A. 1993. Interleukin-1 activates transcription factor NF kappa B in glial cells. *Biochem J,* 294 (Pt 2)**,** 343-7.

MURPHY, E. P. & CREAN, D. 2015. Molecular Interactions between NR4A Orphan Nuclear Receptors and NF-κB Are Required for Appropriate Inflammatory Responses and Immune Cell Homeostasis. *Biomolecules,* 5**,** 1302-18.

MURRAY, R. K., CONNELL, G. E. & PERT, J. H. 1961. The role of haptoglobin in the clearance and distribution of extracorpuscular hemoglobin. *Blood,* 17**,** 45-53.

NAKAJIMA, K. & KOHSAKA, S. 2004. Microglia: neuroprotective and neurotrophic cells in the central nervous system. *Curr Drug Targets Cardiovasc Haematol Disord,* 4**,** 65-84.

NDUBAKU, U. & DE BELLARD, M. E. 2008. Glial cells: old cells with new twists. *Acta Histochem,* 110**,** 182-95.

NIKODEMOVA, M., SMALL, A. L., KIMYON, R. S. & WATTERS, J. J. 2016. Age-dependent differences in microglial responses to systemic inflammation are evident as early as middle age. *Physiol Genomics,* 48**,** 336-44.

NORDEN, D. M., FENN, A. M., DUGAN, A. & GODBOUT, J. P. 2014. TGFβ produced by IL-10 redirected astrocytes attenuates microglial activation. *Glia,* 62**,** 881-95.

NORDEN, D. M., TROJANOWSKI, P. J., VILLANUEVA, E., NAVARRO, E. & GODBOUT, J. P. 2016. Sequential activation of microglia and astrocyte cytokine expression

precedes increased Iba-1 or GFAP immunoreactivity following systemic immune challenge. *Glia,* 64**,** 300-16.

NORTH, R. A. & SURPRENANT, A. 2000. Pharmacology of cloned P2X receptors. *Annu Rev Pharmacol Toxicol,* 40**,** 563-80.

O'GARRA, A. & MURPHY, K. 1994. Role of cytokines in determining T-lymphocyte function. *Curr Opin Immunol,* 6**,** 458-66.

OBERHEIM, N. A., GOLDMAN, S. A. & NEDERGAARD, M. 2012. Heterogeneity of astrocytic form and function. *Methods Mol Biol,* 814**,** 23-45.

OBERHEIM, N. A., TAKANO, T., HAN, X., HE, W., LIN, J. H., WANG, F., XU, Q., WYATT, J. D., PILCHER, W., OJEMANN, J. G., RANSOM, B. R., GOLDMAN, S. A. & NEDERGAARD, M. 2009. Uniquely hominid features of adult human astrocytes. *J Neurosci,* 29**,** 3276-87.

OGAWA, S., LOZACH, J., BENNER, C., PASCUAL, G., TANGIRALA, R. K., WESTIN, S., HOFFMANN, A., SUBRAMANIAM, S., DAVID, M., ROSENFELD, M. G. & GLASS, C. K. 2005. Molecular determinants of crosstalk between nuclear receptors and toll-like receptors. *Cell,* 122**,** 707-21.

OLOVNIKOV, A. M. 1996. Telomeres, telomerase, and aging: origin of the theory. *Exp Gerontol,* 31**,** 443-8.

PAOLICELLI, R. C., BISHT, K. & TREMBLAY, M. E. 2014. Fractalkine regulation of microglial physiology and consequences on the brain and behavior. *Front Cell Neurosci,* 8**,** 129.

PAOLICELLI, R. C. & FERRETTI, M. T. 2017. Function and Dysfunction of Microglia during Brain Development: Consequences for Synapses and Neural Circuits. *Front Synaptic Neurosci,* 9**,** 9.

PARKHURST, C. N., YANG, G., NINAN, I., SAVAS, J. N., YATES, J. R., 3RD, LAFAILLE, J. J., HEMPSTEAD, B. L., LITTMAN, D. R. & GAN, W. B. 2013. Microglia promote learning-dependent synapse formation through brain-derived neurotrophic factor. *Cell,* 155**,** 1596-609.

PASCUAL, G., FONG, A. L., OGAWA, S., GAMLIEL, A., LI, A. C., PERISSI, V., ROSE, D. W., WILLSON, T. M., ROSENFELD, M. G. & GLASS, C. K. 2005. A SUMOylation-dependent pathway mediates transrepression of inflammatory response genes by PPAR-gamma. *Nature,* 437**,** 759-63.

PATRYLO, P. R. & NOWAKOWSKI, R. S. 1994. Morphology and distribution of astrocytes in the molecular layer of the dentate gyrus in NZB/BINJ, Dreher, and C57BL/6J mice. *Glia,* 10**,** 1-9.

PEAREN, M. A. & MUSCAT, G. E. 2010. Minireview: Nuclear hormone receptor 4A signaling: implications for metabolic disease. *Mol Endocrinol,* 24**,** 1891-903.

PEI, L., CASTRILLO, A., CHEN, M., HOFFMANN, A. & TONTONOZ, P. 2005. Induction of NR4A orphan nuclear receptor expression in macrophages in response to inflammatory stimuli. *J Biol Chem,* 280**,** 29256-62.

PERRY, V. H. & TEELING, J. 2013. Microglia and macrophages of the central nervous system: the contribution of microglia priming and systemic inflammation to chronic neurodegeneration. *Semin Immunopathol,* 35**,** 601-12.

POCOCK, J. M. & PIERS, T. M. 2018. Modelling microglial function with induced pluripotent stem cells: an update. *Nat Rev Neurosci,* 19**,** 445-452.

POPICHAK, K. A., HAMMOND, S. L., MORENO, J. A., AFZALI, M. F., BACKOS, D. S., SLAYDEN, R. D., SAFE, S. & TJALKENS, R. B. 2018. Compensatory Expression of Nur77 and

Nurr1 Regulates NF-kappaB-Dependent Inflammatory Signaling in Astrocytes. *Mol Pharmacol,* 94**,** 1174-1186.

PRINZ, M. & PRILLER, J. 2014. Microglia and brain macrophages in the molecular age: from origin to neuropsychiatric disease. *Nat Rev Neurosci,* 15**,** 300-12.

QIAN, Y., CHEN, X. X., WANG, W., LI, J. J., WANG, X. P., TANG, Z. W., XU, J. T., LIN, H., YANG, Z. Y., LI, L. Y., SONG, X. B., GUO, J. Z., BIAN, L. G., ZHOU, L., LU, D. & DENG, X. L. 2019. Transplantation of Nurr1-overexpressing neural stem cells and microglia for treating parkinsonian rats. *CNS Neurosci Ther*.

QIN, L., HE, J., HANES, R. N., PLUZAREV, O., HONG, J. S. & CREWS, F. T. 2008. Increased systemic and brain cytokine production and neuroinflammation by endotoxin following ethanol treatment. *J Neuroinflammation,* 5**,** 10.

QURESHI, O. S., PARAMASIVAM, A., YU, J. C. & MURRELL-LAGNADO, R. D. 2007. Regulation of P2X4 receptors by lysosomal targeting, glycan protection and exocytosis. *J Cell Sci,* 120**,** 3838-49.

RAMESH, G., MACLEAN, A. G. & PHILIPP, M. T. 2013. Cytokines and chemokines at the crossroads of neuroinflammation, neurodegeneration, and neuropathic pain. *Mediators Inflamm,* 2013**,** 480739.

RANSOHOFF, R. M. 2016. How neuroinflammation contributes to neurodegeneration. *Science,* 353**,** 777-83.

RAWJI, K. S., MISHRA, M. K., MICHAELS, N. J., RIVEST, S., STYS, P. K. & YONG, V. W. 2016. Immunosenescence of microglia and macrophages: impact on the ageing central nervous system. *Brain,* 139**,** 653-61.

REU, P., KHOSRAVI, A., BERNARD, S., MOLD, J. E., SALEHPOUR, M., ALKASS, K., PERL, S., TISDALE, J., POSSNERT, G., DRUID, H. & FRISEN, J. 2017. The Lifespan and Turnover of Microglia in the Human Brain. *Cell Rep,* 20**,** 779-784.

RIETSCHEL, E. T., KIRIKAE, T., SCHADE, F. U., MAMAT, U., SCHMIDT, G., LOPPNOW, H., ULMER, A. J., ZÄHRINGER, U., SEYDEL, U. & DI PADOVA, F. 1994. Bacterial endotoxin: molecular relationships of structure to activity and function. *FASEB J,* 8**,** 217-25.

ROCK, R. B., GEKKER, G., HU, S., SHENG, W. S., CHEERAN, M., LOKENSGARD, J. R. & PETERSON, P. K. 2004. Role of microglia in central nervous system infections. *Clin Microbiol Rev,* 17**,** 942-64, table of contents.

ROSSI, F. & LEWIS, C. 2018. Microglia's heretical self-renewal. *Nat Neurosci,* 21**,** 455-456.

ROY, A., JANA, A., YATISH, K., FREIDT, M. B., FUNG, Y. K., MARTINSON, J. A. & PAHAN, K. 2008. Reactive oxygen species up-regulate CD11b in microglia via nitric oxide: Implications for neurodegenerative diseases. *Free Radic Biol Med,* 45**,** 686-99.

ROZOVSKY, I., FINCH, C. E. & MORGAN, T. E. 1998. Age-related activation of microglia and astrocytes: in vitro studies show persistent phenotypes of aging, increased proliferation, and resistance to down-regulation. *Neurobiol Aging,* 19**,** 97-103.

RUSTENHOVEN, J., PARK, T. I., SCHWEDER, P., SCOTTER, J., CORREIA, J., SMITH, A. M., GIBBONS, H. M., OLDFIELD, R. L., BERGIN, P. S., MEE, E. W., FAULL, R. L., CURTIS, M. A., SCOTT GRAHAM, E. & DRAGUNOW, M. 2016. Isolation of highly enriched primary human microglia for functional studies. *Sci Rep,* 6**,** 19371.

SA, Q. & HOOVER-PLOW, J. L. 2011. EMILIN2 (Elastin microfibril interface located protein), potential modifier of thrombosis. *Thromb J,* 9**,** 9.

SAIJO, K., CROTTI, A. & GLASS, C. K. 2013. Regulation of microglia activation and deactivation by nuclear receptors. *Glia,* 61**,** 104-111.

SAIJO, K., WINNER, B., CARSON, C. T., COLLIER, J. G., BOYER, L., ROSENFELD, M. G., GAGE, F. H. & GLASS, C. K. 2009. A Nurr1/CoREST pathway in microglia and astrocytes protects dopaminergic neurons from inflammation-induced death. *Cell,* 137**,** 47-59.

SALTER, M. W. & STEVENS, B. 2017. Microglia emerge as central players in brain disease. *Nat Med,* 23**,** 1018-1027.

SASAKI, A., YAMAGUCHI, H., HORIKOSHI, Y., TANAKA, G. & NAKAZATO, Y. 2004. Expression of glucose transporter 5 by microglia in human gliomas. *Neuropathol Appl Neurobiol,* 30**,** 447-55.

SATOH, J., KINO, Y., ASAHINA, N., TAKITANI, M., MIYOSHI, J., ISHIDA, T. & SAITO, Y. 2016. TMEM119 marks a subset of microglia in the human brain. *Neuropathology,* 36**,** 39-49.

SEO, D. R., KIM, K. Y. & LEE, Y. B. 2004. Interleukin-10 expression in lipopolysaccharide-activated microglia is mediated by extracellular ATP in an autocrine fashion. *Neuroreport,* 15**,** 1157-61.

SEO, D. R., KIM, S. Y., KIM, K. Y., LEE, H. G., MOON, J. H., LEE, J. S., LEE, S. H., KIM, S. U. & LEE, Y. B. 2008. Cross talk between P2 purinergic receptors modulates extracellular ATP-mediated interleukin-10 production in rat microglial cells. *Exp Mol Med,* 40**,** 19-26.

SEVENICH, L. 2018. Brain-Resident Microglia and Blood-Borne Macrophages Orchestrate Central Nervous System Inflammation in Neurodegenerative Disorders and Brain Cancer. *Front Immunol,* 9**,** 697.

SEVER, R. & GLASS, C. K. 2013. Signaling by nuclear receptors. *Cold Spring Harb Perspect Biol,* 5**,** a016709.

SHEHAB, S. A., CRONLY-DILLON, J. R., NONA, S. N. & STAFFORD, C. A. 1990. Preferential histochemical staining of protoplasmic and fibrous astrocytes in rat CNS with GFAP antibodies using different fixatives. *Brain Res,* 518**,** 347-52.

SHERIDAN, G. K. & MURPHY, K. J. 2013. Neuron-glia crosstalk in health and disease: fractalkine and CX3CR1 take centre stage. *Open Biol,* 3**,** 130181.

SMITH, J. A., DAS, A., RAY, S. K. & BANIK, N. L. 2012. Role of pro-inflammatory cytokines released from microglia in neurodegenerative diseases. *Brain Res Bull,* 87**,** 10-20.

SOFRONIEW, M. V. 2009. Molecular dissection of reactive astrogliosis and glial scar formation. *Trends Neurosci,* 32**,** 638-47.

SOFRONIEW, M. V. & VINTERS, H. V. 2010. Astrocytes: biology and pathology. *Acta Neuropathol,* 119**,** 7-35.

SOMJEN, G. G. 1988. Nervenkitt: notes on the history of the concept of neuroglia. *Glia,* 1**,** 2-9.

SOUSA, C., BIBER, K. & MICHELUCCI, A. 2017. Cellular and Molecular Characterization of Microglia: A Unique Immune Cell Population. *Front Immunol,* 8**,** 198.

SPEICHER, A. M., WIENDL, H., MEUTH, S. G. & PAWLOWSKI, M. 2019. Generating microglia from human pluripotent stem cells: novel in vitro models for the study of neurodegeneration. *Mol Neurodegener,* 14**,** 46.

STANSLEY, B., POST, J. & HENSLEY, K. 2012. A comparative review of cell culture systems for the study of microglial biology in Alzheimer's disease. *J Neuroinflammation,* 9**,** 115.

STOGSDILL, J. A., RAMIREZ, J., LIU, D., KIM, Y. H., BALDWIN, K. T., ENUSTUN, E., EJIKEME, T., JI, R. R. & EROGLU, C. 2017. Astrocytic neuroligins control astrocyte morphogenesis and synaptogenesis. *Nature,* 551**,** 192-197.

STREIT, W. J., MRAK, R. E. & GRIFFIN, W. S. 2004a. Microglia and neuroinflammation: a pathological perspective. *J Neuroinflammation,* 1**,** 14.

STREIT, W. J., SAMMONS, N. W., KUHNS, A. J. & SPARKS, D. L. 2004b. Dystrophic microglia in the aging human brain. *Glia,* 45**,** 208-12.

SUDDUTH, T. L., SCHMITT, F. A., NELSON, P. T. & WILCOCK, D. M. 2013. Neuroinflammatory phenotype in early Alzheimer's disease. *Neurobiol Aging,* 34**,** 1051-9.

TABATA, H. 2015. Diverse subtypes of astrocytes and their development during corticogenesis. *Front Neurosci,* 9**,** 114.

TABATABAIE, L., KLOMP, L. W., BERGER, R. & DE KONING, T. J. 2010. L-serine synthesis in the central nervous system: a review on serine deficiency disorders. *Mol Genet Metab,* 99**,** 256-62.

TAMASHIRO, T. T., DALGARD, C. L. & BYRNES, K. R. 2012. Primary microglia isolation from mixed glial cell cultures of neonatal rat brain tissue. *J Vis Exp***,** e3814.

TAUPIN, P. 2008. Adult neurogenesis, neuroinflammation and therapeutic potential of adult neural stem cells. *Int J Med Sci,* 5**,** 127-32.

TIAN, L., MA, L., KAARELA, T. & LI, Z. 2012. Neuroimmune crosstalk in the central nervous system and its significance for neurological diseases. *J Neuroinflammation,* 9**,** 155.

TIMMERMAN, R., BURM, S. M. & BAJRAMOVIC, J. J. 2018. An Overview of in vitro Methods to Study Microglia. *Front Cell Neurosci,* 12**,** 242.

TRANG, T., BEGGS, S., WAN, X. & SALTER, M. W. 2009. P2X4-receptor-mediated synthesis and release of brain-derived neurotrophic factor in microglia is dependent on calcium and p38-mitogen-activated protein kinase activation. *J Neurosci,* 29**,** 3518-28.

TREMBLAY, M. E., LECOURS, C., SAMSON, L., SANCHEZ-ZAFRA, V. & SIERRA, A. 2015. From the Cajal alumni Achucarro and Rio-Hortega to the rediscovery of never-resting microglia. *Front Neuroanat,* 9**,** 45.

TRIANTAFILOU, M. & TRIANTAFILOU, K. 2002. Lipopolysaccharide recognition: CD14, TLRs and the LPS-activation cluster. *Trends Immunol,* 23**,** 301-4.

TSUDA, M. 2016. Microglia in the spinal cord and neuropathic pain. *J Diabetes Investig,* 7**,** 17-26.

TSUDA, M., SHIGEMOTO-MOGAMI, Y., KOIZUMI, S., MIZOKOSHI, A., KOHSAKA, S., SALTER, M. W. & INOUE, K. 2003. P2X4 receptors induced in spinal microglia gate tactile allodynia after nerve injury. *Nature,* 424**,** 778-83.

TSUDA, M., TOZAKI-SAITOH, H. & INOUE, K. 2012. Purinergic system, microglia and neuropathic pain. *Curr Opin Pharmacol,* 12**,** 74-9.

UBOGU, E. E., COSSOY, M. B. & RANSOHOFF, R. M. 2006. The expression and function of chemokines involved in CNS inflammation. *Trends Pharmacol Sci,* 27**,** 48-55.

ULMANN, L., HATCHER, J. P., HUGHES, J. P., CHAUMONT, S., GREEN, P. J., CONQUET, F., BUELL, G. N., REEVE, A. J., CHESSELL, I. P. & RASSENDREN, F. 2008. Up-regulation of P2X4 receptors in spinal microglia after peripheral nerve injury mediates BDNF release and neuropathic pain. *J Neurosci,* 28**,** 11263-8.

VAN DER POEL, M., ULAS, T., MIZEE, M. R., HSIAO, C. C., MIEDEMA, S. S. M., ADELIA, SCHUURMAN, K. G., HELDER, B., TAS, S. W., SCHULTZE, J. L., HAMANN, J. & HUITINGA, I. 2019. Transcriptional profiling of human microglia reveals grey-white matter heterogeneity and multiple sclerosis-associated changes. *Nat Commun,* 10**,** 1139.

VENEGAS, C. & HENEKA, M. T. 2017. Danger-associated molecular patterns in Alzheimer's disease. *J Leukoc Biol,* 101**,** 87-98.

VERKHRATSKY, A., PANKRATOV, Y., LALO, U. & NEDERGAARD, M. 2012. P2X receptors in neuroglia. *Wiley Interdiscip Rev Membr Transp Signal,* 1.

VERMEIREN, C., NAJIMI, M., MALOTEAUX, J. M. & HERMANS, E. 2005. Molecular and functional characterisation of glutamate transporters in rat cortical astrocytes exposed to a defined combination of growth factors during in vitro differentiation. *Neurochem Int,* 46**,** 137-47.

VILLA, A., GELOSA, P., CASTIGLIONI, L., CIMINO, M., RIZZI, N., PEPE, G., LOLLI, F., MARCELLO, E., SIRONI, L., VEGETO, E. & MAGGI, A. 2018. Sex-Specific Features of Microglia from Adult Mice. *Cell Rep,* 23**,** 3501-3511.

VOGEL, C. & MARCOTTE, E. M. 2012. Insights into the regulation of protein abundance from proteomic and transcriptomic analyses. *Nat Rev Genet,* 13**,** 227-32.

VOLAKAKIS, N., KADKHODAEI, B., JOODMARDI, E., WALLIS, K., PANMAN, L., SILVAGGI, J., SPIEGELMAN, B. M. & PERLMANN, T. 2010. NR4A orphan nuclear receptors as mediators of CREB-dependent neuroprotection. *Proc Natl Acad Sci U S A,* 107**,** 12317-22.

VOUTSINOS-PORCHE, B., BONVENTO, G., TANAKA, K., STEINER, P., WELKER, E., CHATTON, J. Y., MAGISTRETTI, P. J. & PELLERIN, L. 2003. Glial glutamate transporters mediate a functional metabolic crosstalk between neurons and astrocytes in the mouse developing cortex. *Neuron,* 37**,** 275-86.

WALCO, G. A., DWORKIN, R. H., KRANE, E. J., LEBEL, A. A. & TREEDE, R. D. 2010. Neuropathic pain in children: Special considerations. *Mayo Clin Proc,* 85**,** S33-41.

WANG, W. Y., TAN, M. S., YU, J. T. & TAN, L. 2015. Role of pro-inflammatory cytokines released from microglia in Alzheimer's disease. *Ann Transl Med,* 3**,** 136.

WANG, Z., BENOIT, G., LIU, J., PRASAD, S., AARNISALO, P., LIU, X., XU, H., WALKER, N. P. & PERLMANN, T. 2003. Structure and function of Nurr1 identifies a class of ligand-independent nuclear receptors. *Nature,* 423**,** 555-60.

WATKINS, L. R. & HUTCHINSON, M. R. 2014. A concern on comparing 'apples' and 'oranges' when differences between microglia used in human and rodent studies go far, far beyond simply species: comment on Smith and Dragunow. *Trends Neurosci,* 37**,** 189-90.

WEYDT, P., YUEN, E. C., RANSOM, B. R. & MOLLER, T. 2004. Increased cytotoxic potential of microglia from ALS-transgenic mice. *Glia,* 48**,** 179-82.

WOODLING, N. S., WANG, Q., PRIYAM, P. G., LARKIN, P., SHI, J., JOHANSSON, J. U., ZAGOL-IKAPITTE, I., BOUTAUD, O. & ANDREASSON, K. I. 2014. Suppression of Alzheimer-associated inflammation by microglial prostaglandin-E2 EP4 receptor signaling. *J Neurosci,* 34**,** 5882-94.

WU, S., XUE, R., HASSAN, S., NGUYEN, T. M. L., WANG, T., PAN, H., XU, J., LIU, Q., ZHANG, W. & WEN, Z. 2018. Il34-Csf1r Pathway Regulates the Migration and Colonization of Microglial Precursors. *Dev Cell,* 46**,** 552-563 e4.

YE, S. M. & JOHNSON, R. W. 2001. Regulation of interleukin-6 gene expression in brain of aged mice by nuclear factor kappaB. *J Neuroimmunol,* 117**,** 87-96.

YIP, P. K., KAAN, T. K., FENESAN, D. & MALCANGIO, M. 2009. Rapid isolation and culture of primary microglia from adult mouse spinal cord. *J Neurosci Methods,* 183**,** 223-37.

YOU, L. H., YAN, C. Z., ZHENG, B. J., CI, Y. Z., CHANG, S. Y., YU, P., GAO, G. F., LI, H. Y., DONG, T. Y. & CHANG, Y. Z. 2017. Astrocyte hepcidin is a key factor in LPS-induced neuronal apoptosis. *Cell Death Dis,* 8**,** e2676.

ZAMANIAN, J. L., XU, L., FOO, L. C., NOURI, N., ZHOU, L., GIFFARD, R. G. & BARRES, B. A. 2012. Genomic analysis of reactive astrogliosis. *J Neurosci,* 32**,** 6391-410.

ZETTERSTRÖM, R. H., SOLOMIN, L., JANSSON, L., HOFFER, B. J., OLSON, L. & PERLMANN, T. 1997. Dopamine neuron agenesis in Nurr1-deficient mice. *Science,* 276**,** 248-50.

ZHANG, F., VADAKKAN, K. I., KIM, S. S., WU, L. J., SHANG, Y. & ZHUO, M. 2008. Selective activation of microglia in spinal cord but not higher cortical regions following nerve injury in adult mouse. *Mol Pain,* 4**,** 15.

ZHANG, H., NIESEL, D. W., PETERSON, J. W. & KLIMPEL, G. R. 1998. Lipoprotein release by bacteria: potential factor in bacterial pathogenesis. *Infect Immun,* 66**,** 5196-201.

ZHANG, Q., KANG, R., ZEH, H. J., LOTZE, M. T. & TANG, D. 2013. DAMPs and autophagy: cellular adaptation to injury and unscheduled cell death. *Autophagy,* 9**,** 451-8.

ZHANG, X., ZENG, L., YU, T., XU, Y., PU, S., DU, D. & JIANG, W. 2014. Positive feedback loop of autocrine BDNF from microglia causes prolonged microglia activation. *Cell Physiol Biochem,* 34**,** 715-23.

ZHANG, Z., ARTELT, M., BURNET, M., TRAUTMANN, K. & SCHLUESENER, H. J. 2006. Lesional accumulation of P2X4 receptor+ monocytes following experimental traumatic brain injury. *Exp Neurol,* 197**,** 252-7.

ZHAO, B. & SCHWARTZ, J. P. 1998. Involvement of cytokines in normal CNS development and neurological diseases: recent progress and perspectives. *J Neurosci Res,* 52**,** 7-16.

ZHAO, Y., HOWATT, D. A., GIZARD, F., NOMIYAMA, T., FINDEISEN, H. M., HEYWOOD, E. B., JONES, K. L., CONNEELY, O. M., DAUGHERTY, A. & BRUEMMER, D. 2010. Deficiency of the NR4A orphan nuclear receptor NOR1 decreases monocyte adhesion and atherosclerosis. *Circ Res,* 107**,** 501-11.

ZHUO, M., WU, G. & WU, L. J. 2011. Neuronal and microglial mechanisms of neuropathic pain. *Mol Brain,* 4**,** 31.

ZUJOVIC, V., BENAVIDES, J., VIGE, X., CARTER, C. & TAUPIN, V. 2000. Fractalkine modulates TNF-alpha secretion and neurotoxicity induced by microglial activation. *Glia,* 29**,** 305-15.